AFRRI Reports

1990

July

August

September

Defense Nuclear Agency

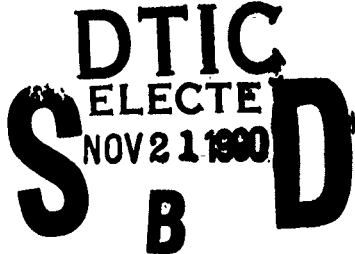# Armed Forces
Radiobiology Research
Institute

Bethesda, Maryland 20889-5145

REPORT DOCUMENTATION PAGE

Public reporting burden for this collection of information is estimated to average 1 hour per response, including the time for reviewing instructions, searching existing data sources, gathering and maintaining the data needed, and completing and reviewing the collection of information. Send comments regarding this burden estimate or any other aspect of this collection of information, including suggestions for reducing this burden, to Washington Headquarters Services, Directorate for Information Operations and Reports, 1215 Jefferson Davis Highway, Suite 1204, Arlington, VA 22202-4302, and to the Office of Management and Budget, Paperwork Reduction Project (0704-0188), Washington, DC 20503

1. AGENCY USE ONLY (Leave blank)	2. REPORT DATE 1990 October	3. REPORT TYPE AND DATES COVERED Reprints/Technical

4. TITLE AND SUBTITLE

AFRRI Reports, Jul-Sep 1990

5. FUNDING NUMBERS

NWED QAXM

6. AUTHOR(S)

7. PERFORMING ORGANIZATION NAME(S) AND ADDRESS(ES)

Armed Forces Radiobiology Research Institute
Bethesda, MD 20889-5145

8. PERFORMING ORGANIZATION REPORT NUMBER

SR90-11 - SR90-24

9. SPONSORING/MONITORING AGENCY NAME(S) AND ADDRESS(ES)

Defense Nuclear Agency
Washington, DC 20305

10. SPONSORING/MONITORING AGENCY REPORT NUMBER

11. SUPPLEMENTARY NOTES

12a. DISTRIBUTION/AVAILABILITY STATEMENT

Approved for public release; distribution unlimited.

12b. DISTRIBUTION CODE

13. ABSTRACT (Maximum 200 words)

This volume contains AFRRI Scientific Reports SR90-11 through SR90-24 for Jul-Sep 1990.

DTIC
ELECTE
NOV 21 1990
S
B
D

14. SUBJECT TERMS	15. NUMBER OF PAGES 132
	16. PRICE CODE

17. SECURITY CLASSIFICATION OF REPORT	18. SECURITY CLASSIFICATION OF THIS PAGE	19. SECURITY CLASSIFICATION OF ABSTRACT	20. LIMITATION OF ABSTRACT
UNCLASSIFIED	UNCLASSIFIED	UNCLASSIFIED	same as report

NSN 7540-01-280-5500

Standard Form 298 (Rev. 2-89)
Prescribed by ANSI Std 239-18
298-102

90 11 21 086

CLASSIFIED BY:

DECLASSIFY ON:

CONTENTS

Scientific Reports

Dist | Avail and/or Special
Codes
A-1

REACTION OF VANADYL WITH HYDROGEN PEROXIDE. AN ESR AND SPIN TRAPPING STUDY

ALASDAIR J. CARMICHAEL

Radiation Biochemistry Department, Armed Forces Radiobiology Research Institute, Bethesda, MD 20814-5145 U.S.A.

Vanadyl reacts with hydrogen peroxide forming hydroxyl radicals in a Fenton-like reaction. The hydroxyl radicals were spin trapped and identified using 5,5-dimethyl-1-pyrroline-N-oxide (DMPO). The quantity of hydroxyl radicals spin trapped during the reaction between vanadyl and hydrogen peroxide are equal to half of the hydroxyl radicals spin trapped during the reaction between ferrous ions and hydrogen peroxide. Experiments in the presence of formate show that this hydroxyl radical scavenger effectively competes with DMPO preventing the formation of the DMPO-OH adduct. However, in experiments using ethanol as the hydroxyl radical scavenger it was not possible to completely prevent the formation of DMPO-OH. The formation of this additional DMPO-OH in the presence of ethanol does not depend on the concentration of dissolved oxygen, but does depend on the concentration of hydrogen peroxide added to the vanadyl solution. The results suggest that the additional DMPO-OH formed in the presence of ethanol originates from a vanadium (V) intermediate. This intermediate may oxidize DMPO leading to the formation of DMPO-OD which rapidly decomposes forming DMPO-OH.

KEY WORDS: Vanadium, vanadyl, hydrogen peroxide, hydroxyl radicals, ESR, spin trapping.

INTRODUCTION

The oxycation of vanadium (IV), vanadyl (VO^{+2}), has been used for many years as a spin probe for the metal binding sites in proteins.[1,2] Since vanadyl has a single unpaired electron in its lowest nondegenerate d_{xy} orbital,[3] in a magnetic field this electron interacts with the ^{51}V nucleus (99.7 percent abundant) which has a nuclear spin, $I = 7/2$, producing a sharp isotropic eight line ESR spectrum at room temperature. An important property of vanadyl as a spin probe is the susceptibility of the VO^{+2} ESR spectrum to the motion of the cation in solution. For instance, the ESR spectrum of VO^{+2} bound to a large slowly tumbling protein is anisotropic. It resembles the ESR spectrum of immobilized VO^{+2} ions in a polycrystalline state or frozen solution. This difference between the bound and unbound VO^{+2} ESR spectrum has provided important information with regard to metal ion properties in metalloproteins.

In addition to these VO^{+2} spectroscopic properties, some aspects of the VO^{+2} chemistry may also prove to be important in biological studies. It has been suggested for some time that VO^{+2} participates, in the presence of H_2O_2, in a Fenton-like reaction generating hydroxyl radicals ($\cdot OH$).[4] Brooks et al.[4] studied the kinetics of this reaction, however, their emphasis was on the VO^{+2} ESR. Recently, Keller et al.[5] using spin trapping have studied the effects of vanadium on lipid peroxidation in micelles of purified and partially peroxidized fatty acids. In this study it was shown than VO^{+2} was the active vanadium species that initiated conjugated diene formation and in the vanadium-catalyzed decomposition of fatty acid hydroperoxides. Further-

more, it was also implied that following the addition of VO^{+2} and H_2O_2 to a micellar suspension, $\cdot OH$ was involved in the production of conjugated dienes. Keller et $al.$ have also studied the vanadium-stimulated oxidation of NADH.[6]

The purpose of the present study is to address, using spin trapping, some important unanswered questions about the reaction between VO^{+2} and H_2O_2. These questions involve: (1) Is the product of the VO^{+2}/H_2O_2 reaction really $\cdot OH$ or is it possible for other activated oxygen species to be produced; (2) Are other oxidizing species produced which may possible mediate free radical mechanisms; (3) If $\cdot OH$ is produced, how effective is VO^{+2} in comparison with ferrous ions to produce these in a Fenton-like reaction?

MATERIALS AND METHODS

Vanadyl Sulfate and Ferrous Ammonium Sulfate were obtained from Fisher Scientific Co. (Fair Lawn, NJ). The concentration of vanadyl solutions was determined spectrophotometrically ($\lambda = 750\,nm$, $\varepsilon = 18\,M^{-1}cm^{-1}$).[7] Ferrous Ammonium Sulfate was titrated with a standard potassium permanganate solution to determine the ferrous ion concentration.[8] Hydrogen Peroxide was obtained from Sigma (St. Louis, MO) and its concentration was also determined by titration with potassium permanganate.[8] The spin trap 5,5-dimethyl-1-pyrroline-N-oxide (DMPO) was purchased from Aldrich (Milwaukee, WI) and was purified following the method described by Buettner and Oberley.[9] This method consists of successively treating the DMPO with activated charcoal until all free radical impurities disappear as verified by ESR. The concentration of DMPO was measured spectrophotometrically ($\lambda = 227\,nm$, $\varepsilon = 8 \times 10^3\,M^{-1}cm^{-1}$).[10]

To eliminate any trace metals, all glassware was kept permanently soaking in a 1:1 mixture of concentrated sulfuric and nitric acids. Immediately prior to use, the glassware was rinsed with metal free water and dried under a stream of nitrogen. The metal-free water was prepared by further treating water obtained from a Sybron/ Barnstead NANO pure system with a 0.001 percent dithizone (Sigma) solution in carbon tetrachloride. This treatment is carried out successively in a separating funnel until the green color of the dithizone persists. The water was then boiled to rid it of residual organic material.

Experiments requiring deaerated or oxygen-free conditions were carried out in an apparatus described by Russell et $al.$[11] and Evans.[12] This apparatus consists of a U-tube connected to an ESR quartz flat cell via a ground glass joint. Nitrogen bubbling through the samples was used to remove oxygen from the solutions. The required quantities of hydrogen peroxide mixed with metal-free water was placed in one stem of the U-tube and the DMPO, metal ions and scavengers ethanol or formate (when required) were placed in the other stem. Nitrogen bubbling was carried out for 20 minutes. However, in experiments requiring ethanol as a scavenger, the solutions and pure ethanol were saturated separately with nitrogen by vigorously bubbling prior to placing in the appropriate amounts in the U-tube. After sealing the U-tube, nitrogen was bubbled through the solutions for approximately 3–5 minutes to insure that the ethanol concentration remained fairly constant. Once nitrogen bubbling was completed, solutions were mixed in the U-tube and the ESR spectrum recorded.

Experiments carried out under air-saturated conditions were done by mixing DMPO, metal ions, ethanol or formate (when required) immediately prior to addition

of the appropriate amount of hydrogen peroxide. After addition of the hydrogen peroxide, the samples were rapidly mixed and transferred to an ESR quartz flat cell (60 × 10 × 0.25 mm) and their ESR spectrum recorded.

All ESR spectra were recorded on a Varian E-9 X-band spectrometer at 100 KHz magnetic field modulation. The magnetic field was set at 3350 G, microwave power, 10 mW; modulation amplitude, 0.5 G; and microwave frequency, 9.510 GHz. The hyperfine coupling constants were obtained by computer simulation generating a theoretical ESR spectrum that matches the experimental spectrum.

RESULTS AND DISCUSSION

When hydrogen peroxide is mixed with a vanadyl solution containing the spin trap DMPO, an ESR spectrum consisting of a 1:2:2:1 quartet is obtained. This quartet with hyperfine coupling constants, $a_N = a_H^\beta = 14.9$ G, corresponds to the DMPO-OH spin adduct.[13] In order to verify that the DMPO-OH spin adduct originates from the reaction of hydroxyl radicals with DMPO, two experiments were done using formate and ethanol as ·OH scavengers.[14] Figure 1 shows the results obtained after mixing H_2O_2 (1 mM) with the vanadyl solution (0.1 mM) each containing DMPO (100 mM) and different concentrations of formate. The ESR spectra from these solutions change from the DMPO-OH spectrum (Figure 1A), obtained when the concentration of DMPO is larger than the formate concentration by a factor of ten, to an ESR spectrum consisting of a triplet of doublets (Figure 1C) with hyperfine coupling constants, $a_N = 15.6$ G and $a_H^\beta = 18.7$ G. This ESR spectrum is observed when the concentration of formate is larger than the DMPO concentration by a factor of ten. The hyperfine coupling constants are consistent with those reported for the DMPO-CO₂⁻ spin adduct,[13] which is produced subsequent to the reaction of hydroxyl
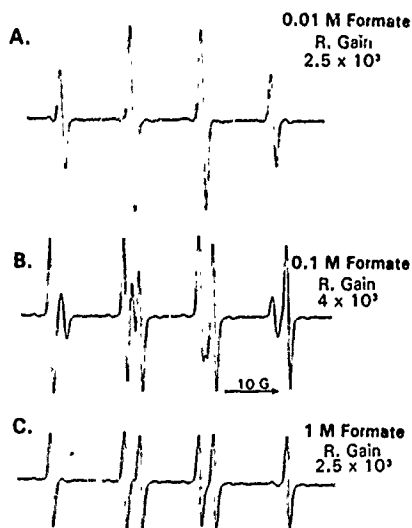
FIGURE 1   ESR spectra of DMPO-OH and DMPO-CO₂⁻ spin adducts obtained in the reaction of VO⁺² with H_2O_2 in the presence of DMPO and varying concentrations of formate.

radicals with formate in the presence of DMPO. Figure 1B shows the ESR spectra of DMPO-OH and DMPO-CO$_2^-$. These spectra are obtained when the formate and DMPO concentration are approximately equal. The results shown in Figure 1 are consistent with DMPO and formate, which react with hydroxyl radicals at similar rates ($k > 10^9 m^{-1} s^{-1}$),[15] competing for hydroxyl radicals in the solution. Therefore, the results in Figure 1 verify that hydroxyl radicals are produced in the reaction between vanadyl and hydrogen peroxide.

Ethanol and DMPO also react with hydroxyl radicals at similar rates. However, the results obtained from experiments in which vanadyl and hydrogen peroxide are mixed in the presence of DMPO and varying concentrations of ethanol (Figure 2) are not consistent with the results obtained in the formate experiments. In the experiments using ethanol as a hydroxyl radical scavenger, the DMPO-OH ESR spectrum persists at high concentrations of ethanol. Figure 2A shows the DMPO-OH ESR spectrum obtained when vanadyl (0.1 mM) is mixed with hydrogen peroxide (1 mM) in the presence of DMPO (100 mM) and ethanol (10 mM). When the concentration of ethanol and DMPO are similar two spin adduct ESR spectra are obtained (Figure 2B). One corresponds to the DMPO-OH and the other consists of a triplet of doublets with hyperfine coupling constants, $a_N = 15.8 G$ and $a_H^\beta = 22.8 G$. These parameters are consistent with the reported hyperfine coupling constants for the DMPO spin adduct obtained in the reaction between ethanol and hydroxyl radicals.[13] Figure 2C shows the ESR spectrum obtained following the reaction of vanadyl with hydrogen peroxide in the presence of 1.7 M ethanol. Although this concentration of ethanol is larger than the DMPO concentration by approximately a factor of 20, the DMPO-OH ESR signal persists. The formation of DMPO-OH at high concentrations of ethanol relative to DMPO occurs in air-saturated and nitrogen-saturated
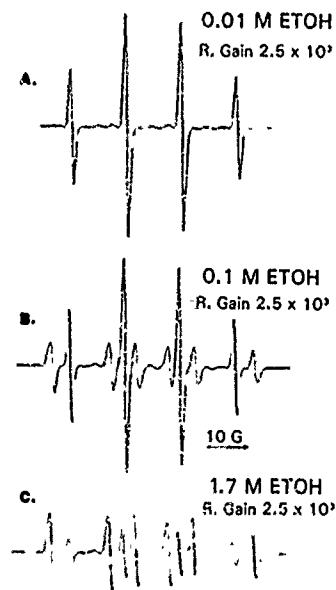

FIGURE 2 ESR spectra of DMPO-OH and DMPO-CH(OH)CH$_3$ spin adducts obtained in the reaction of VO^{+2} with H$_2$O$_2$ in the presence of DMPO and various concentrations of ethanol.
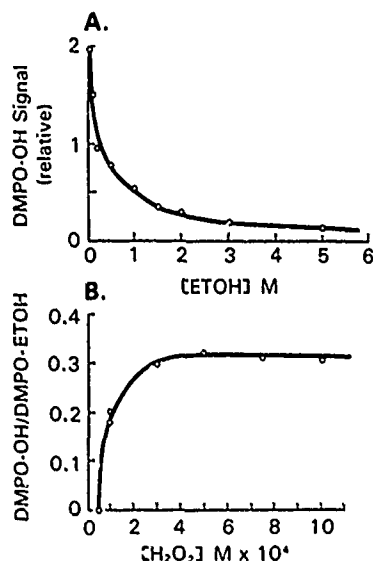
FIGURE 3 (A) DMPO-OH ESR signal intensity as a functions of increasing concentration of ethanol in the VO^{+2}/H$_2$O$_2$ reaction. (B) DMPO-OH ESR signal intensity as a function of hydrogen peroxide concentration obtained during the VO^{+2}/H$_2$O$_2$ reaction in the presence of a constant concentration of ethanol.

solutions, therefore, its production does not depend on the dissolved oxygen in the solution. Furthermore, although this property of the vanadyl/H$_2$O$_2$ reaction is not immediately obvious when formate is used as a hydroxyl radical scavenger, it does occur when other reagents less polar than water such as dimethylsulfoxide are added to the vanadyl solution. It is possible that this property of the vanadyl/H$_2$O$_2$ reaction is due to solvent effects, occurring in solvents less polar than water. The results in Figure 2 suggest that when the reaction of vanadyl with hydrogen peroxide is carried out in the presence of ethanol, another species capable of forming DMPO-OH is generated in addition to hydroxyl radicals.

Since the formation of this additional DMPO-OH is not dependent on the dissolved oxygen, it is important to determine whether or not its production, prior to proposing possible mechanisms, depends on the concentration of hydrogen peroxide. Figure 3 shows the results of these experiments. Figure 3A shows the DMPO-OH ESR signal intensity as a function of ethanol concentration following the mixing of hydrogen peroxide (1 mM) with a vanadyl (0.1 mM) solution containing DMPO (100 mM). It should be noted that at ethanol concentrations above 1 M, virtually no DMPO-OH should be observed if only hydroxyl radicals were responsible for the DMPO-OH signal in the absence of ethanol. Instead, at these concentrations of ethanol relative to DMPO only the triplet of doublets described in Figure 2 should be observed. Figure 3B shows the results obtained after varying the concentration of hydrogen peroxide mixed with several vanadyl solutions (1 mM) containing DMPO (100 mM) and a constant concentration of ethanol (1.7 M). Because the ESR signal intensity of the DMPO-OH and the CH$_3$-ĊHOH adduct of DMPO simultaneously decrease as the hydrogen peroxide concentration is decreased, the ratio of both spin adducts is plotted against the hydrogen peroxide concentration. The results in Figure

3B indicate that the DMPO-OH originating from sources other than the addition of hydroxyl radicals to DMPO, formed directly in the vanadyl/H_2O_2 reaction, depends on the concentration of hydrogen peroxide in the solution. At a concentration of hydrogen peroxide larger than the vanadyl concentration by a factor of three, the formation of additional DMPO-OH remaind constant. At lower concentrations of hydrogen peroxide relative to vanadyl, the additional DMPO-OH decreases until disappearing. This occurs at a concentration of hydrogen peroxide five times lower than the vanadyl concentration.

Other than the reaction of directly formed hydroxyl radicals with DMPO, several pathways leading to the formation of DMPO-OH are possible. One alternative is that superoxide radicals are produced via a mechanism that does not involve dissolved oxygen. It is known that in an aqueous environment the superoxide spin adduct of DMPO, DMPO-O_2^-, rapidly decomposes forming DMPO-OH.[16] It is conceivable that superoxide could be produced via the following reaction:

$$\cdot OH + H_2O_2 \rightarrow H_2O + HO_2^-$$ (1)

However, the rate of this reaction ($k = 2.6 \times 10^7 M^{-1}s^{-1}$) is relatively slow compared to the rate of the reaction between hydroxyl radicals and DMPO.[15] Therefore, for reaction (1) to occur in the experiments described, a concentration of hydrogen peroxide one hundredfold larger than the DMPO concentration would be required.

Another alternative that may cause the formation of DMPO-OH in the vanadyl/ H_2O_2 reaction in the presence of ethanol could be a reactive vanadium intermediate. Several of these intermediates have been reported previously; however, one that seems possible is the vanadium (V) complex, $OVOO^{+2}$.[4] Although the ESR spectrum of this complex is not observed in the aqueous experiments described in this work, it has been observed when higher initial vanadyl concentrations are used.[4] However, in ethanol or DMSO and with the initial vanadyl concentration used in this work, an eight line ESR spectrum similar to the one reported for $OVOO^{+2}$ in water is observed.

There are two reaction schemes which could possibly explain the formation of DMPO-OH as a product of the reaction between DMPO and $OVOO^{+2}$. The first involves a direct addition of $OVOO^{+2}$ to DMPO followed by the decomposition of the spin adduct as shown in reactions (2) and (3):

$$OVOO^{+2} + DMPO \rightarrow DMPO\text{-}OOVO^{+2}$$ (2)

$$DMPO\text{-}OOVO^{+2} \xrightarrow{H^+} DMPO\text{-}OOH + VO^{2+}$$ (3)
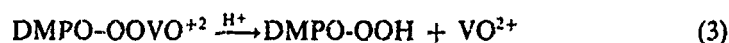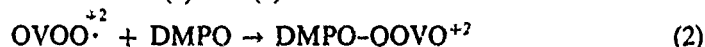
The second scheme shown in reactions (4) through (6) involves the oxidation of DMPO by $OVOO^{+2}$. This reaction could form a $DMPO^+$ intermediate which rapidly adds a hydroxide anion to form DMPO-OH.

$$OVOO^{+2} + DMPO \rightarrow DMPO^+ + VO^{+2} + O_2^-$$ (4)

$$DMPO^+ + OH^- \rightarrow DMPO\text{-}OH$$ (5)

$$DMPO + O_2^- \rightarrow DMPO\text{-}O_2^-$$ (6)
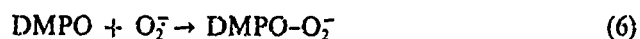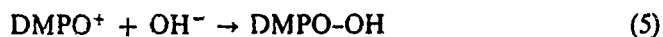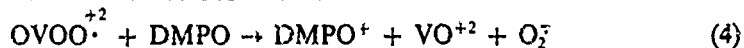
The superoxide spin adduct of DMPO formed in reactions (3) and (6) would rapidly decompose generating DMPO-OH. Since the pH of the reaction mixtures ranged between pH 5 and pH 5.5, due to the instability of vanadyl at pH > 5.5, it would appear the reactions (2) and (3) are favored over reactions (4) through (6). However, at this time it is difficult to differentiate between both reaction schemes because only

the end products, which are the same for both schemes, are observed. A possible explanation for the hydrogen peroxide effect shown in Figure 3B is the following: at lower hydrogen peroxide concentrations relative to DMPO, the hydrogen peroxide is the limiting factor in the reaction and is consumed prior to sufficient formation of OVOO^{+2} for its reaction with DMPO to be observed. However, at high concentrations of hydrogen peroxide relative to DMPO, vanadyl is being generated again (reaction 3 and 4) and continuously reacts with hydrogen peroxide until all the hydrogen peroxide is consumed. Therefore, it is possible that sufficient OVOO^{+2} is produced allowing its effect to be observed. Since in water and at the initial vanadyl concentrations used in the experiments the OVOO^{+2} intermediate is not observed, it is possible that this may be the reason why the results observed in the experiments containing ethanol (Figures 2 and 3) are not similar to those in which formate was used (Figure 1).

At this point, the results have shown that vanadyl in the presence of hydrogen peroxide effectively generates hydroxyl radicals. In addition, the results have suggested that at lower vanadyl concentrations and in environments less polar than water, a vanadium (V) intermediate may be produced which is capable of oxidizing DMPO leading to the formation of DMPO-OH. It is unclear at this time what implications, especially in biological systems, the formation of such an intermediate may have, It is possible that given the appropriate environment, such a vanadium (V) intermediate may act in a similar manner as the intermediate postulated for iron in its reaction with hydrogen peroxide.[17-19]

For biological purposes, it is of interest to determine how vanadyl compares with ferrous ions in its capacity to form hydroxyl radicals in the presence of hydrogen peroxide. Figure 4 shows the results obtained when separate solutions of vanadyl sulfate and ferrous ammonium sulfate of equal concentrations (0.1 mM) are mixed
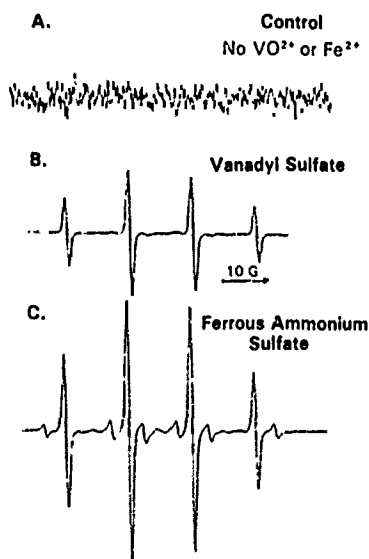

FIGURE 4   DMPO-OH ESR signal obtained in the reactions of vanadyl and ferrous ions with hydrogen peroxide at pH 5-5.5.

with hydrogen peroxide (1 mM) in the presence of DMPO (100 mM). Figure 4A is the control consisting of DMPO (100 mM) mixed with hydrogen peroxide (1 mM) and indicates that no spin adducts are formed. When the metal ions are included in the solutions the results show that the DMPO-OH originating from vanadyl (Figure 4B) is approximately half the DMPO-OH originating from the ferrous ions (Figure 4C). In addition, another DMPO spin adduct is also observed in Figure 4C. This spin adduct consists of a triplet of doublets with hyperfine coupling constants, $a_N = 15.5 G$ and $a_H^\beta = 22.8 G$. These parameters are identical to the hyperfine coupling constants reported by Floyd et al.[20] for the 1-nitrosopyrroline spin adduct of DMPO. Therefore, it is possible that the additional spin adduct observed in Figure 4C corresponds to the interaction of a DMPO radical with DMPO. This triplet of doublets is also observed at higher vanadyl concentrations when reacted with hydrogen peroxide in the presence of DMPO.

Although the experimental results shown in Figure 4 indicate that in the presence of hydrogen peroxide ferrous ions are more efficient than vanadyl in producing hydroxyl radicals, it must be kept in mind that these reactions were carried out using solutions of plain inorganic salts. It remains to be determined if this property is true when these metal ions are chelated by complex biological systems.

Acknowledgement

References

1. Chasteen, N.D. The biochemistry of vanadium. *Structure and Bonding*, **53**, 107–137, (1983).
2. Boyd, D.W. and Kustin, K. Vanadium: A versatile biochemical effector with an elusive biological function. *Adv. Inorg. Biochem.* **6**, 311–365, (1986).
3. Balhausen, C.J. and Gray, H.B. The electronic structure of the vanadyl ion. *Inorg. Chem.* **1**, 111–122, (1962).
4. Brooks, H.B. and Sicilio, F. Electron spin resonance kinetic studies of the oxidation of vanadium (IV) by hydrogen peroxide. *Inorg. Chem.* **10**, 2530–2534, (1971).
5. Keller, R.J., Sharma, R.P., Grover, T.A. and Piette, L.H. Vanadium and lipid peroxidation: Evidence for involvement of vanadyl and hydroxyl radical. *Arch. Biochem. Biophys.*, **265**, 524–533, (1988).
6. Keller, R.J., Coulombe, Jr., R.A., Sharma, R.P., Grover, T.A. and Piette, L.H. Importance of hydroxyl radical in the vanadium-stimulated oxidation of NADH. *Free Rad. Biol. and Med.*, **6**, 15–22, (1989).
7. Fitzgerald, J.J. and Chasteen, N.D. Determination of the vanadium content of protein solutions by electron paramagnetic resonance spectroscopy. *Anal. Biochem.*, **60**, 170–180, (1974).
8. Kolthoff, I.M., Sandell, E.B., Meehan, E.J. and Bruckenstein, S. In Quantitative Chemical Analysis (Fourth Ed.), The Macmillan Co., p. 828 and 834, (1969).
9. Buettner, G.R. and Oberley, L.W. Considerations in spin trapping of superoxide and hydroxyl radicals in aqueous solutions using 5,5-dimethyl-1-pyrroline-1-oxide. *Biochem. Biophys. Res. Commun.*, **83**, 69–74, (1978).
10. Kalyanaraman, B., Felix, C.C. and Sealy, R.C. Photoionization of melanin precursors: An electron spin resonance investigation using the spin trap, 5,5-dimethyl-1-pyrroline-1-oxide (DMPO). *Photochem. Photobiol.*, **36**, 5–12, (1982).
11. Russell, G.A., Janzen, E.G. and Strom, E.T. Electron-transfer process. I. The scope of the reaction between carbanions or nitranions and unsaturated electron acceptors. *J. Am. Chem. Soc.*, **86**, 1807–1814, (1964).
12. Evans, C.A. Spin trapping. *Aldrichim. Acta*, **12**, 23–29, (1979).
13. Buettner, G.R. Spin trapping ESR parameters of spin adducts. *Free Rad. in Biol. and Med.*, **3**, 259–303, (1987).

14. Ononye, A.I., McIntosh, A.R. and Bolton, J.R. Mechanisms of the photochemistry of p-benzoquinone in aqueous solutions. I. Spin trapping and flash photolysis electron spin resonance studies. *J. Phys. Chem.*, **90**, 6266-6270, (1986).

15. Farhataziz and Ross, A.B. Selected specific rates of reactions of transients from water in aqueous solution. III. Hydroxyl radical and perhydroxyl radical and their radical ions. NSRDS-NBS 59. U.S. Govt. Printing Office, Washington, D.C., (1977).

16. Finkelstein, E., Rosen, G.M., Rauckman, E.J. and Paxton, J. Spin trapping of superoxide. *Mol. Pharmacol.*, **16**, 676-685, (1979).

17. Aust, S.D., Morehouse, L.A. and Thomas, C.E. Role of metals in oxygen radical reactions. *J. Free Rad. Biol. Med.*, **1**, 3-25, (1985).

18. Kohler, H. and Jenzer, H. Interaction of lactoperoxidase with hydrogen peroxide. Formation of enzyme intermediates and generation of free radicals. *Free Rad. Biol. Med.*, **6**, 232-339, (1989).

19. Sutton, H.C. and Winterbourn, C.C. On the participation of higher oxidation states of iron and copper in Fenton reactions. *Free Rad. Biol. Med.*, **6**, 53-60, (1989).

20. Floyd, R.A., Soong, L.M., Stuart, M.A. and Reigh, D.L. Spin trapping of free radicals produced from nitrosamine carcinogens. *Photochem. Photobiol.*, **28**, 857-862, (1978).

ARACHIDONIC ACID AND PROSTAGLANDINS ENHANCE POTASSIUM-STIMULATED CALCIUM INFLUX INTO RAT BRAIN SYNAPTOSOMES

S. B. KANDASAMY and W. A. HUNT

Behavioral Sciences Department, Armed Forces Radiobiology Research Institute, Bethesda,
Maryland 20814-5145, U.S.A.

Summary—Exogenous administration of arachidonic acid, prostaglandins $PGF_2\alpha$, PGD_2 and PGE_2 increased potassium-stimulated uptake of calcium in rat brain synaptosomes from the brain of the rat, but had no effect on the basal uptake of calcium. Arachidonic acid-induced uptake of calcium was mediated by its prostaglandin metabolites, because a cylooxygenase inhibitor, indomethacin, inhibited the response. L-Type calcium channel blockers, such as verapamil, diltiazem and nimodipine, blocked both KCl- and prostaglandin-enhanced potassium-stimulated influx of calcium in the brain. These results suggest that prostaglandins act as a calcium ionophore, through L-type voltage-sensitive calcium channels.

The formation of prostaglandins, prostacyclin, thromboxanes or leukotrienes in different cells require arachidonic acid, a naturally occurring *cis*-polyunsaturated fatty acid that is found primarily esterified to membrane lipids in mammalian cells (Samuelson, 1981). The release of arachidonic acid from lipids may be an early step in the mechanism of action of some secretagogues (Samuelson, 1981). Prostaglandins are synthesized in response to various stimuli and are known to modulate numerous physiological functions, including central ones (Chiu and Richardson, 1985; Oliw, Granstrom and Anggard, 1983). Prostaglandins have been demonstrated to be involved in thermoregulation (Milton and Wendlandt, 1970; Ueno, Narumiya, Ogorochi, Nakayama, Ishikawa and Hayaishi, 1982), induction of sleep (Ueno, Ishikawa, Nakayama and Hayaishi, 1982; Ueno, Honda, Inoue and Hayaishi, 1983; Ueno, Osama, Urade and Hayaishi, 1985), nociception (Horiguchi, Ueno, Hyodo and Hayaishi, 1986; Ohkubo, Shibata, Takahashi and Inoki, 1983), anticonvulsive effects (Forestman, Heldt, Knappen and Hertting, 1982), release of neurotransmitters (Higashida, Nakagawa and Miki, 1984; McGee, Simpson, Christain, Mata, Nelson and Nirenberg, 1978) and other actions (Wolfe, 1982; Wolfe and Coceani, 1979). In addition, prostaglandins elevate levels of 3′,5′-cyclic adenosine monophosphate cyclic (cAMP) and cyclic guanosine 3′,5′-monophosphate (cGMP) in neural tissue (Gilman and Nirenberg, 1971; Hamprecht and Schultz, 1973).

Calcium is important in a variety of functions, in both the central nervous system and in peripheral tissues. In neural tissue, the influx of calcium into presynaptic nerve endings initiates events leading to release of neurotransmitter and in heart and in smooth muscle, calcium couples excitation to contraction. The entry of calcium into these tissues appears to be mediated by voltage-sensitive calcium channels (Hagiwara and Byerly, 1981). Several classes of compounds have been shown to interact with these channels. The most important class has been the dihydropyridine calcium antagonists, such as nitrendipine and nimodipine. Drugs from other chemical classes, such as verapamil and diltiazem, also act as calcium antagonists (Schwartz, 1982).

Because arachidonic acid and/or its metabolites may be intracellular effectors of calcium-mediated secretion, the effect of exogenous administration of arachidonic acid and prostaglandins on basal and potassium-stimulated influx of calcium into synaptosomes was studied. In addition, the effect of calcium channel blockers on the uptake of calcium was studied.

METHODS

Materials

Arachidonic acid, prostaglandins $PGF_2\alpha$, PGE_2 and PGD_2, verapamil hydrochloride, diltiazem hydrochloride and indomethacin were purchased from Sigma (St Louis, Missouri) and were dissolved in ethanol. Nimodipine was a gift from Miles Laboratories Inc. (New Haven, Connecticut) and was dissolved in dimethyl sulphoxide (DMSO). Because nimodipine is sensitive to light, experiments were done using amber-colored test tubes. The $^{45}CaCl_2$ was purchased from New England Nuclear.

Preparation of tissue and uptake of calcium

Male Sprague–Dawley rats, weighing 200–300 g (Charles River Breeding Laboratories, Kingston, New York), were used in these experiments. The crude synaptosomal (P_2) fraction was prepared by a modification of the method of Gray and Whittaker, 1962. The final pellet was resuspended in ice-cold incubation medium (NaCl, 136 mM; KCl, 5 mM; $CaCl_2$, 0.12 mM; $MgCl_2$, 1.3 mM; glucose, 10 mM; Tris base 20 mM; pH adjusted to 7.65 with 1.0 M maleic acid), to provide a concentration range of approximately 4–6 mg protein/ml.

For the determination of the uptake of calcium, 0.48 ml of the synaptosomal preparation was pipetted into test tubes and incubated for approximately 14 min at 30°C in a Dubnoff metabolic shaker, in the presence or absence of various concentrations of drugs, as described later. The drugs were added in a 20-μl volume to make final incubation volume of 0.5 ml. For control samples, 20 μl of incubation medium, with various concentrations of ethanol or DMSO, were added. For these experiments, 0.5 ml of depolarizing or nondepolarizing solution containing $^{45}Ca^{2+}$ (3 μCi) was added for 3 sec. The uptake of calcium was terminated by the prompt addition of 5 ml or an ice-cold EGTA stopping solution (NaCl, 136 mM; KCl, 5 mM; $MgCl_2$, 1.3 mM; EGTA [ethylene-glycol-bis-(beta-amino-ethyl ether) *N,N'*-tetraacetic acid], 3 mM; glucose, 10 mM; Tris base, 20 mM; pH adjusted to 7.65 with 1.0 M maleic acid). The composition of the depolarizing solution was the same as that of the incubation medium, except that a portion of the NaCl was isosmotically replaced by KCl, to provide a final concentration of KCl of 65 mM. The nondepolarizing solution had the same composition as the incubation medium, except for the presence of $^{45}Ca^{2+}$. Depolarizing and nondepolarizing solutions, added to drug-exposed synaptosomes, also contained the same concentrations of drug, to maintain the designated molar relationships. Each sample was immediately filtered under vacuum through a Whatman GF/B filter, presoaked with nondepolarizing solution. Each filter was then washed with two 5-ml aliquots of ice-cold incubation medium and placed in a scintillation vial. Radioactivity was determined by liquid scintillation spectrometry.

To calculate the net uptake of $^{45}Ca^{2+}$ into synaptosomes, the uptake in the absence of depolarization (5 mM KCl) was subtracted from the uptake in the presence of depolarization (65 mM KCl). This value is referred to as 'k' (potassium-induced change) and represents net KCl-induced uptake of calcium (Blaustein and Ector, 1975; Leslie, Friedman, Wilcox and Elrod, 1980). Each control and drug experiment was performed using matched synaptosomal preparations from the same batch. The content of protein was determined by the method of Lowry, Rosebrough, Farr and Blaustein, 1951), using bovine

serum albumin as the standard. All data are expressed as the mean $\pm$ SEM of triplicate determinations. Values for the effect of indomethacin or calcium channel antagonists on the enhancement by arachidonic acid, $PGF_2\alpha$, PGD_2 or PGE_2 of the potassium-stimulated uptake of calcium were represented as a percentage of control, i.e. responses to arachidonic acid, $^{\frown}GF_2\alpha$, PGD_2 or PGE_2 in the absence of indomethacin or calcium channel antagonists. Statistical analyses were performed using analysis of variance (ANOVA) (RSI; BBN Software Products Corp., Cambridge, MA), for identifying the main effects, along with subsequent *post hoc* tests, when appropriate. Data were identified as significant if $P < 0.05$.

RESULTS

Prostaglandin $PGF_2\alpha$ (10 nM–10 μM) and arachidonic acid, PGD_2 and PGE_2 (1–30 μM each) increased the entry of potassium-stimulated influx of calcium (Fig. 1) but had no effect on the basal uptake of calcium (data not shown). Arachidonic acid (3 μM)-induced uptake of calcium was inhibited by indomethacin (1–10 μM) (Fig. 2), a cyclooxygenase inhibitor, suggesting that arachidonic acid acted through the formation of prostaglandins. However, indomethacin had no inhibitory effect on the enhancement by $PGF_2\alpha$, PGE_2 aND PGD_2 of the KCl-stimulated influx of calcium (data not shown). Preincubation of the synaptosomes with the voltage-sensitive channel blockers verapamil (5–30 μM), nimodipine (1–10 μM) or diltiazem (50–300 μM), inhibited the potassium-$PGF_2\alpha$- or PGD_2- and PGE_2-enhanced potassium-stimulated influx of calcium (Table 1).
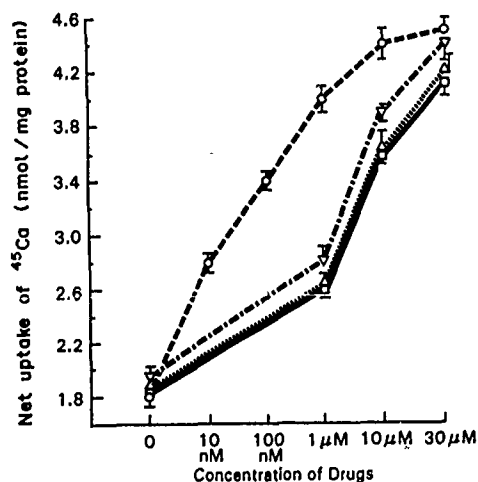

Fig. 1. Effect of arachidonic acid (□), $PGF_2\alpha$ (○), PGD_2 (▽) or PGE_2 (△) on potassium-stimulated uptake of calcium in synaptosomes from the brain of the rat. Points and bars represent mean $\pm$ SEM values from three separate experiments, each using triplicate samples.
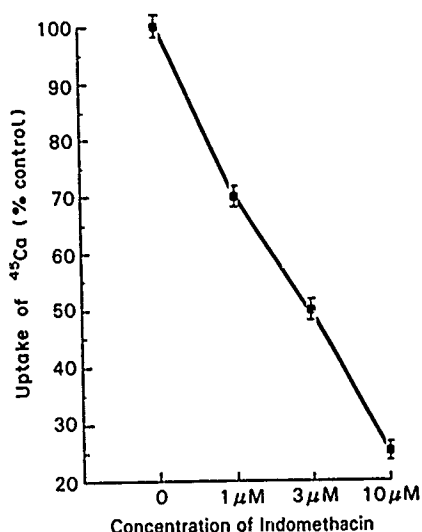
Fig. 2. Effect of indomethacin (■) on arachidonic acid (3 µM)-induced potassium-stimulated uptake of calcium in synaptosomes from the brain of the rat. Values are mean ± SEM of 3 separate experiments, each using triplicate samples, represented as a percentage of control the response, in the absence of indomethacin. Net uptake of calcium evoked by 3 µM arachidonic acid was 2.8 ± 0.05 nmol/mg protein.

DISCUSSION

Synaptosomes provide a useful system for the study of the biochemical mechanisms that mediate stimulation-secretion coupling in neurons. The uptake of $^{45}Ca^{2+}$ into synaptosomes was comparable on an nmol/mg basis to other reports (Leslie, McCormick and Gonzales, 1982; Leslie, Barr and Chandler, 1983). Potassium-induced depolarization of synaptosomes from the brain of the rat stimulates endogenous phospholipase A_2 which, in turn, releases arachidonic acid from the phospholipids (Bradford,

Marinetti and Abood, 1983). The released arachidonic acid may then be metabolized by lipoxygenase or cyclooxygenase to form leukotrienes, hydroxyeicosatetraenoic acids or prostaglandins (Samuelson, 1981).

It is possible that some metabolites of arachidonic acid (lipoxygenase products) act as intracellular second messengers for presynaptic inhibition, while others (cyclooxygenase products) act as first messengers on the postsynaptic cell for stimulation (Piomelli, Shapiro, Feinmark and Schwartz, 1987a).

Pharmacological experiments, performed on the identified Aplysia interneuron L10 (Shapiro, Piomelli and Schwartz, 1987) and on Aplysia sensory cells (Piomelli et al., 1987a; Piomelli, Volterra, Dale, Siegelbaum, Kandel, Schwartz and Belardetti, 1987b), have demonstrated the involvement of lipoxygenase products of arachidonic acid in presynaptic inhibition. In both types of cells, the responses to inhibitory transmitters were mimicked when arachidonic acid was applied (Piomelli et al., 1987a). Likewise, cyclooxygenase products of arachidonic acid are first messengers on the postsynaptic cell for stimulation (Piomelli et al., 1987a) and have been implicated as the biologically active factor(s), because cyclooxygenase inhibitors were shown to inhibit stimulated secretion, while the exogenous administration of one of several metabolites of cyclooxygenase was shown to reproduce the biological response (Whitting and Barritt, 1982). However, many have provided evidence in support of the idea that arachidonic acid itself may be biologically active (Kolesnick, Musacchio, Thaw and Gershengorn, 1984).

Because arachidonic acid and its metabolites have been shown to affect calcium homeostasis in several types of cell (Barritt, 1981), it is possible that secretion, stimulated by arachidonic acid or its

Table 1. Effect of calcium antagonists on the enhancement by $PGF_2\alpha$, PGD_2 or PGE_2 of the potassium chloride-stimulated uptake of calcium or potassium chloride-stimulated uptake of calcium in synaptosomes from the brain of the rat

Concentration of calcium antagonists:	Concentration of prostaglandins and KCl			
	100 nM $PGF_2\alpha$	3 µM PGD_2	3 µM PGE_2	65 mM KCl
Verapamil:				
5 µg	85% ± 0.03	90% ± 0.02	88% ± 0.01	75% ± 0.02*
10 µg	65% ± 0.01*	68% ± 0.02*	70% ± 0.01*	50% ± 0.02*
30 µg	50% ± 0.01*	45% ± 0.02*	50% ± 0.01*	30% ± 0.02*
Nimodipine:				
1 µM	80% ± 0.01*	82% ± 0.02*	80% ± 0.02*	75% ± 0.02*
3 µM	68% ± 0.02*	68% ± 0.01*	66% ± 0.01*	52% ± 0.02*
10 µM	40% ± 0.01*	40% ± 0.01*	35% ± 0.02*	25% ± 0.01*
Diltiazem:				
50 µM	85% ± 0.01	90% ± 0.02	88% ± 0.02	72% ± 0.02*
100 µM	65% ± 0.02*	68% ± 0.02*	67% ± 0.01*	50% ± 0.02*
300 µM	48% ± 0.02*	47% ± 0.02*	50% ± 0.02*	35% ± 0.02*

Values are mean ± SEM of three separate experiments, each using triplicate samples, represented as a percentage of control ($PGF_2\alpha$, PGD_2, PGE_2 or KCl) response in the absence of calcium antagonists. Net uptake of calcium by 100 nM $PGF_2\alpha$ was 2.7 ± 0.03 nmol/mg; 3 µg PGD_2 was 2.7 ± 0.05 nmol/mg; 3 µM PGE_2 was 2.6 ± 0.03 nmol/mg and 65 mM² KCi was 1.9 ± 0.03 nmol/mg protein.
*Significantly different from control ($PGF_2\alpha$, PGD_2, PGE_2 or KCl) value, without calcium antagonists: $P < 0.05$.

metabolites, is mediated by calcium. Inhibition of arachidonic acid-induced influx of calcium by indomethacin in this study demonstrated that arachidonic acid acts through its cyclooxygenase metabolites, prostaglandins, in stimulating the influx of calcium, supporting the results of most previous studies. The failure of indomethacin to inhibit prostaglandin-induced influx of calcium suggests that it interferes only with the synthesis of prostaglandins.

The prostaglandins $PGF_2\alpha$, PGE_2 and PGD_2 are the major ones produced (Abdel-Halim, Hamberg, Sjoquist and Anggard, 1977; Miwa, Sugino, Ueno and Hayaishi, 1988; Narumiya, Orgorochi, Nakao and Hayaishi, 1982; Sun, Chapman and McGuire, 1977) in the CNS and their possible functions in the CNS have been reviewed (Wolfe, 1982; Wolfe and Coceani, 1979). However, it is not known whether prostaglandins in the brain are involved in intracellular calcium homeostasis. In this study, $PGF_2\alpha$, PGD_2 and PGE_2 did not enhance the basal influx of calcium, which contradicts the results in neuroblastoma of the mouse and glioma hybrid NG108-15 cells in the rat, where prostaglandins also induce the influx of calcium (Miwa et al., 1988). However, in the present study, these prostaglandins only enhanced the potassium-stimulated influx of calcium indicating that prostaglandins cannot act directly to promote the influx of calcium. At the present time, it cannot be explained why prostaglandins have no effect on the basal levels of uptake of calcium, however, some suggest that it is due to the inhibition evoked by the released arachidonic acid, by depolarization (Lazarewicz, Leu, Sun and Sun, 1983; Piomelli et al., 1987a).

Although the calcium channel antagonists nimodipine, verapamil and diltiazem represent a chemically heterogeneous group of agents (Schwartz, 1982), they act through a common locus: the voltage-sensitive calcium channel. Several types of calcium channels exist and can be distinguish both physiologically and pharmacologically. The calcium channel blockers exert their actions at the L-class of channel, which is characterized by large conductances, of long duration. Radioligand binding and chemical studies have demonstrated that nimodipine, verapamil and diltiazem interact at discrete sites, associated with a major protein of the calcium channel (Triggle and Janis, 1984; Triggle and Janis, 1987). This protein, the $\alpha1$ subunit, with a molecular weight of 170–195 kdaltons, is one of several components of the L-type calcium channel (Catterall, 1988).

Calcium channel blockers, used in this study, blocked the potassium-stimulataed influx of calcium and the prostaglandin-enhanced, potassium-stimulated influx of calcium, suggesting that, in the brain, prostaglandins and potassium may activate L-type voltage-sensitive calcium channels. These results support the finding that nicardipine, another dihydropyridine calcium channel blocker, suppressed the uptake of calcium induced by $PGF_2\alpha$ (Koyama,

Kitayama, Dohi and Tsujimoto, 1988) in a primary culture of bovine adrenal chromaffin cells.

In summary, these results indicate that arachidonic acid induces the uptake of calcium in the brain, an effect that is mediated through the formation of prostaglandins and that the potassium-stimulated influx of calcium and prostaglandin-enhanced, potassium-stimulated influx of calcium may be mediated through the L-type voltage-sensitive calcium channels.

REFERENCES

Abdel-Halim M. S., Hamberg M., Sjoquist B. and Anggard E. (1977) Identification of prostaglandin D_2 as major prostaglandin in homogenates of rat brain. *Prostaglandins* **14:** 633–643.

Barritt G. J. (1981) A proposal for the mechanism by which α-adrenergic agonists, vasopressin, antiotensin and cyclic AMP induce calcium release from intracellular stores in the liver cell: a possible role for metabolites of arachidonic acid. *Cell Calcium* **2:** 53–63.

Blaustein M. P. and Ector S. (1975) Barbiturate inhibition of calcium uptake by depolarized nerve terminals *in vitro*. *Molec. Pharmac.* **11:** 369–378.

Bradford P. G., Marinetti G. V. and Abood L. G. (1983) Stimulation of phospholipase A_2 and secretion of catecholamines from brain synaptosomes by potassium and A23187. *J. Neurochem.* **41:** 1684–1693.

Catterall W. A. (1988) Structure and function of voltage-sensitive ion channels. *Science* **242:** 50–62.

Chiu E K. Y. and Richardson J. S. (1985) Behavioral and neurochemical aspects of prostaglandins in brain function. *Gen. Pharmac.* **16:** 163–175.

Forestmann U., Heldt R., Knappen F. and Hertting G. (1982) Potential anticonvulsive properties of endogenous prostaglandins formed in mouse brain. *Brain Res.* **240:** 303–310.

Gilman A. G. and Nirenberg M. (1971) Regulation of adenosine $3',5'$-cyclic monophosphate metabolism in cultured neuroblastoma cells. *Nature* **234:** 356–358.

Gray E. G. and Whittaker V. P. (1962) The isolation of nerve endings from brain: an electron-microscopic study of cell fragments derived by homogenization and centrifugation. *J. Anat.* **96:** 79–87.

Hagiwara S. and Byerly L. (1981) Calcium channel. *Ann. Rev. Neurosci.* **4:** 69–125.

Hamprecht B. and Schultz J. (1973) Stimulation by prostaglandin E_1 of adenosine $3',5'$-cyclic monophosphate formation in neuroblastoma cells in the presence of phosphodiesterase inhibitors. *FEBS Lett.* **34:** 85–89.

Higashida H., Nakagawa Y. and Miki N. (1984) Facilitation of synaptic transmission by prostaglandin D_2 at synapes between NG108-15 hybrid and muscle cells. *Brain Res.* **295:** 113–119.

Horiguchi S., Ueno R., Hyodo M. and Hayaishi O. (1986) Alterations in nociception after intracisternal administration of prostaglandin D_2, E_2 or $F_2\alpha$ to conscious mice. *Eur. J. Pharmac.* **122:** 173–179.

Kolesnick R. N., Musacchio I., Thaw C. and Gershengorn M. C. (1984) Arachidonic acid mobilizes calcium and stimulates prolactin secretion from GH3 cells. *Am. J. Physiol.* **246:** E458–E462.

Koyama Y., Kitayama S., Dohi T. and Tsujimoto A. (1988) Evidence that prostaglandins activate calcium channels to enhance basal and stimulation-evoked catecholamine release from bovine adrenal chromaffin cells in culture. *Biochem. Pharmac.* **37:** 1725–1730.

Lazarewicz J. W., Leu V., Sun G. Y. and Sun A. Y. (1983) Arachidonic acid release from K^+-evoked depolarization of brain synaptosomes. *Neurochem. Int.* **5:** 471–478.

Leslie S. W., Barr E. and Chandler L. J. (1983) Comparison of voltage-dependent $^{45}Ca^{2+}$ uptake rates by synaptosomes isolated from rat brain regions. *J. Neurochem.* **41:** 1602–1605.

Leslie S. W., Friedman M. B., Wilcox R. E. and Elrod S. Y. (1980) Acute and chronic effects of barbiturates on depolarization-induced calcium influx into rat synaptosomes. *Brain Res.* **185:** 409–417.

Leslie S. W., McCormick J. and Gonzales R. (1982) Lack of morphine effect on potassium-stimulated calcium uptake by whole brain synaptosomes. *Biochem. Pharmac.* **31:** 2697–2698.

Lowry O. H., Rosenbrough N. J., Farr A. L. and Blaustein M. P. (1951) Protein measurement with the Folin phenol reagent. *J. biol. Chem.* **193:** 265–275.

McGee R., Simpson P., Christain C., Mata M., Nelson P. and Nirenberg M. (1978) Regulation of acetylcholine release from neuroblastoma x glioma hybrid cells. *Proc. natn. Acad. Sci. U.S.A.* **75:** 1314–1318.

Milton A. S. and Wendlandt S. (1970) A possible role for prostaglandin E_1 as a modulator for temperature regulation in the central nervous system of cat. *J. Physiol., Lond.* **207:** 76–77.

Miwa N., Sugino H., Ueno R. and Hayaishi O. (1988) Prostaglandin induces Ca^{2+} influx and cyclic GMP formation in mouse neuroblastoma x rat glioma hybrid NG108-15 cells in culture. *J. Neurochem.* **50:** 1418–1424.

Narumiya S., Orgorochi T., Nakao K. and Hayaishi O. (1982) Prostaglandin D_2 in rat brain, spinal cord, and pituitary: basal level and regional distribution. *Life Sci.* **31:** 2093–2103.

Ohkubo T., Shibata M., Takahashi H. and Inoki R. (1983) Effect of prostglandin D_2 on pain and inflammation. *Jap. J. Pharmac.* **33:** 264–266.

Oliw E., Granstrom E. and Anggard E. (1983) The prostaglandins and essential fatty acid. In: *Prostaglandins and Related Substances* (Pace-Asciak C. and Granstom E., Eds), pp. 1–44. Elsvier, Amsterdam.

Piomelli D., Shapiro E., Feinmark S. J. and Schwartz J. H. (1987a) Metabolites of arachidonic acid in the nervous system of aplysia: possible mediators of synaptic modulation. *J. Neurosci.* **7:** 3675–3686.

Piomelli D., Volterra A., Dale N., Siegelbaum S. A., Kandel E. R., Schwartz J. H. and Belardetti F. (1987b) Lipoxygenase metabolites of arachidonic acid as second messengers for presynaptic inhibition of aplysia sonsory cells. *Nature* **328:** 38–43.

Samuelson B. (1981) Prostaglandins, thromboxanes and leukotrienes: formation and biological roles. *Harvey Lect.* **75:** 1–40.

Schwartz A. (Editor) (1982) Symposium on cardiovascular disease and calcium antagonists. *Am. J. Cardiol.* **49:** 497.

Shapiro E. D., Piomelli D. and Schwartz J. H. (1987) Evidence that arachidonic acid cascade generates second messengers that mediate presynaptic inhibition in an identified cell circuit in aplysia. *Soc. Neurosci. Abstr.* **13:** 597.

Sun F. F., Chapman J. P. and McGuire J. (1977) Metabolism of prostaglandin endoperoxide in animal tissues. *Prostaglandins* **14:** 1055–1074.

Triggle D. J. and Janis R. A. (1984) Calcium channel antagonists: new perspectives from the radioligand binding assay. In: *Modern Methods in Pharmacology* (Liss A. R., Ed.), pp. 1–28. New York.

Triggle D. J. and Janis R. A. (1987) Calcium channel ligands. *Ann. Rev. Toxic.* **27:** 347–369.

Ueno R., Honda K., Inoue S. and Hayaishi O. (1983) Prostaglandin D_2, a cerebral sleep-inducing substance in rats. *Proc. natn. Acad. Sci. U.S.A.* **80:** 1735–1737.

Ueno R., Ishikawa Y., Nakayama T. and Hayaishi O. (1982) Prostaglandin D_2 induces sleep when microinjected into preoptic area of conscious rats. *Biochem. biophys. Res. Commun.* **109:** 576–582.

Ueno R., Narumiya S., Ogorochi T., Nakayama T., Ishikawa Y. and Hayaishi O. (1982) Role of prostaglandin D_2 in the hypothermia of rats caused by bacterial lipopolysaccharide. *Proc. natn. Acad. Sci. U.S.A.* **79:** 6093–6097.

Ueno R., Osama H., Urade Y. and Hayaishi O. (1985) Changes of enzymes involved in prostaglandin metabolism and prostaglandin binding proteins in rat brain during development and aging. *J. Neurochem.* **45:** 483–489.

Whitting J. A. and Barritt G. J. (1982) On the mechanism by which hormones induce the release of Ca^{2+} from mitochondria in the liver cell. *Biochem. J.* **206:** 121–129.

Wolfe L. S. (1982) Eicosnoids: prostaglandins, thromboxanes, leukotrienes, and other derivatives of carbon-20 unsaturated fatty acid. *J. Neurochem.* **38:** 1–14.

Wolfe L. S. and Coceani F. (1979) The role of prostaglandins in the central nervous system. *Ann. Rev. Physiol.* **41:** 669–684.

Emesis and Defecations Induced by the 5-Hydroxytryptamine (5-HT$_3$) Receptor Antagonist Zacopride in the Ferret[1]

GREGORY L. KING

Department of Physiology, Armed Forces Radiobiology Research Institute, Bethesda, Maryland

Accepted for publication February 16, 1990

ABSTRACT

Three antiemetic compounds (zacopride, batanopride, granisetron [BRL43694]) were evaluated for the production of gastrointestinal side effects in the conscious ferret after i.v. or p.o. administration. Zacopride evoked multiple emetic and defecatory responses at clinically relevant doses (0.003–0.3 mg/kg) and in a dose-dependent manner. The oral route was the more potent one for eliciting emesis (ED$_{50}$ 0.033 mg/kg). At 0.3 mg/kg p.o., zacopride reliably evoked an 80 to 100% incidence of emesis and a 40 to 80% incidence of defecation. In contrast, batanopride and BRL43694 i.v. evoked a small (10%) incidence of these side effects, but only at 0.1 to 10 mg/kg doses. When given p.o. (0.00003–10 mg/kg), these latter compounds never evoked emesis and significantly reduced (P < .05) the incidence of defecation below that of vehicle. Responses to zacopride (0.3 mg/kg p.o.) were challenged by i.p. pretreatment with the 5-hydroxytryptamine receptor agonist 2-methyl serotonin, the 5-hydroxytryptamine receptor antagonist BRL43694, the quaternary atropine derivative glycopyrrolate, the dopamine receptor antagonist domperidone or selective abdominal vagotomies. All compounds and either bilateral or dorsal vagotomy significantly reduced the incidence of emesis, but did not abolish it. Latency to first emesis was delayed by BRL43694, domperidone or dorsal vagotomy. The data suggest that the emetic response to p.o. zacopride is mediated in part by 5-hydroxytryptamine receptors residing on either enteric neurons or vagal afferents. However, the underlying pharmacology of the response may also include activation of cholinergic and dopaminergic pathways.

Several substituted benzamides and 5-hydroxytryptamine (5-HT$_3$) receptor antagonists are effective antiemetics for radiation- and cytotoxin-induced emesis in many vomiting species (Miner *et al.*, 1987; Bermudez *et al.*, 1988; Dubois *et al.*, 1988; Gylys *et al.*, 1988), including humans (Gralla *et al.*, 1981; Cunningham *et al.*, 1987; Priestman *et al.*, 1988; Kris *et al.*, 1988). As part of their pharmacological action, some of the substituted benzamides also promote gastric motility (Schulze-Delrieu, 1979; Alphin *et al.*, 1986; Cooper *et al.*, 1988). Although the gastric stimulant properties exhibited by some of these compounds can benefit the patient by reinstating normal peristalsis, they may also increase the incidence of diarrhea (Meyer *et al.*, 1984; Kris *et al.*, 1985). The incidence of such unwanted side effects has, in some cases, prompted development of 5-HT$_3$ receptor antagonist antiemetics with limited gastric stimulant properties (Fake *et al.*, 1987).

Zacopride (4-amino-N-[1-azabicyclo(2.2.2)oct-3-yl]-5-chloro-2-methyoxybenzamide[E]-2-butenedioate), a substituted benzamide and 5-HT$_3$ receptor antagonist (Smith *et al.*, 1988b), is a potent antiemetic for radiation- or cytotoxin-induced emesis in dogs, cats, non-human primates, and ferrets (Costall *et al.*, 1987; Cohen *et al.*, 1989; Dubois *et al.*, 1988; Smith *et al.*, 1988a). In the dog, zacopride has been shown to promote gastric motility (Alphin *et al.*, 1986). Recently we observed in the ferret that zacopride, when given i.p. at antiemetic doses, also evoked brief episodes of retching, emesis and defecation during the 20-min period before irradiation (King *et al.*, 1988). Because the emetic phenomenon seemed paradoxical for an antiemetic compound, the studies reported here were initiated to: 1) explore further the dose-response properties of zacopride-induced emesis and defecations; 2) determine whether and to what degree the occurrence of these responses depended on route of administration; and 3) compare the incidence of these side effects to zacopride with their incidence in response to other compounds with somewhat similar antiemetic and pharmacological properties, *i.e.*, granisetron [BRL43694; Endo-N-[9-methyl-9-azabicyclo-(3,3,1)-non-3-yl]-1-methyl-indazole-3-carboxamide; Bermudez *et al.*, 1988] and batanopride (BMY25801; 4-amino-5-chloro-N-[2-(diethylamino)ethyl]2-[1-methyl-2-oxopropoxy]

ABBREVIATIONS: 5-HT, 5-hydroxytryptamine (serotonin); 2-CH$_3$-5-HT, 2-methyl serotonin; BMY25801, batanopride; BRL43694, granisetron; GI,

benzamide HCl; Gylys et al., 1988). In addition, emesis to oral zacopride was challenged with anticholinergic, antidopaminergic, or 5-HT$_3$ receptor-specific ligands, and selective peripheral nerve lesions to determine the underlying receptor specificity and the peripheral anatomical basis for that response.

Methods

Subjects. Experiments were performed on adult male, fitch, castrated and descented ferrets (1-1.5 kg) obtained from Marshall Farms (North Rose, NY). All animals were quarantined upon arrival and screened for evidence of disease prior to release from quarantine. Animals were housed in stainless-steel modified rabbit or cat cages and provided commercial ferret chow and water ad libitum. The animal quarters were maintained at 15-21°C, 45 to 55% humidity, and 12-hr light/12-hr dark photocycle.

Catheter implantation. Ferrets with indwelling jugular catheters for i.v. administration of compounds underwent the behavioral adaptation and surgical procedures described by Jackson et al. (1988). Briefly, the animals were first adapted to wearing a nylon jacket connected to a stainless-steel cable, which in turn was attached to a brass swivel at the cage top. After habituation to this tether-harness system, each animal received a surgically implanted (under aseptic conditions) catheter in its right jugular vein. The catheter exited the animal between the scapulae and fed through the cable to the swivel where it was capped. The catheter was flushed daily with 0.5 ml of 0.1% heparinized sodium chloride (NaCl, 0.9%). The drug studies began 1 week after the surgical procedure. Animals on tether were individually caged.

Dose dependence and route of administration studies. Eight to 11 individual animals were used to test each dose of each drug administered by any single route. Each animal was weighed weekly and then randomly received, at ≥ 48-hr intervals, a single i.v. or p.o. dose (range of values in parentheses) of one of the following compounds: zacopride (0.00003-0.03 mg/kg i.v., 0.001-3 mg/kg p.o.), BMY25801 (0.003-10 mg/kg i.v., p.o.), BRL43694 (0.003-10 mg/kg i.v.; 0.003-3 mg/kg p.o.) or 2-methyl-serotonin (2-CH$_3$ 5-HT, 0.003-3 mg/kg i.v., p.o.). Vehicle was 0.9% NaCl for i.v., 5% dextrose and H$_2$O for p.o. All i.v. injections were given as a bolus in a volume of less than 1 ml; p.o. volume varied between 1 ml and 3 ml; p.o. administration was with a syringe so that the animal was required to swallow the solution.

Pharmacological blockade of emesis and defecation to p.o. zacopride. In order to determine whether and to what degree the emetic response to p.o. zacopride reflected action at 5-HT$_3$ or other receptors, the following compounds were given as pretreatment (i.p.) 20 min prior to p.o. zacopride (0.3 mg/kg).

1. The 5-HT$_3$ receptor antagonist BRL43694 (Sanger and Nelson, 1989) was given at a dose equipotent to that of zacopride (0.3 mg/kg). BRL43694 and zacopride show similar inhibition constant values for binding to homogenates of entorhinal cortex (1.98 nM for zacopride, 2.72 nM for BRL43694; Barnes et al., 1988a).

2. The 5-HT$_3$ receptor agonist 2-CH$_3$ 5-HT was given at doses (1.2 mg/kg or 3 mg/kg) that more closely approximate the difference between the inhibition constant values for it and zacopride (1128 nM for 2-CH$_3$ 5-HT; Barnes et al., 1988a). 2-CH$_3$ 5-HT does not cross the blood-brain barrier.

3. The potent quaternary atropine derivative glycopyrrolate (Robanul®) was given at a dose (0.1 mg/kg) fourfold greater than that which abolishes intestinal contractions in the conscious dog for 20 min (Franko et al., 1962). Glycopyrrolate does not cross the blood-brain barrier and acts primarily on GI function.

4. The D$_2$-dopamine receptor antagonist, domperidone, was given at a dose (1 mg/kg) that may ameliorate radiation-induced emesis in the dog (Dubois et al., 1984; Cordts et al., 1987). Domperidone does not readily cross the blood-brain barrier and has a high affinity for GI tissue (see Brogden et al., 1982).

For these experiments three different groups (A, B and C) of 10 animals were used. Each animal served as its own control. That is, 48

hr prio to challenge with a compound selected from the list just shown, each animal received vehicle (i.p.) as pretreatment, followed 20 min later by zacopride. These data were used to establish both the baseline incidence of emesis/defecation to zacopride and the control values for emetic and defecatory parameters. All animals were retested for their emetic response to p.o. zacopride with vehicle as pretreatment at the conclusion of the experiments.

For group A the emetic response to zacopride was first challenged with BRL43694. After a 48 hr interval, responders to zacopride (vomiting animals) were challenged with glycopyrrolate. Nonresponders (nonvomiting animals) were retested with vehicle pretreatment in order to re-establish that a response to zacopride would occur. After another 48 hr interval, these latter animals were then challenged with glycopyrrolate. For group B the treatment protocols were identical, except that animals were first tested with the lesser dose of 2-CH$_3$ 5-HT, then the greater. For group C only a single dose of domperidone was tested.

Vagotomy studies. Four groups of abdominally vagotomized animals were used in this series of experiments. bilateral ($n = 20$), ventral ($n = 8$), dorsal ($n = 8$) and sham (laparotomy only, $n = 9$). The methods for vagotomy are described in King and Landauer (1990). Each animal was tested for an emetic response to p.o. zacopride (0.3 mg/kg) 48 to 72 hr prevagotomy and 2 to 41 days postvagotomy. The average number of days postvagotomy on which each group was tested was 15 for bilateral, 15 for ventral, 18 for dorsal and 36 for sham.

Data collection and statistical analysis. Individual animals were observed for 30 min following: 1) i.v. and p.o. drug administration to evaluate dose-response effects, and 2) p.o. zacopride administration in control conditions, e.g., with vehicle pretreatment or prevagotomy. The observation period was 1 hr after challenge of response to p.o. zacopride with receptor ligands or vagotomy. The observer recorded the frequency of, and latency to, all expulsions, retches and defecations. Episodes of emesis and retching separated by ≥ 4 min were considered single events. The following parameters were analyzed from all recorded data: 1) latency to first emesis or retch; 2) number of emetic or retching *episodes*; 3) number of expulsions and/or retches; and 4) latency to and number of defecations (including attempts to defecate). Parameters 1 to 3 can be individually altered by vagotomy and/or 5-HT$_3$ receptor antagonist treatment (Andrews and Hawthorn, 1987; Hawthorn et al., 1988; Andrews, et al., 1990). All parameters were tabulated as mean ± S.E. for vomiting and retching animals in each group. For graphic representation in the dose-response curves, vomiting and retching-only animals were pooled. Data obtained from the dose-response curves were tested for statistical significance by chi-square analysis of proportions using a contingency table. The ED$_{50}$ value for emesis to oral zacopride was determined by log-probit analysis. Data obtained from the pharmacologic pretreatments and nerve lesions were compared with the test for significance of difference between two proportions and the Student's t test (Bruning and Kintz, 1977). Statistical significance was assumed when $P < .05$.

Drugs used. All drugs were prepared weekly (except 2-CH$_3$ 5-HT and domperidone, which were prepared daily) and refrigerated. For p.o. administration, the compounds were dissolved in a 5% dextrose and water solution, for i.v. or i.p. administration, a 0.9% NaCl solution. Domperidone was prepared and injected as a suspension made from a 2% carboxymethyl cellulose vehicle in NaCl. 2-CH$_3$ 5-HT was obtained from Research Biochem., Inc. (Natick, MA); both zacopride and glycopyrrolate are compounds from the research of A. H. Robins (Richmond, VA); BMY25801, Bristol-Myers (Wallingford, CT); and BRL43694, Beecham Pharmaceuticals (Harlow, Essex, UK). Domperidone was a gift from Janssen Pharmaceutica, Inc. (Piscataway, NJ). Doses of BRL43694 refer to the base; all others to the salt.

Results

Emesis and defecations to antiemetic compounds. Figure 1 illustrates that, of the three antiemetics tested for an emetic response by either the i.v. or p.o. administration route, only zacopride produced any significant incidence of emesis.
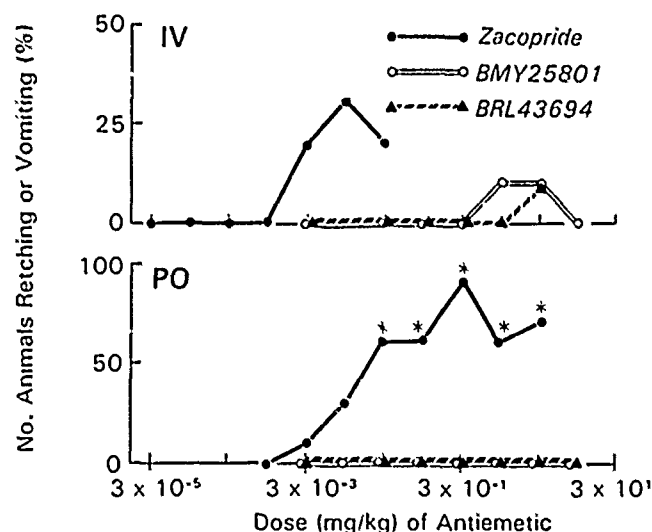
Fig. 1. Dose-dependent incidence of emetic or retching responses to zacopride contrasted with BRL43694 and BMY25801 as a function of administration route. Ferrets observed for 30-min period after drug administration. Top: response to i.v. (bolus) administration. All compounds were dissolved in NaCl. Each data point for BMY25801 and BRL43694 represents tests in eight to 10 individual animals, zacopride, 10 to 11. No emetic/retching responses to vehicle were observed ($n = 30$). Bottom: response to p.o. administration. All compounds were dissolved in 5% dextrose/H_2O. Each point represents tests in 10 to 14 animals. Statistical significance (*$P < .05$) for individual data points was seen at all doses of zacopride greater than 0.030 mg/kg. For the entire dose-response curve, 42% of those animals tested vomited after zacopride ($P < .05$), compared with none for BMY25801 or BRL43694. No emetic/retching responses to vehicle were observed ($n = 30$).

Fig. 2. Dose-dependent incidence of defecatory responses to zacopride contrasted with BRL43694 and BMY25801 as a function of administration route. Ferrets observed for 30-min period after drug administration. Top: response to i.v. (bolus) administration. All compounds were dissolved in NaCl. Each data point for BMY25801 and BRL43694 represents tests in eight to 10 individual animals; zacopride, 10 to 11. No defecatory responses to vehicle were seen ($n = 30$). Bottom: response to p.o. administration. All compounds were dissolved in 5% dextrose/water. Each data point represents tests in 10 to 14 animals. Significant individual differences were observed among compounds (*, †) and vehicle (††) at doses equal to or greater than 0.1 mg/kg ($P < .05$). For all doses that ranged from 0.003 to 3 mg/kg, defecation to zacopride was 62%; BMY25801, 12%; BRL43694, 13%. This incidence of defecation to zacopride differed significantly ($P < .05$) from that for BMY25801, BRL43694 and vehicle (dashed line, $n = 10/30$). The incidence of defecation to both BMY25801 and BRL43694 was significantly ($P < .05$) less than that of vehicle.

When given i.v. at doses ranging between 0.003 and 0.3 mg/kg, zacopride evoked a 20 to 30% ($n = 10$/dose) incidence of emesis or retching at each dose. In contrast, neither BMY25801 nor BRL43694 given i.v. evoked emesis at doses less than 1 mg/kg. BMY25801 elicited a 10% incidence of emesis at 1 to 3 mg/kg ($n = 10$/dose) and BRL43694 evoked a 9% incidence of emesis at 3 mg/kg ($n = 1/11$). The total incidence of emesis to all i.v. doses of zacopride (9.9%) did not significantly differ from the total incidence for all i.v. doses of BMY25801 (3%) or BRL43694 (2%). When given p.o., the emetic responses to zacopride were more pronounced than when given i.v., whereas BMY25801 and BRL43694 failed to elicit emesis at any dose tested. 2-CH_3 5-HT (data not shown) produced only a single emetic episode when given i.v. (3 mg/kg; $n = 1/9$), but never at lower i.v. doses ($n = 38$, 9–10/dose) or any p.o. dose ($n = 40$, 9–10/dose). Although most emetic responses were prompt, the range of emetic latencies varied from 2 to 25 min, regardless of administration route or compound. No emesis was observed to i.v. or p.o. vehicle. The emetic responses to both i.v. and p.o. zacopride also appeared dose dependent. The ED_{50} value for emesis to p.o. zacopride was calculated as 0.033 mg/kg (95% confidence limits = 0.015, 0.077 mg/kg).

Figure 2 shows that zacopride also evoked a greater incidence of a defecatory response than did BMY25801 or BRL43694, regardless of administration route. When given i.v. at doses ranging between 0.00003 and 0.03 mg/kg, zacopride produced a 9 to 50% incidence of defecation that appeared dose dependent ($n = 10$–11/dose). In contrast, a low incidence of defecations occurred in response to BMY25801 ($n = 4/40$) and BRL43694 ($n = 3/50$), but only at doses greater than or equal to 0.1 mg/kg. A defecatory response was never seen after vehicle. Like

the emetic response, the defecatory response to p.o. zacopride was more pronounced than when given i.v. and it too appeared to be dose dependent. In p.o. doses that ranged from 0.003 to 3 mg/kg, the overall incidence of defecation was 62% for zacopride, 12% for BMY25801 and 13% for BRL43694. The 62% incidence of defecation to zacopride was significantly greater ($P < .05$) than for BMY25801, BRL43694 or vehicle ($n = 10/30$). In contrast, the incidence of defecation to either BMY25801 or BRL43694 was significantly lower ($P < .05$) than for vehicle. Animals ($n = 6/33$) also defecated after all p.o. doses of 2-CH_3 5-HT (data not shown), but the incidence did not differ from that for vehicle.

Analysis of the dose-response data for zacopride showed that both the emetic and defecatory responses were likely to occur with similar frequency to an identical dose of the drug. That is, the dose-response curves for the two side effects appeared identical for i.v. zacopride ($r = 0.9754$, $P < .05$) and very similar for p.o. zacopride ($r = 0.7094$, $P < .10$). In addition, the responses were likely to occur in the same animal. No such correlation between the two side effects was observed for either BRL43694 or BMY25801. The latency to emesis after p.o. zacopride (0.003-0.3 mg/kg) was inversely correlated with the dose of zacopride ($r = -0.8119$, $P < .05$) whereas the latency to defecation was not ($r = -0.1949$); p.o. zacopride (>0.003 mg/kg) also produced multiple episodes of both emesis/retching and defecation. Multiple episodes of emesis or defecation never occurred in response to BMY25801, BRL43694, 2-CH_3 5-HT or vehicle.

Behavioral responses other than emesis and defecation were

also observed after i.v. zacopride. At a threshold dose of 0.001 mg/kg all doses of zacopride produced a brief behavioral arousal that was characterized by standing, then circling the cage. The arousal period was followed by 20 to 30 sec of an increased depth and rate of respiration (panting), then 5 ᵥ 3 min of apparent listlessness or sedation from which the animal could be aroused. Because it was unclear as to whether the apparent sedation was life-threatening, zacopride was not tested at greater i.v. doses. Salivation was also occasionally observed, but none of these behavioral responses was explored in detail. After 2-CH₃ 5-HT was given i.v., brief episodes of arousal (0.03-3 mg/kg, $n = 25/39$), panting (0.03-3 mg/kg, $n = 14/39$) and listlessness (0.1-3 mg/kg, $n = 15/29$) were also observed. Panting was observed after i.v. BRL43694 only at the highest dose tested (3 mg/kg, $n = 1/11$). No similar, or other, behavioral effects were observed in response to i.v. BMY25801 or vehicle. These responses were never observed with any compound given p.o.

Pharmacological antagonism of emesis and defecations to p.o. zacopride by 5-HT₃ receptor ligands, 2-CH₃ 5-HT and BRL43694. The lower dose (1.2 mg/kg) of 2-CH₃ 5-HT reduced the incidence of zacopride-induced emesis from 90 to 50% but that reduction was not statistically significant (table 1). This dose of 2-CH₃ 5-HT also failed to affect the latency to emesis, the incidence of defecations or their latency to onset. However, as seen in table 1, both the larger dose of 2-CH₃ 5-HT and BRL43694 significantly reduced the incidence of emesis to oral zacopride, but did not abolish it. Vomiting animals were also protected by these compounds, as evidenced by the significant increased latency to first emesis by BRL43694. Both compounds also significantly reduced the number of retches. The frequency of retches returned to control values during the second 30-min observation period after BRL43694 and 1.2 mg/kg 2-CH₃ 5-HT (data not shown). The number of expulsions was not altered by either compound (data not shown). During the second 30-min observation period after BRL43694 pretreatment an additional animal vomited. Although BRL43694 did not affect the defecatory response to zacopride, 2-CH₃ 5-HT at 3 mg/kg totally abolished it.

Pharmacological antagonism of emesis and defecations to p.o. zacopride by the muscarinic or dopamine receptor antagonists, glycopyrrolate or domperidone. As seen in table 2, both compounds significantly reduced the incidence of emesis to oral zacopride, but did not abolish it.

During the second 30-min observation period after glycopyr-rolate pretreatment, an additional animal vomited. The latency to the first emetic episode was significantly increased by dom-peridone pretreatment. Table 2 also shows that both compounds completely abolished the defecatory response to zaco-pride for the first 30-min observation period. Two glycopyrro-late-treated animals and one domperidone-treated animal defecated during the second 30-min observation period.

Vagotomy vs. emesis and defecation to oral zacopride. Table 3 shows that both bilateral and dorsal abdominal vagot-omy significantly (P < .05) reduced the incidence of emesis to zacopride. Bilateral vagotomy also: 1) reduced (but not signifi-cantly) the number of retches; and 2) abolished expulsions to zacopride in the two responding animals. Dorsal vagotomy significantly increased the latency to first emesis (P < .05); ventral abdominal vagotomy had no effect. Of those seven animals that vomited to zacopride treatment after ventral vagotomy, five had multiple episodes. Only in two animals (one ventral, one sham) did an emetic episode occur during the second 30-min observation period postvagotomy.

Sham vagotomy had a marked effect on the emetic response to oral zacopride. After this procedure significantly more ani-mals (P < .05) vomited after zacopride treatment. In addition, the number of both expulsions and retches significantly in-creased in the responding animals (P < .05).

The latency of the defecatory response to p.o. zacopride was significantly increased by dorsal vagotomy (P < .05). Another dorsally vagotomized animal defecated during the second 30-min observation period. Sham vagotomy caused a significant reduction in the incidence of defecations (P < .05). For those animals ($n = 8$) that showed multiple defecations to zacopride prior to vagotomy, this incidence was reduced to 25% after bilateral or dorsal vagotomy (data not shown).

Discussion

Dose-response curves for emesis and defecations to zacopride, BMY25801 and BRL43694. The principal and most significant finding of this study is that dose-dependent *emetic* responses were evoked in the ferret by i.v. or p.o. administration of the *antiemetic* zacopride, a compound that is being evaluated for clinical use. Zacopride also evoked dose-dependent defecatory responses and other behavioral changes. These side effects to zacopride occurred at clinically relevant,

TABLE 1

Suppression of emetic or defecatory responses to zacopride (0.3 mg/kg p.o.) by pretreatment with the 5-HT₃ antagonist BRL43694 or the 5-HT₃ agonist 2-CH₃ 5-HT

Values are means ± S.E.

Parameter	Pretreatment[a]					
	Vehicle	BRL43694	Vehicle	2-CH₃ 5-HT₁	Vehicle	2-CH₃ 5-HT₂
No. vomiting or retch-ing/tested	9/10	3/10*	9/10	5/10	9/10	1/10*
Latency to 1st episode (min)	13.3 ± 3.0	26.1 ± 2.6*	9.4 ± 2.8	15.2 ± 4.0	10.7 ± 1.9	[6.0][b]
No. retches	17.1 ± 5.1	5.7 ± 0.7*	14.9 ± 2.4	8.0 ± 2.5*	11.6 ± 2.0	[6.0]
No. defecating/tested	6/10	7/10	4/10	4/10	5/10	0/10*
Latency to defecation (min)	9.4 ± 3.1	18.1 ± 4.1	6.0 ± 2.2	13.8 ± 4.3	6.8 ± 3.1	—

[a] Vehicle (NaCl) or drug (BRL43694, 0.3 mg/kg; 2-CH₃ 5-HT₁, 1.2 mg/kg; 2-CH₃ 5-HT₂, 3 mg/kg) given i.p. 20 min before zacopride administration. All data were recorded during the 1st 30-min interval after zacopride administration.

[b] Numbers in brackets represent $n = 1$.

* Statistical significance (P < .05) between vehicle and drug pretreatment by the test for significance of difference between two proportions or the Student's t test for paired data.

TABLE 2

Suppression of emetic or defecatory responses to zacopride (0.3 mg/kg p.o.) by pretreatment with a muscarinic (glycopyrrolate) or dopamine (domperidone) receptor antagonist

Values are means ± S.E.

Parameter	Pretreatment[*]			
	Vehicle	Glycopyrrolate	Vehicle	Domperidone
No. vomiting or retch-ing/tested	9/10	4/10[*]	10/10	5/10[*]
Latency to 1st epi-sode (min)	14.8 ± 3.0	20.0 ± 3.4	6.2 ± 1.7	14.4 ± 4.0[*]
No. retches	10.9 ± 2.5	15.0 ± 4.6	12.4 ± 1.9	8.6 ± 1.6
No. defecating/tested	5/10	0/10[*]	4/10	0/10[*]
Latency to defecation (min)	8.0 ± 2.8	57.5 ± 0.5[b*]	7.5 ± 1.9	—

[*] Vehicle (NaCl) or drug (glycopyrrolate, 0.1 mg/kg, domperidone, 1 mg/kg) given i.p. 20 min before zacopride administration. All data (except [b]) were recorded during the 1st 30-min interval after zacopride administration.

[b] Recorded during the 2nd 30-min interval after zacopride administration.

[*] Statistical significance (P < .05) between vehicle and drug pretreatment by the test for significance of difference between two proportions or the Student's *t* test for paired data.

antiemetic doses (Costall *et al.*, 1987; King and Landauer, 1990). The actions of zacopride contrasted significantly with the actions of BMY25801 and BRL43694, antiemetics with profiles somewhat similar to those of zacopride in classic models for testing 5-HT$_3$ receptor characteristics of compounds. BMY25801 and BRL43694 evoked only isolated emetic responses when given i.v. and never when given p.o. Defecatory responses to these latter compounds were not dose-dependent when given i.v. and were significantly less than vehicle when given p.o.

Emesis and defecation in response to zacopride were previously observed in ferrets after i.p. administration (King *et al.*, 1988; King and Landauer, 1990). Emesis to p.o. zacopride in ferrets has recently been confirmed by Sancilio *et al.* (1990) and their ED$_{50}$ value (0.03 mg/kg; A. H. Robins, personal communication) for that emetic response is similar to that reported here (0.033 mg/kg). In contrast, Costall *et al.* (1987) reported no side effects to i.v. zacopride in ferrets, but the animals were anesthetized for its administration and then allowed 15 to 20 min to recover. The sedation associated with recovery from anesthesia in that study may have prevented or masked the side effects reported here. Others have reported no side effects in response to doses of zacopride ranging from

0.00003 to 0.5 mg/kg (i.v., p.o. or i.p.) in cats (Smith *et al.*, 1988a), dogs (Alphin *et al.*, 1986; Cohen *et al.*, 1989; Smith *et al.*, 1988b), nonhuman primates (Dubois *et al.*, 1988; Sancilio, personal communication) and humans (Sancilio, personal communication). The lack of observed side effects in these studies probably reflects differences among species and routes of administration.

The isolated instances of emesis and defecation to i.v. BMY25801 and BRL43694 have also not been previously observed (Gylys *et al.*, 1988; Bermudez *et al.*, 1988). However, the doses of BMY25801 and BRL43694 evaluated in this study and that evoked these responses exceeds the doses used by those authors. In addition, emesis and defecations as side effects could have been overlooked by those authors. These events could have been masked by emesis/defecations that occur normally in response to cytotoxins and radiation. For example, BMY25801 was not fully protective for emesis against these latter stimuli (Gylys *et al.*, 1988; King and Landauer, 1990). In humans also, emesis has not been reported in response to either BMY25801 or BRL43694 when given i.v. (Zussman *et al.*, 1988; Carmichael *et al.*, 1988; Cassidy *et al.*, 1988; Plezia *et al.*, 1988; Smaldone *et al.*, 1988). Although no GI side effects were reported for BRL43694, 38% of patients receiving BMY25801 reported loose stools (Plezia *et al.*, 1988). This latter pattern of clinically observed GI side effects was found in the present study in ferrets.

It is especially noteworthy that both BMY25801 and BRL43694, when given p.o., significantly reduced the incidence of defecations when compared with vehicle. Such data suggest that, when given orally, these compounds could be useful for counteracting lower GI motility disorders.

Emetic response to oral zacopride. The selective action of dorsal vagotomy to reduce the incidence of emesis to oral zacopride suggests that the predominant afferent pathway for initiation of that emetic response is the dorsal vagus nerve. In ferrets, the dorsal vagus primarily innervates the dorsal aspects of the stomach and the coeliac ganglion (MacKay and Andrews, 1983). Andrews *et al.* (1990) have reported that the emetic latency to certain compounds given p.o. (*e.g.*, copper sulfate) to the ferret varies inversely with the time of recovery after vagotomy. It is thus unlikely that the increased latency to emesis after dorsal vagotomy is confounded by the time of testing with zacopride.

TABLE 3

Effect of vagotomy on emetic or defecatory responses to zacopride (0.3 mg/kg p.o.)

Values are means ± S.E.

Parameter[*]	Sham		Vagotomy					
			Bilateral		Unilateral			
					Dorsal		Ventral	
	Pre	Post	Pre	Post	Pre	Post	Pre	Post
No. vomiting or retching/tested	5/9	9/9[*]	16/20	2/20[*]	8/8	2/8[*]	6/8	7/8
Latency to 1st episode (min)	13.8 ± 3.4	8.6 ± 1.6	11.9 ± 1.9	13.5 ± 5.5	12.2 ± 2.2	23.0[*] ± 2.0	11.2 ± 1.7	12.4 ± 1.9
No. expulsions	1.2 ± 0.4	2.3[*] ± 0.3	1.4 ± 0.2	0	1.7 ± 0.2	1.0 ± 0.0	1.4 ± 0.3	1.7 ± 0.2
No. retches	6.4 ± 2.4	14.6[*] ± 2.4	10.3 ± 4.8	3.0 ± 2.0	—	—	—	—
No. defecating/tested	4/9	0/9[*]	13/20	11/20	5/8	4/8	0/8	1/8
Latency to defecation (min)	13.0 ± 5.1	—	13.1 ± 2.6	9.2 ± 1.1	8.6 ± 2.0	21.3[*] ± 4.7	—	22.0

[*] All data were recorded for 30 min after zacopride administration; — indicates that data were not recorded.

[*] Statistical significance (P < .05) between pre- and postvagotomy values by the test for significance of difference between two proportions or the Student's *t* test for paired data.

The antiemetic action of glycopyrrolate implies that zacopride may facilitate ACh release from myenteric neurons, which in turn may play some role in the eme is to zacopride. Zacopride enhances the ACh mediated muscle-twitch in guinea-pig ileum (Craig and Clarke, 1989) but does not bind at muscarinic ACh receptors (Barnes et al., 1988a). Likewise, the antiemetic action of domperidone also suggests a role for dopamine in media ing this emetic response. Although the precise role for a dopaminergic mechanism in zacopride-induced emesis is unclear from these data, other evidence suggests that central 5-HT₃ and dopamine receptors interact (see Tricklebank, 1989). Costall et al. (1989) recently reported that the 5-HT₃ receptor antagonist ICS 205-930 can partially prevent apomorphine-induced emesis in the ferret.

The data also strongly suggest that the emesis to p.o. zacopride results from an action at the 5-HT₃ receptor. This was demonstrated by the reduced emesis seen after pretreatment with either the 5-HT₃ receptor antagonist BRL43694 or agonist 2-CH₃ 5-HT. Although emesis was not completely abolished by either compound, those animals still vomiting after BRL43694 exhibited both a significantly: 1) increased latency to the first emetic episode; and 2) reduced number of retches. Likewise, the number of retches was significantly reduced by the lower dose of 2-CH₃ 5-HT. The action by the 5-HT₃ receptor ligands to ameliorate retching but not vomiting suggests that subtle pharmacological differences exist between the underlying mechanisms for the two events. Such a differential effect on vomiting vs. retching has been observed with zacopride and BRL43694 when used as antiemetics for cytotoxin- and radiation-induced emesis (Andrews and Hawthorn, 1987; Dubois et al., 1988; Hawthorn et al., 1988). These authors, however, found a greater percentage decrease in emetic rather than retching events.

If one accepts that the emetic response to p.o. zacopride is mediated predominantly by 5-HT₃ receptor action, the reduced emesis in response to dorsal vagotomy implies that these receptors are distributed primarily along the dorsal wall of the stomach, possibly within the myenteric plexus or along vagal afferents. In support of this notion, Bingham (1987) has shown that close intra-arterial injections of 5-HT and 5-hydroxytryptophan in μg/kg doses will evoke an (atropine-sensitive) antral contraction in the stomacn of the anesthetized ferret. However, a separate (peripheral or central) pathway must be involved in the emetic response to oral zacopride since vagotomy does not completely abolish the emesis.

Several alternative explanations exist that can account for the partial abolition of zacopride-induced emesis by the 5-HT₃ receptor ligands. For example, because 5-HT₃ receptors are found throughout the peripheral nervous system (Bradley et al., 1986), BRL43694 and 2-CH₃ 5-HT could act at other sites along the emetic pathway to prevent the emesis. Their distribution or duration of action could also vary across individual animals. It seems unlikely that the specific challenging doses chosen for these compounds were inadequate. Of the three pretreatments, only BRL43694 failed to abolish the defecatory response to zacopride.

The enhanced emetic responses to zacopride following sham vagotomy were unexpected. Although the reason for this response is unknown, it could reflect an increased level of GI 5-HT production in the response to anesthesia and laparotomy. According to Gomes et al. (1985), this may last for up to 5 weeks postvagotomy.

Defecatory response to oral zacopride. In contrast to the emetic response to oral zacopride, the incidence of a defecatory response was totally abolished by glycopyrrolate, domperidone and the higher dose of 2-CH₃ 5-HT. Its latency to onset was also increased by dorsal vagotomy. Because oral zacopride enhances gastric emptying (Dubois et al., 1988), that preparation may have passed into the intestine and activated the more proximal myenteric neurons to stimulate peristalsis. This could explain the rapidity of the defecatory response and the fact that dorsal vagotomy significantly increased the latency of this response. The vagus does contain two motor pathways that are reflexly excited by vagal afferent input, one of which is cholinergic (Collman et al., 1984a,b). However, such a mode of action for zacopride can only be speculated because the distribution of vagal fibers in the ferret has not been traced anatomically beyond the coeliac ganglion (MacKay and Andrews, 1983).

Other side effects to zacopride administration. It was also observed that clinically relevant doses of i.v. zacopride, but not BMY25801 or BRL43694, produced sedation or listlessness, which was preceded by a central arousal and labored respiration. We have previously reported sedative-like response to i.p. zacopride, expressed as a depression of vertical exploratory behavior (King and Landauer, 1990). In contrast, Costall et al. (1987) reported that their animals remained alert and active during the recording period. Such differences could be attributed to varied observation methods (see King and Landauer, 1990).

The arousal and labored respirations followed by listlessness induced by low doses of i.v. zacopride were mimicked only by similar doses of i.v. 2-CH₃ 5-HT. Although the arousal and listlessness from zacopride may result from central action, 2-CH₃ 5-HT does not cross the blood-brain barrier. It is thus likely that all of these side effects were in response to action on peripheral 5-HT₃ receptors by these compounds. Activation of 5-HT₃ receptors in the epicardium, juxtapulmonary capillary bed and carotid body produce numerous reflexive autonomic responses. These peripheral responses, which include bradycardia, hypo- and hypertension, rapid shallow breathing and inhibition of somatic muscles (for review, see McQueen and Mir, 1989), could account for the observed behaviors.

General significance of results. The most compelling result from the pharmacological studies was that emesis to oral zacopride was not totally abolished by any single compound. In contrast, the defecatory response was completely abolished by glycopyrrolate, domperidone and 2-CH₃ 5-HT. Based on these data, the most likely explanation for these results is that zacopride acts in the GI tract in a manner analogous to that of metoclopramide, which stimulates motility by facilitating ACh release from myenteric neurons (Schulze-Delrieu, 1979; Sanger, 1985, 1987). That zacopride enhances ACh-mediated contractions in the guinea-pig ileum (Craig and Clarke, 1989), an action that is mimicked by 5-HT (Sanger, 1985, 1987), supports this hypothesis. As suggested by the action of domperidone, however, zacopride may also facilitate dopamine release from the myenteric plexus, but this has yet to be confirmed in vitro. Zacopride antagonized 2-CH₃ 5-HT-induced contractions of guinea-pig ileum (Cohen et al., 1989), but the transmitter mediating these contractions was not defined. It is also possible that the antidefecatory action of these receptor antagonists reflects a nonspecific action by zacopride on GI motility. The incidences of a defecatory response to NaCl plus zacopride

during one series of experiments (vehicle: tables 1 and 2) were not significantly greater than that to p.o. vehicle alone in another (fig. 2 *lower, dashed line*; n = 10/30).

Undoubtedly, the mechanism by which zacopride evokes an emetic and/or defecatory response varies with the route of administration. The emetic responses to i.v. zacopride may result from action at the chemoreceptor trigger zone in the area postrema (Borison and Wang, 1953). 5-HT$_3$ receptor binding has been shown in the ferret area postrema (Barnes et al., 1988b) and emesis to i.v. neurotransmitter receptor agonists is abolished by area postrema lesion (Carpenter et al., 1984). A similar action at the chemoreceptor trigger zone might explain the emetic responses to i.v. BMY25801 and BRL43694, although the greater doses necessary to evoke emesis would suggest some other, non-5-HT$_3$ selective action. Alternatively, emesis to i.v. zacopride could be in response to activation of epicardial 5-HT$_3$ receptors (see McQueen and Mir, 1989). The mechanism for evoking a defecatory response after i.v. administration is unknown.

It can only be speculated as to what attribute zacopride has that would explain its ability to evoke emetic or defecatory responses and thus distinguish it so markedly from BMY25801 and BRL43694. Both zacopride (Smith et al., 1988b) and BRL43694 (Sanger and Nelson, 1989) are potent 5-HT$_3$ receptor antagonists, but the former stimulates gastric motility (Alphin et al., 1986) and the latter does not (Sanger and Nelson, 1989). BMY25801 has not been tested for 5-HT$_3$ receptor affinity (Monkovic et al., 1988). All three compounds attenuate the Bezold-Jarisch reflex in a dose-response fashion, although BMY25801 only at greater doses (Gylys et al., 1988). The complete pharmacological profile exists only for BRL43694.

Zacopride could act as either a partial agonist or mixed agonist-antagonist at the 5-HT$_3$ receptor (see Craig and Clarke, 1989). Such agonist action would explain the finding that i.v. zacopride and 2-CH$_3$ 5-HT evoke similar physiological responses and that zacopride can be both emetic and antiemetic. However, agonist action by zacopride would not explain an emetic response to zacopride but not 2-CH$_3$ 5-HT. Alternatively, zacopride is a racemate and the isomers show different effects on gastric emptying (Wade et al., 1989). Thus the emetic or antiemetic and other properties of zacopride may be related to a specific stereoisomer.

In summary, the 5-HT$_3$ receptor antagonist and antiemetic zacopride has also been shown to demonstrate emetogenic properties at antiemetic doses. This was not seen in response to two other somewhat similar compounds, BMY25801 and BRL43694. The emetic response to zacopride was most pronounced when it was given orally and that emetic response was attenuated, but not abolished, by prior administration of various receptor ligands or dorsal vagotomy. That zacopride shows both emetic and antiemetic properties at similar doses is a paradox that has yet to be resolved.

References

ALPHIN, R. S., SMITH, W. L., JACKSON, C. B., DROPPLEMAN, D. A. AND SANCILIO, L. F.: Zacopride (AHR-11190B). A unique and potent gastro-intestinal prokinetic and antiemetic agent in laboratory animals. Dig. Dis. Sci. **31**: 482S, 1986.

ANDREWS, P. L. R., DAVIS, C. J., BINGHAM S., DAVIDSON, H. I. M., HAWTHORN, J. AND MASKELL, L.: The abdominal visceral innervation and the emetic reflex. Pathways, pharmacology, and plasticity. Can. J. Physiol. Pharmacol. **68**: 325-345, 1990.

ANDREWS, P. L. R. AND HAWTHORN, J.: Evidence for an extra-abdominal site of action for the 5-HT$_3$ receptor antagonist BRL24924 in the inhibition of radiation-evoked emesis in the ferret. Neuropharmacology **26**: 1367-1370, 1987.

BARNES, N. M., COSTALL, B. AND NAYLOR, R. J.: [^{3}H]Zacopride: Ligand for the identification of 5-HT$_3$ recognition sites. J. Pharm. Pharmacol. **40**: 548-551, 1988a.

BARNES, N. M., COSTALL, B., NAYLOR, R. J. AND TATTERSALL, F. D.: Identification of 5-HT$_3$ recognition sites in the ferret area postrema. J. Pharm. Pharmacol. **40**: 586-588, 1988b.

BERMUDEZ, J., BOYLE, E. A., MINER, W. D. AND SANGER, G. J : The antiemetic potential of the 5-hydroxytryptamine$_3$ receptor antagonist BRL 43694. Br. J. Cancer **58**: 644-650, 1988.

BINGHAM, S.: A comparison of the effects of 5-HT and vagal stimulation on antral motility in the anaesthetized ferret. J. Physiol. (Lond.) **382**: 186P, 1987.

BORISON, H. L. AND WANG, S. C.: Physiology and pharmacology of vomiting. Pharmacol. Rev. **5**: 193-230, 1953.

BRADLEY, P. B., ENGEL, G., FENUIK, W., FOZARD, J. R., HUMPHREY, P P A., MIDDLEMISS, D. N., MYLE-CHARANE, E. J., RICHARDSON, B. P. AND SAXENA, P. R.: Proposals for the classification and nomenclature of functional receptors for 5-hydroxytryptamine. Neuropharmacology **25**: 563-576, 1986.

BROGDEN, R. N., CARMINE, A. A., HEEL, R. C., SPEIGHT, T. M. AND AVERY, G. S.: Domperidone: A review of its pharmacological activity, pharmacokinetics and therapeutic efficacy in the symptomatic treatment of chronic dyspepsia and as an antiemetic. Drugs **24**: 360-400, 1982.

BRUNING, J. L. AND KINTZ, B. J.: Computational Handbook of Statistics, 2nd edition. Scott, Foresman and Co., Glenview, IL, 1977.

CARMICHAEL, J., CANTWELL, B. M. J., EDWARDS, C. M., RAPEPORT, W. G. AND HARRIS, A. L.: The serotonin type 3 receptor antagonist BRL43694 and nausea and vomiting induced by cisplatin. Br. Med. J. **297**: 110-111, 1988.

CARPENTER, D. O., BRIGGS, D. B. AND STROMINGER, N. L.: Peptide-induced emesis in dogs. Exp. Brain Res. **11**: 277-281, 1984.

CASSIDY, J., RAINA, V., LEWIS, C., ADAMS, L., SOUKOP, M., RAPEPORT, W. G., ZUSSMAN, B. D., RANKIN, E. M. AND KAYE, S. B.: Pharmacokinetics and antiemetic efficacy of BRL43694, a new selective 5-HT-3 antagonist. Br. J. Cancer **58**: 651-653, 1988.

COHEN, M. L., BLOOMQUIST, W., GIDDA, J. S. AND LACEFIELD, W.: Comparison of the 5-HT$_3$ receptor antagonist properties of ICS 205-930, GR38032F and zacopride. J. Pharmacol. Exp. Ther. **248**: 197-201, 1989.

COLLMAN, P. I., GRUNDY, D. AND SCRATCHERD, T.: Vagal control of colonic motility in the anesthetized ferret: Evidence for a non-cholinergic excitatory innervation. J. Physiol. (Lond.) **348**: 35-42, 1984a.

COLLMAN, P. I., GRUNDY, D., SCRATCHERD, T. AND WACH, R. A.: Vago-vagal reflexes to the colon of the anesthetized ferret. J. Physiol. (Lond.) **352**: 395-402, 1984b.

COOPER, S. M., McCLELLAND, M., McRITCHIE, B. AND TURNER, D. H.: BRL24924. A new and potent gastric motility stimulant. Br. J. Pharmacol **8**: suppl. A, 383P, 1988.

CORDTS, R. E., YOCHMOWITZ, M. G. AND HARDY, K. A.: Evaluation of domperidone as a modifier of gamma-radiation-induced emesis. Int. J. Radiat. Oncol. Biol. Phys. **13**: 1333-1337, 1987.

COSTALL, B., DOMENEY, A. M., NAYLOR, R. J. AND TATTERSALL, F. D.: Emesis induced by cisplatin in the ferret as a model for the detection of antiemetic drugs. Neuropharmacology **9**: 1321-1326, 1987.

Costall, B., Naylor, R. J., Owera-Atepo, J. B. and Tattershall, F. D.: The responsiveness of the ferret to apomorphine induced emesis. Br. J. Pharmacol. **96**: suppl, 329P, 1989.

CRAIG, D. A. AND CLARKE, D. E.. Gaddum's M receptor does not equate with the 5-HT-3 receptor in guinea-pig ileum. FASEB J. **3**: A1199, 1989.

CUNNINGHAM, D., HAWTHORN, J., POPLE, A., GAZET, J.-C., FORD, H. T., CHALLONER, T. AND COOMBES, R. C.: Prevention of emesis in patients receiving cytotoxic drugs by GR38032F, a selective 5-HT$_3$ receptor antagonist. Lancet I: 1461-1462, 1987.

DUBOIS, A., FIALA, N., BOWARD, C. A. AND BOGO, V.: Prevention and treatment of the gastric symptoms of radiation sickness. Radiat. Res. **115**: 595-604, 1988.

DUBOIS, A., JACOBUS, J. P., GRISSOM, M. P., ENGS, R. R., DURAKOVIC, A. AND CONKLIN, J. J.: Altered gastric emptying and prevention of radiation-induced vomiting in dogs. Gastroenterology **86**: 444-448, 1984.

FAKE, C. S., KING, F. D. AND SANGER, G. J.: BRL43694: A potent and novel 5-HT$_3$ receptor antagonist. Br. J. Pharmacol. **91**: suppl, 335P, 1987.

FRANKO, B. V., ALPHIN, R. S., WARD, J. W. AND LUNSFORD, C. D.: Pharmacodynamic evaluation of glycopyrrolate in animals. Ann. N. Y. Acad. Sci. **99**: 131-149, 1962.

GOMES, G. M. P., DAHLSTROM, A., GRIMELIUS, L., JOHANSSON, H. AND AHLMAN, H.: The effect of truncal vagotomy on serotonin distribution in the rat gastrointestinal tract. J. Surg. Res. **38**: 13-16, 1985.

GRALLA, R. J., ITRI, L. M., PISKO, S. E., SQUILLANTE, A. E., KELSEN, D. P., BRAUN, D. W., BORDIN, L. A., BRAUN, T. J. AND YOUNG, C. W.: Antiemetic efficacy of high-dose metoclopramide: Randomized trials with placebo and prochlorperazine in patients with chemotherapy-induced nausea and vomiting. N. Engl. J. Med. **305**: 905-909, 1981.

GYLYS, J. A., WRIGHT, R. N., NICOLOSI, W. D., BUYNISKI, J. P. AND CRENSHAW, R. R.. BMY 25801, an antiemetic agent free of D_2-dopamine receptor antagonist properties. J. Pharmacol. Exp. Ther. **244:** 830–837, 1988.

HAWTHORN, J., OSTLER, K. J. AND ANDREWS, P. L. R.. The role of the abdominal visceral innervation and 5-hydroxytryptamine M receptors in vomiting induced by the cytotoxic drugs cyclophosphamide and cis-platin in the ferret. Q. J. Exp. Physiol. **73:** 7–21, 1988.

JACKSON, R. K., KIEFFER, V. A., SAUBER, J. J. AND KING, G. L.. A tethered-restraint system for blood collection from ferrets. Lab. Animal Sci. **38:** 625–628, 1988.

KING, G. L. AND LANDAUER, M. R.. Effects of zacopride and BMY25801 (batanopride) on radiation-induced emesis and locomotor behavior in the ferret. J. Pharmacol. Exp. Ther. **253:** 1026–1033, 1990.

KING, G., LANDAUER, M., KIEFFER, V., KESSLER, D. AND DAVIS, H.: Zacopride, a 5HT₃ antagonist, modifies emetic and behavioral responses to radiation in the ferret. FASEB J. **2:** 325, 1988.

KRIS, M. G., GRALLA, R. J., CLARK, R. A. AND TYSON, L. B.: Dose-ranging evaluation of the serotonin antagonist GR-C507/75 (GR38032F) when used as an antiemetic in patients receiving anticancer chemotherapy. J. Clin. Oncol. **6:** 659–662, 1988.

KRIS, M. G., GRALLA, R. J., TYSON, L. B., CLARK, R. A., KELSEN, D. P., REILLY, L. K., GROSHEN, S., BOSL, G. J. AND KALMAN, L. A.: Improved control of cisplatin-induced emesis with high-dose metoclopramide and with combinations of metoclopramide, dexamethasone, and diphenhydramine. Results of consecutive trials in 255 patients. Cancer **55:** 527–534, 1985.

MACKAY, T. W AND ANDREWS, P. L. R.: A comparative study of the vagal innervation of the stomach in man and the ferret. J. Anat. **136:** 449–481, 1983.

MCQUEEN, D. S. AND MIR, A. K.: 5-Hydroxytryptamine and cardiopulmonary and carotid body reflex mechanisms. *In* The Peripheral Actions of 5-Hydroxytryptamine, ed. by J. R. Fozard, pp. 301–326, Oxford University Press, New York, 1989.

MEYER, B. R., LEWIN, M, DRAYER, D. E., PASMANTIER, M., LONSKI, L. AND REIDENBERG, M. M.: Optimizing metoclopramide control of cisplatin-induced emesis. Ann. Intern. Med. **100:** 393–395, 1984.

MINER, W. D., SANGER, G. J. AND TURNER, D. H.: Evidence that 5-hydroxytryptamine₃ receptors mediate cytotoxic drug and radiation-evoked emesis. Br. J. Cancer **56:** 159–162, 1987.

MONKOVIC, I., WILLNER, D., ADAM, M. A., BROWN, M., CRENSHAW, R. R., FULLER, C. E., JUBY, P. F., LUKE, G. M, MATISKELLA, J. A. AND MONTZKA, T. A.: Substituted benzamides. 1. Potential nondopaminergic antagonists of chemotherapy-induced nausea and emesis. J. Med. Chem. **31:** 1548–1558, 1988.

PLEZIA, P. M., DAVIS, L. E., ALBERTS, D. S., DAVIS, A., GAREWAL, H. S.,

GREENBERG, B. R., SMALDONE, L. AND FAIRCHILD, C.. BMY25801: An effective single agent antiemetic for cisplatin-induced nausea and vomiting. Proc. Am. Soc. Clin. Oncol. **7:** 294, 1988.

PRIESTMAN, T., CHALLONER, T., BUTCHER, M. AND PRIESTMAN, S.. Control of radiation induced emesis with GR38032F. Proc. Am. Sci. Clin. Oncol. **7:** 281, 1988.

SANCILIO, L. F., PINKUS, L. M., JACKSON, C. B. AND MUNSON, JR., H. R.: Emetic activity of oral zacopride in ferrets and its antagonism by ip zacopride, ICS 205-930, and prochlorperazine. FASEB J. **4:** A474, 1990.

SANGER, G. J.: The effects of various pharmacological agents on the metoclopramide-induced increase in cholinergic-mediated contractions of rat isolated forestomach. Eur. J. Pharmacol. **114:** 139–145, 1985.

SANGER, G. J.: Increased gut cholinergic activity and antagonism of 5-hydroxytryptamine M-receptors by BRL43694: Potential clinical importance of BRL24924. Br. J. Pharmacol. **91:** 77–87, 1987.

SANGER, G. J. AND NELSON, D. R.: Selective and functional 5-hydroxytryptamine₃ receptor antagonism by BRL43694 (granisetron). Eur. J. Pharmacol. **159:** 113–124, 1989.

SCHULZE-DELRIEU, K.: Metoclopramide. Gastroenterology **77:** 768–779, 1979.

SMALDONE, L., FAIRCHILD, C., ROZENCWIEIG, M., AAPRO, M., SARTIANO, G., PLEZIA, P. AND ALBERTS, D.: Dose-ranging evaluation of BMY-25801: A nondopaminergic antiemetic. Proc. Am. Soc. Clin. Oncol. **7:** 280, 1988.

SMITH, W. L., CALLAHAM, E. M. AND ALPHIN, R. S.: The emetic activity of centrally administered cisplatin in cats and its antagonism by zacopride. J. Pharm. Pharmacol. **40:** 142–143, 1988a.

SMITH, W. L., SANCILIO, L. F., OWERA-ATEPO, J. B., NAYLOR, R. J. AND LAMBERT, L.: Zacopride, a potent 5-HT₃ antagonist. J. Pharm. Pharmacol. **40:** 301–302, 1988b.

TRICKLEBANK, M. D.: Interactions between dopamine and 5-HT₃ receptors suggest new treatments for psychosis and drug addiction. Trends Pharmacol. Sci. **10:** 127–129, 1989.

WADE, P. R., BRANCHEK, T. A., MAWE, G. M. AND GERSHON, M. D.: Use of stereoisomers of zacopride to distinguish between 5-HT receptor subtypes: An intracellular study of myenteric neurons and gastric emptying. The Neuropharmacology of Serotonin. New York Academy of Sciences, New York, July 10–13, 1989.

ZUSSMAN, B. D., CLARKSON, A., COATES, P. E. AND RAPEPORT, W. G.: The pharmacokinetic profile of BRL43694, a novel 5HT-3 receptor antagonist in healthy male volunteers. Br. J. Clin. Pharmacol. **25:** 107P, 1988.

Effects of Zacopride and BMY25801 (Batanopride) on Radiation-Induced Emesis and Locomotor Behavior in the Ferret[1]

GREGORY L. KING and MICHAEL R. LANDAUER

Departments of Physiology (G.L.K.) and Behavioral Sciences (M.R.L.), Armed Forces Radiobiology Research Institute, Bethesda, Maryland

Accepted for publication February 16, 1990

ABSTRACT

The antiemetic and locomotor effects of two substituted benzamides, zacopride and batanopride (BMY25801), were compared in ferrets after bilateral ^{60}Co irradiation at 2, 4 or 6 Gy. Both zacopride and BMY25801 were effective against emesis and related signs. Zacopride, tested at several doses (0.003, 0.03 and 0.3 mg/kg), appeared to be more potent because it abolished emesis at 100-fold lower doses than did BMY25801 (3 mg/kg). The ED_{50} value for the antiemetic effect of zacopride was 0.026 mg/kg (confidence levels = 0.0095, 0.072 mg/kg). However, analysis of emetic parameters recorded from vomiting animals (e.g., latency to first emesis) demonstrated that BMY25801 provided greater antiemetic protection in this population than zacopride without any apparent side effects. Locomotor activity was significantly depressed by both radiation (all doses) and zacopride alone (0.03 mg/kg and 0.3 mg/kg). BMY25801 alone did not affect locomotor activity, and protected against the radiation-induced locomotor decrement. Although zacopride potentiated the locomotor decrement to radiation, no clear dose-response relationship was evident. Bilateral abdominal vagotomy significantly increased the latency to the first emetic episode and significantly reduced the number of retches, but did not alter the duration of the prodromal response to 4-Gy irradiation. Unilateral vagotomies had no effect. Zacopride (at 0.03 mg/kg and 0.3 mg/kg) remained an effective antiemetic in animals that received a bilateral vagotomy, abolishing emesis in four of eight and two of eight ferrets, respectively. These data suggest that the antiemetic action of zacopride does not fully depend on intact vagal innervation and also acts via other pathways.

Several 5-HT$_3$ receptor antagonists and substituted benzamides provide antiemetic protection for both cytotoxins and radiation in animal models (Miner and Sanger, 1986; Costall et al., 1986; Bermudez et al., 1988) and humans (Priestman et al., 1988; De Haan et al., 1988; Cassidy et al., 1988). One such 5-HT$_3$ receptor antagonist and substituted benzamide, zacopride, is 10-fold more potent than two other 5-HT$_3$ receptor antagonists [ICS 205-930 and GR38032F (ondansetron)] in its ability to reduce the incidence and severity of cisplatin-induced emesis in the dog (Cohen et al., 1989). Another compound, the substituted benzamide batanopride (BMY25801), is presently in clinical trials as an antiemetic (Plezia et al., 1988; Smaldone et al., 1988). Although BMY25801 partially antagonizes the Bezold-Jarisch reflex (an abrupt bradycardia and hypotension in response to i.v. serotonin; see McQueen and Mir, 1989) in a dose-dependent manner (Gylys et al., 1988), it has not yet been shown to possess 5-HT$_3$ receptor antagonist properties.

Both zacopride and BMY25801 have been evaluated for antiemetic action in several vomiting species following different emetic stimuli (Costall et al., 1987; Gylys et al., 1988; Dubois et al., 1988; Smith et al., 1989). However, their antiemetic action has not been directly compared in a single species and in response to a common emetic stimulus. For this study, we chose the ferret as the animal model and radiation as the emetic stimulus. Using this experimental paradigm, both the threshold and the ED_{50} values for emesis are the lowest described for any species tested to date (King, 1988).

Although no significant side effects were reported after zacopride or BMY25801 treatment, more recent evidence contradicts these findings for zacopride. For example, i.v. zacopride produced a sedative-like action in the ferret (King, 1990). Mild sedation has also been observed in humans in response to the 5-HT$_3$ receptor antagonist ondansetron given i.v. (De Haan et al., 1988; Hesketh et al., 1989; Kris et al., 1989). Sedation, a side effect of some antiemetics, has been quantitatively measured by decreases in locomotor activity (see Jenner and Marsden, 1979). In this study, we evaluated the locomotor behavior of the ferret following administration of zacopride or BMY25801 alone or in combination with radiation.

The purposes of this study were to determine: 1) the effective antiemetic dose of zacopride for radiation-induced emesis in

ABBREVIATIONS: 5-HT, 5-hydroxytryptamine (serotonin); BMY25801, batanopride.

the ferret, 2) whether zacopride or BMY25801 provides better antiemetic protection for radiation-induced emesis, 3) the effects of zacopride and BMY25801 on locomotor behavior at antiemetic doses; and 4) whether peripheral vagal innervation is required for the antiemetic action of zacopride. These results have been communicated in part as abstracts (King and Kieffer, 1988; King et al., 1988).

Methods

Subjects. Experiments were performed on castrated, descented, adult male (fitch) ferrets (1-1.5 kg) obtained from Marshall Farms (North Rose, NY). All animals were quarantined upon arrival and screened for evidence of disease. Ferrets were housed in stainless-steel modified rabbit or cat cages and provided commercial ferret chow and water *ad libitum*. The animal quarters were maintained at 15-21°C, 45 to 55% humidity, and 12-hr-light/12-hr-dark photocycle. At the end of the experiments, all animals were anesthetized (sodium pentobarbitol, 80 mg/kg, i.p.) and then euthanatized (T-61, 0.3 mg/kg, i.p.).

Experimental design. In experiment I, zacopride and BMY25801 were evaluated for their antiemetic properties and effects on locomotor behavior. In experiment II, the mechanism by which zacopride exerts its antiemetic action was investigated by selective vagotomy.

Effects of antiemetics. Animals received i.p. injections of either sodium chloride (0.9%, vehicle), zacopride (0.003, 0.03, 0.3 mg/kg), or BMY25801 (3 mg/kg) 20 min before irradiation or sham irradiation. There were six to 11 animals per group. All compounds were given in a volume less than 1 ml. The dose of 3 mg/kg for BMY25801 was chosen for optimum antiemetic action, based on the results of Gylys et al. (1988).

Effects of vagotomy. Radiation treatment was preceded with vehicle in ferrets that had previously undergone sham ($n = 9$), bilateral ($n = 8$), dorsal ($n = 8$) or ventral ($n = 8$) abdominal vagotomy. Two additional groups of animals underwent bilateral abdominal vagotomy, and were also administered zacopride i.p. at 0.03 mg/kg ($n = 8$) or 0.3 mg/kg ($n = 8$) before irradiation.

All abdominal vagotomies were performed under sterile conditions. Animals were not fed for 12 to 16 hr before surgery, water was provided *ad libitum*. The following morning, ferrets were medicated (i.m.) with 30 mg/kg ketamine hydrochloride (Vetalar, Parke-Davis) and 25 mg/kg acetylpromazine maleate (Acepromazine Maleate Injection, Tech America); anesthesia was then maintained with isoflurane (1-1.5%) in 0.5 liters/min O₂. For all animals, a ventral midline incision was made below the diaphragm, and the vagi exposed along the esophagus. A 5-mm section of nerve was then removed from the vagotomized animals. The muscle layer was closed with nonabsorbable proline suture, and the skin with 4.0 chromic absorbable gut. Animals were monitored frequently over a 18-hr postoperative period to ensure uneventful recovery from the surgical procedure. All animals were completely recovered by the time of irradiation.

Radiation procedure and source. In all experiments, animals received either sham irradiation or bilateral, head-shielded ⁶⁰Cu radiation at 1 Gy/min as described by King (1988). In experiment I, a 2-, 4- or 6-Gy dose of radiation was combined with pretreatment of vehicle, zacopride or BMY25801. In experiment II, all ferrets received a 4-Gy radiation dose. The average number of days between vagotomy and radiation exposure was 17 for bilateral, 17 for ventral, 19 for dorsal and 38 for sham.

Recording of emesis and emesis-related behaviors. Following irradiation or sham irradiation, each animal was placed in a 41 cm × 41 cm × 41 cm, well-ventilated Plexiglas arena for 2 hr. An observer recorded: 1) the latency, number and duration of emetic expulsions and retches, 2) the number of burrowing and lip-licking episodes, and 3) the number of defecations. Episodes of emesis or retching separated by ≥4 min were considered single episodic events. This 4-min interval allowed animals to recover from the characteristic posture and other behaviors (e.g., burrowing) that accompany emesis in this species (King, 1988). All behaviors were timed from termination of irradiation.

Recording of locomotor activity. Locomotor behavior of each animal was recorded throughout the 2-hr observation period by an automated animal activity monitor (Opto-Varimex; Columbus Instruments, Columbus, OH) surrounding the Plexiglas chamber. Infrared photocells detected horizontal (ambulatory) and vertical (rearing) movements. Only vertical activity was analyzed because the burrowing behavior that accompanied emesis (King, 1988; Bermudez et al., 1988) interfered with recording naturally occurring horizontal movements. Locomotor activities of ferrets were monitored following irradiation with and without drug treatment. The sham-irradiated animals received drug ($n = 6$/compound) or vehicle ($n = 12$) as described previously. Animals were not habituated to the test chamber to optimize the levels of locomotor activity.

Data collection and statistical analysis. The following parameters were analyzed from the data recorded by the observer: 1) latency to first emesis; 2) duration of prodromal period of the acute radiation syndrome, or time interval between the start of the first emetic or retching episode and the termination of the final episode (King, 1988; in humans, the prodromal phase of radiation sickness [see Young, 1986] occurs hours to days postirradiation, and is manifest by nausea, vomiting, diarrhea, abdominal cramping and fatigue); 3) time spent vomiting or summed duration of all individual bouts; 4) number of emetic episodes; 5) individual expulsions and retches; 6) expulsions and retches per episode; 7) defecations (including attempts to defecate); 8) burrowing events, and 9) lip-licking episodes. Parameters 1 to 5 and 7 are linearly correlated with radiation dose in the ferret (King, 1988). Retching can be dissociated from vomiting with 5-HT₃ receptor antagonists or vagotomy (Andrews and Hawthorn, 1987; Hawthorn et al., 1988). Parameters 8 and 9 may represent, in ferrets, the behavioral concomitants of nausea in humans (Bermudez et al., 1988).

The above parameters were tabulated as mean ± S.E. for all vomiting animals in each group. Some data are presented graphically as a percentage of emetic control (saline + irradiation) animals. The nonparametric test for proportions (Bruning and Kintz, 1977) was used to calculate the significant incidence (percent) of emesis in response to drug treatment or vagotomy. Log-probit analysis was used to obtain the ED₅₀ values for the antiemetic effect of zacopride across radiation doses. The effect of drug treatment or vagotomy (with or without drug treatment) on each parameter was analyzed by analysis of variance. The nonparametric Wilcoxon test (Siegel, 1956) was used to compare the vertical activity of the locomotor control group (saline + sham-irradiation) of animals and the emetic control group (saline + irradiation) with those receiving other treatments. Statistical significance was assumed when P < .05.

To determine whether zacopride (at any single dose) or BMY25801 provided greater antiemetic protection for vomiting animals, the group-mean data for each emetic parameter (e.g., latency to first emesis and duration of prodromal period) were evaluated (table 1). If a significant difference from the emetic control value was determined by analysis of variance, the Newman-Keuls' multiple range test for unequal group means (Kramer, 1956) was applied to that parameter. This test was used to determine significant differences among drug treatments for each parameter at each radiation dose. Based on the results of this analysis, the group mean value for each parameter (at a single drug and radiation dose) was scored and ranked. A group mean value received a score of zero if it did not significantly differ from that of emetic control. A score of 1 indicated that a group-mean value significantly differed from emetic control. A score of 2 indicated that a group-mean value significantly differed from a group-mean score of 1. Group means received equal scores if they did not significantly differ from one another. The ranked scores for each drug treatment (e.g., 3 mg/kg BMY25801) effect on each parameter (e.g., latency to emesis) for each radiation dose (e.g., 2 Gy) were then summed. Averages were taken from these summed scores, and these averages were ranked according to the results given by the Kruskal Wallis test for the average rank sum.

Data from the vagotomized animals were also analyzed by analysis of variance and the Newman-Keuls' multiple range test for unequal

TABLE 1

Analysis of emetic parameter, latency to first emesis, in partially protected (vomiting) ferrets

Parameter	Radiation Dose (Gy)	Vehicle	Antiemetic Compound[a] (mg/kg)			BMY25801
			Zacopride			
			0.003	0.03	0.3	3.0
Latency to first emesis[b] (min)	2	21.7 ± 3.1	19.2 ± 1.6	42.3 ± 13.9	00[c]	[55][d]
	4	12.8 ± 0.4	19.0 ± 2.5	26.3 ± 0.7	[71.2]	47.7 ± 3.9
	6	10.7 ± 0.9		64.7 ± 2.2	18.0 ± 11	35.6 ± 3.2
Latency to first emesis[e] (rank)	2	0	0	1	nt	nt
	4	0	0	1	nt	2
	6	0	nt	2	0	1

[a] All compounds given i.p. 20 min before ^{60}Co irradiation at 1 Gy/min.
[b] All values are means ± S.E.; n for each group found in figure 1.
[c] No retching or emesis during 2-hr recording period.
[d] Numbers in brackets represent $n = 1$.
[e] Significant difference between vehicle and antiemetics determined by analysis of variance. Individual differences among antiemetics determined by the Newman-Keuls multiple range test for unequal group means (Kramer, 1956). Value of zero represents no difference from that for vehicle, value of 1 represents a significant difference (P < .05) from vehicle; value of 2 represents a significant difference (P < .05) from 1; nt = not tested.

group means (Kramer, 1956). Two sets of vagotomized animals were compared. 1) sham vs. ventral vs. dorsal vs. bilateral vagotomy, and 2) bilateral vs. bilateral + 0.03 mg/kg zacopride vs. bilateral + 0.3 mg/kg zacopride.

Drugs used. All drugs were prepared weekly in a 0.9% saline solution and refrigerated. Zacopride (4-amino-N-[1-azabicyclo(2.2.2)oct-3-yl]-5-chloro-2-methyoxybenzamide[E]-2-butenedioate] was a gift from A. H. Robins (Richmond, VA); BMY25801 (4-amino-5-chloro-N-[2-(diethylamino)ethyl]2-[1-methyl-2-oxoopropoxy] benzamide HCl) was a gift from Bristol-Myers (Wallingford, CT). All drugs were administered as the salt.

Results

Antagonism of radiation-induced emesis by zacopride or BMY25801. The two greater doses of zacopride (0.03 mg/kg, 0.3 mg/kg) and the single dose of BMY25801 (3 mg/kg) significantly reduced the incidence of radiation-induced emesis in the ferret. Table 2 describes the emetic dose-response incidence for all drug treatments and also shows that irradiation with 2, 4 and 6 Gy of ^{60}Co evoked emesis in all saline-treated animals. The elimination of emesis by zacopride appeared to be dose dependent, with 0.003 mg/kg being inactive and 0.3 mg/kg providing the greatest protection. The ED_{50} values for the antiemetic action of zacopride across the 2-Gy and 4-Gy radiation doses were identical at 0.026 mg/kg (table 2).

In addition to preventing emesis to radiation, both zacopride and BMY25801 ameliorated other parameters of the emetic

TABLE 2

Effect of pretreatment with zacopride or BMY25801 on the incidence of radiation-induced emesis

Radiation Dose (Gy)	NaCl	Antiemetic Compound[a] (mg/kg)				BMY25801
		Zacopride				
		0.003	0.03	0.3	ED_{50}[b]	3.0
2	10/10[c]	8/8	3/8*	0/6*	0.0260	1/10*
4	10/10	10/10	3/10*	1/10*	0.0263	11/11
6	8/8	nt[d]	3/10*	2/8*	nt	6/11*

[a] All compounds given i.p. 20 min before ^{60}Co irradiation at 1 Gy/min.
[b] Confidence levels = 0.0095, 0.072 mg/kg for 4-Gy dose; unable to test confidence levels for 2-Gy dose.
[a] Number of animals vomiting per number of animals tested. All animals observed for 2 hr postirradiation.
[d] nt = not tested.
* P < .05 as compared with NaCl treatment; the nonparametric test for proportions (Bruning and Kintz, 1977).

response in vomiting animals. As illustrated in figure 1, when compared with vehicle, both compounds increased the latency to the first emetic episode (table 1) and reduced the duration of the prodromal period of vomiting. The action of zacopride appeared to be dose-dependent for most doses of radiation tested. However, 0.3 mg/kg of zacopride failed to increase the latency to first emesis after 6-Gy irradiation. The attenuation of these factors by BMY25801 diminished with increasing doses of radiation.

Figure 2 shows that both compounds also significantly attenuated several other emetic parameters (table 3) in response to all radiation doses. At 2 Gy and 4 Gy (but not 6 Gy), zacopride acted in a dose-dependent manner to reduce the incidence of the parameters shown in figure 2. After 2-Gy irradiation, however, the reduction of these parameters by zacopride at the lower doses (0.003 mg/kg and 0.03 mg/kg) was not statistically significant. The degree to which these parameters were reduced by either a single dose of zacopride (0.03 mg/kg and 0.3 mg/kg) or BMY25801 did not differ between the 4-Gy and 6-Gy radiation doses. The compounds did not significantly affect the number of expulsions per episode, retches per episode or the incidence of defecations (data not shown). These parameters were not included in the final statistical analysis for ranking because they did not distinguish any ameliorative differences among the drugs and doses used. Thus, based on the analysis of the emetic parameters significantly altered by drug treatment in the partially protected (or vomiting) animals (figs. 1 and 2; table 1), the therapeutic antiemetic potencies of drugs (on a mg/kg basis) were ranked as follows: 3 mg/kg BMY25801 > 0.03 mg/kg zacopride > 0.3 mg/kg zacopride > 0.003 mg/kg zacopride.

During the 20-min interval between zacopride administration (at 0.03 and 0.3 mg/kg) and radiation exposure, several animals ($n = 9/20$) vomited, retched and/or defecated. These paradoxical responses to zacopride were further investigated and are described in a companion paper (King, 1990).

Antagonism of emesis-related behaviors by zacopride and BMY25801. Figure 3 shows that burrowing behavior in response to 4-Gy irradiation was significantly reduced in all animals by pretreatment with either zacopride or BMY25801. The burrowing in response to 2-Gy and 6-Gy irradiation was also reduced by these compounds, but that reduction was significant for only 0.03 mg/kg zacopride and BMY25801 after 2-Gy irradiation. In contrast, lip-licking behavior was not signif-
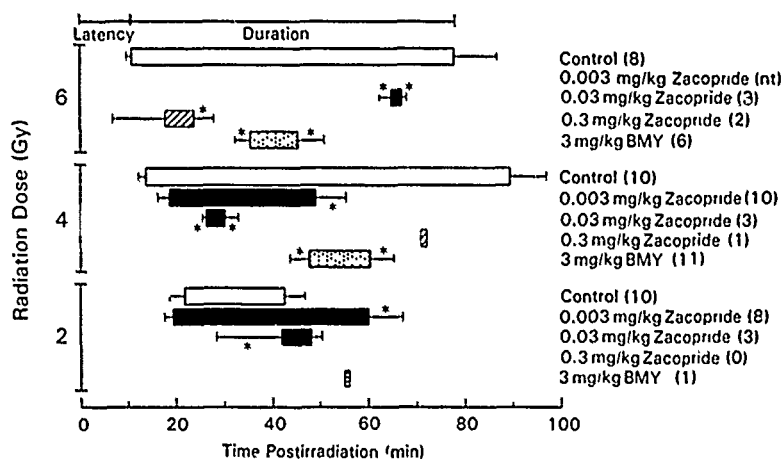
Fig. 1. Zacopride and BMY25801 affect latency to and duration of radiation-induced emesis in partially protected (vomiting) ferrets. Mean latency (±S.E.; left hand error bar) to first emetic episode is represented at time of origin of each bar. Mean duration (±S.E.; right hand error bar) of prodromal period is represented by length of each bar. N for each group is in parentheses after each drug dose; nt: not tested. Control animals were given injections of NaCl and all compounds were injected i.p. 20 min before ^{60}Co irradiation at 1 Gy/min. Animals were observed for 2 hr postirradiation. *P < .05 as compared with each emetic control group (Control); *at left hand error bar = latency; *at right hand error bar = duration.
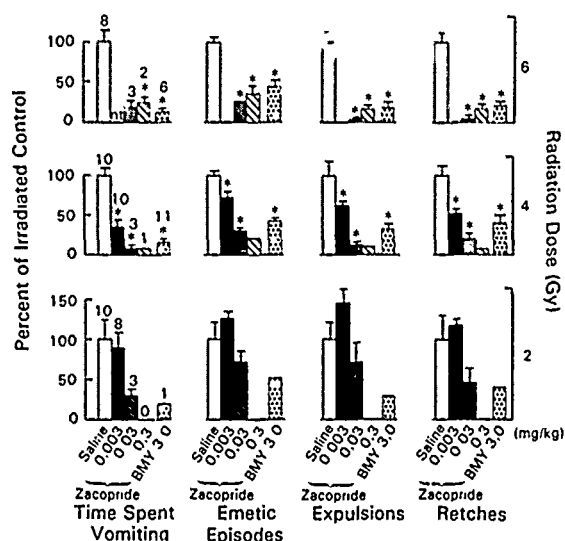

Fig. 2. Pretreatment with zacopride or BMY25801 reduces the incidence of emetic parameters in partially protected (vomiting) ferrets after irradiation. All compounds received injections i.p. 20 min before ^{60}Co irradiation at 1 Gy/min, and animals were observed for 2 hr postirradiation. The number above each bar (mean ± S.E.) represents the sample size of that group; nt = not tested. *P < .05 as compared with each emetic control group (saline) for each radiation dose. Mean values (mean ± S.E.) for the emetic control (saline) groups (table 3).

Fig. 3. Zacopride and BMY25801 reduce the incidence of burrowing episodes in the ferret in response to irradiation. All compounds were injected i.p. 20 min before ^{60}Co irradiation at 1 Gy/min, and animals were observed for 2 hr postirradiation. The number above each bar (mean ± S.E.) represents the sample size of that group; nt = not tested. *P < .05 as compared with each emetic control group (saline) for each radiation dose. The mean values (±S.E.) for the saline groups: 2 Gy, 4.9 ± 1.4; 4 Gy, 7.7 ± 1.8; 6 Gy, 2.9 ± 0.9.

icantly reduced by either zacopride or BMY25801 (data not shown).

Effect of zacopride or BMY25801 on locomotor activity. Most animals in all groups habituated to the recording chamber 1 hr postirradiation and locomotor activity was significantly reduced during the 2nd hr. The data were therefore analyzed for intervals of 1 to 30 min and 31 to 60 min postirradiation.

When compared with the locomotor control group (saline + sham irradiation), ferrets treated with zacopride alone exhibited a dose-dependent decrease in locomotor activity that was significant for the 0.03 mg/kg and 0.3 mg/kg doses during the first hour postirradiation (fig. 4, D1 and D2). Locomotor activity, however, was not affected by BMY25801 (fig. 4, D1 and D2) when administered to the sham-irradiated ferrets.

Radiation alone, at all doses, significantly depressed locomotor activity throughout the 1st hr postirradiation (fig. 4, A1, A2, B1, B2, C1 and C2). During the first 30 min postirradiation, zacopride failed to protect against this behavioral decrement

and, in some cases, potentiated it (fig. 4, A1 and B1). In contrast, BMY25801 maintained locomotor activity at levels comparable with those recorded for the emetic control group of animals for this 30-min period (fig. 4, A1, B1 and C1). During min 31 to 60 postirradiation, all zacopride plus radiation groups exhibited significantly less locomotor activity than the locomotor control group (fig. 4, A2, B2 and C2). By comparison, BMY25801 prevented the depression of locomotor activity at
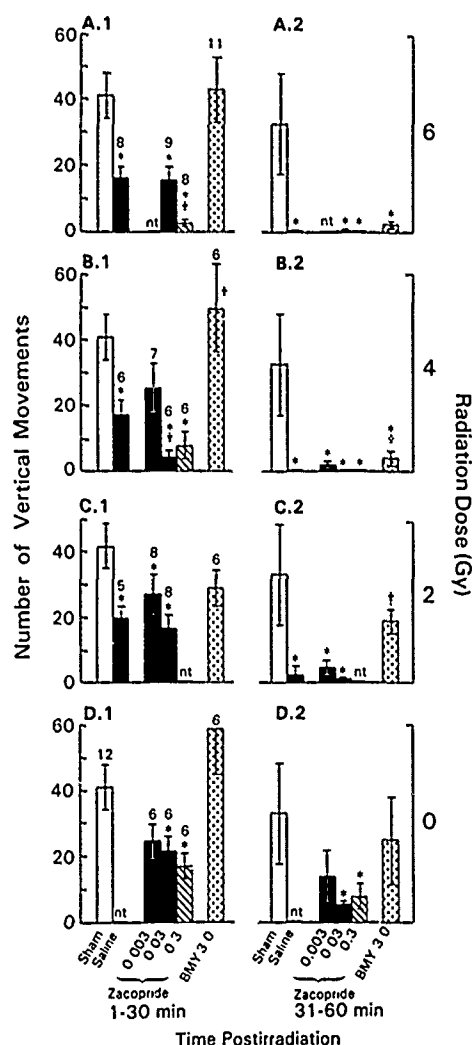
Fig. 4. Effect of zacopride or BMY25801 on vertical locomotor activity following irradiation or sham irradiation. Vertical activity (rearing) was monitored by an automated animal activity monitor. Infrared photodetectors recorded the number of vertical movements. The number above each bar (mean ± S.E.) represents the sample size of that group; nt = not tested. Radiation exposure: A, 6 Gy; B, 4 Gy; C, 2 Gy; D, sham irradiation. 1, First 30-min interval (1–30 min) postirradiation. 2, Second 30-min interval (31–60 min) postirradiation. *P < .05 as compared with locomotor control group (saline + sham irradiation; open bar). †P < .05 as compared with emetic control group (saline + irradiation).

2-Gy and 4-Gy irradiation during min 31 to 60 postirradiation (fig. 4, B2 and C2).

Effect of vagotomy. When compared with sham-vagotomy, only bilateral abdominal vagotomy significantly altered any of the emetic parameters recorded after 4-Gy irradiation (table 4). Bilateral abdominal vagotomy significantly: 1) increased the latency to first emesis; and 2) reduced the number of retches. Neither dorsal nor ventral vagotomy significantly affected any variable. All vagotomized and sham-vagotomized animals exhibited an emetic response to radiation.

The antiemetic action of zacopride was additive to the antiemetic action of bilateral vagotomy. Thus, when vagotomized animals were given zacopride, this treatment combination reduced the incidence of radiation-induced emesis (table 3). When compared with bilaterally vagotomized (vehicle) control animals, this combination significantly altered several emetic parameters: 1) time spent vomiting; 2) number of retches; and

TABLE 3
Emetic parameters[a] recorded for emetic control (saline) groups[b] after various radiation doses

Parameter	Radiation Dose		
	2 Gy	4 Gy	6 Gy
Time spent vomiting (min)	6.2 ± 1.2	15.8 ± 1.4	10.6 ± 1.6
No. emetic episodes	2.4 ± 0.4	4.7 ± 0.3	4.4 ± 0.3
No. expulsions	4.2 ± 0.7	9.7 ± 1.8	9.5 ± 1.3
No. retches	37.7 ± 8.6	68.3 ± 9.4	68.0 ± 8.7

[a] Values are mean ± S.E.
[b] See figure 2 for effects of antiemetics on these parameters

3) number of retches per episode. Although no significant difference was found between the doses of zacopride tested, the trend of ameliorative effect was toward the lower 0.03-mg/kg dose (table 3). This lower zacopride dose also reduced: 1) the number of expulsions, expulsions per episode, and defecations (data not shown); and 2) the incidence of radiation-induced emesis (P < .05).

Locomotor activity was also monitored in these groups of animals. Animals that received a ventral vagotomy showed a significant depression of locomotor activity during the first 30-min recording interval, when compared with the emetic control group (data not shown).

Discussion

Effects of zacopride and BMY25801 on emesis. The principal finding of this study was that two benzamide analogs, zacopride (0.03 mg/kg and 0.3 mg/kg) and BMY25801 (3 mg/kg), provided effective antiemetic protection for ferrets exposed to several 100%-emetic doses of ionizing radiation. Both compounds raised the ED_{50} for radiation-induced emesis in the ferret to values greater than untreated control animals (0.8 Gy; King, 1988), but the small sample of radiation doses precluded the calculation of precise ED_{50} values for that response. Nevertheless, our data do show that, for radiation, the ferret appears as sensitive to the antiemetic properties of zacopride as the nonhuman primate (0.3 mg/kg p.o.; Dubois et al., 1988). The 0.026-mg/kg ED_{50} value for zacopride's antiemetic effect at 4-Gy irradiation was 10-fold lower than that ED_{50} value reported for i.v. BMY25801 (0.24 mg/kg; 95% confidence levels = 0.04, 0.53 mg/kg) at an identical radiation dose (Gylys et al., 1988).

Although zacopride abolished radiation-induced emesis after the low radiation dose (2 Gy), neither compound totally eliminated emesis to the higher doses (4 Gy, 6 Gy). This finding agrees with results of other studies that challenged radiation-induced emesis to high-dose radiation with similar doses of zacopride or BMY25801 (Gylys et al., 1988; Dubois et al., 1988). However, this finding contrasts with studies that used these compounds to challenge cisplatin-induced emesis. In ferrets for example, BMY25801 attenuates the incidence and frequency of cisplatin-induced emesis (Gylys et al., 1988), whereas zacopride totally abolishes it (Costall et al., 1987). In dogs, cisplatin-induced emesis is abolished by both compounds (Gylys et al., 1988; Smith et al., 1989). Such differences in antiemetic action between the two compounds may reflect species differences in responsiveness to either the emetic stimuli or the antiemetics.

From the detailed analysis of the emetic parameters, a second significant finding was that BMY25801 provided a greater antiemetic effect in partially protected (or vomiting) animals than did zacopride. This result was unexpected because zacopride has a strong binding affinity for 5-HT$_3$ receptors (Barnes

TABLE 4

Action of vagotomy on emetic parameters following 4-Gy irradiation[*]

Parameter	Vagotomy					
	Sham	Unilateral		Bilateral[b]		
				Vehicle	+ Zacopride (mg/kg)	
		Dorsal	Ventral		0.03	0 30
No. vomiting/no. tested	9/9	8/8	8/8	8/8	4/8†	6/8
Latency to first emesis (min)	14.6 ± 2.0†	21.4 ± 2.8†	15.1 ± 2.2†	37.4 ± 4.4*	53.0 ± 12.6	39.3 ± 8.2
Time spent vomiting (min)	4.0 ± 1.0	2.7 ± 0.9	3.1 ± 0.6	2.8 ± 0.5	1.0 ± 0.3†	1.4 ± 0.4†
No. retches	42.4 ± 6.5†	30.9 ± 7.0	32.0 ± 4.8	23.8 ± 5.9*	4.3 ± 2.3†	13.7 ± 4.0
Retches per episode	13.2 ± 1.8	12.4 ± 1.9	10.2 ± 1.2	10.0 ± 1.4	3.4 ± 0.9†	9.1 ± 1.6

[*] Values are mean ± S.E.
[b] All compounds given i.p. 20 min before ^{60}Co irradiation at 1 Gy/min.
[*] P < .05, compared with sham vagotomy.
† P < .05, compared with bilateral vagotomy.

et al., 1988a); this affinity has not yet been shown for BMY25801 (Monkovic *et al.*, 1988). The broader antiemetic protection by BMY25801 was also unexpected because zacopride is more potent (on a mg/kg basis) than some other 5-HT₃ receptor antagonists in dogs (Cohen *et al.*, 1989) and is stronger than BMY25801 for cisplatin-induced emesis in ferrets (Costall *et al.*, 1987; Gylys *et al.*, 1988).

Our results may reflect the extent to which the data were analyzed. Gralla *et al.* (1979) also used a ranking system of data analysis (the Kruskal-Wallis rank sum test) to evaluate several antiemetics. These investigators recorded only three parameters of the emetic response: the latency to first emesis, the number of emetic episodes and the duration of emesis (time from first to last emesis). Currently, most investigators rely on a single dose of radiation (or cytotoxin) as the stimulus, and use a more limited number of emetic parameters for data analysis. For example, Gylys *et al.* (1988) used the frequency of emetic episodes as the measure of antiemetic protection by BMY25801. Had we analyzed such limited data, we would have found zacopride to have antiemetic action greater than or equal to BMY25801. Nevertheless, it appears from our data, and by inference from that of Gylys *et al.* (1988), that zacopride is more potent (on a mg/kg basis) in reducing the incidence of radiation-induced emesis. Our data suggest, however, that BMY25801 is the more protective compound for vomiting animals.

The dose-dependent action by zacopride to ameliorate emetic parameters within a single radiation dose was expected. However, zacopride more effectively ameliorated the parameters at 4 Gy and 6 Gy, rather than at 2 Gy. The similar efficacy of zacopride after 4 and 6 Gy would be expected if the two doses of radiation were virtually equivalent. In fact, the emetic responses of the emetic control group of animals were quite similar (*e.g.*, mean number of retches; see table 3). In vomiting animals, however, zacopride (at 0.003 mg/kg and 0.03 mg/kg) was less effective at the 2-Gy radiation dose than at the 4-Gy dose. These results were unexpected and suggest that different mechanisms contribute to emesis produced by low and high doses of radiation. This latter suggestion is not new (see Young, 1986), but our data disagree with what would be expected. Davis *et al.* (1988) reported that radiation-induced emesis in the ferret, in response to low (2 Gy) but not high (8 Gy) doses of radiation, was completely abolished by vagotomy or the 5-HT₃ receptor antagonist granisetron. If radiation-induced emesis in the ferret is vagally mediated by 5-HT₃ receptors, then the two

lower zacopride doses should have been more potent at the low dose of radiation. Our data imply a more complex role for the 5-HT₃ receptor in radiation-induced emesis.

It is possible that the emetic properties of zacopride contributed to its failure to provide better antiemetic protection. For example, when given at 0.3 mg/kg p.o., zacopride evokes an 80 to 100% incidence of emesis (King, 1990); when given 0.3 mg/kg i.p., a 40% incidence. As shown in figure 1, the mean latency to first emesis for animals given 0.3 mg/kg zacopride and exposed to 6-Gy irradiation did not differ from the mean latency observed for the emetic control group. This result does not conform to the dose-response relationship observed for the zacopride dose *vs.* the emetic latency at 2 Gy and 4 Gy, and could result from emetogenic properties of zacopride. When combined with vagotomy, the lower dose (0.03 mg/kg) of zacopride also appeared more protective than the higher dose (0.3 mg/kg; table 4). Such data suggest that the antiemetic potency of zacopride in the ferret cannot be fully appreciated until the emetic and antiemetic properties have been dissociated from one another.

Effects of zacopride and BMY25801 on emesis-related behaviors. Because lip-licking and burrowing by ferrets are attenuated by treatment with the 5-HT₃ receptor antagonist granisetron, they may represent behavioral concomitants of nausea in humans (Bermudez *et al.*, 1988). Lip-licking occurs in the conscious ferret in response to other emetic agents and in the anesthetized ferret to electrical stimulation of the vagus (King, unpublished observations). Unlike its response to granisetron, we found that the incidence of lip-licking was not significantly depressed by zacopride or BMY25801.

Zacopride and BMY25801, like granisetron (Bermudez *et al.*, 1988), significantly reduced burrowing behavior at the lower radiation doses (2 Gy, 4 Gy). The suppression of this behavior was not dose-dependent for zacopride. At the doses used, zacopride and BMY25801 produced similar levels of disruption. In contrast, locomotor activity was reduced by only zacopride (see below). The latter data suggest that the reduced burrowing does not represent a generalized decrease in locomotor behavior. It is uncertain, however, whether reduced burrowing in response to antiemetics truly represents reduced nausea-related behaviors. Burrowing is part of the ferret's normal behavioral repertoire and its occurrence after irradiation may represent a displacement activity. In turn, antiemetics may act in some other central or peripheral manner to reduce the incidence of this behavior.

Action of radiation, zacopride, and BMY25801 on locomotor behavior. In rodents, a decrement in spontaneous locomotor behavior in response to a compound is considered an index of sedation. Although such sedation has been observed in response to antiemetic benzamide analogues (*e.g.*, metoclopramide; see Jenner and Marsden, 1979), locomotor behavior can also be suppressed by other antiemetics (*e.g.*, nabilone; McCarthy and Borison, 1981; Stark, 1982). Without additional measurements (*e.g.*, an electroencephalogram), however, it is unclear whether the radiation- or zacopride-induced suppression of locomotor behavior in the ferret represents a central nervous system sedation. Radiation-induced decreases in locomotor behavior have not been previously reported for the ferret (King, 1988) but have been reported for other species (Landauer *et al.*, 1988). This locomotor decrement may represent a behavioral concomitant of the fatigue typically observed as part of the prodromal response to radiation exposure (see Young, 1986).

Zacopride also produced significant decrements in the ferret's locomotor activity that appeared to be dose-dependent. In addition, zacopride could potentiate the decrement produced by radiation. If this effect of zacopride represents central nervous system sedation, it may have contributed to zacopride's antiemetic action. However, the zacopride-induced decrement in locomotor activity may not result from a central nervous system sedation but rather a peripheral autonomic or somatic action (see McQueen and Mir, 1989; King, 1990). Others (Costall *et al.*, 1987) have failed to observe altered locomotor behavior to i.v. zacopride in the ferret, but their data were collected by gross observation rather than by an automated activity monitor. In addition, their animals were given zacopride while under anesthesia. The 15 to 20 min required to recover from anesthesia may have masked any sedation produced by zacopride.

In contrast to both radiation and zacopride, BMY25801 alone did not affect locomotor behavior in the ferret. More importantly, BMY25801 protected against the radiation-induced locomotor decrement recorded during the first 30 min postirradiation and provided partial protection during the second 30 min. BMY25801 produced significant locomotor decrements in the mouse only at the highest dose tested (100 mg/kg i.p.; Landauer *et al.*, 1990) and lacks sedative effects in both the dog and squirrel monkey at 12 mg/kg (i.v.) and 11 mg/kg (i.m.), respectively (Gylys *et al.*, 1988). Thus, in addition to its antiemetic properties, BMY25801: 1) can protect against some other effects of radiation; and 2) appears to lack behavioral side effects when used at therapeutic doses in several species.

Effect of vagotomy. To determine the site of action for zacopride, its antiemetic effects were evaluated in a series of irradiated animals that had received visceral vagotomies. When compared with laparotomy, bilateral vagotomy significantly increased the latency to the first emesis and reduced the number of retches. The former response has been observed in other species (Wang *et al.*, 1958; Carpenter *et al.*, 1986; Borison *et al.*, 1987). In comparison, zacopride alone produced these effects and also shortened the prodromal duration and reduced the number of expulsions. These results contrast with those of Andrews and Hawthorn (1987), who found that bilateral vagotomy and the 5-HT₃ receptor antagonist BRL24924 produced identical effects (*i.e.*, increased latency, shortened prodromata, and reduced retches and expulsions). Although Carpenter *et al.* (1986) also found that vagotomy did not influence prodromal

duration, the length of postoperative recovery may be a factor in this response. The vagotomized animals of Andrews and Hawthorn (1987) were irradiated within 7 days of surgery; our recovery period averaged 17 days; Carpenter *et al.* (1986) averaged 60 days. Andrews *et al.* (1990) has reported that for the ferret, the latency to emesis in response to some emetic compounds (*e.g.*, copper sulfate) varies inversely with recovery time from vagotomy. Such a relationship may also hold for the duration of radiation-induced emesis.

We extended the studies of Andrews and Hawthorn (1987) by administering zacopride to animals that received bilateral vagotomies and found that the addition of zacopride significantly increased the latency to and reduced the duration of emesis beyond that achieved by bilateral vagotomy alone. Thus, the action of zacopride does not depend on intact vagus nerves. This confirms Andrews' and Hawthorn's suggestion that anatomical sites other than the vagus are involved in the antiemetic action of 5-HT₃ receptor antagonists. One site may be the area postrema because it exhibits binding for 5-HT₃ receptor ligands in the ferret (Barnes *et al.*, 1988b). Intracerebroventricular injection of 5-HT₃ receptor antagonists can ameliorate cytotoxin-induced emesis in ferrets (Higgins *et al.*, 1989) and cats (Smith *et al.*, 1988).

Our vagotomy studies were the first to demonstrate that neither dorsal nor ventral abdominal vagotomy alone will alter radiation-induced emesis in the ferret. This may be a reflection of the bilateral distribution of both dorsal and ventral vagal afferents found in this species (Fitzakerley and Lucier, 1988a,b). This further contrasts with the differential effect of dorsal vs. ventral vagotomy on the ferret's emetic response to agents administered orally (King, 1990).

General significance of findings. In summary, we have compared the antiemetic and locomotor effects of two substituted benzamides, zacopride and BMY25801, in the ferret after irradiation. Zacopride was more potent (on a mg/kg basis), ameliorating emesis at 100-fold lower doses than BMY25801. However, analysis of emetic parameters in animals that vomited despite drug treatment demonstrated that BMY25801 provided broader antiemetic protection than did zacopride. Radiation and zacopride alone, but not BMY25801, also produced significant decrements in locomotor activity. BMY25801 also protected against the radiation-induced depression of locomotor behavior, which in turn could be further depressed by zacopride. The antiemetic action of zacopride appears to be mediated partially by the abdominal vagus nerve, but that action also includes other sites.

The i.p. route of administration used in our studies likely influenced the antiemetic and/or locomotor responses to both zacopride and BMY25801. For example, when given i.v., BMY25801 reduced emesis to 4-Gy irradiation by 50% (Gylys *et al.*, 1988), whereas we observed only a reduction in the intensity of emetic parameters to an identical dose of radiation. As another example, zacopride evokes a sedative-like action when given i.v. to the ferret (King, 1990). This effect is more pronounced than the one reported here, but is absent when given p.o. (King, 1990). The appearance of side effects at antiemetic doses for zacopride may also depend on the animal species tested. Although zacopride did not affect behavioral performance in the nonhuman primate, it was administered p.o. (Dubois *et al.*, 1988).

Nevertheless, our studies confirm that zacopride is an effective antiemetic for radiation in the ferret, as it is in other

species for cytotoxins (Smith *et al.*, 1988, 1989). The ferret continues to show much promise as an animal model for predicting 5-HT₃ receptor antagonists as potential antiemetics for human use (Bermudez *et al.*, 1988; Cassidy *et ai.*, 1988; Plezia *et al.*, 1988). It is likely, therefore, that zacopride will also prove to be an effective antiemetic against radiation- or cytotoxin-induced emesis in the clinic.

Acknowledgments

References

ANDREWS, P. L. R., DAVIS, C. J., BINGHAM, S., DAVIDSON, H. I. M., HAWTHORN, J. AND MASKELL, L.: The abdominal visceral innervation and the emetic reflex: Pathways, pharmacology, and plasticity. Can. J. Physiol. Pharmacol. **68**: 325-345, 1990.

ANDREWS, P. L. R. AND HAWTHORN, J.: Evidence for an extra-abdominal site of action for the 5-HT₃ receptor antagonist BRL24924 in the inhibition of radiation-evoked emesis in the ferret. Neuropharmacology **26**: 1367-1370, 1987.

BARNES, N. M., COSTALL, B. AND NAYLOR, R. J.: [³H]Zacopride: Ligand for the identification of 5-HT₃ recognition sites. J. Pharm. Pharmacol. **40**: 548-551, 1988a.

BARNES, N. M., COSTALL, B., NAYLOR, R. J. AND TATTERSALL, F. D.: Identification of 5-HT₃ recognition sites in the ferret area postrema. J. Pharm. Pharmacol. **40**: 586-588, 1988b.

BERMUDEZ, J., BOYLE, E. A., MINER, W. D. AND SANGER, G. J.: The anti-emetic potential of the 5-hydroxytryptamine₃ receptor antagonist BRL 43694. Br. J. Cancer **58**: 644-650, 1988.

BORISON, H. L., McCARTHY, L. E. AND JOHNSON, J. R.: High dorsal column cordotomy plus subdiaphragmatic vagotomy prevents acute ionizing radiation sickness in cats. Exp. Neurol. **98**: 645-658, 1987.

BRUNING, J. L. AND KINTZ, B. L.: Computational Handbook of Statistics, 2nd edition. Scott, Foresman and Co., Glenview, IL, 1977.

CARPENTER, D. O., BRIGGS, D. B., KNOX, A. P. AND STROMINGER, N. L.: Radiation-induced emesis in the dog: Effects of lesions and drugs. Radiat. Res. **108**: 307-316, 1986.

CASSIDY, J., RAINA, V., LEWIS, C., ADAMS, L., SOUKOP, M., RAPEPORT, W. G., ZUSSMAN, B. D., RANKIN, E. M. AND KAY, S. B.: Pharmacokinetics and antiemetic efficacy of BRL43694, a new selective 5HT-3 antagonist. Br. J. Cancer **58**: 651-653, 1988.

COHEN, M. L., BLOOMQUIST, W., GIDDA, J. S. AND LACEFIELD, W.: Comparison of the 5-HT₃ receptor antagonist properties of ICS 205-930, GR38032F and zacopride. J. Pharmacol. Exp. Ther. **248**: 197-201, 1989.

COSTALL, B., DOMENEY, A. M., NAYLOR, R. J. AND TATTERSALL, F. D.: 5-Hydroxytryptamine M-receptor antagonism to prevent cisplatin-induced emesis. Neuropharmacology **25**: 959-961, 1986.

COSTALL, B., DOMENEY, A. M., NAYLOR, R. J. AND TATTERSALL, F. D.. Emesis induced by cisplatin in the ferret as a model for the detection of antiemetic drugs. Neuropharmacology **26**: 1321-1326, 1987.

DAVIS, C. J , ANDREWS, P. L. R. AND HAWTHORN, J.. The mechanism of radiation induced emesis in the ferret. *In* Symposium on Nausea and Vomiting: A Multidisciplinary Perspective, November 12-13, 1988, University of Ottawa, Ontario, Canada. Satellite Symposium: 18th Annual Meeting Society for Neuroscience, Toronto, Ontario, Canada, 1988.

DE HAAN, J. L., DE MULDER, P. H. M., BEEX, L. V. A. M., DEBRUYNE, F. M. J., CHALLONER, T. AND DE PAUW, R. E.: The efficacy of GR38032F, an antagonist of 5-hydroxytryptamine-3 (5-HT₃) in the prophylaxis of cisplatin (CDDP)-induced nausea and vomiting. Eur. J. Cancer Clin. Oncol. **24**: 1383-1384, 1988.

DUBOIS, A., FIALA, N., BOWARD, C. A. AND BOGO, V.: Prevention and treatment of the gastric symptoms of radiation emesis. Radiat. Res. **115**: 595-604, 1988.

FITZAKERLEY, J. L. AND LUCIER, G. E.. Connections of a vagal communicating branch in the ferret I. Pathways and cell body location. Brain Res. Bull. **20**: 189-196, 1988a.

FITZAKERLEY, J. L. AND LUCIER, G. E.: Connections of a vagal communicating branch in the ferret II. Central projections. Brain Res. Bull. **20**: 479-486, 1988b.

GRALLA, E. J., SABO, J. P , HAYDEN, D. W., YOCHMOWITZ, M. G. AND MATTSSON, J. L.: The effect of selected drugs on first-stage radioemesis in beagle dogs. Radiat. Res. **78**: 286-295, 1979.

GYLYS, J., WRIGHT, R. N., NICOLOSI, W. D., BUYNISKI, J. P. AND CRENSHAW,

R. R.: BMY-25801, an antiemetic agent free of D₂-dopamine receptor antagonist properties. J. Pharmacol. Exp. Ther. **244**: 830-837, 1988.

HAWTHORN, J., OSTLER, K. J. AND ANDREWS, P. L. R.: The role of the abdominal visceral innervation and 5-hydroxytryptamine M-receptors in vomiting induced by the cytotoxic drugs cyclophosphamide and cis-platin in the ferret. Q. J. Exp. Physiol. **73**: 7-21, 1988.

HESKETH, P. J., MURPHY, W. K., LESTER, E. P., GANDARA, D. R., KHOJASTEH, A., TAPAZOGLOU, E., SARTIANO, G. P., WHITE, D. R., WERNER, K. AND CHUBB, J. M.: GR 38032F (GR-C507/75): A novel compound effective in the prevention of acute cisplatin-induced emesis. J. Clin. Oncol. **7**: 700-705, 1989.

HIGGINS, G. A., KILPATRICK, G. J., BUNCE, K. T., JONES, B. J. AND TYERS, M. B.: 5-HT₃ receptor antagonists injected into the area postrema inhibit cisplatin-induced emesis in the ferret. Br. J. Pharmacol. **97**: 247-255, 1989.

JENNER, P AND MARSDEN, C. D.: Minireview: The substituted benzamides—a novel class of dopamine antagonists. Life Sci. **25**: 479-486, 1979.

KING, G. L.: Characterization of radiation-induced emesis in the ferret. Radiat. Res. **114**: 599-612, 1988.

KING, G. L.: Emesis and defecations induced by the 5-hydroxytryptamine (5-HT₃) receptor antagonist zacopride in the ferret. J. Pharmacol. Exp. Ther. **253**: 1034-1041, 1990.

KING, G. L. AND KIEFFER, V. A.: Comparison of the anti-emetic action of two substituted benzamides, zacopride and BMY 25801. Soc. Neurosci. Abstr. **14**: 848, 1988.

KING, G., LANDAUER, M., KIEFFER, V., KESSLER, D. AND DAVIS, H.: Zacopride, a 5HT₃ antagonist, modifies emetic and behavioral responses to radiation in the ferret. FASEB J. **2**: A325, 1988.

KRAMER, C. Y.: Extension of multiple range tests to group means with unequal numbers of replications. Biometrics **12**: 307-310, 1956.

KRIS, M. G., GRALLA, R. J., CLARK, R. A. AND TYSON, L. B.: Phase II trials of the serotonin antagonist GR38032F for the control of vomiting caused by cisplatin. J. Natl. Cancer Inst. **81**: 42-46, 1989.

LANDAUER, M. R., DAVIS, H. D., DOMINITZ, J. A. AND WEISS, J. F.: Long-term effects of radioprotector WR-2721 on locomotor activity and body weight of mice following exposure to ionizing radiation. Toxicology **49**: 315-323, 1988.

LANDAUER, M. R., DAVIS, H. D. AND KING, G. L.: Zacopride and batanopride (BMY-25801): Effects on locomotor behavior of mice. FASEB J. **4**: A811, 1990.

McCARTHY, L. E. AND BORISON, H. L.: Antiemetic activity of N-methylevonantradol and nabilone in cisplatin-treated cats. J. Clin. Pharmacol. **21**: 30S-37S, 1981.

McQUEEN, D. S. AND MIR, A. K.: 5-Hydroxytryptamine and cardiopulmonary and carotid body reflex mechanisms. *In* The Peripheral Actions of 5-Hydroxytryptamine, ed. by J. R. Fozard, pp. 301-326, Oxford University Press, New York, 1989.

MINER, W. D. AND SANGER, G. J.: Inhibition of cisplatin-induced vomiting by selective 5-hydroxytryptamine M-receptor antagonism. Br. J. Pharmacol. **88**: 497-499, 1986.

MONKOVIC, I., WILLNER, D., ADAM, M. A., BROWN, M., CRENSHAW, R. R., FULLER, C. E., JUBY, P. F., LUKE, G. M., MATISKELLA, J. A. AND MONTZKA, T. A.: Substituted benzamides. 1. Potential nondopaminergic antagonists of chemotherapy-induced nausea and emesis. J. Med. Chem. **31**: 1548-1558, 1988.

PLEZIA, P. M., DAVIS, L. E., ALBERTS, D. S., DAVIS, A., GAREWAL, H. S., GREENBERG, B. R., SMALDONE, L. AND FAIRCHILD, C.: BMY-25801: An effective single agent antiemetic for cisplatin-induced nausea and vomiting. Proc. Am. Soc. Clin. Oncol. **7**: 294, 1988.

PRIESTMAN, T., CHALLONER, T., BUTCHER, M. AND PRIESTMAN, S.: Control of radiation induced emesis with GR38032F. Proc. Am. Soc. Clin. Oncol. **7**: 281, 1988.

SIEGEL, S.: Nonparametric Statistics for the Behavioral Sciences. McGraw-Hill, New York, 1956.

SMALDONE, L., FAIRCHILD, C., ROSENCWEIG, M., AAPRO, M., SARTIANO, G., PLEZIA, P. AND ALBERTS, D.: Dose-range evaluation of BMY-25801, a nondopaminergic antiemetic. Proc. Am. Soc. Clin. Oncol. **7**: 280, 1988.

SMITH, W. L., ALPHIN, R. S., JACKSON, C. B. AND SANCILIO, L. F.: The antiemetic profile of zacopride. J. Pharm. Pharmacol. **41**: 101-105, 1989.

SMITH, W. L., CALLAHAN, E. M. AND ALPHIN, R. S.: The emetic activity of centrally administered cisplatin in cats and its antagonism by zacopride. J. Pharm. Pharmacol. **40**: 142-143, 1988.

STARK, P.: The pharmacological profile of nabilone: A new antiemetic agent. Cancer Treat. Rev. **9**: suppl. B, 11-16, 1982.

WANG, S. C., RENZI, A A. AND CHINN, H. I.: Mechanism of emesis following X-irradiation. Am. J. Physiol. **193**: 335-339, 1958.

YOUNG, R. W.: Mechanisms and treatment of radiation-induced nausea and vomiting. *In* Nausea and Vomiting: Mechanisms and Treatment, ed. by C. J. Davis, G. V. Lake-Bakaar, and D. G. Grahame-Smith, pp. 94-109, Springer-Verlag, Berlin, 1986.

Therapeutic use of recombinant human G-CSF (rhG-CSF) in a canine model of sublethal and lethal whole-body irradiation*

T. J. MACVITTIE†, R. L. MONROY†‡, M. L. PATCHEN†
and L. M. SOUZA§

†Department of Experimental Hematology, Armed Forces Radiobiology
Research Institute, Bethesda, MD, U.S.A.
§AMGen., Thousand Oaks, CA, U.S.A.

The short biologic half-life of the peripheral neutrophil (PMN) requires an active granulopoietic response to replenish functional PMNs and to maintain a competent host defence in irradiated animals. Recombinant human G-CSF (rhG-CSF) was studied for its ability to modulate haemopoiesis in normal dogs as well as to decrease therapeutically the severity and duration of neutropenia in sublethally and lethally irradiated dogs. For the normal dog, subcutaneous administration of rhG-CSF induced neutrophilia within hours after the first injection; total PMNs continued to increase (with plateau phases) to mean peak values of 1000 per cent of baseline at the end of the treatment period (12–14 days). Bone-marrow-derived granulocyte–macrophage colony-forming cells (GM-CFC) increased significantly during treatment. For a sublethal 200 cGy dose, treatment with rhG-CSF for 14 consecutive days decreased the severity and shortened the duration of neutropenia and thrombocytopenia. The radiation-induced lethality of 60 per cent after a dose of 350 cGy was associated with marrow-derived GM-CFC survival of 1 per cent. Treatment with rhG-CSF markedly reduced the lethality associated with exposure to 350 cGy of radiation to zero. White blood cell (WBC) and platelet recovery kinetics were correlated with degree of marrow damage. The rhG-CSF reduced the severity and duration of neutropenia. Control animals required antibiotic therapy (WBC $< 1000 \, mm^3$) for a total of 16 days versus 3 days for rhG-CSF-treated dogs. The duration of thrombocytopenia was reduced, although the severity of depletion was unchanged with treatment. These data indicate that in the lethally irradiated dog, effective cytokine therapy with rhG-CSF will increase survival through the induction of earlier recovery of neutrophils and platelets.

1. Introduction

Survival after exposure to high doses of radiation depends on at least two factors: the survival of a critical number of haemopoietic stem cells (HSC) and the ability of these HSCs to generate an effective level of mature granulocytes and platelets within a critical, clinically manageable time period. The short biologic half-life of the peripheral granulocytes and platelets requires an active granulopoietic and thrombocytopoietic response to replenish functional neutrophils and platelets, to restore and maintain a competent host defence and to prevent inopportune haemorrhage.

Until recently we could not, with the exception of marrow transplantation, therapeutically treat radiation-induced stem cell aplasia and consequent sepsis and haemorrhage, except by providing clinical support, such as administration of fluids, antibiotics and platelets. Evidence from recent experiments using purified growth factors in murine (Fujisawa *et al.* 1986, Tsuchuja *et al.* 1987, Shimamura *et al.* 1987, Moore and Warren 1987, Tanikawa *et al.* 1989, Kobayashi *et al.* 1987, Broxmeyer *et al.* 1987, Cohen *et al.* 1987, 1988, Kindler *et al.* 1986, Lord *et al.* 1986), canine (MacVittie *et al.* 1988a,b, Lothrup *et al.* 1988, Lam *et al.* 1989, Schuening *et al.* 1989), and non-human primate (Welte *et al.* 1987, Monroy *et al.* 1988, Krumwieh and Seiler 1989, Mayer *et al.* 1987, Donahue *et al.* 1986) models of radiation-induced or drug-induced myelosuppression and in phase I and II clinical trials (Bronchud *et al.* 1987, Brandt *et al.* 1988, Antman *et al.* 1988, Jakubowski *et al.* 1989, Hammond *et al.* 1989) has provided new and interesting possibilities regarding therapeutic enhancement of stem cell and progenitor cell recovery. Additional evidence from *in vivo* studies has indicated that these recombinant cytokines can also prime end cells, such as granulocytes, to function more efficiently (Mayer *et al.* 1987, Cohen *et al.* 1988, Kaplan *et al.* 1989, Baldwin *et al.* 1988, Sullivan *et al.* 1989). Some clinical trials, however, have shown that therapy with recombinant human granulocyte–macrophage colony-stimulating factor (rhGM-CSF) did not enhance neutrophil function (Buescher *et al.* 1988, Jakubowski *et al.* 1989, Peters *et al.* 1988, Hammond *et al.* 1989). Clearly, the design of competent therapeutic modalities for the use of recombinant cytokines will depend on defining protocols that balance the ability of these proteins to induce self-renewal and differentiation of haemopoietic target cells, activation of mature end cells, and induction of other interactive cytokines.

Here, we studied recombinant human granulocyte colony-stimulating factor (rhG-CSF) for its ability to modulate haemopoiesis in normal dogs and to decrease therapeutically the severity and duration of neutropenia and thrombocytopenia in sublethally and lethally irradiated dogs.

2. Materials and methods

2.1. *Dogs*

Purpose-bred beagles, mean weight 10.0 ± 0.8 kg, were housed in individual stainless-steel cages in conventional holding rooms of the AAALAC-accredited animal facility at the Armed Forces Radiobiology Research Institute. The dogs were provided 10 air changes of 100 per cent fresh air, conditioned to $21 \pm 2°C$ with a relative humidity of 50 ± 10 per cent; they were maintained on a 12-h light/dark full-spectrum lighting cycle with no twilight, and provided with tap water *ad libitum* and commercial canine chow. Research was conducted according to the principles enunciated in the *Guide for the Care and Use of Laboratory Animals*, prepared by the Institute of Laboratory Animal Resources, National Research Council.

2.2. *Irradiation and clinical support*

Dogs were bilaterally exposed to uniform, homogeneous, whole-body ^{60}Co radiation from the AFRRI opposing ^{60}Co sources, at a dose rate of 40 cGy/min; total doses, measured at midline tissue depth, were 200 or 350 cGy. Radiation exposure took place in well ventilated Plexiglas restraint boxes (after prior acclimatization).

Ringer's lactate was administered (20 ml/kg by slow i.v. drip into a lateral cephalic vein over 1 h and 20 ml/kg per day s.q. between the shoulder blades) at signs of dehydration.

An antibiotic regimen was initiated when the white blood cell (WBC) count dipped below 1000/µl and continued daily until the WBC rose above that value for 3 consecutive days. Gentamicin (1·5 mg/kg, q12) and claforan (cephotaxime sulphate, 5 mg/kg, q12) were both given intramuscularly. Fresh, irradiated (1500 cGy) platelets, from a random donor pool, were administered when the platelet count dipped below 40,000/µl. The volume and concentration of platelets infused depended on the yield from donor dogs.

2.3. *Cellular analysis*

Bone marrow aspirations from the iliac crest were performed on intubated dogs anaesthetized with 4 per cent Biotal solution given i.v. by cephalic vein to the desired effect. Bone marrow and peripheral blood cells were separated over ficoll-hypaque; light-density ($<1·077$ g/ml) mononuclear cells (MNC) were washed and diluted in Dulbecco's modified Eagle's medium (DMEM) supplemented with 2 per cent heat-inactivated fetal calf serum. Heparinized peripheral blood was drawn at selected intervals for peripheral haematological values (WBC, haematocrit, platelet counts and differential counts). Marrow smears were also made for differential counts after staining by DifQuik. Body temperatures were taken daily.

2.4. *Canine GM-CFC assay*

Marrow and peripheral blood-derived GM-CFC were assayed using the double-layer agar technique as previously described (MacVittie *et al.* 1984). Briefly, colony-stimulating activity (CSA) was provided from pooled plasma from dogs previously injected with endotoxin. CSA at a concentration of approximately 7 per cent (v/v), was added to the lower agar layer while marrow-derived or blood-derived MNC were plated in the upper agar layer at appropriate concentrations for detection of GM-CFC-derived colonies (>50 cells) after a 10-day incubation at 37°C in 5 per cent CO_2 humidified atmosphere.

2.5. *Treatment protocol*

Normal and irradiated dogs were administered rhG-CSF s.c. in a 5 ml bolus, once per day, on a daily basis. The rhG-CSF was supplied by AMGen Corp., Thousand Oaks, CA. This 174-amino acid protein is a nonglycosylated, single-chain polypeptide, has a molecular weight of 18·6 kilodaltons, is produced by *Escherichia coli*, and is purified by a series of chromatographic steps (Souza *et al.* 1986). The final product was formulated in an aqueous buffer as a sterile solution at a concentration of 0·53 mg/ml. The rhG-CSF was diluted in sterile, pyrogen-free Hanks' balanced salt solution to a final solution for injection.

The dose–response study used three rhG-CSF doses at 10 µg/kg, 2 µg/kg and 1 µg/kg of canine body weight per day for 14 consecutive days. Dogs receiving 200 cGy and 350 cGy exposures were injected with the 10 µg/kg dose for 14 and 21 consecutive days, respectively, beginning at 07.00 the day after irradiation.

3. Results

3.1. *Normal canines: rhG-CSF dose response and haemopoiesis*

A dose-dependent increase in WBC was observed within hours of the first injection of rhG-CSF, and the WBC counts continued to increase to peak values of

approximately 900 per cent, 400 per cent, and 215 per cent of control for 10 μg/kg, 2 μg/kg, and 1 μg/kg doses, respectively (figure 1a). The mature, segmented neutrophil was the predominant cell type, increasing to 1000 per cent of control levels after the 10 μg/kg dose, with periodic increases in the percentage of the less mature band forms. Circulating PMNs returned to normal levels within 3–7 days (depending on dose) after cessation of rhG-CSF injection (figure 1b).
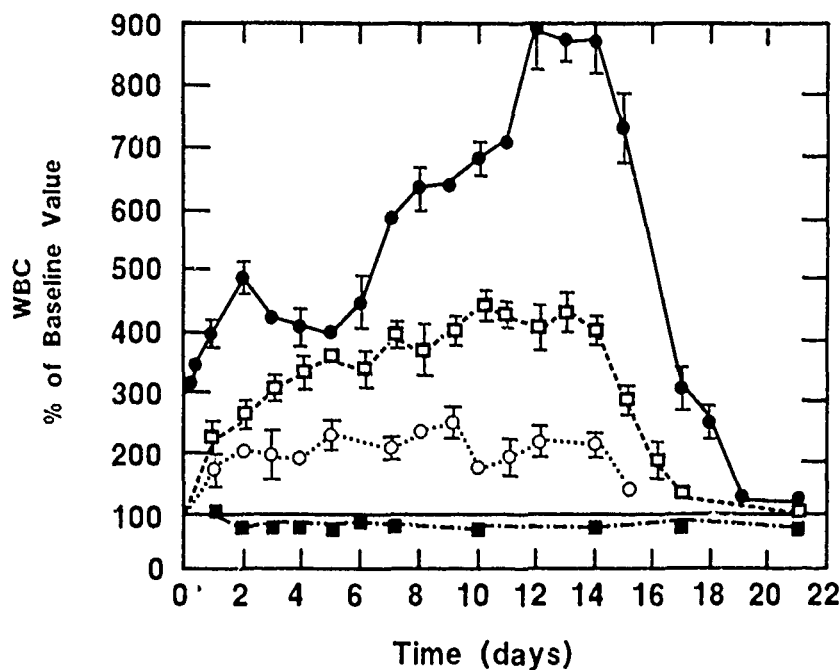
(a)

Figure 1 (a) Peripheral WBC response, as a percentage of baseline values ($\pm$SEM) to injection of rhG-CSF with time (days) during and after injecti n protocol. Dose of 10 μg/kg per day($\bullet$), 2 μg/kg per day ($\square$) and 1 μg/kg per day (O) (n=6, 4, and 4 animals, respectively). ($\blacksquare$) Platelets (10 μg/kg dose) as percentage of baseline values. (b) Peripheral neutrophil response, as a percentage of baseline values($\pm$SEM) in response to treatment with rhG-CSF; 10 μg/kg per day ($\bullet$), 2 μg/kg per day (O), and 1 μg/kg per day ($\blacksquare$).
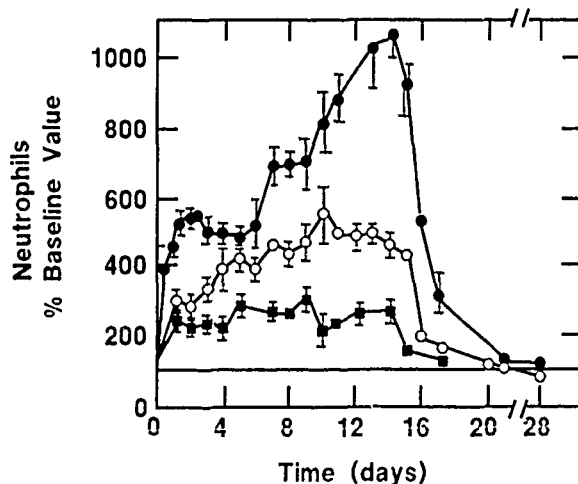
(b)

Bone-marrow-derived GM-CFC (per 10^5 MNC), after an initial drop in concentration, increased to a peak value of 180 per cent of control during the 7th day of rhG-CSF administration (table 1). The concentration of GM-CFC, despite continued rhG-CSF administration, decreased to within the normal range by the end of the treatment period. Peripheral-blood-derived GM-CFC increased significantly within 3–4 days after initiation of rhG-CSF injections to values 2000 per cent of baseline. Elevated levels were maintained throughout the treatment period, however, declining to normal values within 3 days after treatment was terminated.

3.2. *Irradiated dogs: 200 cGy sublethal exposure*

The rhG-CSF administered from Day 1 through Day 15 after irradiation with 200 cGy ^{60}Co significantly reduced the severity and duration of leukopenia (figure 2a). WBC from irradiated control-treated dogs decreased within 8 days to values 25 per cent of baseline, and required 6–7 weeks for recovery to normal values. The injection of rhG-CSF elicited an early rise in WBC (discharge of marrow neutrophils) through the 4th day of treatment. The nadir at Day 5 (WBC levels at 50 per cent of baseline) was followed by a marked increase in WBC, which peaked 1 day after cessation of rh-GCSF treatment at values 145 per cent of baseline. After treatment ended, WBC decreased to a second nadir at 45 per cent of baseline by Day 21, but increased to normal levels by Day 27, 3 weeks ahead of the control animals.

Treatment with rhG-CSF also reduced the duration of thrombocytopenia while having no significant effect on the severity of platelet loss (figure 2b). Platelet levels in control animals remained depressed (5 per cent of baseline) through 21 days after exposure. Recovery occurred later, with platelets reaching normal levels by Day 50. The rhG-CSF-treated animals showed evidence of platelet recovery as early as Day 15, with significant recovery occurring at Day 19, and reached normal levels by Day 35, 15 days ahead of the control animals.

Table 1. Marrow and peripheral blood derived GM-CFC[a]: response to injection of rhG-CSF.

Time (days)	GM-CFC (percentage of baseline[b])	
	Marrow	Blood
2	72±11	125±31
4	163±15	2075±350
7	180±12	—[c]
8	—	1650±425
10	125±8	1775±280
14	102±7	3300±670
16	—	525±225
17	115±5	—
21	110±5	100±20

[a] GM-CFC per 10^5 mononuclear cells as a percentage of baseline values; rhG-CSF was injected at 10 μg/kg per day for 14 consecutive days. Marrow and peripheral blood determinations are from five and six animals, respectively.

[b] Baseline value for marrow GM-CFC/10^5 MNC was 46·4, baseline value for blood GM-CFC was 0·4/10^5 MNC.

[c] Dashed line indicates no data at that time point.

Examination of the marrow-derived GM-CFC concentration revealed a signifi-
cant differential in recovery between rhG-CSF-treated animals and control animals
(table 2). The GM-CFC concentration in rhG-CSF-treated animals reached
levels 50 per cent of control within 7 days, while comparable control animals had
GM-CFC concentrations that were less than 10 per cent of baseline.

3.3. Irradiated dogs: 350 cGy lethal exposure

A midline tissue dose of 350 cGy was lethal for 60 per cent of the exposed dogs
(eight of 12) within the 30-day examination period; mean survival time was 20 ± 2
days. This degree of lethality or survival depended on the dogs receiving clinical
support (see §2). The 350 cGy dose was lethal for all canines not receiving clinical
support. The $LD_{50/30}$ values for unsupported and supported dogs were 260 and
340 cGy, respectively.
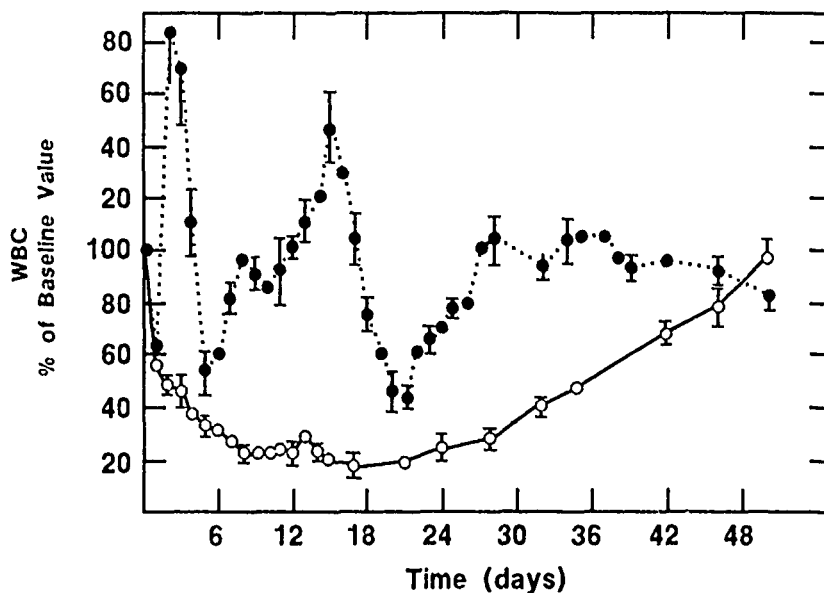
(a)

Figure 2. Recovery pattern
of (a) peripheral WBC:
control (O); rhG-CSF
(●); and (b) circulating
platelets: control (●);
rhG-CSF (■); as a per-
centage of baseline
values (±SEM) after
200 cGy whole-body
^{60}Co irradiation in re-
sponse to treatment
with rhG-CSF. Con-
trol values from 12
animals, rhG-CSF
value from four
animals.
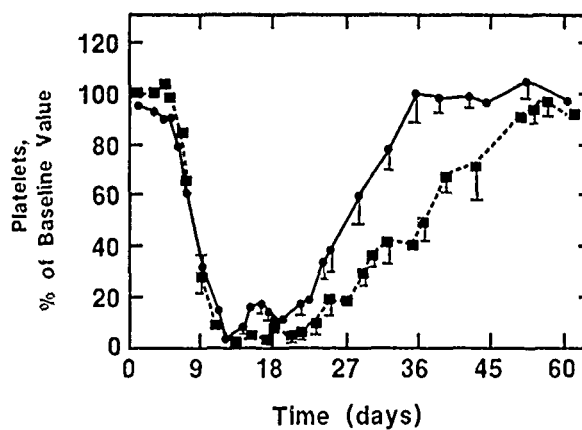
(b)

Table 2. Bone-marrow-derived progenitor cells: GM-CFC recovery after 200 cGy irradiation (percentage of baseline value)[a].

	Treatment	
Day of treatment	Control	rhG-CSF[b]
2	5±1	8±3
4	8±2	13±3
7	8±2	48±8
10	10±2	42±7
14	15±4	50±8
21	20±3	85±8
28	46±5	75±11
35	73±5	88±10

[a] Baseline value control and rhG-CSF-treated dogs was 100.

[b] rhG-CSF was injected at 10 μg/kg per day for 14 consecutive days. Marrow determinations are from 12 animals and four animals for control and rhG-CSF-treated dogs, respectively.

This model was designed to test whether therapeutic administration of rhG-CSF into mid-lethally irradiated dogs would increase survival through expansion of granulopoiesis and production of neutrophils, without exhausting the severely depleted stem cell pool.

Administration of rhG-CSF, beginning at Day 1 after exposure and continuing for 21 consecutive days, reduced lethality to zero, reduced the severity of neutropenia and although the severity of thrombocytopenia remained unaffected, significantly reduced the duration of these respective aplasias (figure 3a,b). All surviving dogs have normal WBC and platelet levels at 300–350 days post-exposure.

WBC in rhG-CSF-treated dogs were reduced to the level of control-irradiated animals for an average of 3 days, versus 15 days for irradiated controls. Recovery of WBC in rhG-CSF-treated dogs began at Days 13–14 and rose to levels approximately 250 per cent of baseline by Day 22, 1 day after treatment ended. WBC decreased over the following 5 days to levels that remained within the normal baseline range. Control-irradiated dogs, in contrast, required 60 days or more to reach within normal levels.

In irradiated controls, platelets required approximately 28 or 29 days to initiate recovery after exposure to 350 cGy, versus 23 or 24 days in rhG-CSF-treated dogs (figure 3b). Normal values were reached within 46 days and 80 days for rhG-CSF-treated and control-irradiated dogs, respectively.

4. Discussion

Our findings demonstrate the therapeutic efficacy of rh-CSF in a canine preclinical model of moderate to severe radiation-induced myelosuppression. The therapeutic administration of rhG-CSF reduced the severity and duration of neutropenia and decreased the period of thrombocytopenia after sublethal and lethal radiation exposure. Administration of rhG-CSF also dramatically increased survival, from 40 per cent to 100 per cent, for the animals exposed to 350 cGy of radiation.
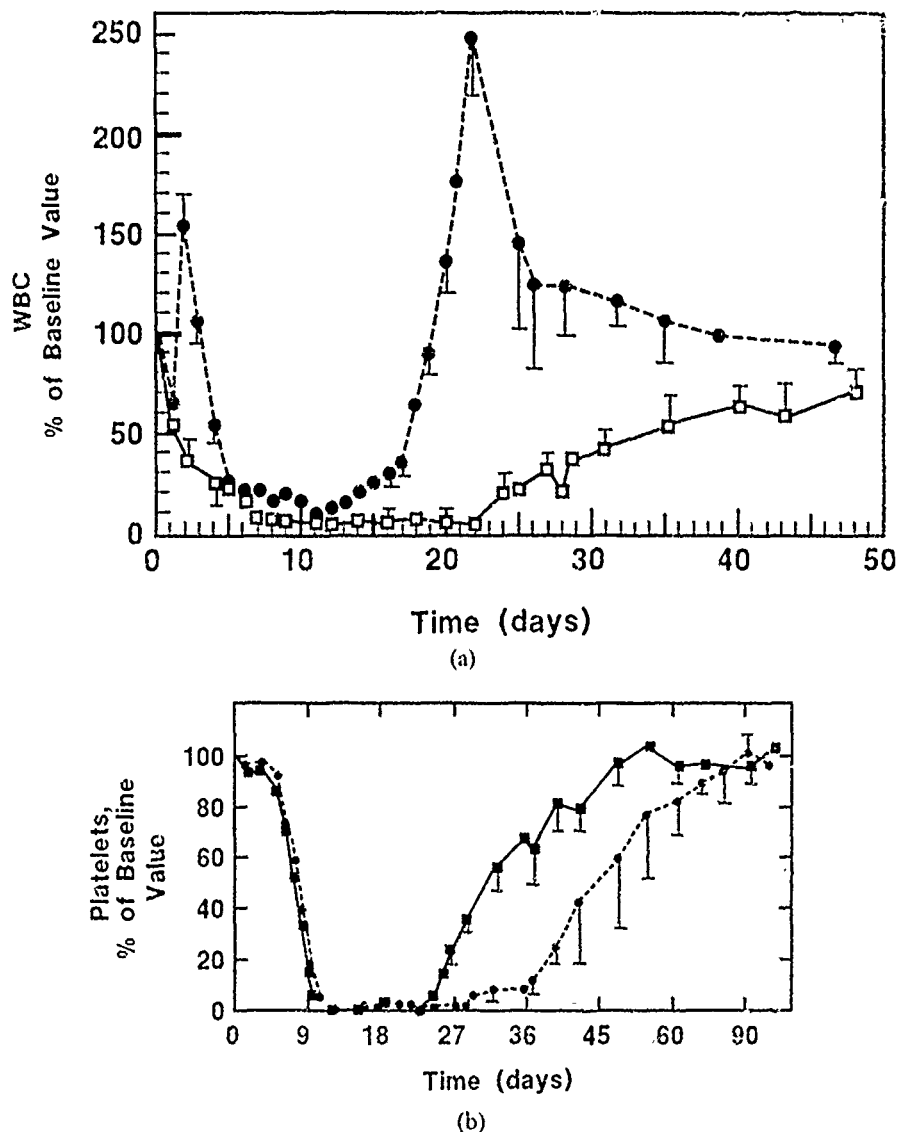
Figure 3. Recovery pattern of (a) peripheral white blood cells (WBC): control (□); rhG-CSF (●); and (b) circulating platelets: control (●); rhG-CSF (■); as a percentage of baseline values (±SEM) after 350 cGy whole-body ^{60}Co irradiation in response to treatment with rhG-CSF. Control values from 12 animals, rhG-CSF values from four animals.

The administration of rhG-CSF to normal dogs demonstrated its efficacy in stimulating marrow-derived granulopoiesis, releasing marrow-derived GM-CFC into the blood, and increasing peripheral WBC and absolute neutrophil levels. Peripheral neutrophil levels were increased in a dose-dependent manner, with a concomitant but modest increase in marrow-derived GM-CFC concentration. Peripheral neutrophil levels increased to values approximately 1000 per cent of baseline within 12–14 days of daily rhG-CSF administration, demonstrating the significant amplification potential of the rhG-CSF target precursor cells. The

efficacy of *in vivo* administration of rhG-CSF to dogs is similar to that observed in mice (Fugisawa *et al.* 1986, Tsuchuja *et al.* 1987, Shimamura *et al.* 1987, Moore and Warren 1987, Kobayashi *et al.* 1987, Tanikawa *et al.* 1989), hamsters (Cohen *et al.* 1987, 1988), and the non-human primates (Welte *et al.* 1987, Krumwieh and Seiler 1989), and serves as the basis for determining its use as a preclinical model for CSF therapy.

4.1. *Exposure to 200 cGy*

The therapeutic action of rhG-CSF in the 200-cGy sublethal dose model confirms the regenerative activity of rhG-CSF observed in the mouse after irradiation (Kobayashi *et al.* 1987, Tanikawa *et al.* 1989) and chemotherapy (Shimamura *et al.* 1987, Moore and Warren 1987, Cohen *et al.* 1987, 1988, Matsumoto *et al.* 1987, Tamura *et al.* 1987), and in the cyclophosphamide-treated non-human primate (Welte *et al.* 1987). Kobayashi *et al.* (1987), using purified G-CSF therapeutically administered to mice from Day 1 to Day 14 after doses of 300 cGy or 500 cGy X-irradiation, reduced the period of neutropenia and significantly enhanced recovery of marrow and splenic-derived GM-CFC, compared with controls. Tanikawa *et al.* (1989), using a murine, high-dose sublethal model (750 cGy), recently showed the therapeutic efficacy of rhG-CSF and rhGM-CSF. This extensive study showed the ability of each of these recombinant CSFs to enhance leukocyte as well as platelet recovery along with the regeneration of CFU-S, GM-CFC, BFU-E, and megakaryocyte CFC. Moore and Warren (1987) also documented the ability of rhG-CSF to induce multilineage CFC recovery in cyclophosphamide-induced myelosuppression in mice. Welte *et al.* (1987) demonstrated that while rhG-CSF effectively reduced the 4-week period of neutropenia after cyclophosphamide treatment to 1 week in the cynomolgus monkey, and induced marrow aspirate recovery of all lineage precursors, rhG-CSF did not induce a differential recovery of platelets. In our study 14 consecutive days of rhG-CSF administration to 200 cGy irradiated dogs induced earlier recovery of circulating platelets and dramatically affected regeneration of granulocytes and marrow-derived GM-CFC. As suggested by Welte *et al.* (1987), these recovery patterns after marrow-ablative radiation or drug treatment indicate that the availability of growth factor is a critical limiting step in recovery of the depleted haemopoietic system: the impressive recovery of recombinant CSF-treated animals after radiation is indicative of the proliferative ability of surviving progenitor cells capable of responding to the CSFs. Our data reported for rhG-CSF, data showing the efficacy of recombinant GM-CSF (Tanikawa *et al.* 1989, Monroy *et al.* 1988), and data on the combined use of rhG-CSF and rhIL-1 (Moore and Warren 1987) demonstrate the inability of therapeutically used lineage-specific factors to deplete the stem cell pool that survives sublethal exposure to radiation or drugs to a level that would not support survival.

4.2. *Exposure to 350 cGy*

Exposure of the dog to midline tissue radiation dose of 350 cGy ^{60}Co is 100 per cent lethal without clinical support with fluids, antibiotics and fresh platelets. The $LD_{50/30}$ without supportive therapy is approximately 260 cGy (MacVittie *et al.* 1984), whereas supportive therapy raises the $LD_{50/30}$ to 340 cGy (unpublished data). Exposure to 350 cGy is 60 per cent lethal with supportive therapy. Thus, clinical support alone produces a dose reduction factor of approximately 1·3, which

is the consequence of spontaneous regeneration of stem and progenitor cells during the increased survival time afforded by the support regimen. Survival time of descendants is increased approximately 6–8 days, that is, from 12–16 days to 18–22 days for unsupported and supported dogs, respectively. Effective therapy for lethally exposed dogs must either influence the spontaneous regeneration of stem cells during the critical period or extend the time of the clinically manageable period.

Data presented here indicate that single-agent therapy with rhG-CSF effectively influences the regeneration kinetics of the surviving haemopoietic cells during the increased clinically manageable time period. Granulocytes and platelets are effectively produced earlier, and the overall severity of neutropenia is reduced, as shown by the diminished period of antibiotic support (i.e. days of WBC $<1000/\mu l$). These results further emphasize the regenerative capacity of the haemopoietic system and the ability of rhG-CSF to stimulate a target cell pool that is normally unable to support survival of more than 40 per cent of all dogs exposed, even when they are given maximum clinical support. The ability of rhG-CSF to influence both granulocyte and platelet recovery suggests that CSF acts on multipotent stem cells and lineage-specific progenitor cells, and/or that rhG-CSF can synergize with other endogenously released CSFs to affect multi- and specific-lineage regeneration. Schuening *et al.* (1989) have most recently shown the effectiveness of rhG-CSF therapy following an $LD_{100/30}$ exposure of 400 cGy. Our data are in accord with these results, although Schuening *et al.* used 10-fold ($100\,\mu g/kg$ per day) our dose ($10\,\mu g/kg$ per day) of rhG-CSF in a divided, twice-daily subcutaneous injection in comparison to our single injection. These authors also did not report any effect on platelet recovery in the lethally irradiated and treated animals.

Although G-CSF was thought to be lineage-specific relative to the more multipotent capacity of GM-CSF, recent data from *in vitro* studies by McNiece *et al.* (1988a) suggest that G-CSF can act in synergy with IL-3 to promote megakaryocyte and platelet development. McNiece *et al.* (1988b, 1989). Williams *et al.* (1987) and Ferrero *et al.* (1989) have also demonstrated the *in vitro* synergistic activity of the major CSFs on proliferation of GM-CFCs and the high proliferative potential CFCs (HPP-CFC) in murine and human-derived marrow. Ikebuchi *et al.* (1988) have demonstrated the ability of G-CSF to synergize with IL-3 to enhance the IL-3-dependent proliferation of multipotent blast cell colonies. They proposed that the synergism was a consequence of shortening the G_0 period for stem cells. Whatever the mechanism of rhG-CSF action, it is apparent that even after lethal doses of radiation, surviving haemopoietic cells are available and capable of responding to the CSF. It is availability of the CSF that limits the rate of response, because the exogenously administered G-CSF can induce regeneration. It may also be possible that the administered G-CSF can interact with limited amounts of endogenously produced IL-3 to promote megakaryocyte and platelet production, induce synthesis and release other cytokines within the haemopoietic micro-environment.

The observation described herein, and that of Schuening *et al.* (1989), that rhG-CSF can increase survival through regeneration of haemopoiesis in an otherwise lethally irradiated dog, emphasizes the efficacy of single-agent CSF therapy in combination with clinical support in severe radiation- or drug-induced myelosup-

pression. These data provide the basis from which to titrate the radiation dose, and thus the degree of stem cell depletion from which recovery with single-agent therapy cannot be induced within the clinically manageable time period. Furthermore, these data provide the framework from which to approach future therapeutic strategies involving combined CSFs and interleukins.

References

ANTMAN, K. S., GRIFFIN, J. D., ELIAS, A., SOCINSKI, M. A., RYAN, L. CANNISTEN, S. A., OETTE, D., WHITLEY, M., FREI E., and SCHNIPPER, L. E., 1988, Effect of recombinant human granulocyte-macrophage colony stimulating factor on chemotherapy-induced myelosuppression. *New England Journal of Medicine,* **319**, 593–598.

BALDWIN, G. C., GASSON, J. C., QUAN, S. G., FLEISCHMANN, J., WEISBART, R., OETTE, D., MITSUYASU, R. T., and GOLDE, D. W., 1988, Granulocyte-macrophage colony-stimulating factor enhances neutrophil function in acquired immunodeficiency syndrome patients. *Proceedings of the National Academy of Sciences, U.S.A.,* **85**, 2763–2766.

BRANDT, S. J., PETERS, W. P., ATWATER, S. K., KURTZBERG, J., BOROWITZ, M. J., JONES, R. B., SHPALL, E. J., BAST, R. C., GILBERT, C. J., and OETTE, D. H., 1988, Effect of recombinant human granulocyte-macrophage colony-stimulating factor on hemopoietic reconstitution after high dose chemotherapy and autologous bone marrow transplantation. *New England Journal of Medicine,* **318**, 869–876.

BRONCHUD, M. N., SCARFFE, J. H., THATCHER, N., CROWTHER, D., SOUZA, L. M., ALTON, N. K., TESTA, N. G., and DEXTER, T. M., 1987, Phase I/II study of recombinant human granulocyte colony-stimulating factor in patients receiving intensive chemotherapy for small cell lung cancer. *British Journal of Cancer,* **56**, 809–813.

BROXMEYER, H. E., WILLIAMS, D. E., COOPER, S., WAHEED, A., and SHADDUCK, R. K., 1987, The influence *in vivo* of murine colony stimulating factor-1 on myeloid progenitor cells in mice recovering from sublethal dosages of cyclophosphamide. *Blood,* **69**, 913–918.

BUESCHER, E. S., MCILHERAN, S. M., and VADHAN-RAJ, S., 1988, Effects of *in vivo* administration of recombinant human granulocyte-macrophage colony-stimulating factor on human neutrophil chemotaxis and oxygen metabolism. *Journal of Infectious Diseases,* **158**, 1140–1142.

COHEN, A. M., ZSEBO, K. M., INOUE, H., HINES, D., BOONE, T. C., CHAZIN, V. R., TSAI, L., RITCH, T., and SOUZA, L. M., 1987, *In vivo* stimulation of granulopoiesis by recombinant human granulocyte colony-stimulating factor. *Proceedings of the National Academy of Sciences, U.S.A.,* **84**, 2484–2488.

COHEN, A. M., HINES, D. K., KORACH, E. S., and RATZKIN, B. J., 1988, *In vivo* activation of neutrophil function in the hamster by recombinant human granulocyte colony-stimulating factor. *Infection and Immunity,* **86**, 2801–2805.

DONAHUE, R. E., WANG, E. A., STONE, D. K., KANEEN, R., WONG, G. G., SCHGAL, P. K., NATHAN, D. G., and CLARK, S. C., 1986, Stimulation of hemopoiesis in primates by continuous infusion of recombinant human GM-CSF. *Nature,* **321**, 872-875.

FERRERO, D., TARELLA, C., BADONI, R., CARACCIOLO, D., BELLENE, G., PILERI, A., and GALLO, E., 1989, Granulocyte-macrophage colony-stimulating factor requires interaction with accessory cells or granulocyte colony-stimulating factor for full stimulation of human myeloid progenitors. *Blood*, **73**, 402–405.

FUJISAWA, M., KOBAYASHI, Y., OKABE, T., TAKAKU, F., KOMATSU, Y., and ITOH, S., 1986, Recombinant human granulocyte colony-stimulating factor induces granulocytosis *in vivo*. *Japanese Journal of Cancer Research*, **77**, 866–869.

HAMMOND, W. P., PRICE, T. H., SOUZA, L. M., and DALE, D. C., 1989, Treatment of cyclic neutropenia with granulocyte colony-stimulating factor. *New England Journal of Medicine*, **320**, 1306–1311.

IKEBUCHI, K., CLARK, S. C., IHLE, J. N., SOUZA, L. M., and OGAWA, M., 1988, Granulocyte colony-stimulating factor enhances interleukin 3-dependent proliferation of multipotential hemopoietic progenitors. *Proceedings of the National Academy of Sciences, U.S.A.*, **85**, 3445–3450.

JAKUBOWSKI, A. A., SOUZA, L. M., KELLY, F., FAIN, K., BUDMAN, D. CLARKSON, B., BONILLA, M. A., MOORE, M. A. S., and GABRILOVE, J., 1989, Effects of human granulocyte colony-stimulating factor in a patient with idiopathic neutropenia. *New England Journal of Medicine*, **320**, 38–42.

KAPLAN, S. S., BASFORD, R. E., WING, E. J., and SHADDUCK, R. K., 1989, The effect of recombinant human granulocyte-macrophage colony-stimulating factor on neutrophil activation in patients with refractory carcinoma. *Blood*, **73**, 636–638.

KINDLER, V., THORENS, B., DEKOSSODO, S., ALLET, B., ELIASON, J. F., THATCHER, D., FARBER, N., and VASSALLI, P., 1986, Stimulation of hemopoiesis *in vivo* by recombinant bacterial murine interleukin-3. *Proceedings of the National Academy of Sciences, U.S.A.*, **83**, 1001–1005.

KOBAYASHI, Y., OKABE, T., URABE, A., SUZUKCI, N., and TAKAKU, F., 1987, Human granulocyte colony stimulating factor produced by *Escherichia coli* shortens the period of granulocytopenia induced by irradiation in mice. *Japanese Journal of Cancer Research*, **78**, 763–768.

KRUMWIEH, D., and SEILER, F. R., 1989, *In vivo* effects of recombinant colony stimulating factors on hematopoiesis in cynomolgus monkeys. *Transplantation Proceedings*, **21**, 2964–2967.

LAM, C., MAYER, P., BESEMER, J., DIETER, D., and KNAPP, W., 1989, Differential activation of dog, human, and monkey peripheral blood granulocytes by recombinant human granulocyte-macrophage colony-stimulating factor, *in vivo* hemopoietic activity in dogs. *Journal of Cellular Biochemistry* (Suppl. 136) H401 (abstr.).

LORD, B. I., MOLINEUX, G., TESTA, N. G., KEELY, M., SPOONCER, E., and DEXTER, T. M., 1986, The kinetic response of hemopoietic precursor cells, *in vivo* recombinant interleukin-3. *Lymphokine Research*, **5**, 97–104.

LOTHRUP, C. D., JR, WARREN, D. J., SOUZA, L. M., JONES, J. B., and MOORE, M. A. S., 1988, Correction of canine cyclic hematopoiesis with recombinant human granulocyte colony stimulating factor. *Blood*, **72**, 1324–1328.

MACVITTIE, T. J., MONROY, R. L., and PATCHEN, M. L., 1984, Acute lethality and radiosensitivity of the canine hemopoietic system to cobalt-60 gamma and mixed neutron-gamma irradiation. *Response of Different Species to Total Body Irradiation*, edited by J. J. Broerse and T. J. MacVittie (Martinus Nijhoff, Boston), pp. 113–129.

MACVITTIE, T. J., D'ALESANDRO, M. M., MONROY, R. L., FARESE, A., PATCHEN, M. L., CLARK, S. C., and DONAHUE, R. E., 1988a, Stimulation of hemopoiesis in the canine by *in vivo* administration of recombinant human GM-CSF (rhGM-CSF). *Journal of Cellular Biochemistry* (Suppl. 12A), 152 (abstr.).

MACVITTIE, T. J., SCHWARTZ, G. N., MONROY, R. L., PATCHEN, M. L., FARESE, A., BENJAMIN, W., and LOMEDICO, P., 1988b, Stimulation of hemopoiesis in the canine by administration of recombinant human interleukin-1. *Experimental Hematology*, **16**, 537, (abstr.).

MATSUMOTO, M., MATSUBARA, S., MATSUNO, T., TAMURA, M., HATTON, K., NOMURA, H., ONO, M., and YOKOTA, T., 1987, Protective effect of human granulocyte colony stimulating factor on microbial infection in neutropenic mice. *Infection and Immunity*, **55**, 2715–2720.

MAYER, P., LAM, C., OBERAUS, H., LIEHL, E., and BESEMER, J., 1987, Recombinant human GM-CSF induces leukocytosis and activates peripheral blood polymorphonuclear neutrophils in nonhuman primates. *Blood*, 70, 206–213.

McNIECE, I. K., ANDREWS, R., STEWART, M., CLARK, S. C., BOONE, T., and QUESENBERRY, P., 1989, Action of interleukin-3, G-CSF, and GM-CSF on highly enriched human hematopoietic progenitor cells: Synergistic interaction of GM-CSF plus G-CSF. *Blood*, 74, 110–114.

McNIECE, I. K., McGRATH, H. E., and QUESENBERRY, P. J., 1988a, Granulocyte colony stimulating factor augments *in vitro* megakaryocyte colony formation by interleukin-3. *Experimental Hematology*, 16, 807–810.

McNIECE, I. K., STEWART, F. M., DEACON, D. M., and QUESENBERRY, P. J., 1988b, Synergistic actions between hematopoietic growth factors as detected by *in vitro* mouse bone marrow colony formation. *Experimental Hematology*, 16, 383–388.

MONROY, R. L., SKELLY, R. R., TAYLOR, P., DUBOIS, A., DONAHUE, R. E., and MACVITTIE, T. J., 1988, Recovery from severe hemopoietic suppression using recombinant human granulocyte-macrophage colony-stimulating factor. *Experimental Hematology*, 16, 344–348.

MOORE, M. A. S., and WARREN, D. J., 1987, Synergy of interleukin-1 and granulocyte colony stimulating factor: *In vivo* stimulation of stem cell recovery and hematopoietic regeneration following 5-fluorouracil treatment of mice. *Proceedings of the National Academy of Sciences, U.S.A.*, 84, 7134–7138.

PETERS, W. P., STUART, A., AFFRONTI, M. L., KIM, C. S., and COLEMAN, R. E., 1988, Neutrophil migration is defective during recombinant human granulocyte-macrophage colony-stimulating factors infusion after autologous bone marrow transplantation in humans. *Blood*, 72, 1310–1315.

SCHUENING, F. G., STORB, R., GOEHLE, S., GRAHAM, T. C., APPELBAUM. F. R., HACKMAN, R., and SOUZA, L. M., 1989. Effect of recombinant human granulocyte colony-stimulating factor on hematopoiesis of normal dogs and cn hematopoietic recovery after otherwise lethal total body irradiation. *Blood*, 74, 1308–1313.

SHIMAMURA, M., KOBAYASHI, Y., YUO, A., URABE, A., OKABE, T., KOMATSU, Y., ITOH, S., and TAKAKU, F., 1987, Effect of human recombinant granulocyte-colony-stimulating factor on hemopoietic injury in mice induced by 5-fluorouracil. *Blood*, 69, 353–355.

SOUZA, L. M., BOONE, T. C., GABRILOVE, J., LAI, P. H., ZSEBO, K. M., MURDOCK, D. C., CHAZIN, V. R., BUSZEWSKI, J., LU, H., CHEN, K. K., BARENDT, J., PLATZER, E., MOORE, M. A. S., MERTELSMANN, R., and WELTE, K., 1986, Recombinant human granulocyte colony-stimulating factor: Effects on normal and leukemic myeloid cells. *Science*, 232, 61–65.

SULLIVAN, R., FREDETTE, J. P., SOCINSKI, M., ELIAS, A., ANTMAN, K., SCHNIPPA, L., and GRIFFIN, J. D., 1989, Enhancement of superoxide anion release by granulocytes harvested from patients receiving granulocyte-macrophage colony-stimulating factor. *British Journal of Haematology*, 71, 475–479

TAMURA, M., HATTORI, K., NOMURA, H., OHEDA, M., KUBOTA, M., IMAZEKI, I., ONO, M., UEYAMA, Y., NAGATA, S., SHIRAFUJI, N., and ASANO, S., 1987, Induction of neutrophilic granulocytosis in mice by administration of purified human native granulocyte colony stimulating factor (G-CSF). *Biochemical and Biophysical Research Communications*, 142, 454–459.

TANIKAWA, S., NAKAO, I., TSUNESKA, K., and NOBIO, N., 1989, Effects of recombinant granulocyte colony-stimulating factor (rG-CSF) and recombinant granulocyte-macrophage colony-stimulating factor (rGM-CSF) on acute radiation hematopoietic injury in mice. *Experimental Hematology*, 17, 883–888.

TSUCHUJA, M., NOMURA, H., ASANO, S., KAZIRO, Y., and NEGATA, S., 1987, Characterization of recombinant human granulocyte colony-stimulating factor produced in mouse cells. *European Molecular Biology Organization Journal*, 6, 611–617.

WELTE, K., BONILLA, M. A., GILLIO, A. P., BOONE, T. C., POTTER, G. K., GABRILOVE, J. L., MOORE, M. A. S., O'REILLY, R. J., and SOUZA, L. M., 1987, Recombinant human granulocytes colony-stimulating factor: effects on hematopoiesis in normal and cyclophosphamide-treated primates. *Journal of Experimental Medicine*, 165, 941–948.

WILLIAMS, D. E., STRANEVA, J. E., COOPER, S., SHADDUCK, R. K., WAHEED, A., GILLIS, S., URDAL, D., and BROXMEYER, H. E., 1987, Interactions between purified murine colony stimulating factors (natural CSF-1, purified recombinant GM-CSF, and purified recombinant IL-3) on the *in vitro* proliferation of purified murine granulocyte-macrophage progenitor cells. *Experimental Hematology*, 15, 1007–1012.

Effects of Ionizing Radiation on Fixed-Ratio Escape Performance in Rats[1]

PAUL C. MELE, CAROL G. FRANZ AND JOHN R. HARRISON

Behavioral Sciences Department, Armed Forces Radiobiology Research Institute
Bethesda, MD 20814-5145

MELE, P. C., C. G. FRANZ AND J. R. HARRISON. *Effects of ionizing radiation on fixed-ratio escape performance in rats.* NEUROTOXICOL TERATOL 12(4) 367–373, 1990.—Adult male rats pressed a lever to terminate scrambled footshock according to a fixed-ratio 20 schedule (FR escape). Separate groups of rats received a single whole-body exposure to 4.5 or 7.5 Gray (Gy) of gamma photon radiation or were sham irradiated. The first postirradiation test session began 5 min after the end of the irradiation. The 4.5 Gy dose failed to produce any significant changes in performance over six weeks of testing after exposure. In contrast, response rates after irradiation with 7.5 Gy were decreased over the first four weeks postexposure. Reductions in response rate were due to both an increase in the latency to the first response of a ratio and to a reduction in running response rate. Performance recovered to preirradiation control levels during weeks 5–6 after exposure to 7.5 Gy. Body weights were decreased dose-dependently to a minimum of 91% of preirradiation control values during the third week after exposure to 7.5 Gy. A significant positive correlation existed for changes in the weekly average response rates and body weights at this dose. When a total dose of 7.5 Gy was delivered as 1.5 Gy per day for five consecutive days (dose fractionation), there were no significant changes in performance over eight weeks of testing although reversible decreases in response rates occurred in three of six rats. By comparison with previous studies these results demonstrate that FR escape performance may provide a more sensitive index of radiation-induced behavioral disruption than performance maintained by several other schedules of negative reinforcement. Moreover, it can be suggested that the type of reinforcing event (positive versus negative) can modulate the sensitivity of FR performance to radiation-induced disruption.

Ionizing radiation   Fixed-ratio escape   Acute exposure   Dose fractionation

NUMEROUS behavioral measures have been evaluated for their usefulness in providing a sensitive index of exposure to ionizing radiation (16,22). Among the behaviors studied, responding maintained by schedules of reinforcement has been shown to be disrupted by ionizing radiation (gamma rays and x-rays) over a wide range of doses. In studies using rats, decreases in responding maintained by positive reinforcers such as food or water have been reported at relatively low, sublethal doses under fixed-ratio (FR) (6, 28, 29, 37), fixed-interval (FI) (28,29), and variable-interval (VI) (21) schedules of reinforcement, while disruptions in FR responding maintained by electrical brain stimulation have also been demonstrated (13,17). In these studies the radiation doses ranged from 3.0–6.75 Gray (Gy). For comparison, the 30 day LD_{50} in rats following exposure to gamma radiation has ranged from an earlier estimate of 7.5 Gy (9) to the recently reported 9.5 Gy (3). [The Gray has recently replaced the rad as the official international unit of measurement of absorbed dose of ionizing radiation (32). For reference, 1 Gy = 100 rad.] This increase in the LD_{50} over the last two to three decades probably reflects improved

methods of animal care (e.g., housing, diet, environment) that have reduced the likelihood of infection-related deaths after irradiation (5). In contrast, effective doses for disrupting schedule-controlled responding have not shown a corresponding rise over this same time period [e.g., (21,28)].

Disruptions in responding maintained by a negative reinforcer such as electric shock have also been reported although these effects have been shown primarily at much higher doses (25–200 Gy) that are well above the LD_{100} for rats (8, 10, 20). Disruptions in responding under shock avoidance schedules at similarly high doses of radiation (>LD_{100}) have been reported in the pig (12) and rhesus monkey (7) also. At sublethal doses in contrast, most studies have found responding under shock-avoidance schedules to be insensitive to radiation In rats irradiated with x-rays, unsignalled (Sidman) avoidance performance was not altered by 1.0–5.0 Gy (21), while signalled (pole-jump) avoidance/escape performance was unaffected by 3.0–9.0 Gy; this highest dose, in fact, killed all rats within one week after irradiation (18). When rhesus monkeys were given sustained low-level exposure to gamma

radiation (total dose of 4.4 Gy delivered at 0.02 Gy per hour), neither signalled nor unsignalled avoidance performance was affected although food-reinforced FR responding was decreased (4). In another study, when rhesus monkeys were given a total dose of 3.0 Gy of gamma radiation over 12 hours of continuous exposure while performing a reaction time task reinforced by either food presentation or shock avoidance, responding slowed under each condition with food reinforced performance affected to a greater degree and/or at a lower cumulative dose than shock avoidance performance (40). For comparison, the acute 30 day LD_{50} for gamma radiation in rhesus monkeys has been estimated to be around 6.0 Gy (9).

These few reports suggest that negatively reinforced responding may be relatively insensitive to sublethal doses of ionizing radiation. However, because this apparent insensitivity could be a function of the specific behavioral tasks and/or radiation parameters (e.g., dose, dose-rate, and quality or type of radiation) used so far, the present study was conducted to further evaluate radiation-induced changes in shock-motivated responding. Because we have previously reported on the effects of gamma radiation on FR responding when milk was the reinforcer (28,29), it was of particular interest to evaluate the effects of gamma radiation on responding under an FR schedule of termination of foot shock (FR escape). Responding under FR escape schedules involving the termination of shock or stimulus-shock complexes has been shown to be useful in the evaluation of the behavioral effects of a variety of pharmacological agents (27). There are no reports to our knowledge concerning the effects of ionizing radiation on schedule-controlled shock-escape performance.

In the present study acute doses of gamma radiation (7.5 Gy, 4.5 Gy and sham exposure) were administered to separate groups of rats responding under an FR 20 escape schedule; performance was monitored for six weeks after exposure. These doses were taken from our previous work which showed that milk-reinforced FR responding was reliably disrupted by 4.5 Gy and above of gamma radiation (28,29). Subsequently, the rats of the sham-exposed group were irradiated with 1.5 Gy per day for five consecutive days (total dose of 7.5 Gy) and tested for an additional seven weeks. This dose-fractionation procedure was used in order to collect some initial data on the effects of multiple low-dose irradiations on FR escape performance.

METHOD

Animals

Adult male Sprague-Dawley rats [Crl:CD(SD)BR] (VAF/Plus) (Charles River breeders) were used. Animals were permitted free access to commercial rodent chow and acidified water (pH = 2.5–3.0) at all times, except during experimental test sessions. Acidified water is commonly used to reduce the possibility of infection in the irradiated organism. Body weights ranged from 500–650 g at the start of testing.

Rats were quarantined on arrival and screened for evidence of disease. They were individually housed in plastic Microisolator cages containing sterilized hardwood-chip bedding. Animal holding rooms were maintained at $21 \pm 1°C$ with $50 \pm 10\%$ relative humidity using at least ten air changes per hour of 100% conditioned fresh air. Full spectrum lights were used to maintain a 12-hr light-dark cycle (lights on from 0600–1800 hr).

Apparatus

Ten operant conditioning chambers were used. The top and one sidewall that served as the entry door were Plexiglas, the remaining three walls were aluminum, and the floor was a grid of 0.64 cm diameter aluminum rods. Each box measured 11 cm high, 24 cm long and 25 cm wide. A response lever mounted on a microswitch (Gerbrands model No. G6312) was located on each side of the front wall, approximately 6.5 cm above the floor and 5.0 cm in from the nearest sidewall. In the middle of the front wall was a Sonalert speaker (model No. SP2A2). A 28-W white house light was located in the middle of the ceiling. The grid floor, aluminum walls and response levers were connected to a constant current AC shocker and scrambling device. Each chamber was enclosed in a sound- and light-attenuating compartment, which also contained an exhaust fan for ventilation. The chambers were placed in a darkened room with white noise present continuously. Control of the chambers and recording of data were accomplished with a PDP-8E computer.

Behavioral Procedure

Training and testing procedures were modified from those reported previously (38). For initial training a rat was placed in the chamber and the house light was turned on. Thirty seconds later scrambled electric shock (0.9 mA) was delivered through the grid floor accompanied by the Sonalert tone (75 dB). The tone and shock remained on until a single response on the left lever was made (an FR 1 escape schedule). This response extinguished both the tone and shock for 30 sec after which the cycle repeated. After several sessions under FR 1, the ratio was increased by one every 3–5 days. Once an FR 10 schedule was in effect, the ratio was increased by two until the final FR 20 schedule was attained. Sessions lasted 60 min, except for when they were terminated early when, after experimental treatments, effective responding was no longer maintained. Each rat was assigned a particular test chamber and time of day for testing. Testing was conducted five days per week, Monday–Friday. Over the course of training, as the FR value was increased, six rats developed and persisted in behaviors that were incompatible with lever pressing [e.g., lying on their back (38)]. Repeated attempts at improving performance by lowering the FR value revealed that these rats typically performed poorly at FR values greater than five; these animals were eliminated from the study. Radiation exposures occurred once the performance of the remaining rats appeared stable.

Radiation Procedure

Rats were assigned to radiation dose groups (n = 5–7 per group) such that group mean baseline response rates were similar prior to treatment. Animals from different dose groups were balanced across test chambers and time of day for testing to the extent possible. For irradiations, rats were placed in well-ventilated, clear plastic restraining tubes. Test sessions began approximately 5 min after exposure ceased. Sham exposures, consisting of placing the animals in the tubes and transporting them to the exposure room, were conducted on at least eight occasions prior to the first irradiation.

For the evaluation of single acute irradiations, bilateral whole-body midline tissue doses of 4.5 and 7.5 Gy of gamma photon radiation were administered at a fixed rate of 2.5 Gy/min from a cobalt-60 source. A third group of rats received a sham exposure. These three groups were tested for six weeks after exposure. Sixteen weeks after the first irradiation and after the addition of one rat, the rats of the sham exposure group received 1.5 Gy of gamma radiation per day for 5 consecutive days to evaluate the effects of a total dose of 7.5 Gy administered in multiple fractions; testing continued for 8 weeks. All irradiations occurred on a Monday, except for the fractionated exposure condition which occurred over Monday–Friday.

Radiation dosimetry was accomplished using paired 0.5 cm³

ion chambers. Measurements were made both free in air and within an acrylic rat phantom enclosed in a standard plastic restraining tube. The dose measured within the phantom was converted to a tissue-equivalent dose. Administered dose was the ratio of the tissue-equivalent dose within the phantom to the dose measured free in air. The estimated difference in absorbed dose over the range of body weights of the rats used here was less than two percent.

Data Collection and Analysis

The overall response rate, running response rate, and latency to the first response of a ratio were calculated for each rat for each session. Overall response rate was calculated by dividing the total number of responses by the total time that the shock was on. Response latency was defined as the time elapsed from the onset of shock to the first response of a ratio. Running response rate was the response rate calculated with the latency to the first response omitted. Control data were taken from 10–15 baseline sessions immediately preceding exposure. Body weights were obtained on a weekly basis.

Overall response rate and body weight data were analyzed statistically using one- and two-factor repeated measures analyses of variance (25). Response rates underwent a $\log(x+1)$ transformation to reduce the variance. Pairwise comparisons among the three treatment groups, and between each radiation dose group and the sham control group, were performed with Newman-Keuls and Dunnett's tests, respectively. Pairwise comparisons between pre- and postirradiation data within a treatment group were performed with t-tests for matched pairs. All pairwise comparisons were two-tailed with the alpha level set at less than 0.05. The Pearson product-moment correlation coefficient was used to determine the relationship between changes in response rates and body weights after irradiation.

One rat in the 7.5 Gy exposure group died on day 31 after exposure; pathological examination determined that the cause of death was unlikely to be radiation-related. The data of this rat were included in the figures and tables. Statistical analysis was performed both with (days 1–30) and without (days 1–40) this rat's data, and the results were highly similar either way. The statistical results presented are those with this rat's data excluded. Also, the data were lost for postirradiation day 33 for one animal each in the sham and 4.5 Gy exposure groups. All available data are presented in the figures for these groups although statistical analysis was performed with day 33 excluded. This accounts for the lower degrees of freedom shown for the results of some of the ANOVAs.

RESULTS

Control Performance

Control rates and patterns of responding were consistent with those reported previously for performance under FR escape schedules (1, 19, 38). Generally, following the onset of shock, there was a short latency to the first lever-press and then a steady rate of responding thereafter until the ratio was completed. In some rats, however, a more erratic pattern was evident in that intermittent pauses in responding commonly occurred during the session. Baseline rates of responding in responses per second (mean ± standard error) were 1.51 ± 0.25 for the sham group, 1.45 ± 0.45 for the 4.5 Gy group, and 1.28 ± 0.37 for the 7.5 Gy group. Baseline response rates did not differ significantly among these three groups, $F(2,14) < 1.0$.

Acute Irradiation

Acute exposure to gamma radiation produced a prolonged,
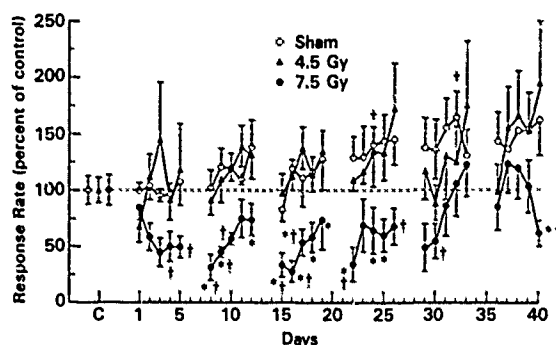

FIG. 1. Effects of acute doses of gamma radiation on FR escape response rates. Separate groups of rats were given a single exposure to 4.5 (n = 6) or 7.5 (n = 7 through day 30, n = 6 thereafter) Gy of gamma radiation or were sham exposed (n = 5). Exposure occurred approximately 5 min before the start of the session on day 1. Each postexposure point represents the group mean, vertical lines represent one SEM. Points at C represent group mean control data. Vertical lines about control points represent the SEM averaged across the individual rats. *$p < 0.05$ versus sham-exposed group (Dunnett's test after ANOVA). †$p < 0.05$ versus preirradiation control (matched pairs t-tests after ANOVA).

dose-related disruption in FR escape response rates (Fig. 1). Analysis of variance on absolute response rates revealed significant effects of radiation dose, $F(2,14) = 4.14$, $p < 0.05$, and day, $F(29,406) = 2.58$, $p < 0.05$, and a radiation dose by day interaction that just failed to achieve the conventional level of significance, $F(58,406) = 1.31$, $p < 0.075$. Overall, the response rate of the 7.5 Gy exposure group (mean of 0.84 responses per second) was significantly lower than that of both the sham and 4.5 Gy exposure groups (means of 1.81 and 1.53 responses per second, respectively), while the response rates of these latter two groups did not differ from each other (Newman-Keuls test).

Because there were clear differences among the treatment groups for changes in response rates over days after irradiation (Fig. 1), the significance level of the interaction term was considered acceptable for performing further analyses. One-way ANOVAs and subsequent Dunnett's tests on response rates from each postirradiation session were performed. This analysis revealed that the response rates of the 7.5 Gy exposure group were significantly lower than those of the sham exposure group on days 8, 9, 12, 15–19, 22, 24, 25 and 40. In contrast, response rates of the 4.5 Gy and sham-exposed groups did not differ significantly on any day after irradiation.

Within each treatment group response rates after irradiation were compared against preexposure baseline values. Response rates of the sham and 4.5 Gy exposed groups generally remained similar to their respective preexposure control values over the first three weeks of testing after irradiation, and then tended to increase above preirradiation control values over the last three weeks of testing (Fig. 1). Responding increased significantly in the sham-exposed group, $F(29,116) = 1.65$, $p < 0.05$, although significant increases occurred on days 24 and 32 only (paired t-test, $p < 0.05$). Exposure to 4.5 Gy of ionizing radiation did not alter rates of responding significantly, $F(29,145) = 1.18$. Responding of the 7.5 Gy exposure group was reduced beginning on day 2 postexposure and remained so for much of the first four and one-half weeks of testing. Over this time period response rates tended to fluctuate; the largest reductions in response rates, to 28–34% of control values, occurred on days 8, 15, 16 and 22 postirradiation. Performance of this group recovered to preexposure levels during the latter part of week 5, though relative response rates tended to

TABLE 1

RUNNING RESPONSE RATES (PERCENT OF CONTROL) UNDER THE
FR 20 ESCAPE SCHEDULE AFTER GAMMA IRRADIATION

Day Control	Sham 1.59 (0.24)	4.5 Gy 1.47 (0.45)	7.5 Gy 1.38 (0.38)
1	97.2 (5.0)	68.7 (13.9)	83.6 (10.2)
2	108.3 (15.6)	111.9 (19.4)	55.3 (11.4)
3	95.3 (4.5)	144.4 (50.6)	43.0 (11.9)
4	82.8 (19.2)	91.7 (17.8)	48.6 (12.6)
5	106.9 (18.6)	120.6 (39.3)	46.6 (9.1)
8	106.3 (17.1)	91.2 (13.5)	31.9 (11.0)
9	121.8 (12.6)	109.9 (20.4)	47.3 (6.1)
10	123.3 (12.9)	119.0 (11.5)	54.5 (4.8)
11	114.0 (4.7)	138.8 (18.2)	69.4 (16.6)
12	142.2 (17.7)	131.6 (21.4)	73.6 (14.2)
15	86.8 (8.4)	98.2 (16.9)	35.5 (10.1)
16	117.5 (6.0)	113.4 (12.9)	26.7 (9.3)
17	110.4 (22.1)	138.3 (19.1)	52.7 (11.3)
18	112.6 (11.8)	114.7 (15.6)	56.2 (12.8)
19	122.8 (21.9)	135.3 (17.9)	70.7 (25.4)
22	127.0 (16.5)	113.6 (13.0)	33.3 (15.1)
23	127.8 (24.8)	117.5 (10.9)	75.3 (29.8)
24	139.7 (11.1)	139.9 (30.8)	70.2 (26.5)
25	139.4 (18.5)	133.6 (24.7)	57.6 (13.3)
26	141.4 (19.0)	173.4 (39.7)	64.6 (16.3)
29	142.1 (23.7)	121.0 (25.6)	50.8 (19.6)
30	132.2 (24.5)	120.6 (39.5)	52.7 (15.3)
31	154.0 (22.9)	130.5 (39.2)	81.6 (26.0)
32	160.8 (19.9)	124.8 (31.1)	98.7 (27.7)
33	126.8 (22.3)	175.3 (56.0)	121.8 (27.9)
36	141.3 (24.6)	101.5 (22.7)	82.2 (19.9)
37	134.2 (29.6)	157.5 (35.1)	124.0 (29.4)
38	147.2 (31.7)	167.6 (38.2)	124.3 (28.7)
39	148.3 (31.8)	158.0 (47.4)	99.0 (23.2)
40	158.2 (29.7)	193.5 (54.8)	60.5 (11.1)

All values are the group mean with the standard error in parentheses. Control response rates are in responses per second. Postirradiation response rates (days 1–40) are percentages of baseline values.

TABLE 2

RESPONSE LATENCIES UNDER THE FR 20 ESCAPE SCHEDULE AFTER
GAMMA IRRADIATION

Day Control	Sham 0.18 (0.38)	4.5 Gy 0.10 (0.05)	7.5 Gy 1.18 (1.54)
1	0.15 (0.24)	0.11 (2.77)	2.09 (1.31)
2	0.22 (0.19)	0.11 (0.13)	5.41 (3.49)
3	0.18 (1.06)	0.07 (0.01)	3.03 (8.15)
4	0.11 (0.04)	0.12 (0.18)	1.67 (24.26)
5	0.12 (0.28)	0.08 (0.04)	1.21 (1.36)
8	0.33 (0.66)	0.12 (0.07)	34.20 (46.63)
9	0.14 (0.34)	0.06 (0.11)	3.97 (7.68)
10	0.18 (1.24)	0.07 (0.06)	0.70 (6.70)
11	0.17 (1.47)	0.11 (0.11)	1.52 (8.28)
12	0.12 (1.02)	0.05 (0.12)	0.94 (10.00)
15	0.19 (1.24)	0.20 (0.13)	8.35 (17.98)
16	0.18 (0.12)	0.14 (0.22)	4.22 (30.25)
17	0.43 (0.28)	0.13 (0.10)	9.39 (7.13)
18	0.12 (0.18)	0.08 (0.12)	2.28 (10.77)
19	0.10 (0.06)	0.09 (0.17)	2.70 (8.86)
22	0.15 (0.27)	0.07 (0.30)	8.60 (49.80)
23	0.46 (0.46)	0.16 (0.16)	6.61 (19.33)
24	0.13 (0.05)	0.54 (0.34)	8.97 (16.69)
25	0.08 (0.09)	0.09 (0.08)	4.55 (11.99)
26	0.19 (0.10)	0.16 (0.14)	3.11 (5.27)
29	0.09 (0.11)	0.13 (1.52)	4.31 (50.34)
30	0.06 (0.09)	0.09 (0.04)	1.95 (2.61)
31	0.09 (0.04)	0.11 (0.10)	1.84 (2.42)
32	0.05 (0.04)	0.07 (0.05)	1.28 (0.99)
33	0.04 (0.61)	0.07 (0.29)	0.92 (5.06)
36	0.07 (0.05)	0.08 (1.41)	4.23 (7.47)
37	0.11 (0.11)	0.08 (0.31)	3.03 (2.64)
38	0.05 (0.02)	0.22 (0.18)	2.99 (2.38)
39	0.04 (0.07)	0.05 (3.86)	1.71 (1.89)
40	0.05 (0.03)	0.05 (0.01)	2.84 (1.23)

Values are the group median and the semi-interquartile range in parentheses in seconds. Control values are the group median and semi-interquartile range of individual control means.

be lower than those of the sham exposure group through the remainder of the testing period. One-way, repeated measures ANOVA revealed a significant effect of days for this group, $F(30,150) = 2.47$, $p < 0.0005$; response rates were reduced significantly on days 4, 5, 8–10, 15–17, 22, 26, 30 and 40.

Radiation-induced changes in running response rates are shown in Table 1. It can be seen that there were no differences among the three groups in control running rates. Following irradiation, changes in running response rates within each treatment group closely paralled the changes (both increases and decreases) in overall response rates shown in Fig. 1.

Radiation-induced changes in the latency to the first response of a ratio are presented in Table 2. There were no significant differences in control latencies between any pair of groups (all p's > 0.05, Mann-Whitney test). There were no consistent changes in the latencies of the sham exposure group over the first four weeks of testing; during the final two weeks, there was a small but consistent decrease in latencies (both median and semi-interquartile range). The 4.5 Gy dose of gamma radiation failed to produce

any consistent changes in median latencies; the intermittent increases in the semi-interquartile range that occurred were due primarily to increases in latencies of two rats. Irradiation with 7.5 Gy of gamma radiation increased median latencies during approximately one-half of the sessions over the first four weeks postexposure, while the semi-interquartile range was increased during most of these sessions. Although these increases in latencies generally corresponded with decreases in overall response rates, changes in latencies and overall response rates could be dissociated. For example, overall response rates were decreased to about the same degree on days 5 and 17 after exposure to 7.5 Gy (Fig. 1), while latencies were unaltered or increased, respectively. During weeks five and six after exposure to 7.5 Gy, latencies were returning toward preirradiation control values.

Dose Fractionation

After the completion of the evaluation of the single acute irradiations, the five rats of the sham exposure group plus one
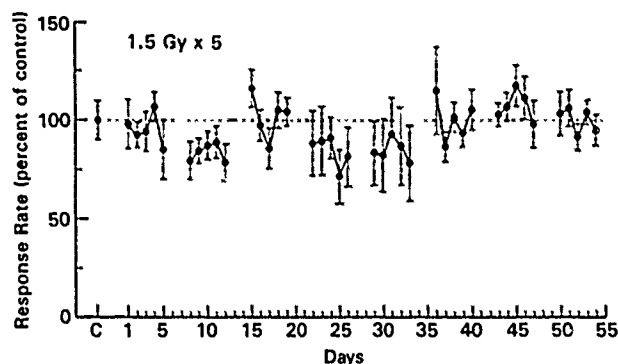
FIG. 2. Effects of repeated exposures to gamma radiation on FR escape response rates. Five exposures to 1.5 Gy occurred over days 1–5 (n = 6). Test sessions on irradiation days began approximately 5 min after exposure ceased. Each postexposure point represents the group mean, vertical lines represent one SEM. Points at C represent group mean control data. Vertical lines about control points represent the SEM averaged across the individual rats.

additional rat were tested under baseline conditions for ten more weeks. After this additional training, response rates appeared to be quite stable in that no systematically increasing or decreasing changes in rates were evident. These rats were then exposed to 1.5 Gy per day for five consecutive days and tested for an additional seven weeks (Fig. 2). The preirradiation control response rate (mean ± standard error) for this group of six rats was 2.76 ± 0.46 responses per second. ANOVA on response rates revealed that the fractionated exposure did not produce significant changes from preirradiation control values over the first two, four or all eight weeks of testing (p > 0.05 for all Fs). Even though the fractionated exposure condition did not alter performance significantly, three of six rats had response rates decreased below their individual control ranges on 12, 8 and 4 of 40 sessions. Recovery of control response rates was evident in each of these rats during the last 2–3 weeks of this phase.

Body Weight

Preirradiation body weights (mean ± standard error) for the sham, 4.5 and 7.5 Gy exposure groups were, respectively, 584.9 ± 26.3, 579.1 ± 8.5 and 618.4 ± 19.9 g. Acute irradiation produced a small but dose-related decrease in body weight (Fig. 3, top). Over eight weeks after exposure, the sham-irradiated group showed gradual weight gain to 106.3% of preexposure control levels. The 4.5 Gy group had a slight reduction in body weight to 97.1% of preirradiation control on day 5, body weight recovered and then increased thereafter. The 7.5 Gy group showed a more pronounced drop in body weight on day 5 that was followed by additional loss over the subsequent 2 week period before reversal of this trend was observed. The maximal reduction in body weight to 91.3% of control levels occurred during the third week (day 17) postexposure. Over the entire 8-week period, however, only the main effect of day, F(8,112) = 15.89, p < 0.001, was significant. When evaluation of body weight was restricted to the first four weeks after irradiation, a significant effect of radiation dose, F(2,14) = 5.67, p < 0.025, was evident.

Comparison between Figs. 1 and 3 (top) indicate that decreases in weekly response rates and body weights followed a roughly similar time-course after the 7.5 Gy exposure. At this dose changes in weekly average response rates and body weights were positively correlated (r = .94, p < 0.01).
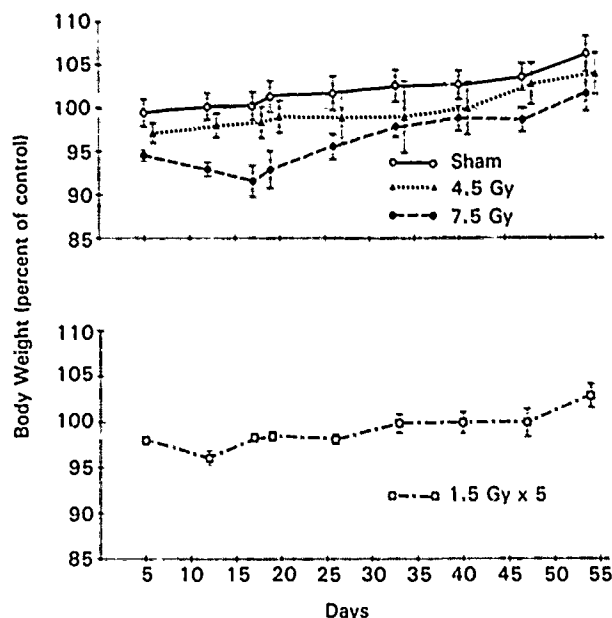

FIG. 3. Effects of gamma radiation on body weight. The top panel shows the effects of single exposures. On day 1 separate groups of rats were given a single exposure to 4.5 (n = 6) or 7.5 (n = 7 through day 30, n = 6 thereafter) Gy of gamma radiation or were sham-exposed (n = 5). The bottom panel shows the effects of irradiation with 1.5 Gy per day over days 1–5 (n = 6). Each point represents the group mean, vertical lines represent one SEM. Body weights were measured at the end of each week (on Fridays); an additional measurement was made in the middle of week 3 (day 17).

The mean preexposure body weight of the group of rats receiving 1.5 Gy per day for five consecutive days was 635.7 ± 35.6 g. This fractionated exposure reduced body weight to a small degree over the first four weeks postexposure, with the largest reduction observed on day 12 (Fig. 3, bottom). Recovery and a subsequent increase in body weight occurred thereafter.

DISCUSSION

The major finding of the present study was that gamma radiation produced a dose-related disruption of FR escape performance. Acute exposure to 7.5 Gy of gamma radiation decreased response rates, while 4.5 Gy did not alter performance significantly. There are few previous reports of disruptions of negatively reinforced responding by sublethal doses of ionizing radiation. In studies using rats, acute x-ray doses of 1.0–5.0 Gy failed to alter unsignalled (Sidman) avoidance performance over 14 days postexposure (21), while 3.0 and 6.0 Gy delivered acutely did not alter performance of a signalled (pole-climb) avoidance-escape task over 30 days after irradiation (18). This latter study also reported that performance was unaffected by 9.0 Gy up until the death of all rats by the sixth day after exposure. Prolonged low-level exposure to gamma radiation (4.4 Gy delivered at 0.02 Gy per hour) was ineffective in altering performance on several avoidance tasks in rhesus monkeys (4). However, in a shock avoidance reaction time task extended gamma exposure (3.0 Gy delivered at 0.25 Gy per hour) lengthened response latencies slightly (40). Compared to these earlier reports, the behavioral disruption reported in the present study may have been due to the radiation parameters used and/or to a greater sensitivity of FR escape performance to

radiation-induced disruption. Among the radiation parameters to be considered, dose is likely the most critical here, although dose-rate and radiation quality (type) cannot be ignored. In terms of behavioral factors, differences between the present study and previous ones include escape versus avoidance contingencies, shock levels, baseline rates of responding, and the number of responses required to meet the reinforcement contingency. Each of these are potentially important factors and each needs to be systematically examined.

In contrast to the present results, other findings from this laboratory showed that doses of gamma radiation as low as 4.5 Gy reliably reduced rates of responding under FR 20 and 50 schedules of milk presentation; there were no differences in radiosensitivity as a function of these FR values (28,29). An earlier study reported that 3.0 Gy of x-rays reduced FR 20 response rates when food pellets were used as reinforcers (6). These results suggest that the dose-effect function for radiation-induced decreases in FR responding maintained by shock termination is shifted to the right of those for FR responding maintained by milk or food delivery. This implies that the type of reinforcing event may be an important determinant of the sensitivity of FR performance to disruption by ionizing radiation. Two previous reports showed that food reinforced responding under an FR schedule in monkeys (4) and a VI schedule in rats (21) was disrupted by doses of ionizing radiation that did not alter Sidman avoidance performance. However, because the schedules of food delivery and shock avoidance differed in each of these studies, and because there were marked differences in the baseline rates and patterns of responding generated by each schedule, it is unclear as to which specific factor or factors were primarily responsible for the observed differences in radiosensitivity (2).

Comparing across studies from this laboratory revealed that radiation disrupted performance under FR schedules of shock termination and milk presentation in a similar manner in that overall and running response rates were decreased and latencies to the first response were increased. In these studies, baseline performance measures maintained by these FR schedules were similar in several potentially important ways. For one, similar baseline rates of responding have occurred under these two types of FR schedules; overall FR response rates were approximately 1.5 responses per second here and in one study when milk was the reinforcer (28). Secondly, a similar pattern of baseline responding was evident regardless of the reinforcing event in that once an FR run of responses was initiated it usually continued at a high, steady rate until reinforcement occurred. The primary difference between baseline performance under these schedules was in the latency to the first response of a ratio. These latencies were shorter under the escape schedule (1 sec or less) than under the milk delivery schedule (3–8 sec). Overall, the similarity in baseline performance and in the radiation-induced disruption in performance under these FR schedules further suggests that the reinforcing event itself was an important determinant of the sensitivity of responding to gamma irradiation.

In addition to differences in radiosensitivity, another characteristic of radiation-induced disruption of FR responding that appears to vary with the type of reinforcing event is the time-course over which performance changes occur. Under the FR escape schedule the largest reductions in response rates occurred during the second, third and fourth weeks after exposure to 7.5 Gy. Response rates recovered to preexposure levels during the subsequent two weeks. The possibility that performance decrements were not fully reversed, however, was suggested by the tendency for the response rates of this treatment group to remain below those of the sham exposure group throughout the final week of testing. In contrast, at doses up to 9.0 Gy, maximal reductions in milk-reinforced FR responding occurred during the first week

after exposure; reductions in responding during subsequent weeks were considerably smaller or were no longer evident (28.29).

Following irradiation, changes in body weights were correlated with the week-to-week changes in FR escape response rates. Since reductions in free-feeding body weights have been shown to disrupt shock escape and avoidance performance (26, 30, 36), it is possible that the reduced body weights caused or contributed to the concurrent deficits in responding reported here. In those studies, however, body weight reductions of about 20% were necessary to produce consistent changes in established performance, whereas here, the maximal reduction in body weight was less than 9% (weeks 2–3 after irradiation). Moreover, response rates were significantly reduced when body weights were within 5% of preexposure levels (weeks 1 and 4). Based on the data from those earlier studies, it seems unlikely that such relatively small reductions in body weight alone would account for the large disruptions in performance observed here.

Although the weight-reducing effects of ionizing radiation are well established (15, 24, 31, 35), there is evidence to suggest that the weight loss reported here was not solely a consequence of radiation exposure. These earlier studies reported that maximal weight loss occurred within the first week after exposure, and that this was followed by steady weight gain thereafter. Although the 4.5 Gy exposure group here showed minor changes in weight over time consistent with these earlier studies, there was a definite trend of steady weight loss in the 7.5 Gy exposure group over the first three weeks after irradiation. Perhaps the prolonged decrements in performance and/or body weight observed here following sublethal radiation exposure are indicative of radiation's effects under highly stressful (i.e., shock motivated) environmental conditions. It has been demonstrated previously that a variety of other environmental stressors (e.g., exhaustion, cold, and trauma) are capable of enhancing radiation-induced lethality (11, 23, 34).

When 7.5 Gy of ionizing radiation was delivered as five daily fractions, smaller decreases in response rates and body weights were evident than when this dose was given as a single exposure. These two measures indicate that the cumulative effect of these multiple exposures was less than additive. This is consistent with an extensive amount of data on radiation-induced lethality at both the cellular and organismic level (33,39). The reduced effectiveness of dose fractionation has been shown to be a function of exposure parameters such as the total dose administered, the number of fractions, the time between fractions, and the type or quality of ionizing radiation. Although the fractionated dosing condition used here did not produce a significant change in performance, the reversible behavioral disruption observed in three of six rats indicates that this exposure nevertheless had important functional consequences.

Several behavioral factors need to be considered when making comparisons between the effects reported here for 7.5 Gy delivered as a single acute dose and as multiple fractions. One is that the baseline response rates of the rats given the fractionated exposure were twice those of the rats given the single exposure. Because baseline response rate has been shown to be an important determinant of the effects of a number of agents on schedule-controlled responding [e.g., the rate-dependency relationship (14,27)], it is possible that these baseline rate differences contributed in some way to the differential effectiveness of these two exposure conditions. Based on rate-dependency, however, it would be expected that for a given treatment that reduces rates of responding, higher rates would be decreased more than or at least similarly to lower rates under a particular schedule of reinforcement. That rats with higher baseline response rates showed smaller reductions after irradiation can be viewed as further support for the conclusion that the cumulative effect of the fractionated exposure condition was less than additive. Obviously, this interpretation

rests with the assumption that gamma radiation produces greater reductions in escape response rates of rats as a function of increasing baseline rate, this has yet to be experimentally determined. At this time the opposite relationship that higher FR escape response rates are less susceptible to disruption by radiation than lower rates seems unlikely, but cannot be entirely discounted.

A second potentially important factor is the increased amount of training given to the animals in the fractionated exposure condition prior to irradiation. To our knowledge radiosensitivity as a function of training time has not been evaluated. However, that

continued training per se does not decrease radiosensitivity is indicated by the finding that disruptions in responding under FR schedules of milk delivery were highly replicable when 2–3 repeated exposures occurred at 6–8 week intervals (28,29)

In summary, the present results demonstrate that aversively motivated behavior can provide a more sensitive index of exposure to ionizing radiation than previously thought. Further evaluation of the specific behavioral and radiobiological factors accounting for this enhanced sensitivity are warranted.

REFERENCES

1. Arzin, N. H., Holtz, W. C., Hake, D. F., Ayllon, T. Fixed-ratio escape reinforcement. J. Exp. Anal. Behav. 6:449–456; 1963.

2. Barrett, J. E., Katz, J. L. Drug effects on behavior maintained by different events. In: Thompson, T.; Dews, P. B.; McKim, W. A., eds. Advances in behavioral pharmacology, vol 3. New York. Academic Press; 1981.

3. Bogo, V. Behavioral radioprotection. Pharmacol. Ther. 39:73–78; 1988.

4. Braun, R. G., Farrer, D. N., Zappini, W., Crook, G. H. Performance of rhesus monkeys during continuous low-level gamma radiation: an exploratory study. Technical report ARL-TR-66-18, 6571st Aeromedical Research Laboratory, Holloman AFB, NM 88330; 1966.

5. Broerse, J. J., MacVittie, T. J. Response of different species to total body irradiation. Dordrecht, The Netherlands: Martinus Nijhoff; 1984.

6. Brown, W. L. Response rate during x-irradiation and recovery following irradiation. J. Genet. Psychol. 108.117–120, 1966.

7. Bruner, A., Bogo, V., Jones, R. K. Delayed match-to-sample performance decrement in monkeys after 60Co irradiation. Radiat. Res. 63:83–96; 1975.

8. Burkhardt, W. F., Hunt, W. A. Characterization of radiation-induced performance decrement using a two-lever shock-avoidance task. Radiat. Res. 103:149–157; 1985.

9. Casarett, A. P. Radiation biology. Englewood Cliffs, New Jersey: Prentice-Hall; 1968.

10. Casarett, A. P., Comar, C. L. Incapacitation and performance decrement in rats following split doses of fission spectrum radiation. Radiat. Res. 53:455–461; 1973.

11. Chapman, W. H., Sipe, C. R., Eltzholtz, D. C., Cronkite, E. P., Chambers, F. W. Sulfhydryl-containing agents and the effects of ionizing radiation. Radiology 55.865–873, 1950.

12. Chaput, R. L., Barron, E. L. Postirradiation performance of miniature pigs as modified by tasks. Radiat. Res. 53:392–401; 1973.

13. Christensen, H. D., Flesher, A. M., Haley, T. J. Changes in brain self-stimulation rates after exposure to X-irradiation. J. Pharm. Sci. 58:128–129; 1969.

14. Dews, P. B., Wenger, G. R. Rate-dependency and the behavioral effects of amphetamine. In. Thompson, T., Dews, P. B., eds. Advances in behavioral pharmacology, vol 1. New York. Academic Press; 1977.

15. Fishler, M. C., Cole, L. J., Bond, V. P., Milne, W. L. Therapeutic effect of rat bone marrow injection in rats exposed to lethal whole body x-irradiation. Am. J. Physiol. 177:236–242; 1954.

16. Furchtgott, E. Behavioral effects of ionizing radiation. In. Furchtgott, E., ed. Pharmacological and biophysical agents and behavior. New York: Academic Press; 1971:1–64.

17. Haley, T. J., Bach-Y-Rita, P., Komesu, N. Effect of X-irradiation on self-stimulation of the brain. Nature 192.1307, 196..

18. Haley, T. J.; Fonesca, J.; Komesu, N.; Williams, P. Inability of whole body x-irradiation to produce extinction of conditional avoidance in rats. Arch. Int. Pharmacodyn. 134:148–15'; 1961.

19. Hineline, P. N., Rachlin, H. Notes on fixed-ratio and fixed-interval escape responding in the pigeon. J. Exp. Anal. Behav 12.397–401, 1969.

20. Hunt, W. A. Comparative effects of exposure to high-energy electrons and gamma radiation on active avoidance behavior. Int. J. Radiat. Biol. 44:257–260; 1983.

21. Jarrard, L. E. Effects of X-irradiation on operant behavior in the rat. J. Comp. Physiol. Psychol. 56:608–611; 1963.

22. Kimeldorf, D. J., Hunt, E. L. Ionizing radiation Neural function and behavior. New York: Academic Press; 1965.

23. Kimeldorf, D. J., Jones, D. C. The relationship of radiation dose lethality among exercised animals exposed to Roentgen rays. Am. J. Physiol. 167:626–632; 1951.

24. Kimeldorf, D. J.; Jones, D. C.; Castanera, T. J. Effect of x-irradiation upon the performance of daily exhaustive exercise by the rat Am J Physiol. 174:331–335; 1953.

25. Kirk, R. E. Experimental design: Procedures for the behavioral sciences. Belmont: Brooks/Cole; 1968.

26. Leander, J. D. Effects of food deprivation on free-operant avoidance behavior. J. Exp. Anal. Behav. 19:17–24; 1973.

27. McMillan, D. E.; Leander, J. D. Effects of drugs on schedule-controlled behavior. In. Glick, S. D., Goldfarb, J , eds Behavioral pharmacology. St. Louis: The C. V, Mosby Co.; 1976:85–139.

28. Mele, P. C.; Franz, C. G.; Harrison, J. R. Effects of sublethal doses of ionizing radiation on schedule-controlled performance in rats Pharmacol. Biochem. Behav. 30:1007–1014; 1988.

29. Mele, P. C., McDonough, J. H. Effects of ionizing radiation on multiple schedule performance in rats. Paper presented at the 7th Annual Meeting of the Behavioral Toxicology Society, Savannah, GA: 1988.

30. Meyer, M. E.; Adams, W. A.; Worthen, V. K. Deprivation and escape conditioning with various intensities of shock. Psychon. Sci. 14:212–214; 1969.

31. Nims, L. F.; Sutton, E. Weight changes and water consumption of rats exposed to whole-body x-irradiation. Am. J. Physiol. 171:17–21; 1952.

32. Radiation quantities and measurements. International Commission on Radiation Units and Measurements, Report No 33 Washington, DC; 1980.

33. Sacher G. A. Reparable and irreparable injury a survey of the position in experiment and theory. In. Claus, W. D , ed Radiation biology and medicine. Reading: Addison-Wesley; 1958.

34. Smith, W. W.; Highman, B. J.; Mitchell, J. R.; Blount, H. C., Jr. Effect of environmental temperature on the response of mice to whole-body roentgen radiation. Proc. Soc. Exp Biol. Med 71· 498–501; 1949.

35. Smith, D. E.; Tyree, E. B. Influence of x-irradiation upon body weight and food consumption of the rat. Am J. Physiol. 177· 251–260; 1954.

36. Ukai, M., Holtzman, S G. Restricted feeding does not modify discriminative stimulus effects of morphine in the rat. Pharmacol. Biochem. Behav. 29:201–203; 1988.

37. Wicker, J. E., Brown, W. L. The effect of gamma radiation upon operant water-reinforcement behavior. J. Genet. Psychol. 106:295–299; 1965.

38. Winograd, E. Escape behavior under different fixed ratios and shock intensities. J. Exp. Anal. Behav. 8:117–124; 1965.

39. Withers, H. R. The four R's of radiotherapy. In· Lett, J. T.; Adler, H., eds. Advances in radiation biology. New York· Academic Press; 1975.

40. Yochmowitz, M. G., Brown, G. C. Performance in a 12-hour, 300-rad profile. Aviat. Space Environ. Med. 48:241–247; 1977.

Brain μ and δ opioid receptors mediate different locomotor hyperactivity responses of the C57BL/6J mouse

G. Andrew Mickley, Maureen A. Mulvihill, and Mark A. Postler

Behavioral Sciences Department, Armed Forces Radiobiology Research Institute, Bethesda, MD 20814-5145, USA

Abstract. Morphine induces a dose-dependent stereotypic locomotor hyperactivity in the C57BL/6J mouse. Although morphine is the prototypical opioid μ receptor agonist, it also binds at δ sites. This has led to speculation as to which set(s) of receptor subtypes mediate opiate-induced locomotor hyperactivity. Here we use selective μ and δ receptor agonists as well as a sophisticated activity measuring apparatus to investigate the neuropharmacology of opioid-induced locomotion in the mouse. Male C57BL/6J mice were implanted with chronic bilateral cannula aimed at the lateral ventricles. Following recovery from surgery, mice received a series of bilateral 1 μl intraventricular (i.vent.) injections of [D-Ala^2-MePhe^4-Glyol^5] enkephalin (DAGO) (0.1, 1.0, 2.0 μg), [D-Pen^2, D-Pen^5] enkephalin (DPDPE) (2.5, 5.0, 10.0, 30.0 μg) (compounds with respective μ and δ opioid receptor selectivity), morphine sulfate (10.0, 20.0, 60.0 μg), or saline. Injections were separated by at least 3 days and were presented in a randomized order. We measured several locomotor parameters following each injection. DAGO, DPDPE and morphine each produced horizontal locomotor hyperactivity and lengthened the average distance per move. While morphine and DAGO significantly reduced vertical activity (rearing) and produced thigmotaxis (wall-hugging), DPDPE-injected mice were similar to controls on these locomotor parameters. These data reveal that mouse locomotor hyperactivity can be observed following injections of either morphine or more-selective opioid μ or δ receptor agonists. However, within the drug/dose regimens used here, we noticed qualitative differences in the locomotor topography produced by the selective μ and δ receptor agonists.

Key words: Opiates – Locomotion – Mice – Opioid receptors – Thigmotaxis

While many animals manifest lethargy and a reduction in behavioral responsiveness following a sufficiently large dose of morphine (Browne et al. 1979), some strains of

Offprint requests to · G.A. Mickley, Radiation Sciences Division (RZP), USAF School of Aerospace Medicine, Brooks AFB, TX 78235–5301, USA

mice become hyperactive (Oliverio and Castellano 1974, Teitelbaum et al. 1979). The C57BL/6J mouse, for example, exhibits a dose-dependent, stereotypic locomotor hyperactivity ("running fit") (Oliverio 1975) and an elevated "Straub" tail (Aceto et al. 1969; Oliverio 1975). This morphine-induced running response is predominantly characterized by long-duration horizontal movements – mostly around the test chamber perimeter. The drug also produces a muscular stiffness and raised hindquarter posture that contributes to the "compulsive", "robotic" appearance of the locomotion (Stevens et al. 1986).

Recent identification of opioid receptor subtypes (i.e., μ_1, μ_2, δ, κ, σ and ε) (Lord et al. 1977; Wuster et al. 1979; Wolozin and Pasternak 1981; Martin 1984) has raised the question of possible differences in the functions mediated by each of the opioid receptor populations and their ligands. Experiments aimed at determining the physiological mediators of locomotor behaviors have been facilitated by the use of ligands with selective opioid receptor binding properties. For example, β-endorphin (active at the ε receptor) does not produce locomotor hyperactivity in mice (Wei et al. 1977; Puglisi-Allegra et al. 1982). Similarly, κ agonists seem more likely to depress rather than stimulate C57 mouse locomotion (Castellano et al. 1984). However, stimulation of opioid μ receptors (with FK 33-824; Castellano 1981) produces a robust mouse locomotor hyperactivity, as does stimulation of the reportedly enkephalin-selective δ receptors (Wei et al. 1977; Katz et al. 1978; Kameyama and Ukai 1981, 1983; Puglisi-Allegra et al. 1982).

While morphine is the prototypical μ receptor agonist (Kosterlitz et al. 1977), it may act at the δ receptor as well (Takemori et al. 1986; Takemori and Portoghese 1987). Therefore, the morphine-induced locomotor response of the C57BL/6J mouse may be mediated by either, or both, of these receptors. A comparison of the locomotor responses produced by morphine with responses following injections of selective μ or δ receptor ligands may help reveal the roles played by these sites in the production of opiate-induced locomotion. The locomotor topographies produced by morphine and the δ-selective enkephalins have just begun to be compared, and the results of these studies have not always been consistent. In fact, mor-

phine- and enkephalin-induced locomotion have been described by different authors as either quite similar (Katz et al. 1978) or, in many ways, dissimilar (Kameyama and Ukai 1983).

In the current study we injected highly selective μ or δ opioid receptor agonists (DAGO or DPDPE, respectively) or morphine sulfate into the brains of C57BL/6J mice in order to more fully characterize and differentiate the locomotor response produced by these compounds.

Materials and methods

Subjects. Male C57BL/6J mice (15–20 g) were obtained from Jackson Laboratories (Bar Harbor, ME), screened for evidence of disease, and housed in a facility accredited by the American Association for Accreditation of Laboratory Animal Care. Temperature and relative humidity in the animal rooms were held at 19–21° C and 50% ± 10%, respectively, with at least ten air changes/h. Full-spectrum lighting was cycled at 12 h intervals (lights on at 0600 hours) with no twilight. Groups of ten mice were initially housed in micro-isolator, polycarbonate cages on hardwood chip contact bedding. Animals were individually housed beginning 2 weeks before the experiment. Food (Wayne) Rodent Blox and acidified water (pH 2.5 using HCl) (McPherson 1963) were available ad lib.

Locomotion measurements. Locomotor behaviors were automatically recorded in a dimly lighted room between 0700 and 1100 hours using Digiscan Animal Activity Monitors, Model DCM-16 (Omnitech Electronics, Columbus, OH) connected to an IBM-PC/XT computer. Monitors consisted of a square acrylic arena (40 × 40 × 30 cm). Horizontal movement parameters were recorded by a 16 × 16 array of infrared photodetectors placed 2.54 cm apart and 1.3 cm above the chamber floor. An additional 16 photodetectors (spaced 2.54 cm apart and 6.3 cm above the floor) were used to detect vertical movements. In these experiments we analyzed three locomotor parameters: (1) Total Distance Traveled (i.e., the system calculates distance traveled for each sample period by recording both straight and diagonal movements within the horizontal photobeam grid); (2) Average Distance / Move (i.e., Total Distance Traveled divided by the number of horizontal moves. A move is completed when there is a > 1 s break in horizontal activity); (3) Vertical Activity (i.e., total number of photobeam interruptions that occur in the vertical sensors).

Stereotaxic surgery. Using stereotaxic surgical procedures, bilateral stainless-steel guide cannulas (23 gauge) were placed in the lateral ventricles of each mouse (0 8 mm anterior to bregma, 0.8 mm lateral to the midline and 3.0 mm below the skull; Slotnick and Leonard 1975). Wire stylettes were placed in the guide cannulas to keep them patent. Prior to surgery, mice received atropine sulfate (0.4 mg/kg, IP) followed by 75 mg/kg (IP) sodium pentobarbital. Methoxyflurane was also used (as required) as an auxiliary anesthetic. Behavioral testing was begun not earlier than 1 week following the surgery. At the end of these experiments mice were anesthetized with methoxyflurane and perfused with heparinized saline, followed by a 10% buffered formalin solution. Brains were removed, sliced (20 μ sections) and stained with thionin in order to confirm cannula placements.

Procedures On drug treatment days, stylettes were removed from the guide cannulas and a 30-gauge injection cannula (0.5 mm longer than the guide) was inserted. Mice (N = 49) received bilateral intraventricular (i.vent.) injections (1 μl / hemisphere) of an opioid agonist or vehicle (saline) at a rate of 1 μl / min. Injection cannulas were left in the guides for an additional 30 s at the end of the injection before mice were placed in the activity monitors. Locomotor activity was recorded for 20 min although only data from the 10–20 min interval were analyzed See statistical analysis section

below. Subjects had multiple drug injections (not exceeding five) separated by at least 3 days. The order of the drug treatments was randomized. Mice were injected with the following compounds (see Fig. 1 for doses and number of subjects receiving each dose): (1) the selective μ opioid receptor agonist [D-Ala^2-MePhe^4-Glyol^5] enkephalin (DAGO) (Handa et al. 1981; Kosterlitz and Paterson, 1981; Pasternak 1988); (2) the selective δ opioid receptor agonist [D-Pen^2, D-Pen^5] enkephalin (DPDPE) (Mosberg et al. 1983; Goldstein, 1987); (3) morphine sulfate, (4) vehicle (saline). The enkephalins were purchased from Sigma Chemical Co., St Louis, MO, USA.

In vitro studies suggest that DAGO and DPDPE are two of the most selective agonists for the μ and δ opioid receptors, respectively. DPDPE is 3164 times more selective for δ receptors over μ receptors (Mosberg et al. 1983). DAGO has a μ/δ selectivity of 220/1 (Miller 1986). In vivo binding assays support similar conclusions about the high degree of receptor selectivity of these opioid agonists (Sanchez-Blazquez and Garzon 1989). Further, Porreca et al. (1987) and Cowan et al. (1986) have found that opioid antagonists selective for the δ receptor blocked the behavioral effects of DPDPE but not μ receptor ligands. Thus, the literature seems to consistently support the conclusion that DPDPE and DAGO are useful tools in discriminating the particular functions of δ and μ opioid receptors.

Statistical analysis. During the first 10 min after our intracranial injections we noticed that opioid-stimulated locomotor activity increased rapidly, while the activity of saline-injected mice became reduced. In order to get a more stable response that was not so strong, a reflection of environmental novelty and/or drug absorption, we analyzed data collected from 10–20 min after the drug/control treatments. Pilot studies from our own laboratory and others (Stevens et al. 1986; Hart et al. 1989) suggest that data within this time period more accurately reflect the plateau phase of locomotor responding following ICV opiate injections. The data from these experiments were not normally distributed and the group variances were frequently non-homogeneous. Consequently, we analyzed the data through a nonparametric ANOVA (Kruskal-Wallis) (Siegel 1956). Individual group differences were determined by using the Mann-Whitney U test (Siegel 1956). An α of 0.05 was set throughout these studies. In circumstances in which multiple group comparisons would significantly increase the probability of a Type I error, the α was partitioned according to the procedure of Bonferroni (Miller 1981) and the overall probability reported.

Results

The selective μ and δ opioid agonists (DAGO and DPDPE) and morphine each produced horizontal locomotor hyperactivity (enhanced total distance traveled) in the C57BL/6J mouse. Despite the fact that certain doses of opioid agonists caused an increase in the total distance traveled (as compared to saline controls, see Fig. 1), ANOVAs calculated to determine dose-dependent activities within particular agonists did not reveal statistically significant differences (P > 0.05, Kruskal-Wallis). Therefore, the data derived from all doses of the same drug were combined. This composite analysis confirmed that DAGO, DPDPE and morphine produced levels of horizontal locomotion that were all significantly higher than that observed in saline controls (P < 0.05, Mann-Whitney U). Further, the selective δ and μ opioid agonists stimulated the total distance traveled to levels significantly higher than those produced by morphine (P < 0.05, Mann-Whitney U).

The opioid agonists also significantly enhanced the length of the average distance per move. This suggests that locomotion was infrequently interrupted by breaks
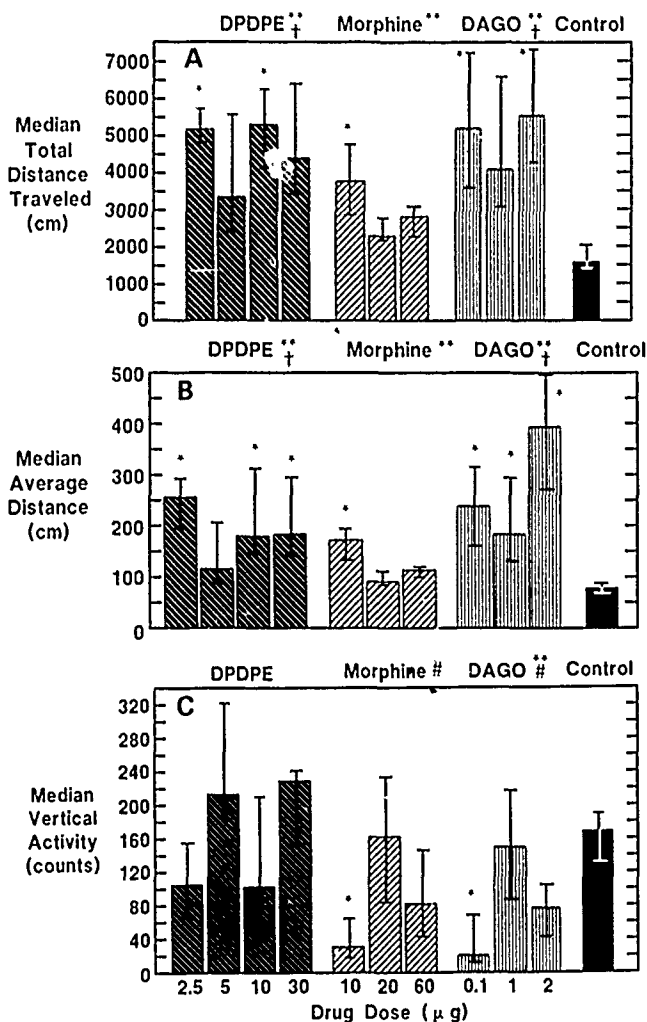
Fig. 1A–C. Median distance traveled (A), average length of individual movements (average distance/move) (B) and vertical activity (C) exhibited by C57BL/6J mice in a 10-min period following intraventricular doses of opioid agonists [DPDPE (selective for δ receptors), morphine or (DAGO) (selective for μ receptors)] or saline vehicle (control). The following drug doses (in μg) were administered to the subjects through bilateral injections (i.e., half the indicated amount was injected into each hemisphere in 1 μl vehicle: DPDPE −2.5 (N = 10), 5.0 (N = 5), 10.0 (N = 7), 30.0 (N = 8), DAGO − 0.1 (N = 10), 1.0 (N = 10), 2.0 (N = 10), Morphine sulfate − 10.0 (N = 10), 20.0 (N = 7), 60.0 (N = 9), Vehicle control (saline) (N = 19). Variance indicators represent the semi-interquartile range. The * indicates a significant (P < 0.05, Mann-Whitney U) difference from the saline control group. There were no statistically significant differences between the locomotor responses to various doses of particular compounds. The ** identifies differences (P < 0.05, Mann-Whitney U) from saline control mice when all the animals receiving a particular agonist were combined. The † reflects statistically significant differences from morphine-injected mice, while the # indicates differences from DPDPE-treated mice (P < 0.05, Mann-Whitney U)
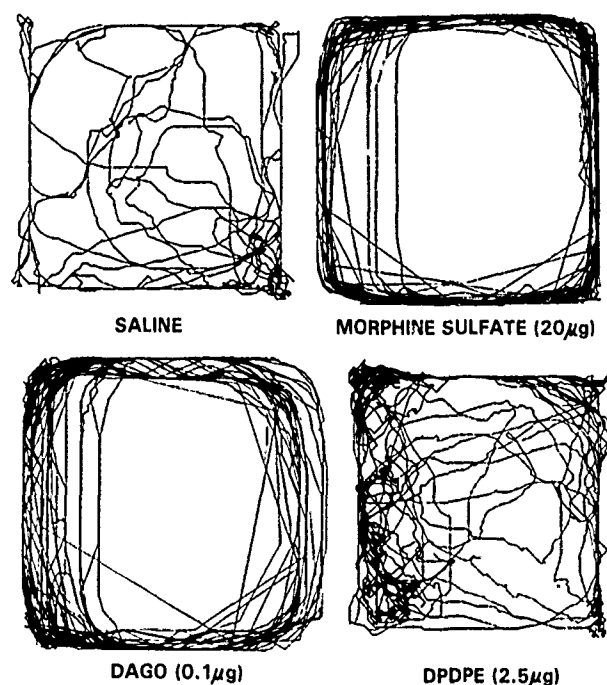

Fig. 2. Examples of horizontal activity tracings produced by individual C57BL/6J mice in a 6-min period following bilateral injections (i. vent.) of the indicated opioid agonist or saline

(P < 0.05, Mann-Whitney U). Both the selective δ and μ opioid receptor agonists produced longer horizontal moves than did morphine (P < 0.05, Mann-Whitney U).

Vertical activity (rearing) was reduced (compared to saline-injected mice) only after certain doses of morphine (10 μg) or DAGO (0.1 μg) (Fig. 1). Overall, however, changes in vertical activity were drug dependent but not dose dependent (P > 0.05, Kruskal-Wallis comparing the vertical activity associated with various doses of each drug). Therefore, when we combined the vertical activity data from all the animals receiving all doses of a particular opioid agonist and compared these data with the rearing counts of saline-injected mice, a suppression of vertical activity was revealed in DAGO-treated mice only (P < 0.05, Mann-Whitney U). Overall, the vertical activity evoked by DPDPE was not quantitatively different from that observed in saline-injected mice and it was significantly greater than that produced by doses of either morphine or DAGO (P < 0.05, Mann-Whitney U).

The qualitative aspects of the locomotion evoked by each of the opioid agonists were different in several respects. Morphine-induced locomotor hyperactivity was characterized by "robotic" movements, of long duration. These movements were almost exclusively thigmotaxic, i.e., made around the periphery of the test chamber (see Fig. 2). Like others (Aceto et al. 1969; Katz et al. 1978; Oliverio et al. 1984), we observed Straub tails, a muscular stiffness and elevation of the hind quarters in these opiate-treated animals. The topography of locomotion of DAGO-injected mice was dose independent and quite similar to that of mice that received morphine. Straub tails were rarely observed in the DPDPE-injected mice. Rearing was also observed less frequently in DAGO-injected mice than in morphine-injected subjects. While

of > 1 s. The group differences observed using this parameter closely paralleled those just described for the total distance traveled (Fig. 1). Once begun, movements of mice treated with DAGO, DPDPE or morphine were significantly longer (medians = 242.0, 206.9, and 113.6 cm, respectively, for combined drug doses) than were movements of the saline-injected controls (74.9 cm)

mice injected with DPDPE covered as much, or more, distance as the subjects receiving either DAGO or morphine (Fig. 1) their movements were much less stereotypic, did not follow the contours of the test chamber (Fig. 2), and included a strong vertical component.

Discussion

Within the constraints of the drug/dose regimens used here, we observed that mouse locomotion following i.vent. injections of morphine is, in many ways, similar to that produced by the μ receptor agonist DAGO. However, morphine-induced locomotion is dissimilar from the hyperactivity observed after injection of an opioid agonist (DPDPE) selective for the δ receptor. These observations support and extend the findings of others (Carroll and Sharp 1972; Castellano and Oliverio 1975; Shuster et al. 1975; Kameyama and Ukai 1983; Oliverio et al. 1984; Cowan et al. 1986).

Different locomotor effects have been reported following injections of enkephalins that act, with some selectivity, at the δ receptor. For example, Bhargava (1978) reported a suppression of locomotion following an i.vent. injection of methionine-enkephalin in mice (Swiss-Webster) known to exhibit morphine-induced hyperactivity. Whereas, Katz et al. (1978) observed a sustained increase in locomotion following i.vent. injections of enkephalin analogues (D-Ala^2 Leu and Met-enkephalin-amides) in the Swiss-Webster mouse. Similarly, Puglisi-Allegra et al. (1982) reported stimulated locomotion after i.vent. injections of D-Ala^2, Leu-enkephalin-amide in the C57BL/5 mouse. These previous studies used enkephalins that are less selective for δ receptors than is DPDPE (Mosberg et al. 1983). Still, our data agree with the preponderance of evidence that δ receptor agonists can cause mouse locomotor hyperactivity.

Despite the fact that DPDPE stimulated horizontal locomotion to levels similar to those produced by morphine and DAGO, our findings suggest that the character of movements produced by opioid δ receptor activation is quite dissimilar from that observed following an injection of a μ receptor agonist. In particular, δ opioid receptor activation caused frequent rearing and non-stereotypic hyperactivity throughout all areas of the test chamber. On the other hand, the μ receptor ligand suppressed rearing and caused thigmotaxis. This observation of different locomotor topographies induced by μ or δ receptor agonists seems consistent with other reports (Volterra et al 1984) suggesting that a selective δ receptor antagonist (ICI 154129) does not influence the stimulant effect of morphine on mouse horizontal locomotion. Further, Cowan et al. (1986) found that DPDPE-induced vertical rearing (in the rat) was selectively reduced by an injection of the δ receptor antagonist ICI 174864.

Thigmotaxic responses recorded following injections of either DAGO or morphine were profound and, in some ways, similar to those observed in rats following scopolamine, apomorphine (Geyer et al. 1986) or lysergic acid diethylamide (LSD) (Adams and Geyer 1985). Since thigmotaxis involves avoidance of novel central areas in an open field, some investigators have interpreted this response as being characteristic of an increase in "emotionality" (Hall 1934; Royce 1977) or hallucinogenic activity (Adams and Geyer 1985; Gold et al. 1988). Our data suggest that what Hall (1934) described as "emotional" components of opioid-stimulated motor activity may be mediated more directly by μ than δ opioid receptor subtypes.

The fact that C57 mouse locomotion is quite sensitive to the stimulatory effects of the original prototypical μ agonist, morphine (Moskowitz et al. 1985), along with the finding that this mouse strain has a large number of μ receptors in brain motor areas (Moskowitz and Goodman 1985), has suggested the hypothesis that μ receptors play a prominent role in the production of opiate-induced running fits (Oliverio et al. 1984). This hypothesis is supported by our findings, since DAGO induced a motor response topographically similar to that produced by morphine. Based on the present data, however, we cannot exclude some synergistic action of morphine at both μ and δ receptors. The involvement of multiple receptor sites in the production of morphine-stimulated locomotion is consistent with previously reported data suggesting that the variable proportions of μ and δ opioid receptors in different mouse strains may explain the dissimilarities in their quantity of morphine-induced locomotion (Reggiani et al. 1980; Castellano et al. 1984; Oliverio et al. 1984). Recently, an additional receptor (μ_1) with high affinities for both opiates and enkephalins has been identified (Pasternak 1988). Future investigations might test the hypothesis that the μ_1 receptor plays a role in integrating the behavioral effects mediated by either the μ_2 sites (which preferentially bind morphine) and δ sites (which selectively bind enkephalins).

Most of our behavioral effects were dose independent. This is surprising, since morphine has been shown to produce a dose-dependent hyperactivity when it is administered to C57 mice via a peripheral route (Castellano and Oliverio 1975). Since the i.vent. doses of all the opioid agonists employed in the current study produced surprisingly flat dose/response functions, this leads us to speculate that we may not have tested morphine, DAGO and DPDPE over their full range of activity. If this is true, it is difficult to make unequivocal statements about the identity of the receptors mediating quantitative differences in opioid-stimulated locomotion. For example, different amounts of horizontal activity following DAGO and morphine may represent different parts of an as-yet-fully-described dose/response curve. Perhaps the distinct qualitative differences observed in locomotor topography (e.g., rearing, thigmotaxis) and postures (Straub tail) may more readily allow us to characterize components of locomotion produced by the selective μ or δ opioid receptor agonists used here.

The dose-independence of our behavioral phenomena belies the fact that the levels of agonist used in the present study covered a relatively wide gamut. The intraventricular doses of morphine administered in this study were both higher (60 μg) and lower (10, 20 μg) than those previously reported (Stevens et al. 1986). In the

case of the opioid μ receptor agonist DAGO, we employed doses spanning a 20-fold range. DPDPE (δ receptor agonist) and morphine sulfate were administered in dose ranges that encompassed 12 and 6 orders of magnitude, respectively. The concentrations of intraventricular DAGO, DPDPE and morphine we selected are of similar size and range as those used by others characterizing opioid receptor involvement in mouse behavior (Heyman et al. 1987; Porreca et al. 1987). Further, the doses used here were chosen with knowledge of the relative behavioral potencies of these opioid agonists (i.e., DAGO > DPDPE > morphine) in producing analgesia (Dickenson et al. 1987, Galligan et al. 1987) or place conditioning (Bals-Kubik et al. 1989). Our data highlight the fact that the selection of appropriate drug doses is a complicated issue that is dependent on receptor populations present, selectivity and potency of the agonists, distribution and kinetics of the drug in the test system, and knowledge of the behavior of interest.

It should be noted that the relatively flat dose/response curves reported here are not unprecedented. Others have found similar relationships between pain responsivity and intraventricular injections of DPDPE (administered within the range also used in the current experiment, Heyman et al. 1987). Further, when mouse vertical activity (rearing) is the dependent variable, a relatively flat dose/response relationship exists following a 10-fold range of injections of DPDPE (3–30 mg/kg, SC) (Cowan et al. 1986). Our data corroborate these previous reports and reveal the unexpected finding that the locomotor stimulation evoked by our three different opioid agonists are strikingly insensitive to dose manipulation.

In summary, morphine and opioid agonists more selective for either μ or δ receptors all produced locomotor hyperactivity in the C57BL/6J mouse. Different horizontal movement response topographies and enhanced rearing distinguished DPDPE-stimulated locomotor hyperactivity from that following morphine or DAGO. Although we administered opioid agonists in a variety of doses, locomotion was rather insensitive to this dose manipulation. Future studies may reveal more apparent dose dependent locomotor phenomena and thereby allow a complete characterization of the role of μ and δ opioid receptors in C57BL/6J mouse hyperactivity.

References

Aceto MD, McKean DB, Pearl J (1969) Effects of opiates and opiate antagonists on the Straub tail reaction in mice. Br J Pharmacol 36:225–239

Adams LM, Geyer MA (1985) A proposed model for hallucinogens based on LSD's effects on patterns of exploration in rats. Behav Neurosci 99:881–900

Bals-Kubik R, Shippenberg T, Herz A (1989) Reinforcing effects of opioids in the rat: selective antagonism by β-endorphin-(1-27). In: Cros J, Meunier J-Cl, Hamon M (eds) Advances in the biosciences, vol 75, Progress in opioid research. Pergamon Press, Oxford New York, pp 667–669

Bhargava HN (1978) Effects of methionine-enkephalin and morphine on spontaneous locomotor activity. antagonism by naloxone. Pharmacol Biochem Behav 9.167–171

Browne RG, Derrington DC, Segal CS (1979) Comparison of opiate and opioid-peptide-induced immobility. Life Sci 24:933–942

Carroll BJ, Sharp P (1972) Monoamine mediation of the morphine induced activation of mice. Br J Pharmacol 46:124–139

Castellano C (1981) Strain dependent effects of the enkephalin analogue FK 33-824 on locomotor activity in mice. Pharmacol Biochem Behav 15:729–734

Castellano C, Oliverio A (1975) A genetic analysis of morphine-induced running and analgesia in the mouse. Psychopharmacologia 41:197–200

Castellano C, Pavone F, Sansone M (1984) Locomotor depression by the opioid benzodiazepine tifluadom in mice. Arch Int Pharmacodyn Ther 270:318–323

Cowan A, Rance MJ, Blackburn TP (1986) In vivo studies on delta opioid receptors. Natl Inst Drug Abuse Monogr Ser 75:473–476

Dickenson AH, Sullivan AF, Knox R, Zajac JM, Rogues BP (1987) Opioid receptor subtypes in the rat spinal cord: electrophysiological studies with μ- and δ-opioid receptor agonists in the control of nociception. Brain Res 413:36–44

Galligan JJ, Mosberg HI, Hurst R, Hruby VJ, Burks TF (1984) Cerebral delta opioid receptors mediate analgesia but not the intestinal motility effects of intracerebroventricularly administered opioids. J Pharmacol Exp Ther 229:641–648

Geyer MA, Russo PV, Masten VL (1986) Multivariate assessment of locomotor behavior: pharmacological and behavioral analyses. Pharmacol Biochem Behav 25:277–288

Gold LH, Koob GF, Geyer MA (1988) Stimulant and hallucinogenic behavioral profiles of 3,4,-methylenedioxymethamphetamine and N-ethyl-3,4,-methylenedioxymethamphetamine in rats. J Pharmacol Exp Ther 247:547–555

Goldstein A (1987) Binding selectivity profiles for ligands of multiple receptor types: focus on opioid receptors. TIPS 8:456–459

Hall CS (1934) Emotional behavior in the rat. I. Defecation and urination and measures of individual differences in emotionality. J Comp Psychol 18:385–403

Handa BK, Lane AC, Lord JAH, Morgan BA, Rance JM, Smith CFC (1981) Analogues of β-LPH 61-64 processing selective agonists at mu opiate receptors. Eur J Pharmacol 70:531–540

Hart SL, Friend SC, Cowan DA (1989) Alteration of δ and κ opioid receptor mediated activity in mice by an anabolic steroid. In. Cros J, Meunier J-Cl, Hamon M (eds) Advances in the biosciences, vol 75, Progress in opioid research. Pergamon Press, Oxford New York, pp 656–662

Heyman JS, Mulvaney SA, Mosberg HI, Porreca F (1987) Opioid δ-receptor involvement in supraspinal and spinal antinociception in mice. Brain Res 420:100–108

Kameyama T, Ukai M (1981) Multi-dimensional analysis of behavior in mice treated with α-endorphin. Psychopharmacology 20:247–250

Kameyama T, Ukai M (1983) Multi-dimensional analyses of behavior in mice treated with morphine, endorphins and [Des-tyrosine¹]-γ-endorphin. Pharmacol Biochem Behav 19.671–677

Katz RJ, Carroll BJ, Baldrighi G (1978) Behavioral activation by enkephalins in mice. Pharmacol Biochem Behav 8:493–496

Kosterlitz HW, Hughes J, Lord JAH, Waterfield AA (1977) Enkephalins, endorphins, and opiate receptors. In: Approaches to the cell biology of neurons. Society for Neuroscience Symposia, vol II. Society for Neuroscience, Bethesda, MD, pp 291 307

Kosterlitz HW, Paterson SJ (1981) Tyr-D-Ala-Gly-MePhe-NH(CH₂)₂-OH is a selective ligand for the mu opiate binding site. Br J Pharmacol 73:299

Lord JAH, Waterfield AA, Hughes J, Kosterlitz HW (1977) En-

dogenous opioid peptides: multiple agonists and receptors. Nature 267:495-499

Martin WR (1984) Pharmacology of opioids. Pharmacol Rev 35:283-323

McPherson CW (1963) Reduction of *Pseudomonas aeruginosa* and coliform bacteria in mouse drinking water following treatment with hydrochloric acid and chlorine. Lab Anim Care 13:737-745

Miller G (1981) Simultaneous statistical inference, 2nd edn. Springer, Berlin Heidelberg New York, pp 6-8

Miller RJ (1986) Peptides as neurotransmitters: focus on the enkephalins. In: DeWeid D, Gispen WH, VanWimersma Greidanus TjB (eds) Neuropeptides and behavior, vol 1. Pergamon Press, New York, Toronto, pp 95-136

Mosberg HI, Hurst R, Hruby VJ, Gee K, Yamamura HI, Galligan JJ, Burks TF (1983) Bis-penicillamine enkephalins possess highly improved specificity toward δ-opioid receptors. Proc Natl Acad Sci USA 80:5871-5874

Moskowitz AS, Goodman RR (1985) Autoradiographic analysis of mu_1, mu_2 and delta opioid binding in the central nervous system of C57BL/6BY and CXBK (opioid receptor-deficient) mice. Brain Res 360:108-116

Moskowitz AS, Terman GW, Carter KR, Morgan MJ, Liebeskind JC (1985) Analgesic, locomotor and lethal effects of morphine in the mouse: strain comparisons. Brain Res 361:46-51

Oliverio A (1975) Genotype-dependant electroencephalographic, behavioral and analgesic correlates of morphine. an analysis in normal mice and in mice with septal lesions. Brain Res 83:135-141

Oliverio A, Castellano, C (1974) Genotype-dependant sensitivity and tolerance to morphine and heroin. dissociation between opiate-induced running and analgesia in the mouse. Psychopharmacologia 39:13-22

Oliverio A, Castellano C, Puglisi-Allegra S (1984) Psychobiology of opioids. Int Rev Neurobiol 25:277-337

Pasternak GW (1988) Multiple mu opiate receptors. ISI Atlas Sci: Pharmacol 148-154

Porreca F, Heyman JS, Mosberg HI, Omnaas JR, Vaught JL (1987) Role of mu and delta receptors in the supraspinal and spinal analgesic effects of [D-Pen^2, D-Pen^5] enkephalin in the mouse. J Pharmacol Exp Ther 241:393-400

Puglisi-Allegra S, Castellano C, Filibeck U, Oliverio A, Melchiorri P (1982) Behavioural data on dermorphins in mice. Eur J Pharmacol 82:223-227

Reggiani A, Battaini F, Kobayashi H, Spano 'P, Trabucchi M

(1980) Genotype-dependent sensitivity to morphine: role of different opiate receptor populations. Brain Res 189:289-294

Royce JR (1977) On the construct validity of open-field measures. Psychol Bull 84:1098-1106

Sanchez-Blazquez P, Garzon J (1989) Evaluation of δ receptor mediation of supraspinal opioid analgesia by in vivo protection against the β-funaltrexamine antagonist effect. Eur J Pharmacol 159:9-23

Shuster L, Webster GW, Yu G, Eleftheriou BE (1975) A genetic analysis of the response to morphine in mice: analgesia and running. Psychopharmacologia 42:249-254

Siegel S (1956) Nonparametric statistics for the behavioral sciences. McGraw-Hill, New York Toronto London, pp 184-193, 116-127

Slotnick BM, Leonard CM (1975) A stereotaxic atlas of the albino mouse forebrain (HEW Publication No. 75-100). US Department of Health Education and Welfare, Rockville, MD

Stevens KE, Mickley GA, McDermott LJ (1986) Brain areas involved in production of morphine-induced locomotor hyperactivity of the C57BL/6J mouse. Pharmacol Biochem Behav 24:1739-1747

Takemori AE, Ikeda M, Portoghese PS (1986) The μ, κ, and δ properties of various opioid agonists. Eur J Pharmacol 123:357-361

Takemori AE, Portoghese PS (1987) Evidence for the interaction of morphine with kappa and delta opioid receptors to induce analgesia in β-funaltrexamine-treated mice. J Pharmacol Exp Ther 243:91-94

Teitelbaum H, Giammatteo P, Mickley GA (1979) Differential effects of localized lesions of n. accumbens on morphine- and amphetamine-induced locomotor hyperactivity in the C57BL/6J mouse. J Comp Physiol Psychol 93: 745-751

Volterra A, Brunello N, Cagiano R, Cuomo V, Racagni G (1984) Behavioural and biochemical effects in C57BL/6J mice after a prolonged treatment with the δ-opiate antagonist ICI 154129. J Pharm Pharmacol 36:849-851

Wei ET, Tseng LF, Loh HH, Li CH (1977) Comparison of the behavioral effects of β-endorphin and enkephalin analogs. Life Sci 21:321-328

Wolozin BL, Pasternak GW (1981) A classification of multiple morphine and enkephalin binding sites in the central nervous system. Proc Natl Acad Sci 78:6181-6185

Wuster M, Schulz R, Herz A (1979) Specificity of opioids towards the mu-, delta- and epsilon-opiate receptors. Neurosci Lett 15:199-204

Note added in proof

Since the draft of this manuscript Michael-Titus et al. [Michael-Titus A, Dourmap N, Costentin J (1989) Mu and delta opioid receptors control differently the horizontal and vertical components of locomotor activity in mice. Neuropeptides 13:235-242] have published a report which is in close agreement with the data presented here.

In Vivo Modulation With Anti–Interleukin-1 (IL-1) Receptor (p80) Antibody 35F5 of the Response to IL-1. The Relationship of Radioprotection, Colony-Stimulating Factor, and IL-6

By R. Neta, S.N. Vogel, J.M. Plocinski, N.S. Tare, W. Benjamin, R. Chizzonite, and M. Pilcher

Interleukin-1 (IL-1) is radioprotective and induces both circulating colony-stimulating factor(s) (CSF) and IL-6 in mice. We evaluated the relationship among these three responses to IL-1 using anti–IL-1 receptor antibody 35F5. This antibody in vitro blocks responses of T cells and fibroblasts, but not of B cells or myeloid cell lines, to IL-1. Administration of 35F5 alone before irradiation reduced the number of surviving mice compared with those not treated with 35F5, demonstrating that endogenous IL-1 participates in the natural resistance to radiation. Thirty micrograms of 35F5 per mouse also reduced by 92% the survival of irradiated mice pretreated with 0.3 μg of IL-1. Similarly, 30 μg of 35F5 reduced by 96% to 98% the induction of IL-6 by IL-1. In contrast, 30 μg of 35F5 resulted in only moderate reduction of circulating CSF. Consequently, the level of circulating CSF after 35F5 treatment was still equivalent to levels of CSF that were induced by doses of IL-1 in the radioprotective range. Because treatment with 35F5 antibody resulted in the blocking of IL-1–reduced radioprotection, the above results suggest that circulating CSF, by itself, may not be sufficient for radioprotection. This conclusion supports our previous results which showed that granulocyte-macrophage CSF (GM-CSF) and G-CSF were radioprotective only when administered with suboptimal doses of IL-1.
This is a US government work. There are no restrictions on its use.

THE MECHANISM(S) that underlie the action of biologic radioprotectors (inflammatory or immunomodulatory agents) remain speculative, despite decades of research. The use of interleukin-1 (IL-1), a radioprotective cytokine that has a recognized range of activities and activates cells by identified specific receptors,[1,2] permits the study of these mechanisms in more detail. Several of the recognized activities of IL-1 have been suggested to provide a basis for its radioprotective effect. IL-1 induces the appearance of colony-stimulating factors (CSFs) and IL-6 in the circulation, and stimulates the production of CSF and IL-6 by cultured fibroblasts, endothelial cells, and macrophages.[3-11] Although not radioprotective when administered alone, both CSFs (granulocyte-CSF [G-CSF] and granulocyte-macrophage-CSF [GM-CSF]) and IL-6 synergized with suboptimal doses of IL-1 to induce radioprotection.[4,12]

Furthermore, IL-1 administration initiates cycling of myeloid progenitor cells in the marrow.[13,14] This cycling is thought to depend on the presence of hematopoietic growth factors, such as CSFs and IL-6, and on direct interaction of IL-1 and IL-6 with early progenitor cells.[15-17] However, direct evidence that the above mechanisms are essential for radioprotection remains to be established.

Recently, a monoclonal antibody to the IL-1 receptor was developed. This agent binds only to T lymphocytes and fibroblasts but not to B-lymphocytes, neutrophils, and myeloid cell lines.[18,19] This antibody may provide a means to dissociate those events induced by IL-1 that occur independent of radioprotection. We used this antibody in mice and compared its effect on the activity of IL-1 as a radioprotector with its effect as an inducer of circulating CSF and IL-6.

MATERIALS AND METHODS

Mice. CD2F1 male mice were purchased from the Animal Genetics and Production Branch, National Cancer Institute, National Institutes of Health (Frederick, MD). Mice were quarantined on arrival and screened for evidence of disease before being released from quarantine. They were maintained in an AAALAC-accredited facility in plastic Micro-isolator cages on hardwood chip contact bedding, and given commercial rodent chow and acidified (HCl to a pH of 2.5) tap water ad libitum. Animal holding rooms were maintained at 70°F ± 2°F with 50% ± 10% relative humidity, using at least 10 air changes per hour of 100% conditioned fresh air. The mice were on a 12-hour light-dark full-spectrum lighting cycle with no twilight. Mice were 8 to 12 weeks old when used. All cage cleaning, handling, and injections were performed in a laminar flow clean air unit.

Reagents. Human recombinant IL-1α and anti–IL-1 receptor antibody (35F5), a rat anti-mouse monoclonal immunoglobulin G$_1$ [IgG$_1$] were prepared at Hoffmann-La Roche (Nutley, NJ). Control rat IgG was purchased from Sigma Chemical Co (St Louis, MO).

The antibody and the recombinant IL-1α were diluted in pyrogen-free saline on the day of injection. The antibody was given intraperitoneally (ip) according to the protocol previously developed at Hoffmann-La Roche (unpublished results, 1989), 6 hours before ip injection of IL-1. Mice were anesthetized with methapane and were exanguinated 2 to 3 hours after IL-1 administration.

Irradiation. Mice were placed in Plexiglass containers and were given whole-body irradiation at 40 cGy/min by bilaterally positioned ^{60}Co elements. The number of surviving mice was recorded daily for 30 days.

Stromal cell culture. Murine bone marrow stromal cell cultures

were established using a modification of the method described by Dexter et al[20] for long-term marrow culutre. Briefly, bone marrow cells from one femur (approximtely 2×10^7 cells) of a 6-week-old C57Bl/6J female mouse (Jackson Laboratory, Bar Harbor, ME) were cultured in a 25-cm³ tissue culture flask (Costar, Cambridge, MA) containing 5 mL minimum essential α medium (GIBCO, Grand Island, NY) supplemented with 25% horse serum, 1×10^{-6} mol/L hydrocortisone 21-hemisuccinate (Sigma, St Louis, MO), and antibiotics. After 1 week of incubation at 33°C in a humidified atmosphere containing 5% CO_2, 95% air, half of the culture medium was replaced. After an additional 2 weeks of cultv e, a sub-confluent monolayer of adherent stromal cells, as well as hematopoietic colonies, could be observed. At this time, the medium was changed to contain 10% fetal bovine serum (HyClone, Logan, UT), plus 10% horse serum and 5×10^{-7} mol/L hydrocortisone, and the cultures were transferred to a 37°C incubator. Once confluent, cultures were trypsinized and passaged at 1- to 2-week intervals. During a 6-month selection period, several phenotypically distinct homogenous adherent stromal cell cultures were isolated. To determine the effect of 35F5 antibody on production of IL-1–stimulated cytokines, stromal culture cells were incubated for 72 hours with 130 pg/mL of IL-1 in the presence or absence of 100 μg/mL 35F5 antibody or rat IgG. Supernatants were assayed as described.

Measurement of IL-6 activity. IL-6 activity in the serum and stromal cell supernatants was determined by using the hybridoma growth factor assay described by Aarden et al.[21] This method uses the IL-6–dependent hybridoma, B9, in a conventional microproliferation assay. Briefly, individual samples were initially treated to several 10-fold dilutions in the assay medium (RPMI 1640, 10% fetal calf serum (FCS), 5×10^{-5} mol/L 2-mercaptoethanol (2ME), and 50 μg/mL gentamycin). Samples were subjected to twofold serial dilutions in 96-well culture plates containing 0.1 mL of assay medium per well. We then added 2,000 B9 cells in 0.1 mL of assay medium to each well (final volume 0.2 mL). The cultures were incubated at 37°C in a humidified atmosphere of 5% CO_2. After 72 hours, the cultures were pulsed with 0.5 μC ³H-thymidine/well for 18 hours, harvested onto glass fiber filters, and counted in a liquid scintillation counter One hybridoma growth factor unit was defined as the reciprocal of the dilution that yielded 50% of the maximal ³H-thymidine incorporation.

Measurement of CSF activity in the serum and supernatant. Mice were bled 2 to 3 hrs after IL-1 injection, and serum was collected by centrifugation after clot formation. CSF activity was measured in pooled serum samples collected from 4 to 5 mice per treatment group per experiment. Supernatants were collected from the stromal cell cultures as described above.The bone marrow colony assay for CSF activity has been described in detail.[3] Briefly, C3H/HcJ bone marrow cells were enriched for mononuclear cells by density gradient centrifugation on lymphocyte separation medium (Litton Bionetics, Charleston, SC). The cells collected from the interface of the gradient were washed and resuspended in RPMI 1640 supplemented with antibiotics, glutamine, sodium bicarbonate, HEPES buffer, and 15% FCS. Three serial twofold dilutions of each serum sample (30%, 15%, and 7.5% vol/vol) or two fourfold dilutions of stromal cells supernatant sample (20% and 5% vol/vol) were prepared in this medium, and 0.2 mL of each dilution was added to each duplicate well in a 6-well tissue culture plate. A final cell suspension was prepared of 1×10^5 cells/mL in complete medium supplemented with 0.35% Bacto-Agar (Difco, Detroit, MI) and maintained at 41°C. Immediately after resuspension of the cells in the agar-medium mixture, 1 mL of this medium was added to each well Once solidified, the cultures were incubated at 37°C, 6% CO_2, for 6 to 7 days, at which time colonies (≥ 25 cells per colony) were counted under a dissecting microscope. CSF activity was expressed

as colony-forming units per milliliter, based on colony count within the linear part of the dilution curve.

Statistical analysis. Statistical evaluation of the results was done using chi-square analysis.

RESULTS

Effect of anti–IL-1 receptor antibody 35F5 on radiation sensitivity of mice. We have shown that pretreatment with IL-1 confers radioprotection on mice.[22] Conversely, others have shown that radiation results in a subsequent increase in IL-1.[23-26] To determine if endogenous IL-1 is important in protection from damage by ionizing radiation, mice were administered the 35F5 antibody, control rat Ig, or saline before midlethal irradiation (Table 1). The results show clearly that pretreatment with the 35F5 antibody reduces the survival of mice significantly.

The effect of 35F5 antibody on radioprotection induced by IL-1. The 35F5 antibody has been shown to block the effect of IL-1 only on selected cell populations: fibroblasts and T-lymphoid cells, but not myeloid cells and B lymphocytes.[18,19] Therefore, we determined whether treatment with 35F5 could reduce the radioprotective effect of IL-1. Experimental mice were administered the 35F5 antibody, while control mice were treated with either rat Ig at equivalent concentrations or saline 6 hours before injection of 0.3 μg of IL-1, and exposed to lethal irradiation 20 hours later. The results demonstrate that even the 30-μg dose of the antibody almost completely blocked the radioprotective action of IL-1 (Table 2).

Dose-dependence of the radioprotective effect and CSF-inducing effects of IL-1. We have previously shown that IL-1 induces the release of CSF into circulation.[3] The increase in circulating CSF and the corresponding increase in radioprotection is dependent on the dose of IL-1 (Table 3). The results show that at IL-1 doses above 0.1 μg, the titers of CSF approach plateau values (Tables 3 and 4). However,

Table 1. Radiosensitization of Mice With Anti–IL-1 Receptor Antibody 35F5

Treatment*	Dead/Total	Survival (%)
Saline	7/16	56
Rat Ig	4/8	50
35F5	21/26	20†

*CD2F1 mice received 100 μg of 35F5 antibody, vehicle, or equivalent amount of rat Ig 6 hours before irradiation with 825 cGy. Combined results of three experiments.

†$P < .05$ compared with saline control.

Table 2. Effect of Anti–IL-1 Receptor Antibody 35F5 on Radioprotection With IL-1

Treatment*	Dead/Total	Survival (%)
Rat Ig	53/54	2
IL-1	15/78	81
IL-1 + 35F5 (30 μg)	44/48	8
IL-1 + 35F5 (150 μg)	48/52	8

*CD2F1 mice received ip injection of 35F5 antibody followed 6 hours later with ip injection of 0.3 μg of IL-1. Control mice received rat IgG (100 μg), followed by saline injection. Twenty hours after injection of IL-1, the mice were irradiated with 950 cGy.

Table 3. Relationship of the Effect of Increasing Doses of IL-1 on Radioprotection and CSF in Serum of Mice

Dose of IL-1 (μg)	CSF titer* (±SEM)	Dead/Total*	Survival (%)
Saline	<20	15/16	6
0.05	1,430 ± 450	14/19	26
0.10	2,140 ± 520	12/20	40†
0.30	3,220 ± 570	5/20	75†
0.50	2,880 ± 280	2/12	83†

*The results are the means (±SEM) of three experiments using pooled serum from three mice per group. Radioprotection results are derived from two experiments (950 cGy).

†$P < .05$ compared with saline controls.

radioprotection increases more gradually, with 0.1 μg of IL-1 conferring 40%; 0.3 μg, 75%; and 0.5 μg, 83% protection. A dose of 0.05 μg of IL-1 conferred only limited radioprotection, but a significant increase in circulating CSF.

The effect of 35F5 antibody on levels of CSF in circulation. To determine if induction of CSF with IL-1 was also blocked by 35F5, we used IL-1 in concentrations of 0.1 μg and 0.5 μg, doses just above and below those used in the radioprotection experiments (0.3 μg). Table 4 shows that both 0.1 μg and 0.5 μg of IL-1 induced high titers of CSF in circulation. The use of 35F5 antibody reduced CSF in a dose-dependent manner: 30 μg of 35F5 reduced by 16% the titers that were induced by a 0.5-μg dose, and reduced by 52% the titers induced by a 0.1-μg dose of IL-1. Thus, we assume that the 35F5 reduction of CSF induced with 0.3 μg of IL-1 is within the above-mentioned percentage range. Thirty micrograms of the 35F5 antibody with 0.1 μg of IL-1 reduced titers of CSF to levels comparable with those induced with 0.05 μg of IL-1 given alone. The same dose of antibody (30 μg) used with 0.5 μg of IL-1 reduced CSF to a level similar to that induced with 0.1 μg of IL-1.

The effect of 35F5 antibody on levels of circulating IL-6. Our previous work established that IL-1 induces high titers of IL-6 in circulation within 2 to 4 hours after injection.[4] We examined the effect of 35F5 antibody on the IL-1-induced increase in serum IL-6. Low doses of 35F5 (30 μg) resulted in 96% and 98% reductions in IL-6 titers at 0.5 μg and 0.1 μg of IL-1, respectively (Table 4). Thus, we observed a more complete abrogation in IL-6 than in CSF.

The effect of 35F5 antibody on production of CSF and IL-6 by stromal cells. IL-1 has been shown to induce production of CSF and IL-6 in bone marrow stromal cells.

The type of IL-1 receptor on these cells has not been determined. Therefore, the effect of 35F5 antibody on IL-1-induced production of CSF and IL-6 by stromal cells was examined in vitro. IL-1-induced production of IL-6 and CSF was found to be reduced in the presence of 35F5 antibody (Table 5). Rat IgG, alone or in the presence of IL-1, did not effect CSF or IL-6 production (results not shown). These results show that 35F5 anti-IL-1 receptor antibody blocks stromal cell responses to IL-1, indicating that these cells express receptors similar to those on EL-4 cells.

DISCUSSION

Anti-IL-1 receptor antibody (35F5) administered to mice before irradiation with 825 cGy rendered them more susceptible to the lethal effects of radiation. This result provides the first direct evidence that endogenously produced IL-1 plays an important role in protection from radiation injury. It has been observed previously that radiation induces production of IL-1.[23-26] In view of the present results, the presence of endogenously produced IL-1 after irradiation may represent a natural defense mechanism of the host against damage from ionizing radiation. Furthermore, our previous finding that treatment with pharmacologic doses of IL-1 (10 μg/mouse) after irradiation protects mice from death,[27] suggests that insufficient amounts of IL-1 may be produced endogenously because an additional exogenous supply of IL-1 is required for a greater degree of protection.

Figure 1 summarizes the effects of 35F5 on radioprotection (Table 2) and on serum CSF and IL-6 production (Table 4). Anti-IL-1 receptor antibody 35F5 administered to mice before injection of recombinant IL-1 reduced the radioprotective effects of IL-1 from 81% survival to 8% survival. Increasing doses of antibody (from 30 μg to 150 μg) had no additional effect. However, the same dose of antibody (30 μg) that blocked the radioprotective effect of IL-1 resulted in a comparatively small (between 16% and 50%) reduction in the titers of circulating CSF. Thus, despite the remaining high titers of circulating CSF, 92% of IL-1-treated mice given antibody succumbed to radiation-induced lethality. Increasing the dose of antibody to 150 μg reduced the CSF production, which was induced by 0.1 μg of IL-1, by 95%. Therefore, it appears that higher doses of 35F5 antibody can block the appearance of CSF in the circulation.

The 30-μg dose of 35F5 antibody not only blocked IL-1-induced radioprotection, but also greatly reduced the level of IL-6 in circulation. These results suggest that cells with

Table 4. Effect of Anti-IL-1 Receptor Antibody 35F5 on IL-1-Induced CSF Production

Treatment (μg)*	CSF Titer (± SEM)	Reduction (%)	IL-6 Titer (± SEM)	Reduction (%)
IL-1 (0.1)	2,300 ± 347	—	7,940 ± 4,860	—
IL-1 (0.5)	2,885 ± 278	—	44,800 ± 6,400	—
IL-1 (0.1) + 35F5 (30)	1,110 ± 330	52	132 ± 68	98
IL-1 (0.5) + 35F5 (30)	2,412 ± 97	16	2,110 ± 1,090	96
IL-1 (0.1) + 35F5 (150)	160 ± 70	95	<100	100
IL-1 (0.5) + 35F5 (150)	1,160 ± 725	60	1,310 ± 290	97
Control	<20	—	<100	100

*CD2F1 mice were bled 2 to 3 hours after IL-1 injection and serum was assayed for the presence of CSF or IL-6 (using the IL-6-dependent hybridoma B9). The results represent the means (±SEM) of three experiments using pooled serum from 3 to 5 mice in each experiment.

Table 5. Inhibition of IL-1 Stimulated Release of IL-6 and CSF From Bone Marrow Stomal Cells by 35F5 Antibody

Treatment*			
IL-1	35F5	IL-6 (U/mL) (±SD)	CSF (U/mL) (±SD)
—	—	60 ± 20	1,650 ± 850
—	+	60 ± 20	1,425 ± 825
+	—	22,400 ± 4,200	5,125 ± 875
+	+	180 ± 60	2,075 ± 475

*Bone marrow stromal cell cultures were incubated with 130 pg/mL IL-1 and/or 100 µg/mL 35F5 antibody. Culture supernatants were collected after 72 hours, and IL-6 and CSF were determined as described in Materials and Methods. Rat IgG in doses equivalent to 35F5 was used as control and had no effect. Results are the average from two experiments.

identical IL-1 receptor participate in radioprotection and IL-1-induced IL-6 release. Although combined therapy with IL-1 and IL-6 achieved synergistic radioprotection,[4] this close correlation of radioprotection and the presence of IL-6 in circulation does not necessarily indicate a role of circulating IL-6 in radioprotection. The importance for radioprotection of serum versus tissue levels of cytokines, such as IL-6 or CSFs, requires further analysis.

It is interesting to note that, in culture, 35F5 interacted only with the type of IL-1 receptor present on T lymphocytes and fibroblast cells, but not with the second type of IL-1 receptor detected on B cells, neutrophils, and myeloid cells.[18,19] In view of these findings, the nearly complete elimination of circulating IL-6 and, at high concentration of 35F5, of CSF, is surprising because macrophages are known to be a source of G-CSF, GM-CSF, and IL-6,[28-30] and are not expected to be blocked by this antibody. One possible explanation for the observed blocking of IL-6 and CSF may be based on the negligible contribution of macrophages to the levels of IL-6 and CSF in circulation. Another explanation may be based on the need for a second factor, in addition to IL-1, to stimulate the macrophages.

The fact that IL-6 has been shown to synergize with a variety of CSFs to enhance colony growth of specific progenitor populations[31-33] may underlie the apparent preferential inhibition of 35F5 on IL-6 versus CSF activity. The whole serum, which presumably contained a mixture of CSFs, may have shown reduced colony-forming activity, not due to decreased production of CSF, but rather due to elimination of synergizing IL-6. Alternatively, a specific species of CSF may have been affected by treatment. Clearly, the use of CSF-type specific antibodies will be necessary to determine whether a lower dose of 35F5 antibody blocks only the release of selected hematopoietic growth factors.

Our results show that an increase of CSF in circulation was initially a function of the dose of IL-1, but reached a plateau at doses exceeding 0.1 µg of IL-1 (Tables 3 and 4),[3] with differences not observed at dose increases ranging from 0.3 to 0.5 µg. In contrast, radioprotection was dose-dependent in a more gradual fashion, with 0.05-µg doses conferring protection to 25% of mice, 0.1 µg protecting 40%, and 0.3 to 0.5 µg protecting 75% to 83% of mice. Comparison of the results leads to the conclusion that the mere presence of high titers of CSF in circulation is not sufficient for radioprotection (Tables 2 through 4). This conclusion is also supported by the observation that IL-1-induced radioprotection is strain-specific,[34] whereas IL-1-induced CSF is observed in all mouse strains.

The finding that 35F5 antibody blocks the release of IL-6 and CSF by IL-1-stimulated stromal cells suggests that stromal cells express T-type IL-1 receptors. Hence, 35F5
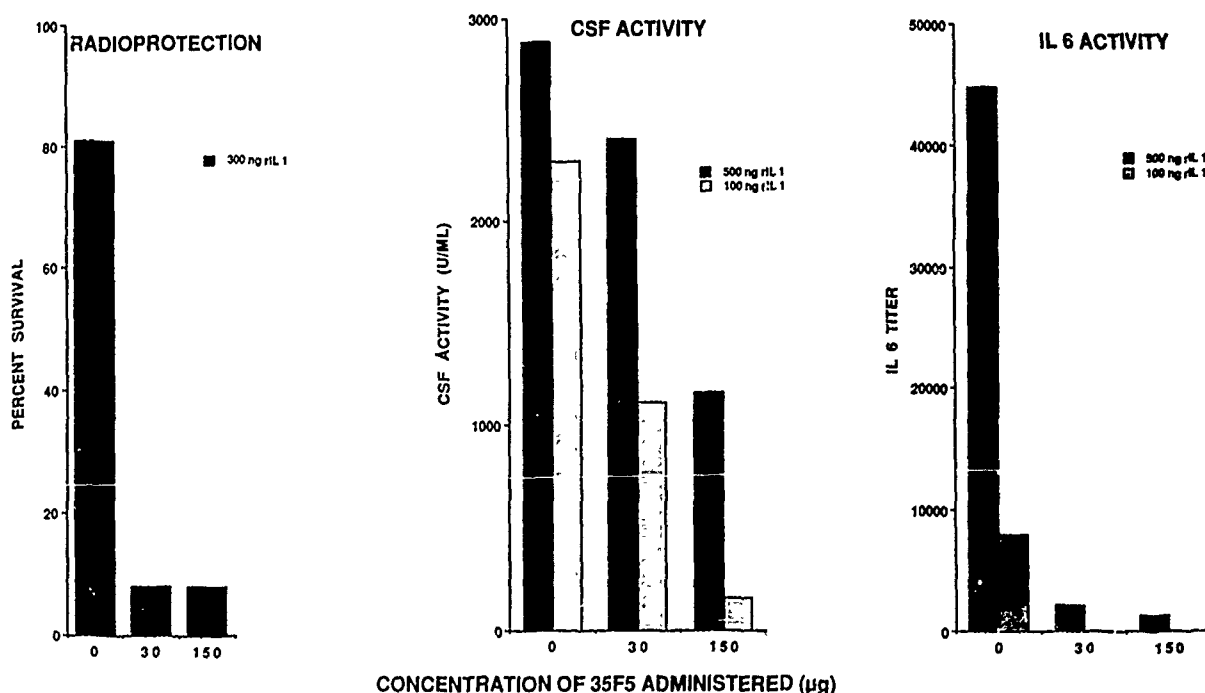
Fig 1. Comparison of the effects of 35F5 anti-IL-1 receptor antibody on Il-1-induced radioprotection and production of IL-6 and CSF.

may directly block CSF and IL-6 production in the bone marrow. 35F5 may also have an indirect effect on bone marrow cells, as indicated by the observation that in IL-1-treated mice, 35F5 greatly reduces efflux of neutrophils (Benjamin et al, unpublished results, 1989). As indicated above, neutrophils are not blocked by 35F5 from binding IL-1. Thus, it appears that release of other IL-1-induced factors, such as IL-8, a chemoattractant of neutrophils, may be blocked or reduced by 35F5.

It is notable that, in vitro, stromal cells produce CSF in substantial quantities within 72 hours, even in the absence of IL-1 (Table 5). However, addition of IL-1 results in much higher CSF titers, which are decreased to background levels by 35F5. This leads to the conclusion that 35F5 blocks IL-1-induced CSF production. These results support the hypothesis that IL-1 stimulates bone marrow stromal cells to produce other cytokines, such as IL-6 and CSF, which synergize with IL-1 to stimulate bone marrow progenitor cells and thus counteract the damaging effects of lethal irradiation.

REFERENCES

1. Durum S, Oppenheim JJ, Neta R. Immunophysiological role of interleukin-1, in Oppenheim JJ, Shevach E (eds): Immunophysiology:Role of Cells and Cytokines in Immunity and Inflammation. Oxford, UK, Oxford University, 1989, p 210

2. Dinarello CA. Interleukin-1 and its biologically related cytokines. Adv Immunol 44:153, 1989

3. Vogel SN, Douches SD, Kaufman EN, Neta R: Induction of colony stimulating factor in vivo by recombinant interleukin 1α and recombinant tumor necrosis factor α. J Immunol 138:2143, 1987

4. Neta R, Vogel SN, Sipe JD, Wong GG, Nordan RP: Comparison of in vivo effects of human recombinant IL 1 and human recombinant IL 6 in mice. Lymphokine Res 7:403, 1988

5. Zucali JR, Dinarello CA, Oblon DJ, Gross MA, Anderson L, Weiner RS: Interleukin 1 stimulates fibroblasts to produce granulocyte-macrophage colony stimulating activity and prostaglandin E2. J Clin Invest 77:1857, 1986

6. Bagby GC, Dinarello CA, Wallace P, Wagner C, Hefeneider S, McCall E: Interleukin 1 stimulates granulocyte-macrophage colony-stimulating activity release by vascular endothelial cells. J Clin Invest 78:1316, 1986

7. Fibbe WE, Van Damme J, Billiau A, Voogt PJ, Duinkerken N, Kluck PMC, Falkenburg JHF. Interleukin-1 (22 K factor) induces release of granulocyte-macrophage colony-stimulating activity from human mononuclear phagocytes. Blood 68:1316, 1986

8. Van Damme J, Cayphas S, Opdenakker G, Biliau A, Van Snick J: Interleukin-1 and poly(rI)-poly(rC) induce production of a hybridoma growth factor by human fibroblasts. Eur J Immunol 17.1, 1987

9. Kohase M, May LT, Tamm I, Vilcek J, Sehgal PB: A cytokine network in human diploid fibroblast. Interactions of beta-interferons, tumor necrosis factor, platelet-derived growth factor, and interleukin 1. Mol Cell Biol 7:273, 1987

10. Billiau A. Interferon-β2 as a promoter of growth and differentiation of B-cells. Immunol Today 8:84, 1987

11. Lee M, Segal GM, Bagby GC: Interleukin 1 induces human bone marrow-derived fibroblasts to produce multilineage hematopoietic growth factors. Exp Hematol 15:983, 1987

12. Neta R, Oppenheim JJ, Douches SD. Interdependence of the radioprotective effects of human recombinant IL 1, TNF, G-CSF, and murine recombinant GM-CSF. J Immunol 140:108, 1988

13. Neta R, Sztein MB, Oppenheim JJ, Gillis S, Douches SD. In vivo effects of IL-1. I. Bone marrow cells are induced to cycle following administration of IL-1. J Immunol 139:1861, 1987

14. Schwartz GN, Neta R, Vigneulle RM, Patchen ML, MacVittie TJ. Recovery of hematopoietic colony-forming cells in irradiated mice pretreated with interleukin-1 (IL-1). Exp Hematol 16.752, 1988

15. Ikebuchi K, Wong GG, Clark SC, Ihle JN, Hirai Y, Ogawa M: Interleukin 6 enhancement of interleukin 3-dependent proliferation of multipotential hemopoietic progenitors. Proc Natl Acad Sci USA 84:9035, 1987

16. Moore MAS, Warren DG: Synergy of interleukin 1 and granulocyte colony-stimulating factor: In vivo stimulation of stem cell recovery and hematopoietic regeneration following 5-fluorouracil treatment of mice. Proc Natl Acad Sci USA 84:7134, 1987

17. Mochizuki DY, Eisenman JR, Conlon PG, Larsen AD, Tushinski RJ. Interleukin 1 regulates hematopoietic activity, a role previously ascribed to hemopoietin 1. Proc Natl Acad Sci USA 84:5267, 1987

18. Chizzonite R, Truitt T, Kilian PL, Stern AS, Nunes P, Parker KP, Kaffka KL, Chua AO, Lugg DK, Gubler U: Two high-affinity interleukin 1 receptors represent separate gene products. Proc Natl Acad Sci USA 86:8029, 1989

19. Bomstzyk K, Sims JE, Stanton TH, Slack J, McMahan CJ, Valentine MA, Dower SK: Evidence for different interleukin 1 receptors in murine B- and T-cell lines. Proc Natl Acad Sci USA 86:8034, 1989

20. Dexter TM, Allen TD, Lajtha LG. Conditions controlling the proliferation of hemopoietic stem cells in vitro. J Cell Physiol 91:335, 1977

21. Aarden LA, De Groot ER, Schaap OL, Landsdorp PJ: Production of hybridoma growth factor by human monocytes. Eur J Immunol 17:1411, 1987

22. Neta R, Douches SD, Oppenheim JJ: Interleukin-1 is a radioprotector. J Immunol 136:2483, 1986

23. Geiger B, Galily R, Gery I. The effect of irradiation on the release of lymphocyte activating factor (LAF). Cell Immunol 7:177, 1973

24. Granstein RD, Sander DN. Whole body exposure to ultraviolet radiation results in increased serum interleukin-1 activity in humans. Lymphokine Res 6:187, 1987

25. Ansel JC, Luger TA, Green I. The effect of in vitro and in vivo UV irradiation on the production of ETAF by human and murine keratenocytes. J Invest Dermatol 81:519, 1983

26. Ansel JC, Luger TA, Green I. Fever and increased serum IL-1 activity as a systemic manifestation of acute phototoxicity in New Zealand white rabbits. J Invest Dermatol 89.32, 1987

27. Neta R, Oppenheim JJ. Cytokines in therapy of radiation injury. Blood 72:1093, 1988

28. Vellenga E, Rambaldi A, Ernst TJ, Ostapovicz D, Griffin JD: Independent regulation of M-CSF and G-CSF gene expression in human monocytes. Blood 71:1529, 1988

29. Sieff CA, Niemeyer CM, Mentzer SJ, Faller DV. Interleukin-1, tumor necrosis factor, and the production of colony-stimulating factors by cultured mesenchymal cells. Blood 72.1316, 1988

30. Nordan RP, Potter M: A macrophage-derived factor required by plasmocytomas for survival and proliferation in vitro. Science 233:566, 1986

31. Ikebuchi K, Ihle JN, Hirai Y, Wong GG, Clark SC, Ogawa M: Synergistic factors for stem cell proliferation: Further studies of the target stem cells and the mechanism of stimulation by interleukin-1, interleukin-6, and granulocyte colony-stimulating factor. Blood 72:2007, 1988

32. Bruno E, Miller ME, Hoffman R: Interacting cytokines regulate in vitro human megakaryocytopoiesis. Blood 73:671, 1989

33. Caracciolo D, Clark SC, Rovera G: Human interleukin-6 supports granulocyte differentation of hematopoietic progenitor cells and acts synergistically with GM-CSF. Blood 73:666, 1989

34. Neta R, Oppenheim JJ, Douches SD, Giclas PC, Imbra RJ, Karin M: Radioprotection with interleukin-1: Comparison with other cytokines. Progr Immunol 6:900, 1986

Original Paper

Therapeutic Administration of Recombinant Human Granulocyte Colony-Stimulating Factor Accelerates Hemopoietic Regeneration and Enhances Survival in a Murine Model of Radiation-Induced Myelosuppression

Myra L. Patchen[a], Thomas J. MacVittie[a], Brian D. Solberg[a], Larry M. Souza[b]

[a]Department of Experimental Hematology, Armed Forces Radiobiology Research Institute, Bethesda, Maryland, USA; [b]Amgen, Thousand Oaks, California, USA

Abstract. The primary cause of death after radiation exposure is infection resulting from myelosuppression. Because granulocytes play a critical role in host defense against infection and because granulocyte proliferation and differentiation are enhanced by granulocyte colony-stimulating factor (G-CSF), this agent was evaluated for the ability to accelerate hemopoietic regeneration and to enhance survival in irradiated mice. C3H/HeN mice were irradiated and G-CSF (2.5 μg/day, s.c.) or saline was administered on days 3-12, 1-12 or 0-12 post-irradiation. Bone marrow, splenic and peripheral blood cellularity, and bone marrow and splenic granulocyte-macrophage progenitor cell recoveries were evaluated in mice exposed to 6.5 Gy. Mice exposed to 8 Gy were evaluated for multipotent hemopoietic stem cell recovery (using endogenous spleen colony-forming units) and enhanced survival. Results demonstrated that therapeutic G-CSF 1) accelerates hemopoietic regeneration after radiation-induced myelosuppression, 2) enhances survival after potentially lethal irradiation and 3) is most effective when initiated 1 h following exposure.

Introduction

Colony-stimulating factors (CSFs) are glycoprotein growth factors capable of controlling the survival, proliferation and differentiation of hemopoietic progenitor cells [1, 2]. At least four different CSFs that affect granulocyte (G-CSF), macrophage (M-CSF/CSF-1), granulocyte-macrophage (GM-CSF) and multipotential (Multi-CSF/IL-3) progenitor cells have been identified. Although the

action of some CSFs appears to be species-specific, several human CSFs cross-react with lower species. One such factor is G-CSF, which recently has been purified [3], molecularly cloned [4] and expressed as a recombinant protein [5]. The cDNA of human G-CSF exhibits a 70% sequence homology to murine G-CSF [6] and in vivo has demonstrated biological activity in mice [7, 8]. G-CSF administration has been shown to significantly increase total granulocyte numbers in normal animals [9, 10] and in drug-induced myelosuppressed animals [8, 11-13], to enhance resistance to microbial infections in neutropenic cyclophosphamide-treated animals [14] and to increase survival after lethal doses of cyclophosphamide [15]. Furthermore, G-CSF has been shown to produce a variety of effects on mature granulocytes, including prolongation of survival in vitro [16], augmentation of antibody-dependent cytotoxicity [17, 18], and enhancement of phagocytosis [1]. Recent clinical trials with cancer patients undergoing cytotoxic chemotherapy have also revealed granulocytopoietic effects of G-CSF in humans [19-21].

Neutropenia is a major factor contributing to infection-induced morbidity and mortality after radiation exposure. Agents capable of enhancing host resistance to infection and/or the regeneration of hemopoietic elements necessary for efficient host defense mechanisms could be useful in circumstances of myelosuppression resulting not only from radiotherapy, but also from accidental radiation exposures, such as those occurring recently in Chernobyl (USSR), Goiania (Brazil) and El Salvador (San Salvador). *Kobayashi et al.* demonstrated that daily administration of G-CSF to mice exposed to 3 Gy or 5 Gy of total-body radiation accelerated peripheral blood leukocyte recovery by five to ten days and stimulated femoral and splenic granulocyte-macrophage colony-forming cells (CFC-gm) regeneration [22]. The studies presented in this paper expand on *Kobayashi's* original work and describe the ability of therapeutically administered G-CSF to increase survival and to stimulate hemopoietic regeneration in more severely irradiated mice.

Materials and Methods

Mice

C3H/HeN female mice (~20 g) were purchased from Charles River Laboratories (Raleigh, NC). Mice were maintained in an accredited American Association for Accreditation of Laboratory Animal Care facility in micro-isolator cages on hardwood-chip, contact bedding and were provided commercial rodent chow and acidified water (pH 2.5) ad libitum. Animal rooms were equipped with full-spectrum light from 6 a.m. to 6 p.m. and were maintained at 70 ± 2°F with 50 ± 10% relative humidity using at least 10 air changes per hour of 100% conditioned fresh air. Upon arrival, all mice were tested for *Pseudomonas* and quarantined until test results were obtained. Only healthy mice were released for experimentation. All animal experiments were approved by the Institute Animal Care and Use Committee prior to performance.

Recombinant Human G-CSF (rhG-CSF)

rhG-CSF was provided by Amgen (Thousand Oaks, CA). This rhG-CSF (Lot #600) was derived from *E. coli* and had a specific activity of 1×10^8 U/mg as assayed by the

CFC-gm assay using normal human bone marrow cells. Endotoxin was undetectable based on the *Limulus* amebocyte lysate assay. rhG-CSF was administered s.c. at a dose of 2.5 µg/day.

Irradiation

The cobalt-60 source at the Armed Forces Radiobiology Research Institute was used to administer bilateral total-body gamma radiation. Mice were placed in ventilated plexiglass containers and irradiated at a dose of 0.4 Gy/min. Dosimetry was determined by ionization chambers. Hemopoietic recovery studies were performed after 6.5 Gy irradiations. Survival and endogenous spleen colony studies were performed after 8.0 Gy irradiations.

Survival Assays

Irradiated mice were returned to the animal facility and cared for routinely. Survival was checked and recorded daily for 30 days; on day 31, surviving mice were euthanized by cervical dislocation. Each treatment group consisted of 10 mice. Experiments were repeated 2-3 times. The percentage of mice surviving 30 days post-exposure was used to analyze survival data.

Granulocyte-Macrophage Colony-Forming Cell (CFC-gm) Assay

Hemopoietic progenitor cells committed to granulocyte and/or macrophage development were assayed using an agar CFC-gm assay. Mouse endotoxin serum (5% v/v) was added to feeder layers as a source of colony-stimulating activity. Colonies (> 50 cells) were counted after 10 days of incubation in a 37°C humidified environment containing 5% CO_2. Triplicate plates mere cultured for each cell suspension, and experiments were repeated 2-3 times. The cell suspensions used for each assay represented tissues from 3 normal, irradiated, or treated irradiated mice at each time point. Cells were flushed from femurs with 3 ml of McCoy's 5A medium (Flow Labs, McLean, VA) containing 10% heat-inactivated fetal bovine serum (Hyclone Labs, Logan, UT). Spleens were pressed through a stainless-steel mesh screen, and the cells were washed from the screen with 6 ml medium. The number of nucleated cells in the suspensions was determined by a Coulter counter. Femurs and spleens were removed from mice euthanized by cervical dislocation.

Peripheral Blood Cell Counts

Blood was obtained from cervically dislocated mice via cardiac puncture using a heparinized syringe attached to a 20-gauge needle. White blood cell (WBC), red blood cell (RBC) and platelet (PLT) cour ts were performed using a Coulter counter. In addition, blood smears were prepared and stained with Diff-Quik to perform WBC differential counts.

Endogenous Spleen Colony-Forming Unit (CFU-s) Assay

The endogenous CFU-s assay was used to measure hemopoietic stem cell recovery in irradiated mice. Mice were exposed to 8.0 Gy of radiation to partially ablate endogenous hemopoietic stem cells. Twelve days later, mice were euthanized by cervical dislocation and spleens were removed. The spleens were fixed in Bouin's solution, and grossly visible spleen colonies arising from the clonal proliferation of surviving endogenous hemopoietic stem cells were counted. Each treatment group consisted of 5 mice. Experiments were repeated 2-3 times.

Statistics

Results of replicate experiments were pooled and are represented as the mean ± SE of pooled data. Student's *t* test was used to determine statistical differences in all but survival data; survival data v ere analyzed using the generalized Savage (Mantel-Cox) procedure. Significance level was set at $p < 0.05$.

Table I. Effect of rhG-CSF on peripheral blood, bone marrow and splenic cellularity in non-irradiated C3H/HeN mice

	Saline[a]	rhG-CSF[b]						
		Day after initiation of rhG-CSF						
		1	4	7	9	10	14	17
WBC/ml (×10⁶)	5.7 ± 0.2	6.0 ± 0.8	7.9[c] ± 0.3	9.4[c] ± 0.5	9.4[c] ± 0.3	6.7[c] ± 0.3	5.2 ± 0.2	6.0 ± 0.5
PMN/ml (×10⁶)	1.7 ± .04	2.5[c] ± 0.1	3.7[c] ± 0.2	4.2[c] ± 0.2	3.5[c] ± 0.2	2.6[c] ± 0.2	1.4 ± 0.1	1.7 ± 0.1
RBC/ml (×10⁹)	6.5 ± 0.2	6.2 ± 0.2	6.1 ± 0.3	6.9 ± 0.5	6.3 ± 0.2	6.8 ± 0.3	6.4 ± 0.2	6.4 ± 0.5
Cells/femur (×10⁶)	4.9 ± 0.2	3.5[c] ± 0.2	3.7[c] ± 0.2	4.1 ± 0.6	5.6[c] ± 0.2	6.6[c] ± 0.3	6.1[c] ± 0.3	4.5 ± 0.2
Cells/spleen (×10⁸)	1.1 ± .05	0.7[c] ± .08	1.6[c] ± .02	1.7[c] ± .05	1.7[c] ± .08	1.3[c] ± .06	1.0 ± .10	1.6[c] ± .09

[a] Average values obtained from non-irradiated mice treated with saline on days 0-9 and assayed on days 1, 4, 7, 9, 10, 14 and 17. No statistical differences were observed in data obtained on individual days; therefore, all saline data were pooled.
[b] rhG-CSF (2.5 μg/mouse/day) was administered s.c. on days 0-9.
[c] $p < 0.05$, with respect to saline values

Results

Hemopoietic Activity of rhG-CSF in Normal C3H/HeN Mice

Because the G-CSF proposed for use in these studies was a recombinant human preparation, preliminary studies were performed to be certain that this rhG-CSF would function as a hemopoietic stimulant in our mice. In these studies, non-irradiated C3H/HeN mice were administered rhG-CSF for 10 days, and at various times after the initiation of rhG-CSF administration, peripheral blood, femoral and splenic cellularity, and femoral and splenic CFC-gm content were evaluated. Peripheral WBC values increased to approximately 165% of normal values by day 7, maintained this level through day 9, then rapidly returned to normal after cessation of rhG-CSF administration (Table I). The increased WBC count observed after rhG-CSF treatment was due primarily to an increase in polymorphonuclear neutrophils (PMNs; Table I). In contrast to the effect of rhG-CSF administration on WBC values, RBC values remained relatively constant, fluctuating within approximately 5% of normal values throughout the experiment (Table I). One day after the initial rhG-CSF administration, femoral cellularity decreased

to 71% of normal values, then gradually increased to 135% by day 10 (1 day after cessation of rhG-CSF administration) and returned to normal values by day 17 (Table I). Femoral CFC-gm content followed a similar pattern, decreasing to 52% of normal values 1 day after initiation of rhG-CSF administration, rising to approximately 160% on days 9 and 10, then falling to 118% by day 17 (Fig. 1). In the spleen, a decrease to 64% of normal cellularity was seen on day 1 after initiation of rhG-CSF administration (Table I). This was followed by an increase to approximately 155% of normal values on days 7 and 9, a return to normal on day 14 and a second increase to 145% of normal values on day 17. Splenic CFC-gm content increased significantly during rhG-CSF administration, reaching a peak of 1335% of normal values on day 7, then rapidly declining to 459% by 1 day after cessation of rhG-CSF treatment (i.e., day 10) and returning to within normal values by day 17 (Fig. 2). These studies demonstrated that the rhG-CSF dose and injection protocol proposed for irradiation studies was capable of inducing significant hemopoietic stimulation in normal C3H/HeN mice.

Therapeutic rhG-CSF Administration Enhances Hemopoietic Recovery in Irradiated C3H/HeN Mice

To evaluate the ability of therapeutically administered rhG-CSF to enhance hemopoietic regeneration after radiation-induced myelosuppression, mice were exposed to a non-lethal dose of 6.5 Gy of cobalt-60 and treated with rhG-CSF on days 3-12 post-exposure. Initiation of rhG-CSF therapy was delayed 3 days post-exposure to allow some post-irradiation repair and regeneration of pluripotent and committed progenitor cells. On days 4, 7, 10, 12, 14, 17 and 20 post-irradiation, bone marrow and splenic cellularity and CFC-gm content were evaluated in non-irradiated, saline-treated mice (i.e., normal control mice) and in irradiated mice treated with either saline or rhG-CSF. Peripheral blood values were also evaluated in these animals on days 7, 12, 17 and 20 post-exposure.

Peripheral WBC values in both saline- and rhG-CSF-treated mice fell to approximately 20% of normal values by 7 days post-irradiation (Fig. 3A). WBC values recovered to only 60% of normal by day 20 in saline-treated mice, while WBC values reached 90% of normal values by day 20 in rhG-CSF-treated mice. An increase in the percentage of neutrophils was also observed in rhG-CSF-treated mice. Interestingly, accelerated recovery of both RBC and PLT values was also observed in rhG-CSF-treated mice (Figs. 3B and 3C). By day 20 post-exposure, RBC values in rhG-CSF-treated mice were 88% of normal values (compared to 55% in saline-treated mice) and PLT values were 66% of normal values (compared to 22% in saline-treated mice).

Based on cellularity and CFC-gm content, femoral and splenic hemopoietic regeneration were also enhanced significantly by rhG-CSF administration. Femoral cellularity in both saline- and rhG-CSF-treated mice decreased to approximately 20% of normal values by 4 days post-exposure (Table II). Interestingly, recovery of femoral cellularity in rhG-CSF-treated mice occurred more slowly than in saline-
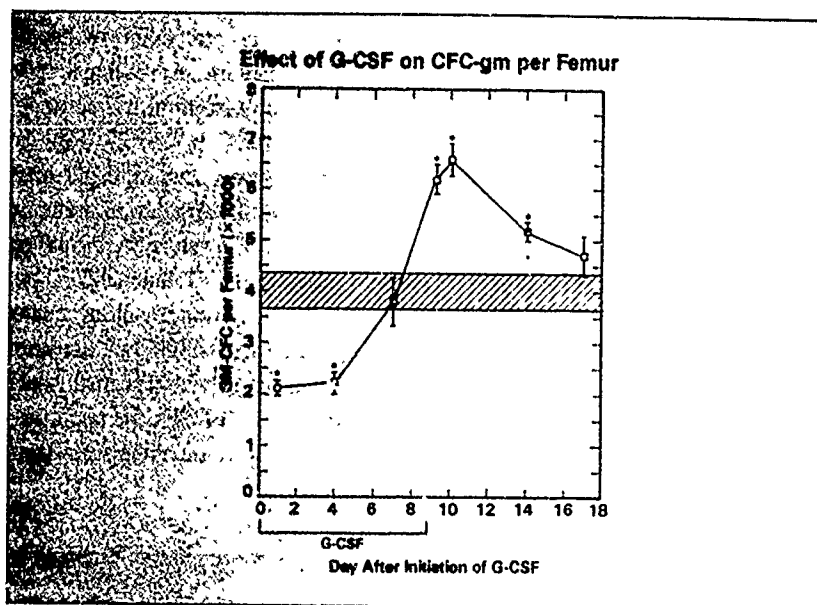
Fig 1. CFC-gm per femur in non-irradiated C3H/HeN mice receiving 2.5 µg/day of rhG-CSF administered s.c. on days 0-9. Shaded area represents femoral CFC-gm content obtained in non-irradiated mice injected with saline. $*$ = $p < 0.05$, with respect to saline controls.
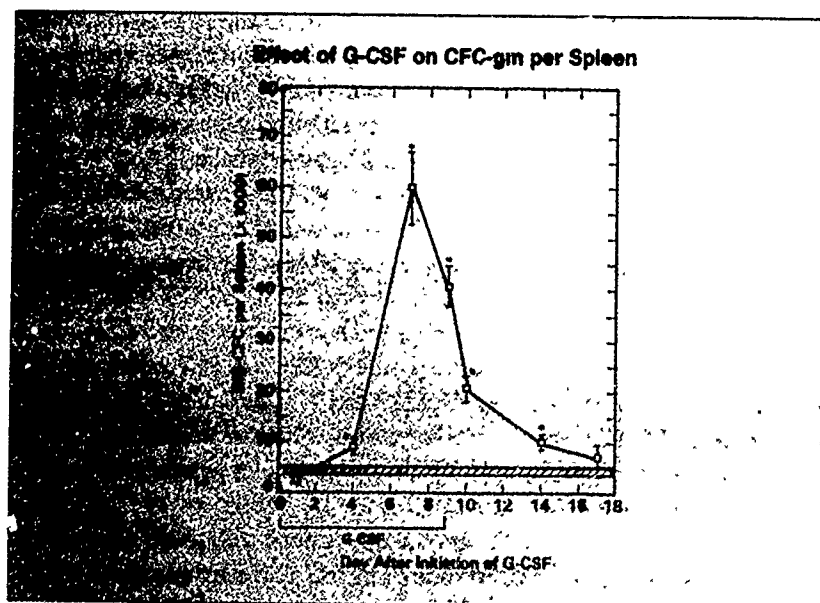

Fig. 2. CFC-gm per spleen in non-irradiated C3H/HeN mice receiving 2.5 µg/day of rhG-CSF administered s c. on days 0-9 Shaded area represents splenic CFC-gm content obtained in non-irradiated mice injected with saline. $*$ = $p < 005$, with respect to saline controls.

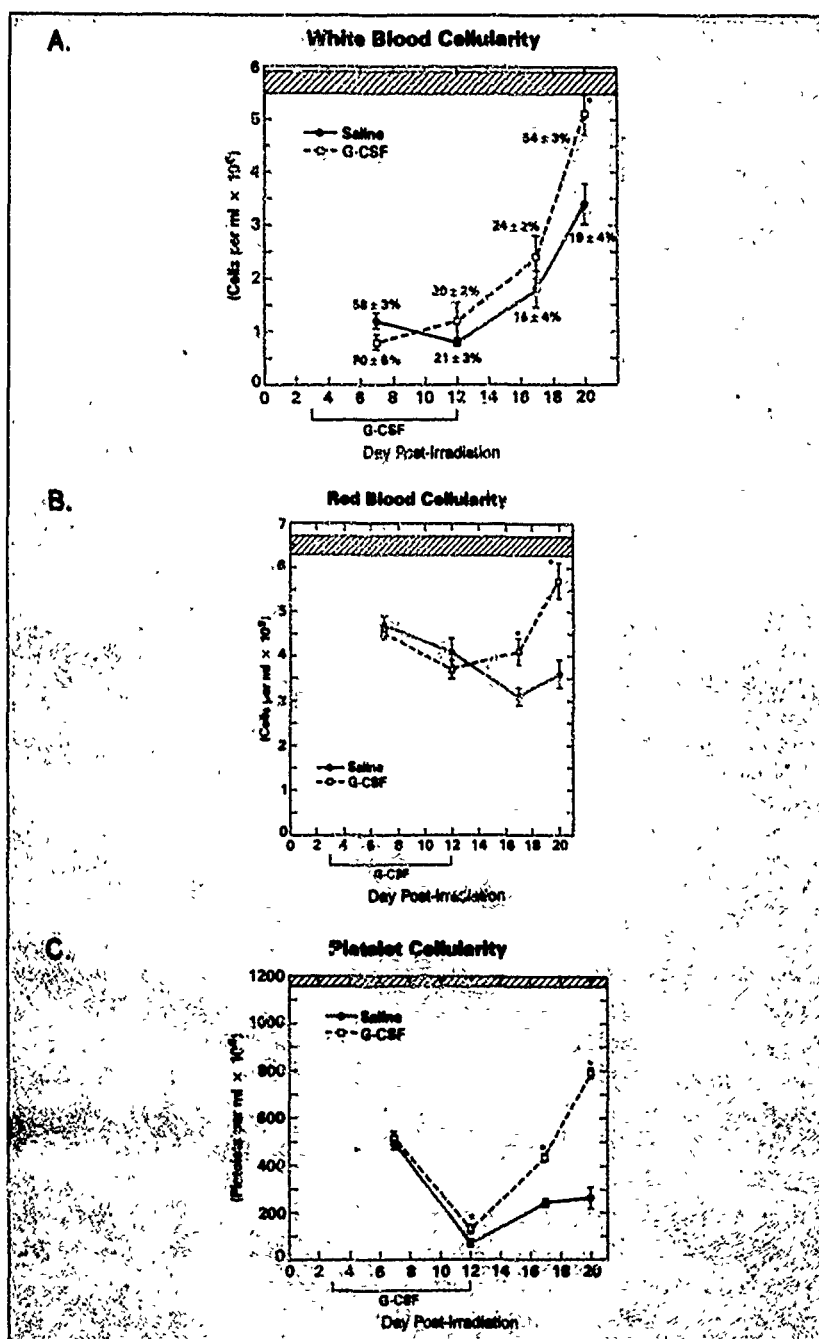**Fig. 3.** Peripheral blood cellularity in C3H/HeN mice after 6.5 Gy. rhG-CSF (2.5 μg/ day) or saline was administered s.c. on days 3-12. Shaded area represents values obtained in non-irradiated mice injected with saline. * = $p < 0.05$, with respect to irradiated saline-treated mice. A = WBC; values in parentheses indicate percentage of neutrophils at each time point. B = RBC. C = PLT.

Table II. Effect of rhG-CSF on bone marrow and splenic cellularity in irradiated C3H/HeN mice[a]

	Day post-irradiation						
	4	7	10	12	14	17	20
Cells/femur[b] ($\times 10^6$)							
Saline	1.2 ± 0.1	2.1 ± 0.2	2.7 ± 0.2	2.6 ± 0.1	2.3 ± 0.2	1.8 ± 0.1	2.1 ± 0.1
rhG-CSF	0.8 ± 0.1	1.4[c] ± 0.2	2.1 ± 0.4	2.8 ± 0.2	2.6 ± 0.1	3.2[c] ± 0.1	3.8[c] ± 0.1
Cells/spleen[d] ($\times 10^8$)							
Saline	.08 ± .006	.09 ± .003	.16 ± .01	.22 ± .005	.39 ± .03	.89 ± .06	1.60 ± .04
rhG-CSF	.10 ± .004	.11 ± .004	.27[c] ± .03	.38[c] ± .04	.47[c] ± .02	1.90[c] ± .07	1.70 ± .05

[a] rhG-CSF (2.5 μg/mouse/day) was administered s.c. on days 3-12 after 6.5 Gy radiation exposure.
[b] Average number of cells per femur in non-irradiated saline-treated mice was $4.9 \pm 0.2 \times 10^6$).
[c] $p < 0.05$, with respect to values obtained from irradiated and saline-treated mice
[d] Average number of cells per spleen in non-irradiated saline-treated mice was $1.1 \pm 0.05 \times 10^8$.

treated mice through day 10. However, enhanced cellular recovery was observed in rhG-CSF-treated mice on days 17 and 20. Femoral cellularity in rhG-CSF-treated mice was 78% of normal values by day 20, compared to 43% in saline-treated mice. Bone marrow CFC-gm recovery was also enhanced significantly in rhG-CSF-treated mice, increasing from 7% of normal values on day 12 post-exposure to 58% on day 20; CFC-gm recovery in saline-treated mice during this time increased from 2% to only 17% of normal values (Fig. 4). Splenic cellularity in both groups of mice decreased to approximately 10% of normal values until 10 days post-exposure (Table II). Recovery occurred in both treatment groups on days 10-20; it occurred more rapidly, however, in rhG-CSF-treated mice. By day 17 post-exposure, splenic cellularity in rhG-CSF-treated mice was 173% of normal values, compared to 81% in saline-treated mice. Recovery of splenic CFC-gm content in rhG-CSF-treated mice also increased dramatically compared to saline-treated mice (Fig. 5). By day 14 post-exposure, CFC-gm content in rhG-CSF mice had reached 63% of normal values, compared to 1% in saline-treated mice. In addition, CFC-gm contents in rhG-CSF mice were 937% and 505% of normal values on days 17 and 20, compared to 57% and 212% in saline-treated mice.
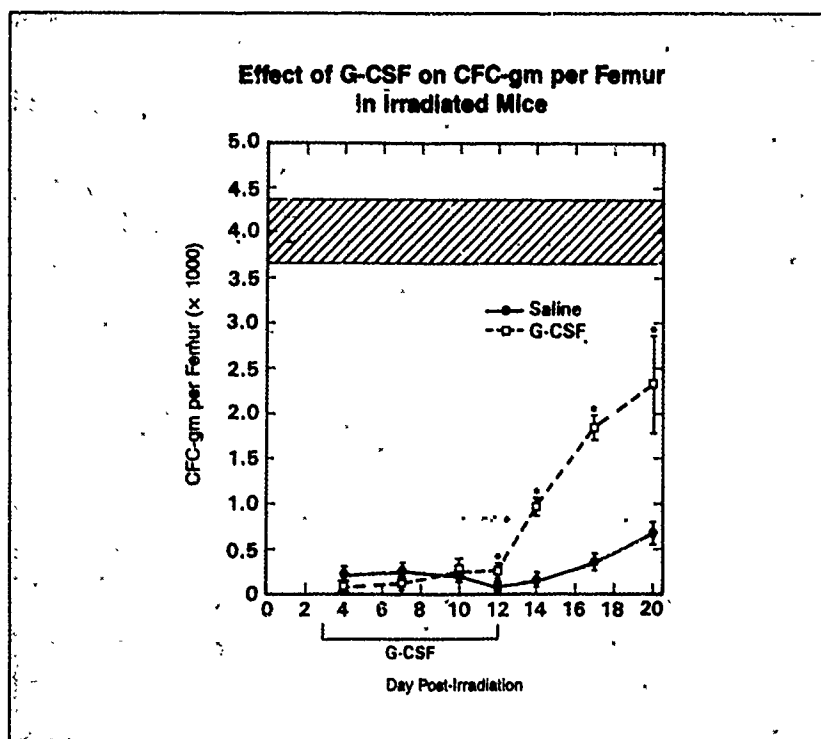
Fig. 4. CFC-gm per femur in C3H/HeN mice after 6.5 Gy. rhG-CSF (2.5 μg/day) or saline was administered s.c. on days 3-12. Shaded area represents femoral CFC-gm content obtained in non-irradiated mice injected with saline. * = $p < 0.05$, with respect to irradiated saline-treated mice.

rhG-CSF therapy enhanced the recovery of not only WBC counts, but also RBC and PLT counts in irradiated mice. This finding suggested that rhG-CSF may stimulate hemopoiesis at a more primitive progenitor level than that of the CFC-gm. Because of this, the endogenous spleen colony assay was used to determine the effects of rhG-CSF therapy on multipotent hemopoietic stem cell recovery in irradiated mice. In these studies, mice were exposed to 8 Gy of radiation and injected with rhG-CSF on days 3-12, 1-12 or 0-12 post-irradiation. The first rhG-CSF treatment in the latter group was administered 1 h post-irradiation. The day 1-12 and day 0-12 injection treatments were added to these experiments to evaluate possible effects of rhG-CSF therapy on stem cell burnout. Mice treated with rhG-CSF on days 3-12 exhibited significantly more endogenous spleen colonies than did saline-treated mice (3.6 ± 0.4 vs. 1.3 ± 0.4), indicating that therapeutic rhG-CSF was capable of stimulating proliferation of multipotential hemopoietic progenitors (Fig. 6). Interestingly, when rhG-CSF therapy was initiated 1 day or 1 h post-irradiation, even greater CFU-s responses were observed.
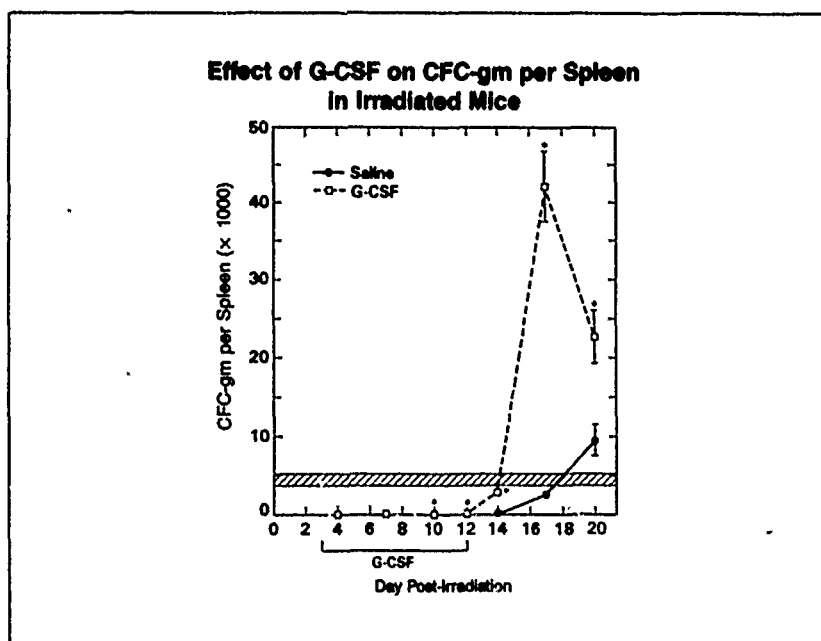
Effect of G-CSF on CFC-gm per Spleen In Irradiated Mice

Fig. 5. CFC-gm per spleen in C3H/HeN mice after 6.5 Gy. rhG-CSF (2.5 μg/day) or saline was administered s.c. on days 3-12. Shaded area represents splenic CFC-gm content obtained in non-irradiated mice injected with saline. $* = p < 0.05$, with respect to irradiated saline-treated mice. Although difficult to detect, CFC-gm values in G-CSF-treated mice at days 10 and 12 (38.0 ± 9.0 and 49.0 ± 5.0, respectively) were significantly greater than CFC-gm values in saline-treated mice (0.4 ± 0.2 and 1.0 ± 0.2, respectively).

Therapeutic rhG-CSF Administration Enhances Survival of Irradiated C3H/ HeN Mice

To evaluate whether rhG-CSF-induced hemopoietic recovery could result in survival enhancement following severe radiation exposure, mice were exposed to 8 Gy of radiation and administered rhG-CSF on days 3-12, 1-12 or 0-12 post-irradiation. All rhG-CSF treatments enhanced survival (Fig. 7). Respectively, these treatments resulted in 57%, 70% and 95% survival, compared with 27% survival in saline-treated mice.

Discussion

Both radiation and chemotherapy destroy hemopoietic stem and progenitor cells, leading to a critical depletion of functional WBC within one to two weeks after treatment. As a result, the host is compromised with respect to natural defenses against exogenous infectious diseases, as well as endogenous gut-derived bacteria and their associated toxins [23-25]. Hemopoietic regeneration requires pluripotent stem cells capable of self-renewing, as well as differentiating into multi-
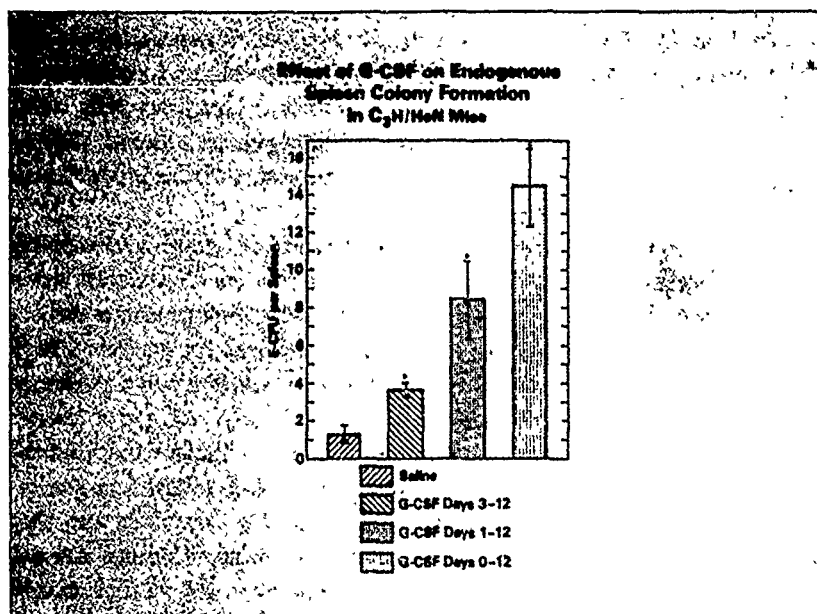
Fig. 6. Endogenous spleen colcny formation in C3H/HeN mice after 8 0 Gy. rhG-CSF (2.5 µg/day) or saline was administered s.c. on days 3-12, 1-12 or 0-12 post-irradiation. * = $p < 0.05$, with respect to irradiated saline-treated mice.

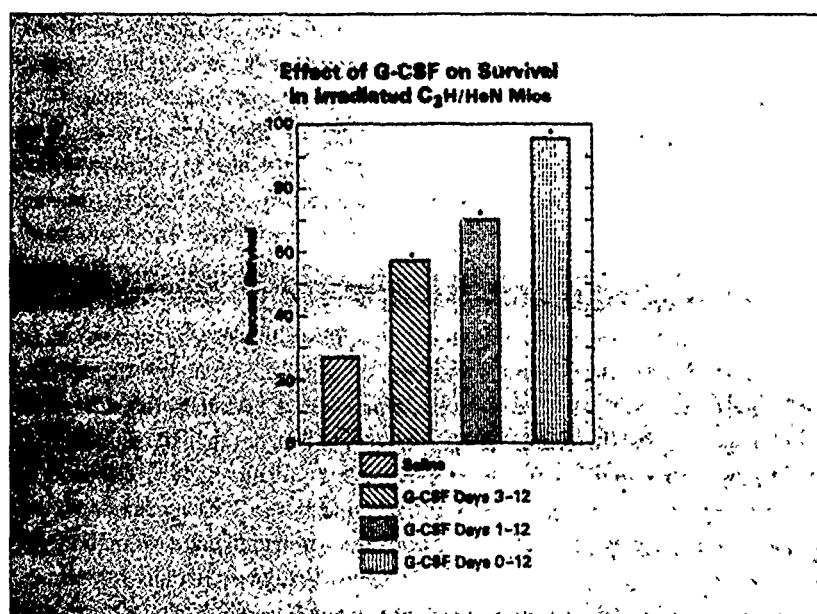**Fig. 7.** Survival in C3H/HeN mice after 8 0 Gy rhG-CSF (2 5 µg/day) or saline was administered s.c. on days 3-12, 1-12 or 0-12 post-irradiation (20-30 mice per group). * = $p < 0.05$, with respect to irradiated saline-treated mice.

potent and committed progenitors capable of giving rise to mature cells with specialized functions. These processes are regulated by specific molecules produced within specialized accessory cells constituting the hemopoietic microenvironment. Hence, in addition to direct effects on hemopoietic stem and progenitor cells, radiation and chemotherapy may also impair hemopoietic regeneration through destruction and/or injury to accessory cell populations necessary for the production of essential hemopoietic growth factors [26-29].

Until recently, with the exception of fluid, antibiotic and platelet support, no effective means to therapeutically treat myelosuppression and consequent sepsis and hemorrhage have been available [30-32]. However, developments in the isolation, purification and molecular cloning of hemopoietic growth factors have opened new possibilities regarding therapeutic enhancement of stem and progenitor cell recovery. rhG-CSF is one such recently cloned hemopoietic growth factor. Although originally recognized for its ability to stimulate the in vitro proliferation of progenitor cells giving rise to neutrophils [33], this factor has been demonstrated to also stimulate granulopoiesis in normal healthy animals in vivo. Our present studies in normal C3H/HeN mice reconfirmed such in vivo data obtained by others in normal C57BL/6 mice [7, 15], normal hamsters [10], normal canines [34], and normal primates [12] in which rhG-CSF administration was shown to increase peripheral WBC counts, as well as to increase CFC-gm progenitors. In addition to in vitro and in vivo effects on granulocyte proliferation and differentiation, rhG-CSF has also been demonstrated to prime and/or activate mature granulocytes to function more efficiently [1, 17, 18].

Several studies have demonstrated the ability of rhG-CSF therapy to enhance recovery from drug-induced myelosuppression. For example, hemopoietic regeneration of peripheral blood neutrophils in hamsters treated with 5-fluorouracil (5-FU) was accelerated two days with rhG-CSF therapy [10]. Similar peripheral effects as well as stimulatory effects on CFC-gm recovery have also been demonstrated in mice treated with 5-FU [8] or cyclophosphamide [14]. More recently, the ability of rhG-CSF therapy to accelerate granulocyte recovery in cyclophosphamide-treated primates [12] and humans receiving a variety of chemotherapeutic agents [4, 20, 21, 35] has also been demonstrated.

In the studies described in this paper, we additionally demonstrate the ability of rhG-CSF to enhance recovery from severe radiation-induced myelosuppression. Furthermore, survival in severely irradiated mice was increased by rhG-CSF treatment, suggesting that the mature cells (presumably the neutrophils) resulting from accelerated hemopoietic recovery were capable of enhancing host resistance to otherwise lethal post-irradiation opportunistic infections. This appears to be consistent with the fact that rhG-CSF has been demonstrated to increase survival [15] and to enhance resistance to microbial infection in cyclophosphamide-treated neutropenic mice [14]. Our current studies in mice confirm and expand our previous work in which enhanced peripheral blood neutrophil recovery, increased bone marrow hemopoiesis and increased survival were observed in irradiated canines

receiving more extended courses of rhG-CSF therapy [36]. These studies also confirm and expand previous work by *Kobayashi et al.* who demonstrated accelerated hemopoietic regeneration in rhG-CSF-treated mice exposed to less severe 3-5 Gy doses of total-body radiation [22].

In this study, rhG-CSF therapy accelerated hemopoietic recovery by four to five days based on femoral and splenic CFC-gm values. Because CFC-gm progenitors are ultimately derived from multipotent hemopoietic progenitor cells, we suspected that intensive rhG-CSF therapy may drain multipotent stem cell pools by driving these cells toward differentiation at the expense of self-renewal. The CFU-s data presented in these studies, however, suggests that this does not occur. In fact, rhG-CSF administration actually increased CFU-s numbers, with the greatest increase being observed when rhG-CSF therapy was initiated 1 h post-irradiation. The survival-enhancing effect of rhG-CSF therapy was also best when initiated 1 h post-irradiation.

Contrary to the in vitro effects of rhG-CSF, which appear to be specific for granulocyte proliferation, differentiation and function, in vivo rhG-CSF therapy stimulated regeneration of multiple hemopoietic cell lineages. Specifically, WBC, RBC and PLT recoveries were all accelerated in rhG-CSF-treated mice. This discrepancy between in vitro and in vivo rhG-CSF effects suggests that the multilineage in vivo effects of rhG-CSF may be indirectly mediated. For example, GM-CSF has been demonstrated to stimulate the release of interleukin 1 from mature granulocytes [27, 37], which in turn has been demonstrated to stimulate the release of other pleotrophic hemopoietic cytokines, such as interleukin 6, GM-CSF, G-CSF and M-CSF from endothelial cells and fibroblasts [38-41]. If rhG-CSF similarly affects granulocytes, rhG-CSF-mediated stimulation of multipotential progenitor cell proliferation could be postulated via such a cascade.

In conclusion, these studies have demonstrated the ability of therapeutically administered rhG-CSF to accelerate hemopoietic regeneration and to increase survival after radiation-induced myelosuppression. rhG-CSF therapy accelerated the regeneration of multiple hemopoietic lineages and, contrary to stem cell burn out, actually appeared to stimulate multipotent stem cell proliferation. rhG-CSF should offer great promise for the treatment of radiation and/or drug-induced myelosuppression and its infectious consequences.

Acknowledgments

References

1   Nicola NA, Vadas M. Hemopoietic color_ stimulating factors. Immunol Today 1984;5:76-81.

2   Metcalf D. The molecular biology and functions of the granulocyte-macrophage colony-stimulating factors. Blood 1986;67:257-267.

3   Welte K, Platzer E, Lu L, et al. Purification and biochemical characterization of human pluripotent hematopoietic colony-stimulating factor. Proc Natl Acad Sci USA 1985; 82:1526-1530.

4   Zsebo KM, Cohen AM, Murdock DC, et al. Recombinant human granulocyte colony-stimulating factor: molecular and biological characterization. Immunobiology 1986; 172:175-184.

5   Souza LM, Boone TC, Gabrilove J, et al. Recombinant human granulocyte colony-stimulating factor: effects on normal and leukemia myeloid cells. Science 1986;232: 61-65.

6   Tsuchiya M, Asano S, Koziro Y, Nagata S. Isolation and characteri   on of the cDNA for murine granulocyte colony-stimulating factor. Proc Natl Acad   . USA 1986;83: 7633-7637.

7   Fujisawa M, Kobayashi Y, Okabe T, Takaku F, Komatsu Y, Itoh S. Recombinant human granulocyte colony-stimulating factor induces granulocyt   in vivo. Jpn J Cancer Res 1986;77:866-869.

8   Shimamura M, Kobayashi Y, Yuo A, et al. Effect of human recombinant granulocyte colony-stimulating factor on hematopoietic injury in mice induced by 5-fluorouracil. Blood 1987;69:353-355.

9   Metcalf D. The molecular control of normal and leukaemic granulocytes and macrophages. Proc R Soc Lond (Biol) 1987;230:389-423.

10 Cohen AM, Zsebo KM, Inoue H, et al. In vivo stimulation of granulopoiesis by recombinant human granulocyte colony-stimulating factor. Proc Natl Acad Sci USA 1987; 84:2484-2488.

11 Tamura M, Hattori K, Nomura H, et al. Induction of neutrophilic granulocytosis in mice by administration of purified human native granulocyte colony-stimulating factor (G-CSF). Biochem Biophys Res Commun 1987;142:454-460.

12 Welte K, Bonilla MA, Gillio AP, et al. Recombinant human granulocyte colony-stimulating factor: effects on hematopoiesis in normal and cyclophosphamide-treated primates. J Exp Med 1987;165:941-948.

13 Moore MA, Warren DS. Synergy of interleukin-1 and granulocyte colony stimulating factor: in vivo stimulation of stem cell recovery and hemopoietic regeneration following 5-fluorouracil treatment of mice. Proc Natl Acad Sci USA 1987;84:7134-7138.

14 Matsumoto M, Matsubara S, Matsuno T, et al. Protective effect of human granulocyte colony-stimulating factor on microbial infectio. in neutropenic mice. Infect Immun 1987;55:2715-2720.

15 Talmadge JE, Tribble H, Pennington R, et al. Protective, restorative, and therapeutic properties of recombinant colony-stimulating factor. Blood 1989;73:2093-2103.

16 Begley CG, Lopez AF, Nicola NA, et al. Purified colony-stimulating factors enhance the survival of human neutrophils and eosinophils in vitro. A rapid and sensitive microassay for colony-stimulating factors. Blood 1986;68:162-166.

17 Lopez AF, Nicola NA, Burgess AW, et al. Activation of granulocyte cytotoxic function by purified mouse colony-stimulating factors. J Immunol 1983;131:2983-2987.

18 Vadas MA, Nicola NA, Metcalf D. Activation of antibody-dependent cell-mediated cytotoxicity of human neutrophils and eosinophils by separate colony-stimulating factors. J Immunol 1983;130:795-799.

19 Bronchud MH, Scarffe JH, Thatcher N, et al. Phase I/II study of recombinant human granulocyte colony-stimulating factor in patients receiving intensive chemotherapy for small cell lung cancer. Br J Cancer 1987;56:809-813.

20 Morstyn G, Campbell L, Souza LM, et al. Effect of granulocyte colony-stimulating factor on neutropenia induced by cytotoxic chemotherapy. Lancet 1988;i:667-671.

21 Gabrilove JL, Jakubowski A, Scher H, et al. Effect of a granulocyte colony-stimulating factor on neutropenia and associated morbidity due to chemotherapy for transitional-cell carcinoma of the urothelium. N Engl J Med 1988;318:1414-1422.

22 Kobayashi Y, Okabe T, Urabe A, Suzuki N, Takaku F. Human granulocyte colony-stimulating factor produced by *Escherichia coli* shortens the period of granulocytopenia induced by irradiation in mice. Jpn J Cancer Res 1987;78:763-766.

23 Benacerraf B. Influence of irradiation on resistance to infection. Bacteriol Rev 1960; 24:35-40.

24 Hammond CW, Tompkins M, Miller CP. Studies on susceptibility to infection following ionizing radiation; time of onset and duration of endogenous bacteremias in mice. J Exp Med 1954;99:405-410.

25 Durack DT. Infection in compromised hosts. In: Lachmann PJ, Peters DK, eds. Clinical Aspects of Immunology. Oxford: Blackwell Scientific Publishers, 1982:1713-1723.

26 Broudy V, Kaushansky K, Segal G, Harlan J. Tumor necrosis factor type alpha stimulates human endothelial cells to produce granulocyte-macrophage colony-stimulating factor. Proc Natl Acad Sci USA 1986;83:7467-7471.

27 Moore RN, Oppenheim JJ, Farrar JJ, Carter CS, Waheed A, Shadduck RK. Production of lymphocyte-activating factor (interleukin-1) by macrophages activated with colony-stimulating factors. J Immunol 1980;125:1302-1305.

28 Sieff CA. Hemopoietic growth factors. J Clin Invest 1987;79:1549-1577.

29 Le PT, Tuck DT, Dinarello CA, Haynes BF, Singer KH. Human thymic epithelial cells produce interleukin 1. J Immunol 1987;138:2520-2527.

30 Sorensen DK, Bond VP, Cronkite EP, Perman V. An effective therapeutic regimen for the hemopoietic phase of the acute radiation syndrome in dogs. Radiat Res 1960; 13:669-685.

31 Perman V, Sorensen DK, Usenik EA, Bond VP, Cronkite EP. Hemopoietic regeneration in control and recovery of heavily irradiated dogs following severe hemorrhage. Blood 1962;19:738-742.

32 MacVittie TJ, Monroy RL. Potential improvement in the management of seriously irradiated persons. In: Ricks RC, Fry SA, eds. The Medical Basis for Radiation Accident Preparedness; Clinical Experiences and Follow-Up Since 1979. New York: Elsevier Science Publishing (in press).

33 Metcalf D. Colony stimulating factors. Science 1985;229:16-22.

34 MacVittie TJ, Schwartz GN, Vriesendorp H, et al. Stimulation of granulopoiesis in normal and sublethally irradiated canines by in vivo administration of recombinant human granulocyte colony-stimulating factor (rhG-CSF). Noordwijkerhout, The Netherlands: 5th International Symposium on Infection in Immunocompromised Hosts, 1988.

35 Duhrsen U, Villeval J, Boyd J, Kannourakis G, Morstyn G, Metcalf D. Effects of recombinant human granulocyte colony-stimulating factor on hemopoietic progenitor cells in cancer patients. Blood 1988;72:2074-2081.

36 MacVittie TJ, Vriesendorp H, Monroy RL, et al. Rescue of lethally irradiated canines using therapeutic administration of either recombinant human G-CSF (rhG-CSF) or GM-CSF (rhGM-CSF). Exp Hematol 1989;17:579a.

37 Lindemann A, Riedel D, Oster W, et al. Granulocyte-macrophage colony-stimulating factor induces interleukin-1 production by human polymorphonuclear neutrophils. J Immunol 1988;140:837-839.

38 Kupper TS, Lee F, Birchall N, Clark S, Dower S. Interleukin 1 binds to specific receptors on human keratinocytes and induces granulocyte-macrophage colony-stimulating factor mRNA and protein. J Clin Invest 1988;82:1787-1792.

39 Sironi M, Breviario F, Proserpio P, et al. IL-1 stimulates IL-6 production in endothelial cells. J Immunol 1989;142:549-553.

40 Seelentag W, Mermod J, Vassalli P. Interleukin-1 and tumor necrosis factor alpha increase the levels of granulocyte-macrophage and granulocyte colony stimulating factor (CSF) mRNA in human fibroblasts. Eur J Immunol 1989;19:209-212.

41 Fibbe WE, Van Damme J, Billiau A, et al. Human fibroblasts produce granulocyte-CSF, macrophage-CSF and granulocyte-macrophage-CSF following stimulation by interleukin-1 and poly(rI)-poly(rC). Blood 1988;72:860-866.

● *Original Contribution*

COMBINED MODALITY RADIOPROTECTION: THE USE OF GLUCAN AND SELENIUM WITH WR-2721

MYRA L. PATCHEN, PH.D.,* THOMAS J. MACVITTIE, PH.D.* AND JOSEPH F. WEISS, PH.D.[†]

Armed Forces Radiobiology Research Institute, Bethesda, MD 20814-5145

Glucan, WR-2721, and selenium, three agents with distinct radioprotective mechanisms, were evaluated in C3H/HeN mice for survival-enhancing and hemopoietic-regenerating effects when administered alone or in combinations before exposure to ^{60}Co radiation. At LD50/30 radiation doses (radiation doses lethal for 50% of mice within 30 days postexposure), dose reduction factors of 1.21, 1.02, 1.37, 1.51, and 1.66 were obtained following glucan (75 mg/kg i.v., −20 hr), selenium (0.8 mg/kg, i.p., −20 hr), WR-2721 (200 mg/kg, i.p., −30 min), glucan + WR-2721, and glucan + selenium + WR-2721 treatments, respectively. All treatments increased numbers of hemopoietic stem cells as measured by the day 12 endogenous spleen colony-forming unit (E-CFU) assay; the most significant E-CFU effects, however, were observed following glucan + WR-2721 and glucan + selenium + WR-2721 treatments. Combined modality treatments were also more effective than single-agent treatments at accelerating bone marrow and splenic granulocyte-macrophage colony-forming cell (GM-CFC) regeneration. These results demonstrate the value of multiple-agent radioprotectants.

Radioprotection, Glucan, Selenium, WR-2721, Drug interactions, Hemopoiesis.

INTRODUCTION

Recent radiation accidents at Chernobyl (U.S.S.R.) and at Goiania (Brazil) have again focused attention on the potential value of agents that could mitigate the biological effects of radiation exposure. Such agents, commonly called radioprotectants, could be valuable not only for individuals who may be exposed to radiation during accident rescue and/or clean-up activities, but also for astronauts who may be subjected to predictable radiation exposures, and for individuals undergoing radiotherapy.

During the past several decades, studies of numerous radioprotective agents have led to the realization that not all radioprotectants mitigate damage through similar mechanisms (9, 13, 20, 37). Because various radioprotective agents differ in mechanisms of action and in optimal administration times with respect to radiation exposure, the use of multiple agents may in some instances provide significantly better protection than single agents. In the studies described here, combinations of such agents were administered to mice and evaluated for effects on survival

enhancement and on hemopoietic recovery. By design, individual agents were used at doses that induce minimal-to-no toxic or performance-degrading side effects.

These particular studies describe the combined use of glucan, WR-2721, and selenium. Glucan is a β,1-3 polyglucose immunomodulator isolated from the inner cell wall of the yeast *Saccharomyces cerevisiae* (10). This agent has been demonstrated to increase survival by enhancing host resistance to life-threatening postirradiation opportunistic infections and by accelerating hemopoietic regeneration (21, 22, 25, 28, 30). WR-2721 is a synthetic sulfhydryl compound shown to radioprotect by free radical scavenging, hydrogen atom donation, and induction of hypoxia (9, 35, 38). Selenium, an essential trace element, is a component of endogenous antioxidant systems known to be involved in the reduction of radiation-induced reactive oxygen species (8, 15, 37). Our results demonstrate that glucan administered in combination with WR-2721 enhances survival better than either agent administered alone, and that this effect can be further enhanced by the addition of selenium to this treatment

combination. In comparison to single-agent treatments, combination treatments also more effectively accelerate postirradiation hemopoietic recovery.

METHODS AND MATERIALS

Mice

C3H/HeN female mice (~20 g) were used [‡] Mice were maintained in an AAALAC (American Association for Accreditation of Laboratory Animal Care) accredited facility in micro-isolator cages on hardwood-chip, contact bedding and were provided commercial rodent chow and acidified tap water (pH 2.5) ad libitum. Animal rooms were equipped with full-spectrum light from 6 a.m. to 6 p.m. and were maintained at 70 ± 2°F with 50 ± 10% relative humidity, and at least 10 air changes per hour of 100% conditioned fresh air. Upon arrival, all mice were tested for Pseudomonas and quarantined until test results were obtained. Only healthy mice were released for experimentation. Prior to performance, all animal experiments were approved by the Institutional Animal Care and Use Committee of the Armed Forces Radiobiology Research Institute (AFRRI).

Glucan, WR-2721, and selenium

Endotoxin-free particulate glucan (10) was used[§] and intravenously (i.v.) administered (75 mg/kg) to mice ~ 20 hr before the start of irradiation. Selenium, as sodium selenite,** was intraperitoneally (i.p.) administered to mice ~ 20 hr before the start of irradiation at a dose of 0.8 mg selenium/kg. WR-2721 was obtained from Walter Reed Army Institute of Research (Washington, DC) and administered i.p. (200 mg/kg) ~ 30 min before the start of irradiation. All drugs were diluted in pyrogen-free saline and administered in a 0.5-ml volume. Control mice received 0.5-ml injections of pyrogen-free saline. Because no significant differences were observed among control mice receiving i.p., i.v., or both i.p. and i.v. saline injections, data from all saline-treated mice were pooled.

Irradiation

The AFRRI ^{60}Co source was used to administer bilateral total-body gamma radiation. Mice were placed in ventilated Plexiglas containers and irradiated at a dose rate of 0.4 Gy/min. Dosimetry was determined by ionization chambers as previously described (31). Radiation doses ranged from 6–16 Gy.

Survival assays

Irradiated mice were returned to the animal facility and cared for routinely. Survival was checked and recorded daily for 30 days; on day 31, surviving mice were euthanized by cervical dislocation. Each treatment group within

each experiment consisted of ~10 mice. Experiments were repeated to obtain an "n" of at least 40 animals for each treatment group at each radiation dose. The percentage of mice surviving each radiation dose at 30 days postexposure was used to construct probit-plot survival curves (11, 12). Dose reduction factors (DRF's) were calculated by dividing the treatment LD50/30 radiation doses by the saline LD50/30 radiation dose.

Endogenous spleen colony-forming unit assay

Pluripotent hemopoietic stem cell recovery was evaluated using the endogenous spleen colony-forming unit (E-CFU) assay (32). Mice were exposed to 6–13 Gy of total-body radiation to partially ablate endogenous hemopoietic stem cells. Twelve days after irradiation, mice were euthanized by cervical dislocation, their spleens were removed, fixed in Bouin's solution, and the number of grossly visible spleen colonies counted. Each treatment group within each experiment consisted of ~5 mice. Experiments were repeated to obtain an "n" of at least 20 animals for each treatment group at each radiation dose. Student's t-test was used to determine statistical differences in E-CFU data.

Granulocyte-macrophage colony-forming cell assay

Hemopoietic progenitor cells committed to granulocyte and/or macrophage development were assayed by a modification of the in vitro granulocyte-macrophage colony-forming cell (GM-CFC) assay (27). Colonies (>50 cells) were counted after 10 days incubation in a 37°C humidified environment containing 5% CO_2. The cell suspensions used for these assays represented tissues from 3–12 normal, irradiated, or treated and irradiated mice at each time point. Cells were flushed from femurs with 3 ml McCoy's 5A medium†† containing 5% heat-inactivated fetal bovine serum. Spleens were pressed through stainless-steel mesh screen, and the cells were washed from the screen with 6 ml medium. The total number of nucleated cells in each suspension was determined by hemocytometer. Experiments were repeated three times; data were pooled and analyzed using Student's t-test.

RESULTS

Survival-enhancing effects of glucan, WR-2721, and selenium

Compared to saline-treated mice, survival was enhanced by treatment with glucan, WR-2721, or the combination of these agents (Fig. 1). LD50/30 values of 7.82 [7.74, 7.89] Gy, 9.45 [8.22, 10.40] Gy, 10.73 [10.57, 10.89] Gy, and 11.77 [11.23, 12.29] Gy were obtained in mice treated with saline, glucan, WR-2721, and glucan + WR-2721, respectively. These values resulted in DRF's of 1.21
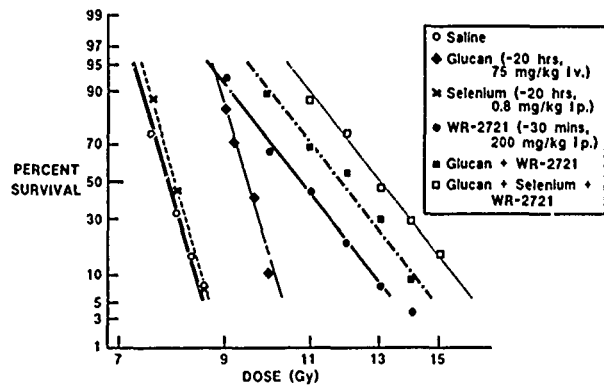
Fig. 1. Effects of combined glucan, selenium, and WR-2721 treatments on survival of irradiated C3H/HeN mice.

for glucan, 1.37 for WR-2721, and 1.51 for glucan + WR-2721 treatments. The slope of the survival curve of glucan-treated mice was identical (i.e., parallel) to that of saline-treated mice. The slopes of the survival curves of WR-2721-treated mice and glucan + WR-2721-treated mice were parallel to each other, however they differed significantly ($p < 0.001$) from those of saline-treated or glucan-treated mice. The administration of selenium in combination with glucan and WR-2721 further enhanced survival, resulting in an LD50/30 value of 12.97 [12.67, 13.27] Gy and a DRF of 1.66. The slope of this survival curve was parallel to those of WR-2721 and glucan + WR-2721. Selenium alone, or the administration of selenium in combination with glucan or WR-2721, did not enhance survival above that induced by saline, glucan alone, or WR-2721 alone. The LD50/30 values for selenium, selenium + glucan, and selenium + WR-2721 were 7.95 [7.68, 8.18] Gy, 9.58 [9.42, 9.75] Gy, and 10.88 [10.67, 11.03] Gy (data not graphed), respectively.

Effects of glucan, WR-2721, and selenium on hemopoietic regeneration

E-CFU studies. E-CFU numbers in saline-treated mice ranged from 7.2 ± 1.0 to 0.2 ± 0.1 following exposure to 6–8 Gy, respectively (Table 1). Glucan treatment significantly increased E-CFU numbers following all radiation exposures. Confluent colony formation (i.e., too many colonies to accurately count) was observed following 6 Gy, while 30.0 ± 2.5, 7.8 ± 1.0, and 3.6 ± 0.7 colonies were observed following 7, 8, and 9 Gy, respectively. WR-2721 treatment also significantly increased E-CFU numbers at all radiation doses, ranging from confluent colony formation at 6, 7, and 8 Gy to 10.4 ± 1.8, 6.7 ± 1.1, and 2.0 ± 0.7 E-CFU's, respectively, at 9, 10, and 11 Gy. Glucan + WR-2721 treatment increased E-CFU numbers more than either agent alone. For example, after a 9-Gy radiation exposure, 34.4 ± 3.9 E-CFU's were observed in mice treated with glucan + WR-2721 compared to 3.6 ± 0.7 E-CFU's in glucan-treated mice and 10.4 ± 1.8 E-CFU's in WR-2721-treated mice. Administration of glucan + selenium + WR-2721 even further increased E-CFU numbers; after an 11-Gy exposure, 8.4 ± 0.9 E-CFU's were observed in mice treated with all three agents compared to only 3.7 ± 0.5 E-CFU's in mice treated with glucan + WR-2721 ($p < 0.0001$).

Cellularity and GM-CFC studies. Recovery of bone marrow and splenic cellularity and GM-CFC's in 9-Gy-irradiated mice pretreated with glucan, WR-2721, selenium, or combinations of these agents was used to further evaluate the hemopoietic effects of these treatments (Tables 2, 3). Bone marrow cellularity in saline-treated mice was reduced to ~3% of normal at day 4 postirradiation and recovered to only ~14% of normal at day 13. Bone marrow cellularities in mice treated with WR-2721, glucan + WR-2721, or glucan + selenium + WR-2721 were significantly greater than that of saline control mice at all

Table 1. Effects of combined glucan, selenium, and WR-2721 on endogenous spleen colony formation in irradiated C3H/HeN mice

| | Radiation Dose (Gy) | | | | | | | |
	6	7	8	9	10	11	12	13
Saline	7.2 ± 1.0	1.6 ± 0.5	0.2 ± 0.1	0 ± 0	**	**	**	**
Glucan	confluent*	30.0 ± 2.5*	7.8 ± 1.0*	3.6 ± 0.7*	0 ± 0	**	**	**
Selenium	8.2 ± 1.1	4.5 ± 0.9*	0.9 ± 0.3*	0 ± 0	**	**	**	**
WR-2721	confluent*	confluent*	confluent*	10.4 ± 1.8*	6.7 ± 1.1	2.0 ± 0.7	0 ± 0	**
Glucan + WR-2721	confluent*	confluent*	confluent*	34.4 ± 3.9*†	25.0 ± 3.9†	3.7 ± 0.5†	0 ± 0	**
Glucan + Selenium + WR-2721	**	**	confluent*	confluent*@	confluent@	8.4 ± 0.9@	4.0 ± 0.8@	1.3 ± 0.5

Glucan (75 mg/kg i.v.) and selenium (0.8 mg/kg i.p.) were administered 20 hours prior to irradiation, WR-2721 (200 mg/kg i.p.) was administered 30 minutes prior to irradiation. Data represent mean ± standard error of spleen colony counts from at least 20 spleens.
* p < 0.05, with respect to saline values.
† p < 0.05, with respect to WR-2721 values.
@ p < 0.05, with respect to Glucan + WR-2721 values.
** Not done.

Table 2. Effect of glucan, selenium, and WR-2721 on bone marrow and splenic cellularity in 9-Gy-irradiated C3H/HeN mice ($\times 10^6$)

Bone Marrow	Day Postirradiation		
	4	9	13
Normal 4.8 ± 0.53			
Saline	0.13 ± 0.02	0.54 ± 0.08	0.68 ± 0.11
Glucan	0.36 ± 0.05*	0.72 ± 0.09	0.94 ± 0.09
WR-2721	1.07 ± 0.11*	2.14 ± 0.32*	3.72 ± 0.58*
Glucan + WR-2721	1.37 ± 0.18*	3.42 ± 0.34*	3.84 ± 0.49*
Selenium	0.29 ± 0.02*	0.61 ± 0.07	0.74 ± 0.14
Glucan + Selenium + WR-2721	1.41 ± 0.12*	3.99 ± 0.56*	5.07 ± 0.73*

Spleen			
Normal 90.4 ± 10.8			
Saline	10.40 ± 0.83	8.30 ± 0.91	5.81 ± 1.11
Glucan	11.88 ± 0.79	12.12 ± 0.96*	12.71 ± 1.10*
WR-2721	13.37 ± 0.81*	16.29 ± 2.33*	26.42 ± 1.90*
Glucan + WR-2721	15.03 ± 0.83*	33.10 ± 2.89*†	53.85 ± 3.62*†
Selenium	11.30 ± 0.94	8.80 ± 1.11	7.23 ± 0.79
Glucan + Selenium + WR-2721	17.77 ± 1.22*	38.16 ± 2.60*	79.00 ± 8.18*@

Glucan (75 mg/kg i.v.) and selenium (0.8 mg/kg i.p.) were administered 20 hours prior to irradiation; WR-2721 (200 mg/kg i.p.) was administered 30 minutes prior to irradiation. Data represent mean ± standard error of three experiments.

* $p < 0.05$, with respect to saline values.
† $p < 0.05$, with respect to WR-2721 values.
@ $p < 0.05$, with respect to Glucan + WR-2721 values.

time points evaluated; cellularities in these mice ranged from ~22–28% of normal at day 4 postexposure to ~77–105% of normal at day 13. Mice treated with only glucan or only selenium exhibited increased bone marrow cellularities at day 4 postexposure, but not at day 9 or 13. Splenic cellularity in saline-treated mice was reduced to ~12% of normal at day 4 postexposure and decreased to ~6% of normal at day 13. In contrast, splenic cellularities

in all mice except those receiving selenium only, increased postirradiation; at day 13, cellularities in mice receiving glucan, WR-2721, glucan + WR-2721, and glucan + selenium + WR-2721, respectively, were ~14%, ~29%, ~60%, and ~87% of normal. In addition, splenic cellularity in mice treated with glucan + WR-2721 was significantly ($p < 0.005$) greater than that in WR-2721-treated mice, and splenic cellularity in mice treated with

Table 3. Effect of glucan, selenium, and WR-2721 on bone marrow and splenic GM-CFC recovery in 9-Gy-irradiated C3H/HeN mice

Bone Marrow	Day Postirradiation		
	4	9	13
Normal 5093 ± 612			
Saline	30 ± 4	2 ± 1	3 ± 1
Glucan	160 ± 21*	17 ± 1*	66 ± 5*
WR-2721	289 ± 33*	58 ± 4*	208 ± 13*
Glucan + WR-2721	626 ± 59*†	308 ± 41*†	465 ± 51*†
Selenium	97 ± 8*	17 ± 3*	26 ± 3*
Glucan + Selenium + WR-2721	776 ± 96*	698 ± 47*@	1014 ± 87*@

Spleen			
Normal 2531 ± 228			
Saline	0 ± 0	0 ± 0	0 + 0
Glucan	0 ± 0	12 ± 2*	140 ± 9*
WR-2721	5 ± 1*	49 ± 3*	528 ± 56*
Glucan + WR-2721	8 ± 1*	166 ± 21*†	1345 ± 169*†
Selenium	0 ± 0	9 ± 1*	64 ± 4*
Glucan + Selenium + WR-2721	12 ± 1*@	294 ± 23*@	3555 ± 569*@

Glucan (75 mg/kg i.v.) and selenium (0.8 mg/kg i.p.) were administered 20 hours prior to irradiation; WR-2721 (200 mg/kg i.p.) was administered 30 minutes prior to irradiation. Data represent mean ± standard error of three experiments.

* $p < 0.05$, with respect to saline values.
† $p < 0.05$, with respect to WR-2721 values.
@ $p < 0.05$, with respect to Glucan + WR-2721 values.

glucan + selenium + WR-2721 was significantly (p < 0.05) greater than that in glucan + WR-2721-treated mice.

Femoral GM-CFC content in saline-treated mice was severely reduced following irradiation, at day 13 postexposure, the number of GM-CFC's per femur in these mice was ~0.06% of normal. Glucan, WR-2721, glucan + WR-2721, selenium, and glucan + selenium + WR-2721 treatments all significantly increased femoral GM-CFC numbers. At day 13 postexposure, the numbers of GM-CFC per femur in mice receiving these treatments were ~1%, ~4%, ~9%, ~0.5%, and ~20% of normal, respectively. In addition, glucan + WR-2721-treated mice exhibited significantly (p < 0.01) more GM-CFC's than WR-2721-treated mice, and glucan + selenium + WR-2721-treated mice exhibited significantly (p < 0.005) more GM-CFC's than glucan + WR-2721-treated mice. Although no splenic GM-CFC's could be detected at any time postirradiation in saline-treated mice (i.e., 0% of normal), all drug-treated groups did exhibit splenic GM-CFC recovery. At day 13, splenic GM-CFC numbers in mice treated with glucan, WR-2721, glucan + WR-2721, selenium, and glucan + selenium + WR-2721 were ~6%, ~21%, ~53%, ~3%, and ~140% of normal, respectively. As in the bone marrow, glucan + WR-2721 produced greater effects than WR-2721 treatment, and glucan + selenium + WR-2721 treatment produced greater effects than glucan + WR-2721 treatment.

DISCUSSION

The exposure of mammals to a single whole-body dose of ionizing radiation results in a complex set of symptoms whose onset, nature, and severity are a function of both total radiation dose and radiation quality (6). In general, radiation injury can be classified into three syndromes affecting the hemopoietic, the gastrointestinal, and the central nervous systems at progressively increasing radiation doses. The hemopoietic syndrome becomes evident at the lowest radiation doses (<10 Gy) and is manifested by hemopoietic stem cell depletion (5, 6) and ultimately by depletion of mature blood cells (2, 29), which, whether destroyed directly by irradiation or lost naturally through attrition, cannot be regenerated without hemopoietic stem cells. In turn, the loss of mature blood cells severely impairs antimicrobial immunity, and ultimately death ensues due to invasive opportunistic infections (3, 14).

A variety of agents can be radioprotective in the dose range of the hemopoietic syndrome. For example, if used at optimal doses, all three agents used in these studies (i.e., glucan, selenium, and WR-2721) can individually enhance survival to varying degrees following radiation doses that induce the hemopoietic syndrome (22, 26, 36, 38). In these particular studies, we have also demonstrated good radioprotective effects of suboptimal doses of these agents when used in combination. Radioprotection following administration of combinations of agents has previously been reported (1, 19). Maisin et al. evaluated primarily combinations of sulfhydryl agents, while Ainsworth et al. evaluated AET used in combination with endotoxin. Our studies differ in that we have evaluated the combined effects of three agents that radioprotect by distinct mechanisms. WR-2721 enhances survival by protecting cells from radiation-induced lethality through free-radical scavenging, hydrogen atom donation, induction of hypoxia, or combinations of these mechanisms (9, 35, 38). Hemopoietic stem and progenitor cells are among the cells best protected by WR-2721; however, WR-2721 also protects a variety of other cell types (9). Because WR-2721 is most effective when administered shortly before radiation exposure, either WR-2721 itself, or immediate metabolites, appear to mediate its radioprotective effects. Unlike WR-2721 which affects multiple cell types, glucan appears to act specifically on cells of hemopoietic origin (Dr. M. L. Patchen, unpublished data, September, 1988). If administered intravenously 15 min before radiation exposure some glucan-containing substances may also radioprotect by free radical scavenging or induction of hypoxia (18). However, evidence suggests that the glucan dose and injection schedule used in the studies presented here radioprotects by enhancing the proliferative capacity of surviving hemopoietic stem and progenitor cells (21, 22, 24, 25, 28). This effect, at least in part, appears to be mediated through the sustained induction of cytokines important in the stimulation and/or regulation of hemopoietic proliferation and function (23, 27). In contrast to either WR-2721 or glucan, induction of endogenous oxidative substances, such as glutathione peroxidase, is the probable mechanism through which selenium mediates its radioprotective effect (37).

The studies presented in this paper demonstrate that, compared to single glucan, selenium, or WR-2721 treatments, combinations of glucan + WR-2721 and glucan + selenium + WR-2721 produce additive-to synergistic survival-enhancing effects. The manner in which single versus combination treatments altered the slopes of their respective survival curves is interesting. For example, as has been shown previously (36), WR-2721 treatment protracts the survival curve, indicating that this agent enhances survival more effectively at high than at low radiation doses. In contrast, neither glucan (this paper) nor selenium (36) alone alter survival curve slopes, indicating equal protection with these agents at both low and high radiation doses. When used in combination with WR-2721, however, both glucan and selenium produce survival curves parallel to that of WR-2721, further increasing WR-2721's ability to selectively enhance survival better at high radiation doses.

Hemopoietic regeneration is also significantly accelerated in mice treated with glucan + WR-2721 and glucan + selenium + WR-2721 when compared to mice receiving single-agent treatments. Furthermore, the hemopoietic effects of these combinations as well as those of the single

agents paralleled their survival-enhancing effects, supporting the concept that accelerated hemopoietic regeneration reduces susceptibility to potentially lethal postirradiation infections, and consequently, enhances survival. Accelerated hemopoietic recovery has previously been demonstrated in mice receiving either WR-2721 or glucan before radiation (16, 21, 28, 33, 34). In the case of WR-2721, such recovery has been attributed to survival of a greater number of stem cells from which hemopoietic regeneration is initiated. In the case of glucan, such recovery has been attributed to enhanced proliferation of surviving stem cells. The further accelerated hemopoietic recovery observed here in mice treated with glucan + WR-2721 could be explained if WR-2721 preserved larger numbers of stem cells on which glucan could then exert its proliferative effects. Whether selenium further contributed to accelerated hemopoietic regeneration by reducing stem cell lethality (as suggested for WR-2721), enhancing stem cell proliferation (as suggested for glucan), or by yet undetermined mechanisms is not clear. We have previously demonstrated that pretreatment of mice with selenium (1.6 mg/kg) increased the radioprotective effect and decreased the lethal toxicity of WR-2721 (36). In the present study, a lower dose of selenium was used, which by itself did not have a radioprotective effect. Although there are a number of possible mechanisms by which selenium could act in conjunction with WR-2721 (37), the most probable mechanism, considering the dose and time of selenium administration, is induction of glutathione peroxidase. This selenium-containing enzyme may reduce stem cell lethality by reducing the level of deleterious hydroperoxides formed during radiation exposure, or perhaps even as byproducts in the metabolism of WR-2721.

The most effective radioprotective combination evaluated in these studies was glucan + selenium + WR-2721, which produced a DRF of 1.66. If used at sufficiently high doses, WR-2721 alone could produce greater DRF's. However, one of the goals of these studies was to evaluate whether relatively high DRF's could be obtained using doses of individual agents that lacked toxic or behavioral effects. High doses of WR-2721 are known to induce both toxicity and detrimental effects on performance (4, 7, 17). In fact, essentially all radioprotectants tested to date result in performance decrements at the best radioprotective dosages (Dr. Michael Landauer, oral communication, August, 1988). Although the side effects (e.g., nausea, vomiting, performance decrements) may not constitute major problems in clinical environments where patients are closely monitored and are not physically active, such effects would be particularly undesirable in radiation rescue and/or clean-up environments where performance and stamina could be critical to the success of the operation. Based on these considerations, doses of WR-2721 and selenium that induce only minimal toxicity (17, 36) were used in these studies. These agents administered in combination with glucan were not toxic; however, the behavioral effects of these combinations remain to be determined.

In conclusion, these studies suggest that a "cocktail" approach to radioprotection allows the exploitation of multiple protective mechanisms. In addition, such an approach allows doses of single agents to be reduced to nontoxic levels while maintaining respectable DRF's. The value of including a hemopoietic stimulant in such cocktails has also been illustrated. Future studies will determine whether agents operating through yet additional radioprotective mechanisms may further enhance the effectiveness of these cocktails.

REFERENCES

1. Ainsworth, E. J.; Larsen, R. M.; Mitchell, F. A., Taylor, J. F. Survival-promoting effects of endotoxin in mice, dogs, and sheep. In: Moroson, H. L., Quintiliani, M., eds. Radioprotection and sensitization. London: Taylor and Francis; 1970:381–388.

2. Anderson, R. E.; Warner, N. L. Ionizing radiation and the immune response. Adv. Immunol. 24:215–335; 1976.

3. Benacerraf, B. Influence of irradiation on resistance to infection. Bacteriol. Rev. 24:35–40; 1960.

4. Bogo, V.; Jacobs, A. J.; Weiss, J. F. Behavioral toxicity and efficacy of WR-2721 as a radioprotectant. Radiat. Res. 104:182–190; 1985.

5. Bond, V. P.; Fliedner, T. M.; Archambeau, J. O. Effects of radiation on the hemopoietic system: The bone marrow syndrome. In: Bond, V. P., ed. Mammalian radiation lethality. New York, NY: Academic Press; 1965:159–230.

6. Broerse, J. J.; MacVittie, T. J., eds. Response of different species to total-body irradiation. Amsterdam: Martinus Nijhoff; 1984.

7. Cairnie, A. B. Adverse effects of the radioprotector WR-2721. Radiat. Res. 94:221–226; 1983.

8. Chow, C. K. Nutritional influence on cellular antioxidant defense systems. Am. J. Clin. Nutr. 32:1066–1081; 1979.

9. Davidson, D. E.; Grenan, M. M.; Sweeney, T. R. Biological characteristics of some improved radioprotectors. In: Brady, L. W., ed. Radiation sensitizers: their use in the clinical management of cancer. New York: Masson Publishing; 1980:309–320.

10. DiLuzio, N. R.; Williams, D. L.; McNamee, R. B.; Edwards, B. F.; Kitahama, A. Comparative tumor-inhibitory and antibacterial activity of soluble and particulate glucan. Int. J. Cancer 24:773–779; 1979.

11. Finney, D. J. Probit analysis, 3rd edition. London: Cambridge University Press; 1971.

12. Finney, D. J. Statistical methods in biological assays, 3rd edition. New York: MacMillan Publishing; 1978.

13. Giambarresi, L.; Jacobs, A. J. Radioprotectants. In: Conklin, J. J., Walker, R. I., eds. Military radiobiology. New York: Academic Press; 1987:265–301.

14. Hammond, C. W.; Tompkins, M.; Miller, C. P. Studies on susceptibility to infection following ionizing radiation; time of onset and duration of endogenous bacteremias in mice. J. Exp. Med. 99:405–410; 1954.

15. Jacobs, A. J.; Rankin, W. A.; Srinivasan, V.; Weiss, J. F. Effects of vitamin E and selenium on glutathione peroxidase activity and survival in irradiated mice. In: Broerse, J. J., Barendsen, G. W., Kal, H. B., Van Der Kogel, A. J., eds.

Proceedings of the 7th International Congress of Radiation Research. Amsterdam: Martinus Nijhoff; 1983:D5–15.

16. Kinnamon, K. E.; Ketterling, L. L.; Stampfli, H. F.; Grenan, M. M. Mouse endogenous spleen counts as a means of screening for anti-radiation drugs. Proc. Soc. Exp. Biol. Med. 164:370–373; 1980.

17. Landauer, M. R.; Davis, H. D.; Dominitz, J. A.; Weiss, J. F. Long-term effects of radioprotector WR-2721 on locomotor activity and body weight of mice following exposure to ionizing radiation. Toxicology 49:315–323; 1988.

18. Maisin, J. R., Kondi-Tamba, A.; Mattelin, G. Polysaccharides induce radioprotection of murine hemopoietic stem cells and increase the LD50/30 days. Radiat. Res. 105:276–281; 1986.

19. Maisin, J. R.; Mattelin, G.; Fridman-Manduzio, A.; Van Der Parren, J. Reduction of short- and long-term radiation lethality by mixtures of chemical protectors. Radiat. Res. 35:26–44; 1968.

20. Nygaard, O. F.; Simic, M. G., eds. Radioprotectors and anticarcinogens. New York: Academic Press; 1983.

21. Patchen, M. L. Immunomodulators and hemopoiesis. Surv. Immunol. Res. 2:237–242; 1983.

22. Patchen, M. L.; D'Alesandro, M. M.; Brook, I.; Blakely, W. F.; MacVittie, T. J. Glucan: mechanisms involved in its radioprotective effect. J. Leukoc. Biol. 42:95–105; 1987.

23. Patchen, M. L., Lotzova, E. The role of macrophages and T-lymphocytes in glucan-mediated alterations of murine hemopoiesis. Biomedicine 34:71–77; 1981.

24. Patchen, M. L.; MacVittie, T. J. Dose-dependent responses of murine pluripotent stem cells and myeloid and erythroid progenitor cells following administration of the immuno-modulatory agent glucan. Immunopharmacology 5:303–313; 1983.

25. Patchen, M. L.; MacVittie, T. J. Stimulated hemopoiesis and enhanced survival following glucan treatment in sublethally and lethally irradiated mice. Int. J. Immunopharmacol. 7:923–932; 1985.

26. Patchen, M. L.; MacVittie, T. J. Comparative effects of soluble and particulate glucans on survival in irradiated mice. J Biol. Response Mod. 5:45–60; 1986.

27. Patchen, M. L.; MacVittie, T. J. Hemopoietic effects of intravenous soluble glucan administration. J. Immunopharmacol. 8:407–425; 1986.

28. Patchen, M. L.; MacVittie, T. J.; Wathen, L. M. Effects of pre- and post-irradiation glucan treatment on pluripotent stem cells, granulocyte, macrophage, and erythroid progenitor cells, and hemopoietic stromal cells. Experientia 40:1240–1244; 1984.

29. Patt, H. M.; Maloney, M. A. A comparison of radiation-induced granulocytopenia in several mammalian species. Radiat. Res. 18:231–235; 1963.

30. Pospisil, M.; Jary, J.; Netikova, J.; Marek, M. Glucan-induced enhancement of hemopoietic recovery in gamma-irradiated mice. Experientia 38:1232–1234; 1982.

31. Schulz, R. J.; Almond, P. R.; Cunningham, J. R.; Holt, J. G.; Loevinger, R.; Suntharalingam, N.; Wright, K. A.; Nath, R.; Lempert, G. D. A protocol for the determination of absorbed dose from high-energy photon and electron beams. Med. Phys. 10:741–771; 1983.

32. Till, J. E.; McCulloch, E. A. Early repair processes in marrow cells irradiated and proliferating *in vivo*. Radiat. Res. 18:96–105; 1963.

33. Travis, E. L.; Fang, M. Z.; Basic, I. Protection of mouse bone marrow by WR-2721 after fractionated irradiation. Int. J. Radiat. Oncol. Biol. Phys. 15:377–382; 1988.

34. Wanger, M.; Sedlmeier, H.; Metzger, E.; Wustrow, T.; Messerschmidt, O. Analysis of the toxicity and radioprotective effect of the chemical radioprotector WR-2721 in dogs (beagles). Strahlentherapie 156:655–662; 1980.

35. Ward, J. F. Chemical aspects of DNA radioprotection. In: Nygaard, O. F., Simic, M. G., eds. Radioprotectors and anticarcinogens. New York: Academic Press; 1983.73–85.

36. Weiss, J. F.; Hoover, R. L.; Kumar, K. S. Selenium pretreatment enhances the radioprotective effect and reduces the lethal toxicity of WR-2721. Free Radic. Res. Commun. 3:33–38; 1987.

37. Weiss, J. F.; Kumar, K. S. Antioxidant mechanisms in radiation injury and radioprotection. In: Chow, C. K., ed. Cellular antioxidant mechanisms, Vol. II. Boca Raton: CRC Press; 1988:163–189.

38. Yuhas, J. M. Biological factors affecting the radioprotective efficiency of S-2-[3-aminopropylamino]ethylphosphorothioic acid (WR-2721): LD 50/30 doses. Radiat. Res. 44:621–628; 1970.

Time- and Dose-Dependent Changes in Neuronal Activity Produced by X Radiation in Brain Slices

T. C. PELLMAR,* D. A. SCHAUER,† AND G. H. ZEMAN†[1]

*Physiology Department and †Military Requirements and Applications Department, Armed Forces
Radiobiology Research Institute, Bethesda, Maryland 20814-5145

PELLMAR, T. C., SCHAUER, D. A., AND ZEMAN, G. H. Time-and Dose-Dependent Changes in Neuronal Activity Produced by X Radiation in Brain Slices. *Radiat. Res.*, 122, 209–214 (1990).

A new method of exposing tissues to X rays in a lead Faraday cage has made it possible to examine directly radiation damage to isolated neuronal tissue. Thin slices of hippocampus from brains of euthanized guinea pigs were exposed to 17.4 keV X radiation. Electrophysiological recordings were made before, during, and after exposure to doses between 5 and 65 Gy at a dose rate of 1.54 Gy/min. Following exposure to doses of 40 Gy and greater, the synaptic potential was enhanced, reaching a steady level soon after exposure. The ability of the synaptic potential to generate a spike was reduced and damage progressed after termination of the radiation exposure. Recovery was not observed following termination of exposure. These results demonstrate that an isolated neuronal network can show complex changes in electrophysiological properties following moderate doses of ionizing radiation. An investigation of radiation damage directly to neurons *in vitro* will contribute to the understanding of the underlying mechanisms of radiation-induced nervous system dysfunction. © 1990 Academic Press, Inc.

INTRODUCTION

Although the nervous system is usually considered to be radioresistant, behavioral studies have shown decrements in performance and acute disorientation at doses of 5–10 Gy (*1, 2*). Ionizing radiation has been shown to modify neuronal activity both *in vivo* (*3–6*) and *in vitro* (*7–9*). Changes in blood pressure and blood flow, altered blood–brain barrier, and release of blood-borne mediators are likely to contribute to the observed damage *in vivo* (*10–16*). In an isolated preparation of neural tissue supplied with oxygen, glucose, and balanced salt solution, damage from ionizing radiation is likely to result from direct effects on the neurons and their microenvironment. By understanding the cellular

changes produced by radiation, we can begin to address the mechanisms of the observed performance decrement.

A previous study on slices of hippocampus isolated from guinea pig brain (*7*) revealed that ^{60}Co radiation decreased the evoked synaptic response and decreased the ability of the synaptic potential to generate a spike. The decrease in the ability to generate a spike potential was not dependent on dose rate; a dose of 75 Gy was necessary to produce the effect at both 5 Gy/min and 20 Gy/min. On the other hand, synaptic damage was dose-rate sensitive. Fifty grays at 20 Gy/min produced damage equivalent to 100 Gy at 5 Gy/min.

The remote location of the cobalt source limited the time resolution and sensitivity of this earlier study. A more sensitive system was established by positioning an X-ray tube directly within a lead-lined Faraday cage (*17*). This allowed observation of electrophysiological parameters in a single slice of brain tissue, immediately before, during, and after exposure to ionizing radiation. This paper reports the effects of radiation from this X-ray system in hippocampal tissue.

METHODS

Slices (400–450 μm thick) of hippocampus were prepared from the brains of euthanized male guinea pigs as described previously (*7, 18–20*). A single slice was positioned in the recording chamber (0.5 ml volume) and constantly perfused (approximately 1 ml/min) with an artificial cerebrospinal fluid (aCSF) containing 124 mM NaCl, 3 mM KCl, 2.4 mM CaCl$_2$, 1.24 mM KH$_2$PO$_4$, 1.24 mM MgSO$_4$, 10 mM glucose, and 26 mM NaHCO$_3$, equilibrated with 95% O$_2$/5% CO$_2$ at 30 ± 1°C. Temperature was continually monitored and did not change with radiation exposure.

The characteristics of the X ray system are described in detail elsewhere (*17*). Briefly, the X-ray source was a Kevex 50 kVp/1-mA unit with a molybdenum (Mo) target, beryllium window, and Mo filter (25 μm). This configuration provided a quasi-monoenergetic spectrum consisting primarily of 17.4-keV photons. Dose rate (1.54 Gy/min) was measured with a Capintec parallel-plate ionization chamber positioned at the location of the tissue. During experimental exposures, the chamber was removed and tissue was exposed for calculated time periods.

The hippocampal slice maintains a large degree of organization that can be observed easily through a dissecting microscope. Using visual cues and a knowledge of this organization, electrodes for stimulation and recording were positioned in defined locations (Fig. 1). A stainless steel concentric bipolar stimulating electrode was positioned in the stratum radiatum which contains afferents to the cells of interest (pyramidal cells) in the CA1 region of the hippocampus. About a millimeter away, a glass microelec-

[1] Present address. AT&T Bell Laboratories, Department of Radiation Protection. Murray Hill, New Jersey 07974-2070
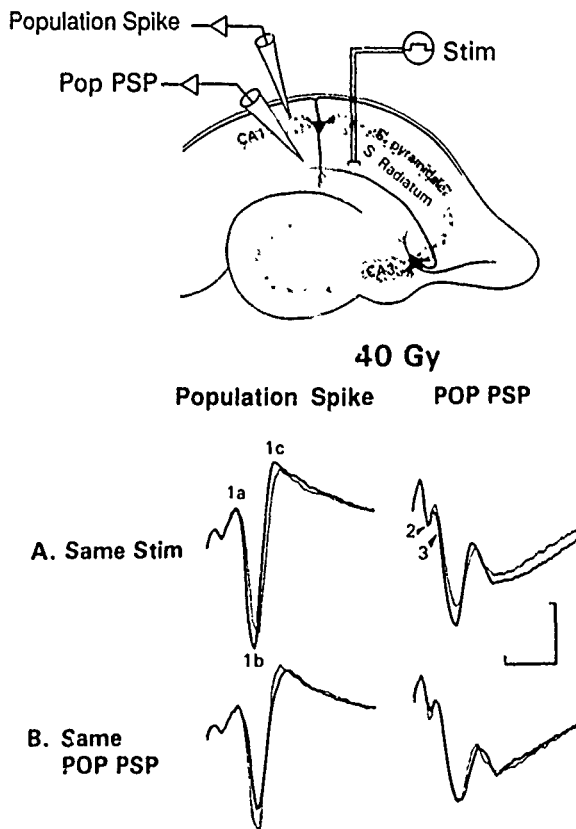
FIG. 1. Schematic diagram of the hippocampal slice preparation showing placement of electrodes. The stimulating electrode is in stratum radiatum of CA1. One recording electrode is in stratum radiatum of CA1 (pop PSP) and another is in stratum pyramidale of CA1 (population spike). Traces obtained from each of these recording sites are shown: On the left are recordings from the stratum pyramidale showing the summation of the responses of the CA1 neurons (population spike). Its amplitude is calculated from the values · . the potentials at 1a, 1b, and 1c: 1/2(a + c) − b. On the right are recordings from the stratum radiatum showing the activation of the afferent fibers (afferent volley) at 2 and the summated response of a population of dendrites of the hippocampal neurons (pop PSP). The pop PSP is quantitated from the slope of the potential at 3. Recordings before and after exposure to 40 Gy X radiation (1.54 Gy/min) are superimposed. The thin line shows control traces and the thick line shows traces following exposure. (A) Using identical stimulus intensities to the afferent pathway produces the same size afferent volley but a larger pop PSP after radiation. The population spike is also larger. (B) If the stimulus intensity to the afferent pathway is reduced to produce a pop PSP of the same size as control, the afferent volley is smaller and the population spike following radiation is also smaller. Calibration pulse: 2 ms, 1 mV population spike, 0.5 mV pop PSP.

trode filled with 2 *M* NaCl also was placed in the stratum radiatum to record the afferent volley (the summation of the potentials from the stimulated afferent fibers) and to record the population postsynaptic potential (pop PSP; the summation of the synaptic responses of the population of neuronal processes in the region of the microelectrode). A typical recording from this microelectrode can be seen in Fig. 1 (traces on right). The afferent volley is the potential at the arrow labeled 2. The rest of the trace reflects the pop PSP. The pop PSP was quantified by measuring the maximal slope at the onset of the response (near arrow 3). A second NaCl-filled microelectrode was positioned in the stratum pyramidale of the CA1 region of the

slice. Through this electrode, we recorded the population spike (the summation of synaptically evoked spike potentials of nearby neurons). Figure 1 also illustrates a typical population spike (traces on left). The amplitude was measured as the difference between the average of the potentials at points 1a and 1c less the potential at point 1b. The electrical potentials recorded from the hippocampal tissue were amplified by a high-gain extracellular amplifier and monitored on an oscilloscope. The data were digitized, stored, and analyzed with a PDP 11-73 computer.

Input–output (I/O) curves for the slice were obtained and analyzed as previously described (7, 20). Briefly, two series of 13 electrically isolated constant-current pulses (0.0 to 1.5 mA, 300 μs, 0.2 Hz) were provided to the stimulating electrode. The responses at the two microelectrodes were recorded. Two curves were plotted from the data. Afferent volley vs pop PSP provided an indication of synaptic efficacy, the ability of the afferent pathway to evoke a synaptic response. Population post-synaptic potential vs population spike amplitude provided an indication of the ability of the synaptic response to generate a population spike (spike generation).

Following placement of electrodes, the X-ray tube (Kevex) was positioned in its holder at a constant distance from the preparation (17) to provide a dose rate of 1.54 Gy/min of 17.4 keV X rays. The lead-lined Faraday cage was closed and the interlock system activated. Tissue was stimulated at 0.2 Hz with a stimulus intensity that produced a population spike of approximately half-maximal amplitude. Every 5 min five traces were averaged and the data stored. At 5 min before radiation exposure and 5 min and 30 min after termination of exposure, input–output curves were obtained. At doses of 40 Gy and less, another I/O curve was obtained approximately 60 min following the end of the exposure. Sham slices were examined intermittently throughout the series of experiments. In the sham slices, I/O curves were obtained and evaluated at time points similar to those used with irradiated tissue. Changes in irradiated tissue were referenced to these control curves. Sham slices changed very little with time, but some trends were evident: maximal population spike amplitude tended to increase while the pop PSP slope decreased slightly. Experiments were limited to a 2-h duration; beyond 2 h, some sham slices began to show decline, most commonly reflected as a severe decrease in the pop PSP size.

Statistical treatment of the I/O curves has been described previously (7, 20). For each experiment, the maximal amplitude during the control period was normalized for the population spike amplitude to 5 mV, pop PSP slope to 0.5 mV/ms, and afferent volley to 2 mV. Average maximal amplitudes of the raw data during control period were 4.7 ± 0.1 mV for the population spike, 0 73 ± 0.03 mV/ms for pop PSP, and 1.4 ± 0.1 mV for volley (n = 60 slices) For each stimulus intensity the data from 5 to 10 slices were averaged for each experimental condition (i.e., radiation dose) to provide a mean I/O curve Two curves (experimental and control) were compared by evaluating the residual sum of squares for the sigmoid functions computer-fitted to the data points of the individual curves and the residual sum of squares for the function fitted to the data of both curves combined Significance was accepted at P < 0.05. Differences between curves were quantified by comparing the ratios of the parameters of the computer-fitted functions.

RESULTS

Exposure of hippocampal slices to X radiation altered their electrophysiological properties. Figure 1 illustrates the changes in a slice exposed to 40 Gy. When the stimulus intensity was held constant, the afferent volley (arrow at 2) was unchanged by radiation exposure. Both the population spike and the pop PSP were increased in size. The increase in the population spike could result from the increased pop PSP and not be a direct effect of radiation. To test this, following irradiation the stimulus strength was decreased to
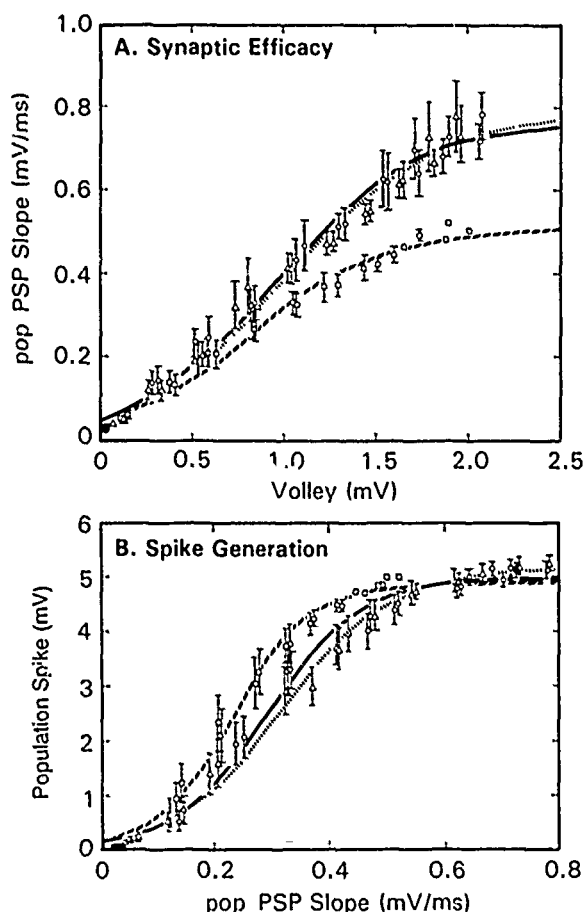
FIG. 2. Input-output curves averaged for six slices exposed to 50 Gy X radiation. Curves were obtained 5 min before exposure (squares; dashed line) and 5 (circles; solid line) and 30 min (triangles; dotted line) following termination of exposure. (A) Plot of afferent volley amplitude vs size of the pop PSP reflects the ability of the afferent pathway to generate a synaptic potential (synaptic efficacy). At all volley amplitudes, the pop PSP is larger following exposure to X radiation. (B) Plot of pop PSP vs population spike reflects the ability of the synaptic potential to generate a spike (spike generation). Following exposure to X radiation, a larger pop PSP is required to produce the same size population spike. Damage to spike generating mechanisms is more severe 25 min following exposure than 5 min following exposure.

less effective in producing a population spike. The I/O curves for 40 Gy (n = 6), 50 Gy (n = 6), and 65 Gy (n = 6) all showed similar changes.

One of the advantages of the X-radiation system used is that measurements of electrophysiological potentials can be made during the exposure. Throughout the exposure, afferents were stimulated at constant intensity. The pop PSP slowly began to increase. The increase progressed with time and continued following termination of exposure although at a slower rate. Following exposure, pop PSP size began to level off but recovery was not observed. Changes in the size of the pop PSP frequently became apparent within about 15 min, corresponding to a cumulative exposure of 23 Gy.

The time course of damage was also evaluated by obtaining I/O curves at two to three time points following termination of exposure to 5, 10, 20, 30, 40, 50, or 65 Gy. The curves for irradiated slices were compared to those for sham-irradiated slices obtained at similar time points in order to control for time-dependent changes not resulting from radiation exposure. Plotting the change in the I/O curves relative to the controls, one can see that the radiation damage progresses with time following exposure. In Fig. 3, data for 20, 30, 40, and 50 Gy are shown. No significant effects were observed with either 20 or 30 Gy. With 30 Gy, however, the trend is apparent. Forty and 50 Gy produced both a significant increase in synaptic efficacy and a significant decrease in the ability to generate the population spike. We observed no recovery during the time of the experiment.

Dose–response curves (Fig. 4) were constructed for the changes in synaptic efficacy and in spike generation from the I/O curves. The curves are plotted for the time point approximately 65–70 min following initiation of irradiation (circles). Also plotted (triangles) are the time points approximately 35–40 min following initiation of irradiation. Significant effects were seen at doses of 40 Gy and greater. The trend was apparent at 30 Gy. The effect at 35 min was always smaller than the effect at 65 min.

produce a smaller afferent volley but the same size pop PSP (Fig. 1B). Under this condition, the population spike was smaller than prior to irradiation. This suggests that radiation has two effects. to increase the pop PSP and to decrease the ability of the pop PSP to generate a population spike.

The two effects can clearly be seen on the I/O curves for doses of 40 Gy and greater. The I/O curves for 50 Gy radiation are illustrated (Fig. 2). Plotting afferent volley amplitude vs the pop PSP size, the increase in the synaptic potential both 5 min and 30 min following exposure was evident (Fig. 2A). This reflects an increase in synaptic efficacy. Following exposure to 50 Gy the plot of pop PSP size vs the amplitude of the population spike was shifted to the right. This shift progressed with time (Fig. 2B). The pop PSP was

DISCUSSION

X radiation has been shown to increase synaptic efficacy and to decrease the ability to generate spikes at doses between 40 and 65 Gy. Synaptic efficacy progressively increases during exposure, with the first noticeable change occurring at a cumulative dose of approximately 25 Gy. Changes in both synaptic efficacy and spike-generating ability continue at a slower rate following exposure. The effects of radiation exposure persist following exposure until the termination of the experiment. Neuronal activity is altered through mechanisms that change the functional characteristics of individual cells without killing those cells.
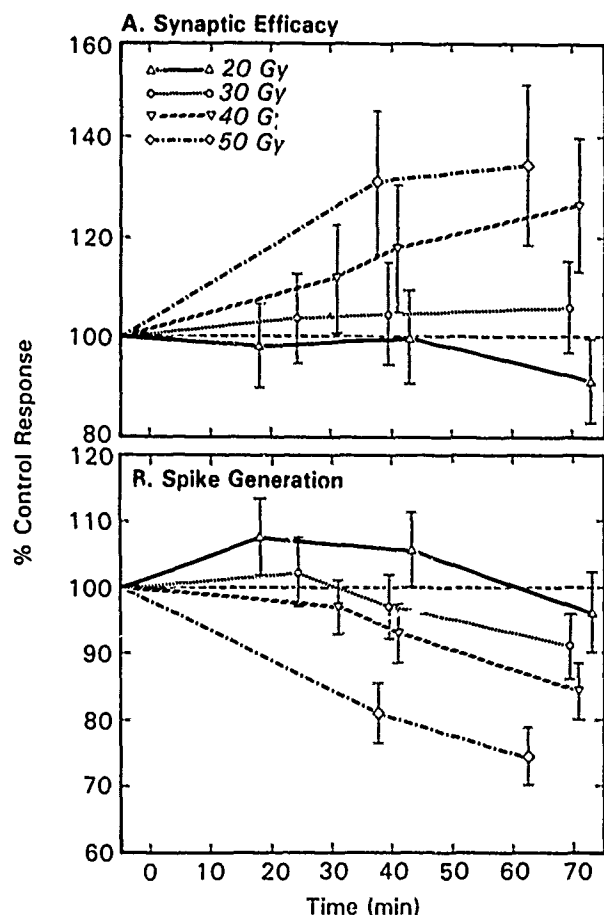
FIG. 3. Time course of radiation damage following exposure to 20, 30, 40, and 50 Gy X radiation. Input–output curves were obtained at the time points plotted. At each dose, the earliest time point was 5 min following termination of exposure. I/O curves were compared to sham-irradiated curves at similar time points. Irradiation was initiated at Time = 0 and terminated at Time = 13 min for 20 Gy, 19.5 min for 30 Gy, 26 min for 40 Gy, and 33 min for 50 Gy. (A) Changes in the curve relating afferent volley to pop PSP size reflect synaptic efficacy. There is no significant change with either 20 or 30 Gy but 40 and 50 Gy produce significant increases. (B) Changes in the curve relating pop PSP size to the population spike amplitude reflect changes in ability to generate spikes. Again, 20 and 30 Gy did not produce statistically significant changes but 40 and 50 Gy significantly depressed spike generation.

Neurons require generation of a spike to transmit their signal to the next cell in a pathway. If the synaptic potentials produced by stimulation of an afferent pathway are increased while the ability .o generate a spike is decreased, the net output of the population of neurons may appear unaltered. Under normal circumstances, however, synaptic input to a cell is not a result of activation of an entire pathway. Rather, the summation of synaptic potentials from a number of discrete inputs is a complicated integrating process. This information processing could be severely compromised by seemingly minor changes. As a consequence, despite the 'balanced' changes in synaptic efficacy and spike

generation, X radiation is likely to modify the functional properties of the hippocampus.

Both X radiation and γ radiation (7) produce deficits in spike generation. In the present study X radiation produced these changes at lower doses than γ radiation did (40 Gy rather than 75 Gy). One very important difference between the two studies is the difference in dose rate. Altering the dose rate from 5 to 20 Gy/min in the previous study did not alter the dose–response characteristics of the tissue for spike generation. A mechanism of lipid peroxidation was suggested as consistent with this observation. Lipid peroxidation is inversely dependent on dose rate at the lower dose rates but becomes relatively insensitive to dose rate at higher levels. This mechanism may also explain the greater sensitivity of the tissue in the present study using a dose rate of 1.54 Gy/min. Alternatively, the quality of radiation could be different enough to explain the effects. Experiments to distinguish these possibilities require a 17.4-keV
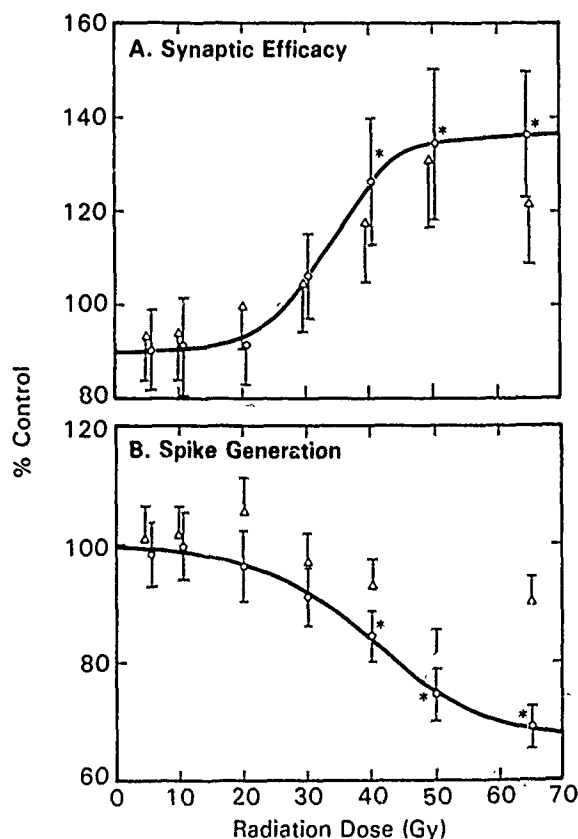
FIG. 4. Dose–response curves for electrophysiological damage to hippocampal tissue following exposure to X radiation. Data from time points 65 to 70 min following initiation of radiation exposure were plotted (circles). Triangles represent response at a time point 35–40 min following initiation of irradiation. (A) Dose–response curve constructed from the changes in the I/O curves relating afferent volley to pop PSP size, reflecting synaptic efficacy (B) Dose–response curve constructed from the changes in the I/O curves relating pop PSP size to population spike amplitude, reflecting spike generation. Control, $n = 11$; 5 Gy, $n = 7$; 10 Gy, $n = 8$; 20 Gy, $n = 10$; 30 Gy, $n = 6$; 40 Gy, $n = 6$; 50 Gy, $n = 6$; 65 Gy, $n = 6$.

X-ray machine capable of providing higher dose rates to the slice preparation. Development of this system is in progress.

The present study demonstrates that X radiation can increase synaptic efficacy. This is in contrast to the γ-radiation studies where synaptic efficacy was reduced (7). Again, as with spik: generation, the differences in dose rate and in radiation quality between these two experiments needs to be considered and evaluated in future experiments. A dose-rate effect seems to be a plausible explanation. At 5 Gy/min a greater dose of γ radiation is required to reduce synaptic efficacy than at a rate of 20 Gy/min (7). In addition, a low dose (625 cGy) of γ radiation at 5 Gy/min actually increased synaptic efficacy slightly, although statistically insignificantly. One might predict that at an even lower dose rate, such as the one used in the present study, reduction of synaptic efficacy would require even higher doses. Removal of the decrease in synaptic efficacy with lower dose rates may allow the expression of a distinct mechanism that increases synaptic efficacy.

An alternative explanation is that the increase and the decrease in synaptic efficacy are due to the same underlying mechanism that is biphasic in nature. We have hypothesized that the decrease is due to an oxidation of cellular proteins because oxidizing agents such as chloramine T and n-chlorosuccinimide can decrease synaptic efficacy in the same way as free radicals generated by peroxide and as exposure to γ irradiation (20). Oxidizing agents, radiation, and free radicals can impair calcium regulation by the mitochondrial, sarcoplasmic reticulum, and/or plasma membranes, resulting in increased intracellular calcium concentration (21-27). Synaptic processes are markedly sensitive to calcium. A relatively small increase in presynaptic calcium levels can increase release of neurotransmitter and increase the synaptic potential. At higher levels of calcium, the divalent cation can block calcium influx and have other toxicological actions. Altered calcium regulation could explain both the increase in synaptic efficacy seen in the present study and the decrease seen with γ radiation at higher doses and dose rates.

There is precedent for biphasic changes in calcium-dependent processes. For example, in cardiac cells from the dog, the calcium-dependent spike is first prolonged and then blocked by exposure to free radicals generated either from peroxide or from dihydroxyfumarate (28, 29). At the synaptic contact between muscle and nerve (the endplate), exposure to mercury first increases and then decreases the synaptic potential (endplate potential) (30). The calcium ionophore X-537a, which allows influx of calcium into the presynaptic terminal, also has a biphasic effect on the endplate potential, first increasing and later decreasing the amplitude (31).

One might expect exposure to radiation in vivo to produce changes in neurons throughout the brain similar to those reported here for neurons in slices of hippocampus.

Although it is difficult to predict from the present study the type of symptoms that might result from general nervous system dysfunction, the disorientation that results from radiation exposure would not be inconsistent. Since the hippocampus is thought to have a role in memory and learning, deficits in these functions may be prevalent if the damage is more specific to hippocampal neurons. In vivo, other factors also come into play. Humoral effects (e.g., increases in levels of prostaglandins or histamine) are likely to influence neuronal activity. In addition, reduced blood flow and alteration in the blood–brain barrier will affect brain function. Changes in glial cells can also alter the neuronal environment. The interactions of all of these factors must be considered before we can arrive at a full understanding of radiation damage to the nervous system.

The data presented in this report demonstrate that doses as low as 40 Gy X radiation can have direct effects on neuronal tissue in vitro. With the availability of an X-ray system that allows investigation into the radiation sensitivity of more complicated neuronal behavior than previously possible, future studies are likely to demonstrate neuronal damage at even lower doses.

REFERENCES

1. R. W. YOUNG, Acute radiation syndrome. In *Military Radiobiology* (J. J. Conklin and R. I. Walker, Eds.), pp. 165-190. Academic Press, New York, 1987.

2. D. J. KIMELDORF and E. L. HUNT, *Ionizing Radiation Neural Function and Behavior.* Academic Press, New York, 1965.

3. M. H. BASSANT and L. COURT, Effects of whole-body γ irradiation on the activity of rabbit hippocampal neurons. *Radiat. Res.* 75, 593-606 (1978).

4. H. GANGLOFF, Acute effects of X irradiation on brain electrical activity in cats and rabbits. In *Effects of Ionizing Radiation on the Nervous System,* pp. 123-135. International Atomic Energy Agency, Vienna, 1962.

5. T. J. HALEY, Changes induced in brain activity by low doses of X irradiation. In *Effects of Ionizing Radiation by the Nervous System,* pp. 171-185. International Atomic Energy Agency, Vienna. 1962.

6. R. L. SCHOENBRUN, E. CAMPEAU, and W. R. ADEY, Electroencephalographic and behavioral effects from X irradiation of the hippocampal system. In *Response of the Nervous System to Ionizing Radiation, Second International Symposium* (T. J. Haley and R. S. Snider, Eds.), pp. 411-428. Little, Brown, Boston, 1964.

7. J. M. TOLLIVER and T. C. PELLMAR, Ionizing radiation alters neuronal excitability in hippocampal slices of the guinea pig. *Radiat. Res.* 112, 555–563 (1987).

8. T. C. PELLMAR and J. M. TOLLIVER, Effects of ionizing radiation on hippocampal excitability. In *Brain Slices. Fundamentals, Applications and Implications* (A. Schurr, T. J. Teyler, and M. T. Tseng, Eds.), pp. 152–156. Karger, Basel, 1987.

9. S. I. PEIMER, A. O. DUDKIN, and A. G. SWERDLOV, Response of hippocampal pacemaker-like neurons to low doses of ionizing radiation. *Int. J. Radiat. Biol.* 49, 597–600 (1986).

10. T. C. PELLMAR, J. M. TOLLIVER, and K. L. NEAL, Radiation-induced impairment of neuronal excitability. *Comments Toxicol.* 2, 253–263 (1988).

11. P. H. CHAPMAN and R. J. YOUNG, effect of cobalt-60 gamma irradiation on blood pressure and cerebral blood flow in the *Macaca mulatta*. *Radiat. Res.* 35, 78–85 (1968).

12. L. G COCKERHAM, T J. CERVANY, and J. D. HAMPTON, Postradiation regional cerebral blood flow in primates. *Aviat. Space Environ. Med.* 57, 578–583 (1986).

13. T. W. GRIFFIN, J. S. RASEY, and W. A. BLEYER, The ffect of photon irradiation on blood brain barrier permeability to methotrexate in mice. *Cancer* 40, 1109–1111 (1977).

14. T. SCHETTLER and C. N. SHEALY, Experimental selective alteration of blood-brain barrier by X irradiation. *J. Neurosurg.* 32, 89–94 (1970).

15. M. DONLON and T. L WALDEN, Release of biological mediators in response to acute radiation injury. *Comments Toxicol.* 4, 205–216 (1988).

16. R HAWKINS and C D FORCINO, Postradiation cardiovascular dysfunction. *Comments Toxicol* 4, 243–252 (1988).

17. D. A. SCHAUER, G. H. ZEMAN, and T. C. PELLMAR, A low energy X-ray irradiator for electrophysiological studie.. *Appl. Radiat. Isot. (Int. J. Radiat. Appl. Instrum. Part A* 40), 7–17 (1989).

18. T. C. PELLMAR, Electrophysiological correlates of peroxide damage in guinea pig hippocampus in vitro. *Brain Res.* 364, 377–381 (1986).

19. T C PELLMAR, Peroxide alters neuronal excitability in the CA1 region of guinea pig hippocampus in vitro *Neuroscience* 23, 447–456 (1987).

20. T. C. PELLMAR and K. L. NEEL, Oxidative damage in the guinea pig hippocampal slice. *Free Radicals Biol. Med.* 6, 467–472 (1989).

21. J. J. ABRAMSON, J. L. TRIMM, L. WEDEN, and G. SALAMA, Heavy metals induce rapid calcium release from sarcoplasmic reticulum vesicles isolated from skeletal muscle. *Proc. Natl. Acad. Sci. USA* 80, 1526–1530 (1983).

22. A. BINDOLI, L. CAVALLINI, N. SILIPRANDI, and F. ZOCCARATO, Action of some thiol oxidizing reagents on mitochondrial sulfhydryl groups. *Bull. Mol. Bikol. Med.* 1, 92–96 (1978).

23. R. P. HEBEEL, O. SHALEV, W. FOKER, and B. H. RANK, Inhibition of erythrocyte Ca2+-ATPase by activated oxygen through thiol- and lipid-dependent mechanisms. *Biochim. Biophys. Acta* 862, 8–16 (1986).

24. M. L. HESS, E. OKABE, and H. A. KONTOS, Proton and free oxygen radical interaction with the calcium transport system of cardiac sarcoplasmic reticulum. *J. Mol. Cell. Cardiol.* 13, 767–772 (1981).

25. J. HIROSUMI, O. YASUYOSHI, and M. WATANABE, Effect of superoxide and lipid peroxide on cytosolic free calcium concentration in cultured pig aortic endothelial cells. *Biochem. Biophys. Res. Commun.* 152, 301–307 (1988).

26. V. McCONNELL, D. B. McINTOSH, and M. C. BERMAN, X irradiation of isolated sarcoplasmic reticulum vesicles. *Radiat. Res.* 85, 505–515 (1981).

27. I. U. SCHRAUFSTATTER, P. A. HYSLOP, D. B. HINSHAW, R. G. SPRAGG, L. A. SKLAR, and C. G. COCHRANE. *Proc. Natl. Acad. Sci. USA*, 83, 4908–4912 (1986).

28. P. L. BARRINGTON, C. F. MEIER, and W. B. WEGLICKI, Abnormal electrical activity induced by free radical generating systems in isolated cardiocytes. *J. Mol. Cell Cardiol.* 20, 1163–1178 (1988).

29. P. L. BARRINGTON, C. F. MEIER, and W. B. WEGLICKI, Abnormal electrical activity induced by H2O2 in isolated canine myocytes. In *Oxygen Radicals in Biology and Medicine* (M. G. Simic, K. A. Taylor, J. F. Ward, and C. von Sonntag, Eds.), pp. 927–932. Plenum, New York, 1989.

30. R. S. MANALIS and G. P. COOPER, Evoked transmitter release increased by inorganic mercury at frog neuromuscular junction. *Nature* 257, 690–691 (1975).

31. N. TANABE and H. KIJIMA, Transmitter release at frog end-plate loaded with a Ca2+-chelator, BAPTA: hypertonicity and erythrosin B augment the release independently of internal Ca2+. *Neurosci. Lett.* 92, 52–57 (1988).

New membrane assembly in IgE receptor-mediated exocytosis

[1]E. A. SCHMAUDER-CHOCK* and [2]S. P. CHOCK[†]

Department of Experimental Hematology, Armed Forces Radiobiology Research Institute, Bethesda, MD, 20814-5145, USA, and
[2]Laboratory of Neurochemistry, NINCDS, NIH, Bethesda, MD, 20892, USA

Summary

The presence of excess membrane has been observed in the secretory granules of mast cells activated via the physiological mechanism of IgE receptor-mediated exocytosis. This excess membrane is the result of a *de novo* assembly from phospholipid, cholesterol, and other membrane components stored in the matrix of the quiescent granule. Following receptor stimulation, membrane bilayer structures of varying size and shape can be seen in the subperigranular membrane space where the perigranular membrane has lifted away from the granule matrix. Vesicles as small as 25 nm in outer diameter are frequently found beneath the perigranular membrane at the site of granule fusion. Membrane in the form of elongated vesicles, tubes, or sheets has also been observed. The wide variation in size and shape of the newly assembled membrane may reflect the spontaneity of the entropy-driven membrane generation process and the fluid characteristic of the biological membrane in general. Fusion of the newly assembled membrane with the perigranular membrane enables the activated granule to enlarge. This rapid expansion process of the perigranular membrane may be the principal mechanism by which an activated granule can achieve contact with the plasma membrane in order to generate pore formation. The fact that new membrane assembly also occurs in the IgE receptor-mediated granule exocytosis, supports our observation that *de novo* membrane generation is an inherent step in the mechanism of mast cell granule exocytosis. Whether new membrane assembly is a common step in the mechanism of secretory granule exocytosis in general, must await careful reinvestigation of other secretory systems.

Introduction

Perigranular membrane lifting and granule enlargement are early morphological changes associated with mast cell exocytosis and histamine release (Bloom & Haegermark, 1965; Bloom & Chakravarty, 1970; Rohlich *et al.*, 1971; Uvnas, 1982). In agreement with the above observation, we have previously proposed a mechanism by which this rapid membrane expansion could be accomplished (Chock & Chock, 1985; Chock & Schmauder-Chock, 1985). The conclusion, which led to our proposing that a *de novo* membrane assembly is an obligatory step in the mechanism of secretory granule exocytosis, was based on the following findings:

(1) Quiescent mast cell granules contain no excess membrane within them, but following stimulation to secrete histamine, membrane vesicles can be observed in association with activated granules.

(2) Purified granules, after their perigranular membranes have been removed, can still generate new bilayer membrane.

(3) New membrane vesicles have been seen fusing with the enlarging perigranular membrane in mast cells activated with detergent (Chock & Schmauder-Chock, 1985).

(4) The activated granule has been observed to triple in its perigranular membrane surface area prior to fusion with the plasma membrane (Schmauder-Chock & Chock, 1987a).

(5) A non-bilayer phospholipid pool, capable of sustaining a trebling of the granule surface area, has been localized in the quiescent mast cell granule (Chock & Schmauder-Chock, 1987, 1989). This phospholipid pool also serves as the source of arachidonic acid needed for the production of prostaglandins and other eicosanoids during exocytosis (Chock & Schmauder-Chock, 1987, 1988; Schmauder-Chock & Chock, 1989).

In order to find out if *de novo* membrane assembly also occurs in the normal physiological mechanism of histamine release, we have now examined the rapid granule changes following an antigen challenge of presensitized mast cells.

Physiologically, the production of immunoglobulin E (IgE) antibodies in response to antigen (e.g. allergens) exposure is the cause of immediate hypersensitivity. The binding of these resulting antibodies to the mast cell surface IgE receptors renders the mast cell sensitive to the antigen (Ishizaka *et al.*, 1970). Challenge of presensitized mast cells with their specific antigen will trigger granule exocytosis and result in the release of histamine. By presensitizing rat peritoneal mast cells with a monoclonal IgE antibody against DNP, and then challenging them with a multivalent DNP antigen, we also found the presence of excess membrane within the activated granules. Since this excess membrane and also that which has been shown in the detergent-activated mast cell are the result of a new assembly, we concluded that *de novo* membrane generation must also occur in the normal IgE receptor-mediated mast cell secretory granule exocytosis. This, in turn, suggests that new membrane assembly may be an inherent step in the mechanism of secretory granule exocytosis.

Materials and methods

Male Sprague-Dawley rats (350–500 g) were either obtained from the NIH animal facility or from NIH animal contract suppliers. Peritoneal lavages were performed after the animals had been killed by carbon dioxide inhalation. A 20 ml cold Hank's balanced salt solution (HBSS, Gibco) containing 0.1% bovine serum albumin was injected into the peritoneal cavity and drained through an incision several minutes later. A fraction, enriched in mast cells, was obtained from the 30 xg, 10 min low speed centrifugation of the combined peritoneal lavages. Passive sensitization against 2,4-dinitrophenol (DNP) epitopes was based primarily on the original procedure of Ishizaka *et al.* (1985). After one wash with calcium-free HBSS, the cell suspension was incubated for one hour at 20°C in the presence of 100 μg ml $^{-1}$ anti-DNP monoclonal IgE antibody to saturate the surface IgE receptors. Unbound antibodies were removed by three subsequent washings of the 35 xg 10 min centrifugation pellets: twice with calcium-free HBSS and once with normal HBSS. After resuspension in HBSS, the sensitized mast cells were challenged with the multivalent antigen DNP cross-linked to human serum albumin (DNP$_{21}$-HSA). After a 45 sec incubation in the presence of 0.6 μg ml^{-1} DNP$_{21}$-HSA at 20°C, the reaction was terminated by adding an equal volume solution of 4% glutaraldehyde, 4 mM MgCl$_2$ in 100 mM sodium cacodylate, pH 7. After 30 min at room temperature, the cells were quickly washed twice with the fixative buffer containing no glutaraldehyde, using a Beckman desktop centrifuge at 1 min each spin. The washed cells were postfixed in 1% osmium tetroxide for 30 min, dehydrated in an acetone series and embedded in Epon-812. Thin

sections were also stained with Reynold's lead citrate and uranyl acetate before examination with a Philips 400 electron microscope.

Results

Rat connective tissue mast cells, isolated by peritoneal lavage, contain a large number of secretory granules (Fig. 1). The quiescent granule is surrounded by a taut perigranular membrane which is often indiscernible due to an overwhelming electron density of the granule matrix. Rapid freezing and freeze-fracture of unstimulated mast cells also reveal the presence of very smooth and well-rounded perigranular membrane (Chandler & Heuser, 1980). Apart from the many mediators of anaphylaxis (Metcalfe *et al.*, 1981; Uvnas, 1982), we recently showed that the mast cell granule also contains a large amount of phospholipid, cholesterol, calcium, phospholipase A$_2$, cyclooxygenase and other enzymes of the arachidonic acid cascade (Chock *et al.*, 1982, 1984; Albers *et al.*, 1985; Chock & Schmauder-Chock, 1987, 1988, 1989; Schmauder-Chock & Chock, 1989). The quiescent granule is very condensed and has a specific gravity of about 1.2 (Kruger *et al.*, 1980). It contains very little or no water. The absence of an aqueous environment in the granule matrix also explains why the matrix-bound phospholipid can exist in a non-bilayer form (Chock & Schmauder-Chock, 1989). The absence of water also prevents the granule enzymes from becoming active before the granule is activated.

A process of *de novo* membrane assembly has been shown to occur (Chock & Chock, 1985; Chock & Schmauder-Chock, 1985) in mast cell granules activated by a detergent. Assembly of the new membrane must have been triggered by an influx of cellular water into the activated granule, which causes a spontaneous sequestration and coalescence of granule-stored phospholipid into membrane vesicles. Fusion of these newly assembled vesicles into the perigranular membrane explains how the perigranular membrane of the activated granule can rapidly enlarge prior to fusion with the plasma membrane (Chock & Schmauder-Chock, 1985, 1989). For the IgE receptor-mediated granule exocytosis, evidence which suggests the occurrence of a similar process can also be observed (Fig. 2).

In Fig. 3, views A–G represent high magnification of areas labelled A–G respectively in Fig. 2. Evidence of excess membrane, frequently in the form of vesicles, is found within granules in the early stages of activation when the granule matrices are still quite electron dense (Fig. 3B, E, F, and G), as well as in granules which have decondensed and become reticular in appearance (Fig. 3A, C and D). Many vesicles are seen to contain matrix material. In Fig. 3A, the matrix material contained within the enclosing membrane.
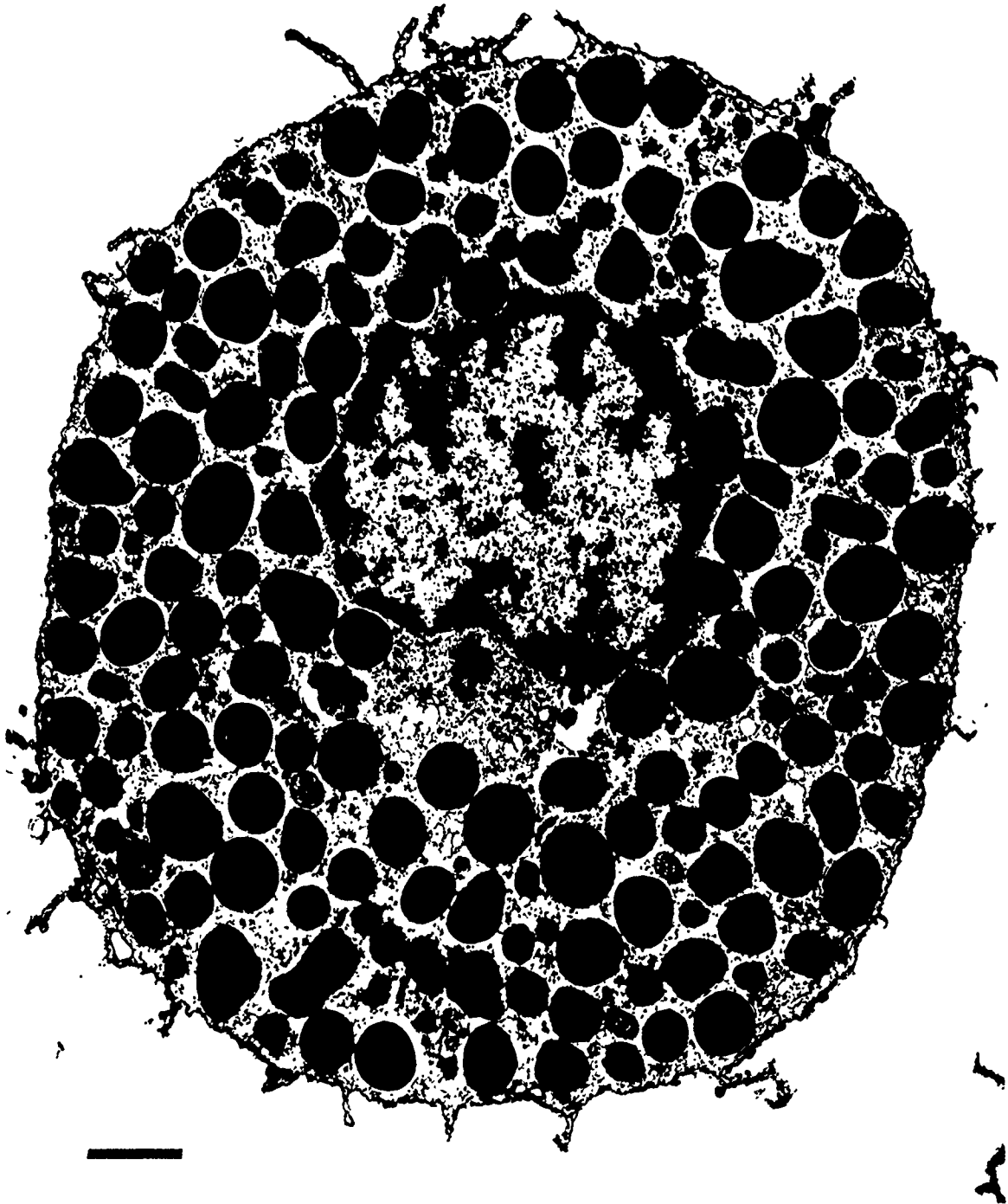
Fig. 1. Unstimulated mast cell. Rat peritoneal mast cells isolated by peritoneal lavage, showing amorphous, electron-dense, membrane-delimited secretory granules. The bar at the lower left corner represents 1 μm

('large vesicle') might have spontaneously assembled into small vesicles in response to a water influx into the enclosing membrane. Some of the enclosed vesicles are as small as 23 nm in outer diameter. Vesicles of around 25 nm in diameter are frequently seen in decondensing granules.

Figure 4A shows a section of a cell in its early stage of activation, most of its granules are still electron dense.

However, many of the perigranular membranes have already lifted away from their matrices. Close observation of selected areas, labelled b-h, can be seen under high magnification (Fig. 4 B-H respectively) to contain newly assembled membrane vesicles (arrows). Of particular interest is the chain of granules in a line from the plasma membrane to the nucleus (labelled h, g, f and e in Fig. 4A). Under high magnification, their

Fig. 2. IgE receptor-mediated mast cell activation. Presensitized mast cells 45 sec after specific antigen challenge show gross transformation of their secretory granules. The areas marked A–G correspond to areas shown at high magnification in Fig. 3. Perigranular membrane lifting and granule matrix dispersion are apparent in several granules throughout the stimulated cell. The bar at the lower left corner represents 1 µm.

fusion with each other becomes apparent (Fig. 4 E–H), and the presence of new membrane vesicles (arrows) at the sites of fusion may suggest their fusogenic role in this case. If the fusion of these granules with each other occurs before their fusion with the plasma membrane (pore formation), this would result in the

formation of a membrane-lined common vacuole. Subsequent fusion of this vacuole with the plasma membrane will result in the formation of a deep channel open to the outside and simultaneous exteriorization of many granule matrices.

Figure 5 shows two different activated granules in
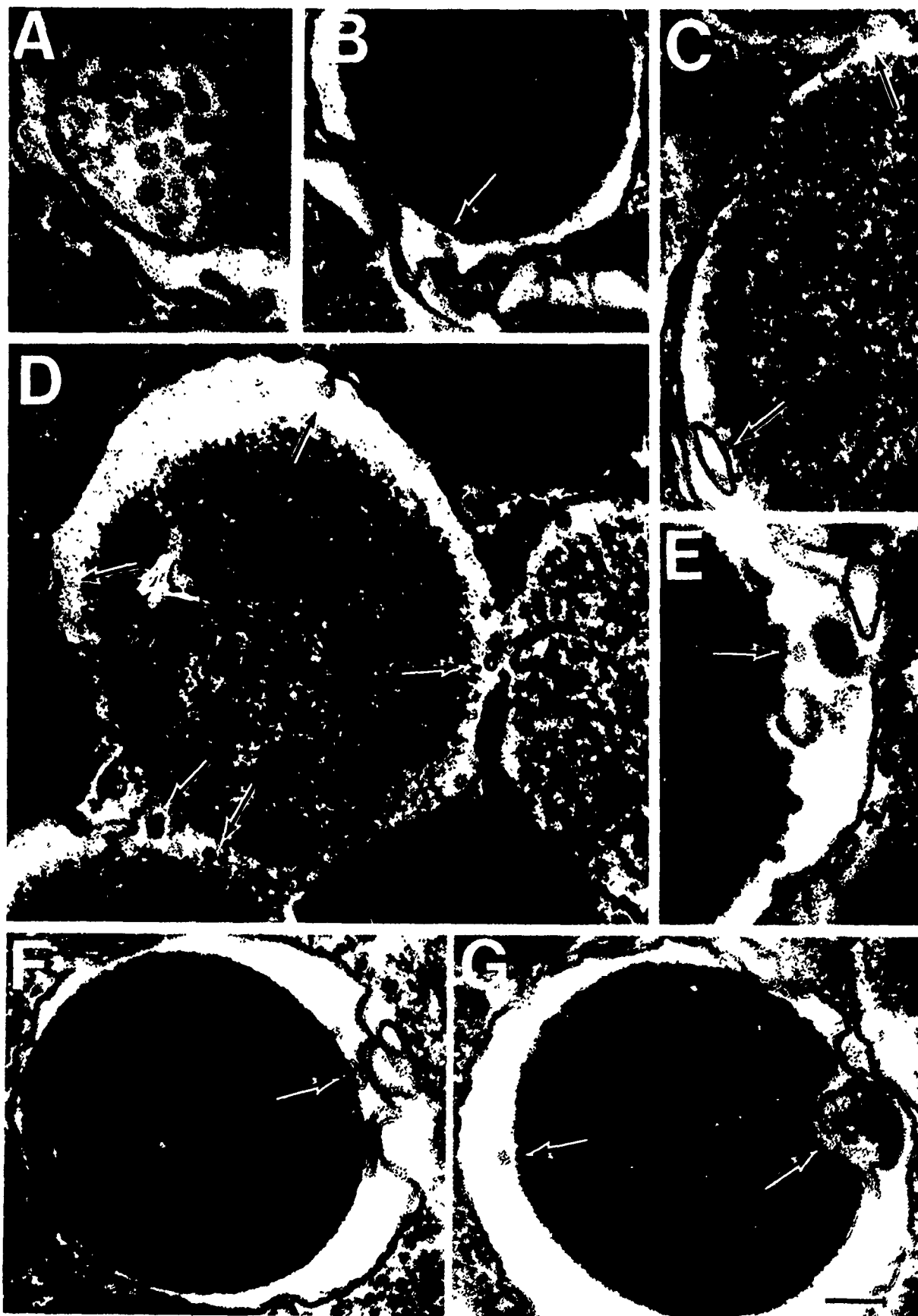
Fig. 3. High magnification of activated granules reveals the presense of new membranes of varying size and shape at the space between the lifted perigranular membrane and granule matrix. In (A), small vesicles, some as small as 23–25 nm in diameter, appear to have formed from matrix components enclosed within the delimiting vesicles in response to a water influx. In (B–G) membranes of varying size and shape (arrows) are seen within the activated granules. The bar at the lower right corner represents 0.1 μm when applied to the images in (B) (C) (E) (F) and (G). The same bar, when applied to the images in (A) and (F) is equivalent to 0.06 and 0.12 μm respectively.
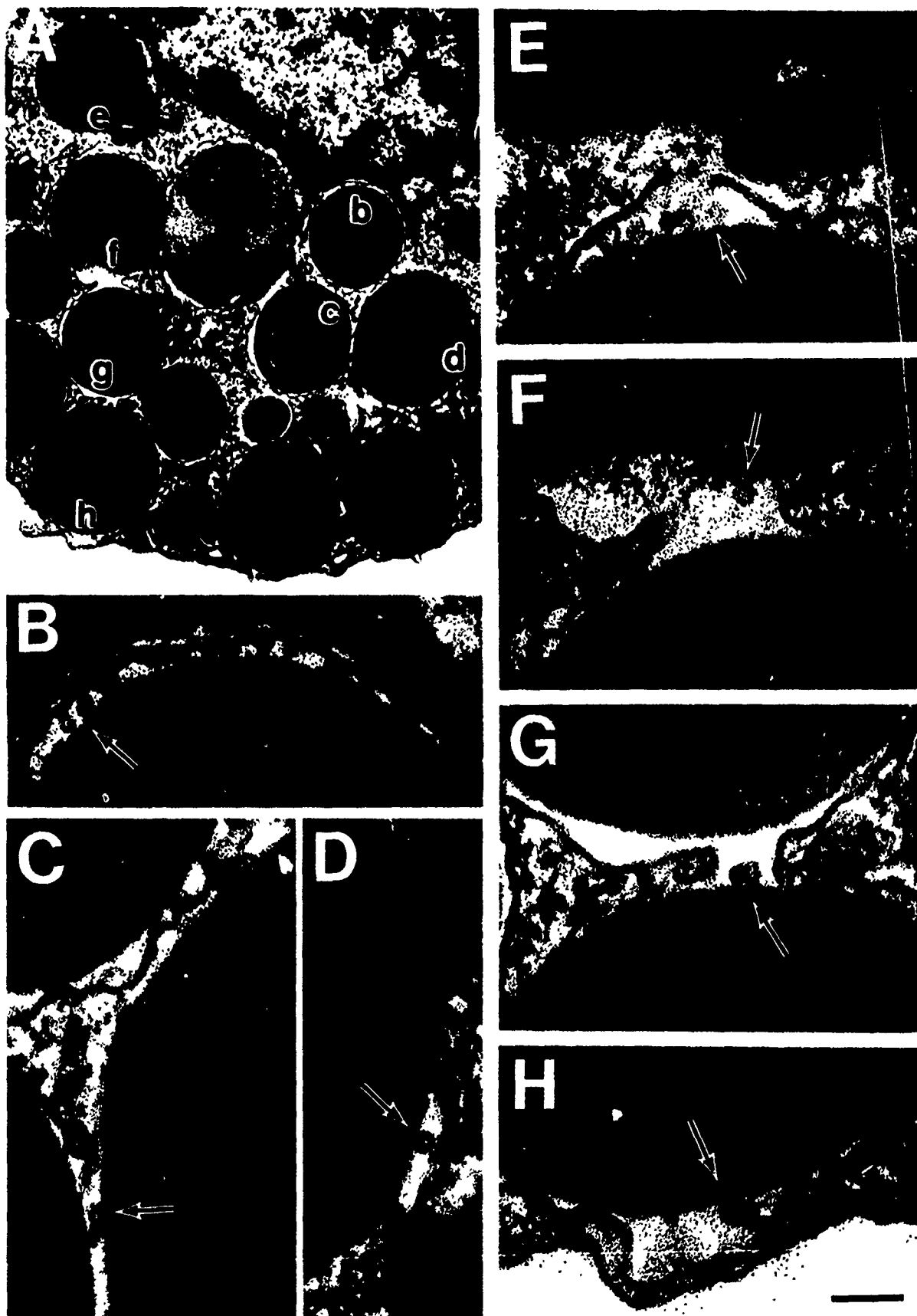
Fig. 4. New membrane vesicles and their presence at the sites of granule fusion during the formation of a membranelined common vacuole. A low magnification image of an antigen-challenged mast cell, showing granules at an early stage of activation A. Areas designated as b–h in (A) are shown under high magnification in (B–H) respectively. Small vesicles (arrows) are shown in subperigranular membrane space in (B–H). Four granules in a line, from the plasma membrane to the nucleus (h, g, f, and e in A) have fused into a connecting channel to form a common vacuole. At the sites of intergranular fusion (E, F and G), new vesicles can also be seen (arrows). The bar at the lower right corner represents 0.49 μm when applied to the image in A, and equals 0.1 μm when applied to the images in (B–H.)

the process of decondensation, at high magnification. Evidence that a new membrane assembly has already occurred is seen in the many membrane vesicles found between the lifting perigranular membrane and granule matrix of each granule. In Fig. 5A, the process of vesicle generation seems to give the impression that they are oozing out of the matrix like soap bubbles. The fact that some of the vesicles (arrowhead) can be assembled deep within the granule matrix suggests that water can penetrate deep into the granule matrix during the process of decondensation. The loosening of the matrix structure can be clearly seen as it takes on a dappled appearance (Fig. 5B). The progression of the membrane assembly process is disguised by the density of matrix which is still osmophilic. It should be noted that many of the newly formed vesicles appear to contain some matrix components. Therefore, fusion of these vesicles into the perigranular membrane would result in ejection of granule matrix materials into the cytoplasm of the activated cell (Chock & Schmauder-Chock, 1989, 1990; Schmauder-Chock & Chock, 1987b).

Discussion

It has been established that the perigranular membrane of an activated granule can enlarge prior to matrix decondensation (Bloom et al., 1965, 1967; Rohlich et al., 1971; Uvnas, 1982). A trebling of the perigranular membrane surface area prior to fusion with the plasma membrane has been seen in granules of mast cells activated by the compound A23187 (Schmauder-Chock & Chock, 1987a). Extensive perigranular membrane enlargement has also been observed for the IgE receptor-mediated mast cell stimulation. An activated granule with an enlarged perigranular membrane equivalent to a surface area increase of about 40% can be seen in Fig. 5A. Since membrane bilayer cannot stretch beyond 2–3% of its original surface area (Kwok & Evans, 1981), and exocytosis is a membrane-delimited event (Palade, 1975), this tremendous enlargement of the perigranular membrane of an activated granule requires the addition of membrane from another source. Since formation of new membrane vesicles and their fusion with the activated perigranular membranes have already been observed in the detergent-activated mast cell granules (Chock & Schmauder-Chock, 1985), it can be inferred that the same process of de novo membrane generation must also have occurred in the IgE receptor-mediated granule exocytosis as observed here.

Several authors have described the presence of various membranous structures in association with activated granules of the mast cell (Lagunoff, 1973; Lawson et al., 1977; Kruger et al., 1980; Lawson, 1980). However, they attributed their observations to a fixation artefact. By using rapid freezing and freeze-

substitution, we have previously demonstrated that the mast cell granule does, indeed, have the potential to generate new membrane. This de novo membrane assembly process was captured in mast cell granules activated by detergent. The fact that a similar process also occurs in the IgE receptor-mediated granule exocytosis, as shown here, further supports our contention that de novo membrane assembly is an integral step in the mechanism of mast cell granule exocytosis. Whether such a process can be a common step in the mechanism of exocytosis in general, cannot yet be answered until more secretory systems are investigated.

However, membrane-like structures have been observed in activated platelet granules, which after stimulation, also secrete a phospholipid-derived clotting factor (Fonio, 1951; White & Krivit, 1966; Marcus et al., 1969). The extensive vesiculation of eosinophil granules following activation by compound A23187, reported by Henderson and Chi (1985), can also be thought of as evidence of a new membrane assembly process similar to that occurring in the activated mast cell granule. Apart from the mast cell granule which has been shown to contain a matrix-bound phospholipid store, many other secretory granules have been suggested to contain phospholipid or lipid-like material. For example, those of the chromaffin cell (Blaschko et al., 1967; Mylroie & Konig, 1971; Helle, 1973), the parotid acinar cell (Simson et al., 1973), the thymus gland cells (Curtis et al., 1979), the prostate gland cells (Kanwar & Kansal, 1980), and the poison gland cells of the centipede (Nagpal & Kanwar, 1981). The possibility that these granule phospholipid stores may also serve as the potential reservoirs for de novo membrane generation during the activation of their respective secretory systems should be investigated.

It should be pointed out that many of the newly assembled vesicles observed here (Figs 3–5), with diameters in the range of 23–25 nm, are similar in size to the unilamellar vesicles formed in vitro by exhaustive sonication of phospholipids in aqueous media (Huang, 1969; Sheetz & Chan, 1972). Small vesicles with diameters less than 40 nm have been shown to be highly unstable and fusogenic below their gel to liquid-crystalline phase transition temperature (Lichtenberg et al., 1981). Their fusion is also enhanced by divalent cations such as calcium, and by the presence of an osmotic gradient across the vesicle membrane (Ohki, 1984). A similar condition conducive to membrane fusion is also believed to exist in the granule.

Due to limitation of the spatial arrangement of phospholipid molecules and geometrical constraints imposed on a minute sphere, there is a high degree of asymmetry between the outer and inner monolayers of a small vesicle. This is illustrated in Fig. 6 for a vesicle of 23 nm in diameter. Since the phospholipid molecules are assumed to be arranged in unit cells
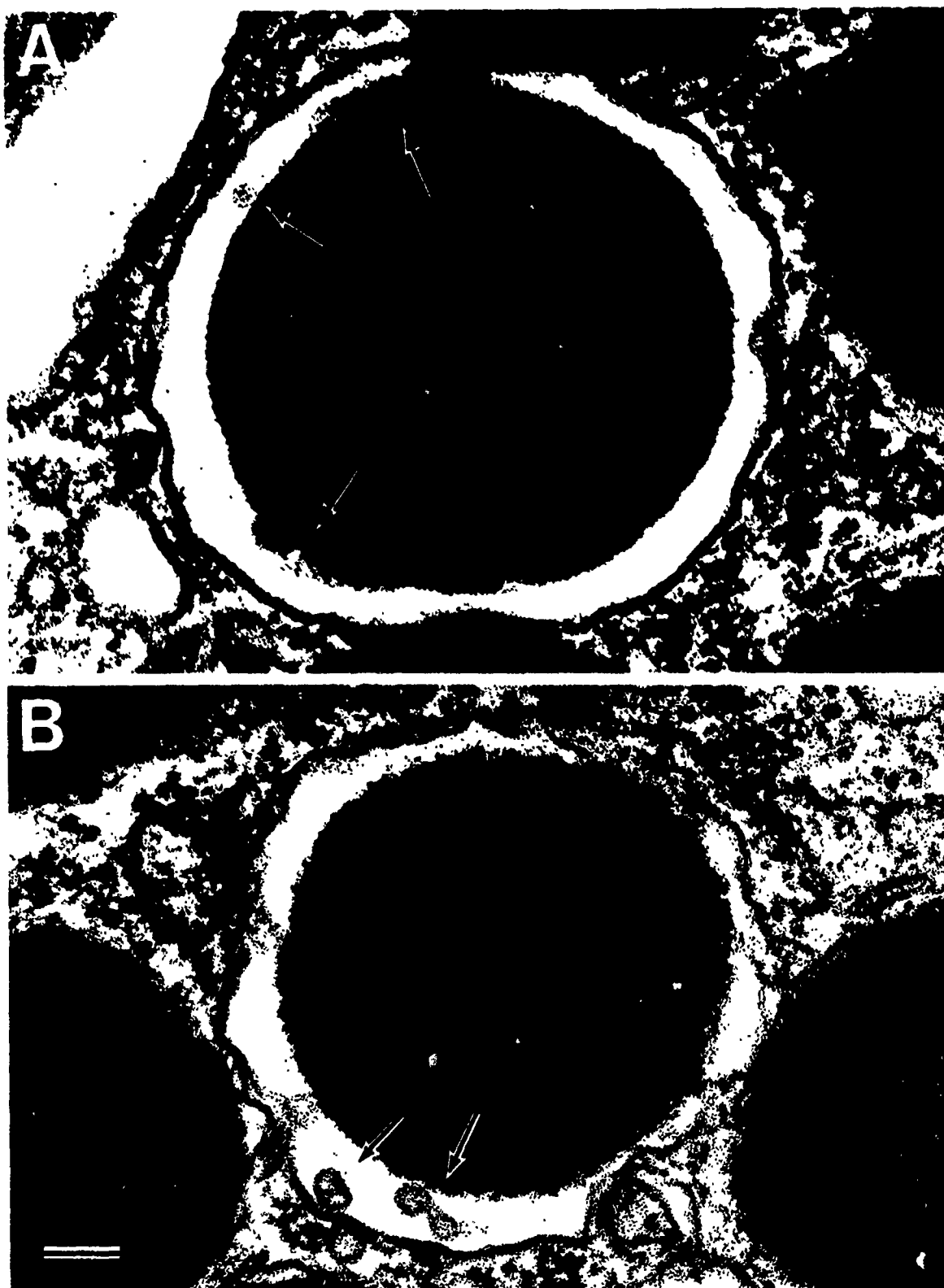
Fig. 5. Granule matrix changes during new membrane assembly. (A) Vesicles (arrows) appear to be emerging from the granule matrix like soap bubbles following activation. Many vesicles also show electron-dense material within them. Vesicles (arrowhead) also appear to be able to emerge from deep within the granule matrix, suggesting a loosening of the matrix to permit water infiltration. Comparison of the perigranular membrane with the granule matrix suggests that the granule radius has increased by about 20%. This increment in radius corresponds to about 40% increase in the perigranular membrane surface area. (B) New vesicles (arrows) appear to have fused with each other. The loosening of the matrix as a result of water infiltration, and the sequestration and coalescence of hydrophobic elements, have caused the matrix to take on a dappled appearance. The bar at the lower left corner represents 0.1 μm.
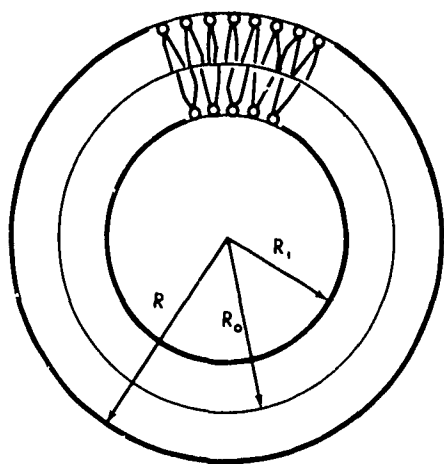
Fig. 6. Cross-section of a small vesicle showing asymmetric packing of phospholipid molecules between the inner and outer phospholipid monolayers. If the diameter of the vesicle is 23 nm, the vesicle radius, R, equals 11.5 nm. If the thickness of the bilayer is 5 nm, then R_o (= $R-2.5$ nm) = 9 nm and R_i = ($R_o-2.5$ nm) = 6.5 nm.

contained within a cone with its apex situated in the centre of the vesicle, the maximum number of molecules that can be packed into the outer monolayer and inner monolayer of this vesicle would depend on the spherical surface areas defined by the radii, R_o and R_i, respectively (Huang & Mason, 1978). If we assume a value of 5 nm for the bilayer thickness (Small, 1967), for a vesicle with a diameter of 23 nm ($R=11.5$ nm), the outer limiting radius, R_o would be equal to 9 nm (11.5 nm minus 2.5 nm); and the inner limiting radius, R_i, would be equal to 6.5 nm (9 minus 2.5 nm). If we assume that the vesicle contains only phospholipid molecules of equal dimension, an equation which defines the ratio of the number of molecules in the outer monolayer (n_o) to that in the inner monolayer (n_i) can be derived.

$$n_o/n_i = (R_o)^2/(R_i)^2 \qquad \text{Equation (1)}$$

By substituting the values of 9 nm for R_o and 6.5 nm for R_i into equation (1), it can be shown that (n_o/n_i) = 1.9. This means that for a vesicle of 23 nm in diameter, there are almost twice as many phospholipid molecules in the outer monolayer as in the inner monolayer. A value of (n_o/n_i) = 2.1 has been approximated for phospholipid vesicles of 21 nm in diameter using a method involving ^{31}P NMR (Yeagle et al., 1976). Since phospholipid molecules cannot readily diffuse from one monolayer into the opposite monolayer, a phenomenon known as 'flip-flop' (Rothman & Lenard, 1977), the fusion of a small vesicle into a planar bilayer may result in the temporary appearance of a small surface curvature or 'bulge' in the planar membrane. This phenomenon might have been observed in the images of perigranular membrane cross-sections (Fig. 4B and C), where the large number of membrane

curvatures or 'kinks' may reflect the insertion of many vesicles.

The biochemical mechanism of how cross-linking of mast cell surface receptor-bound IgE by its specific antigen can trigger the release of histamine, has been studied by T. and K. Ishizaka and their colleagues (T. Ishizaka,1982; Kagey-Sobotka et al., 1982; Metzger et al., 1982; K. Ishizaka, 1985). However, it is still unclear how the receptor-mediated signal transduction can result in the activation of secretory granules throughout the cell. Since spontaneous sequestration and coalescence of phospholipid into the membrane bilayer requires the presence of water, we have proposed earlier that one of the results of signal transduction in the stimulus-secretion coupling process must be the initiation of water influx into the target secretory granules (Chock & Chock, 1985). At the onset of water influx, the matrix-bound phospholipid and other membrane components situated directly under the perigranular membrane are immediately sequestered into bilayer vesicles. Their fusion with the perigranular membrane results in rapid lifting and expansion of the perigranular membrane away from the granule matrix. Since secretory granules have never been seen to migrate rapidly within the filament-filled cytoplasm, or to undergo Brownian movement, a rapid enlargement of the perigranular membrane would provide the necessary mechanism by which an activated granule can achieve contact with the plasma membrane in order that fusion and pore formation can occur.

A graphic representation of such a process is summarized in Fig. 7. This simple scheme may explain how a dense quiescent granule, following activation to secrete histamine, can progressively enlarge prior to fusion with the plasma membrane. The process of new membrane assembly (Fig. 7, stage I) involves the spontaneous sequestration and coalescence of matrix-stored phospholipid and other membrane precursor elements into membrane vesicles. Rapid fusion of these de novo generated vesicles with the perigranular membrane results in enlargement of the perigranular membrane. Since this spontaneous membrane assembly process can also result in incorporation of matrix materials in the new vesicles, their fusion with the perigranular membrane will also result in extrusion of some granule matrix content into the cytoplasm (Schmauder-Chock & Chock, 1987b, Chock & Schmauder-Chock, 1989). In conjunction with this membrane assembly, the granule matrix begins to decondense and sometimes take on a dappled appearance, as shown in Fig. 5B. Subsequently, the expanding perigranular membrane comes into contact with the plasma membrane and their fusion results in pore formation (Fig. 7, stage II). If the expanding perigranular membrane comes into contact with neighbouring granules, their fusion will result in the formation of a
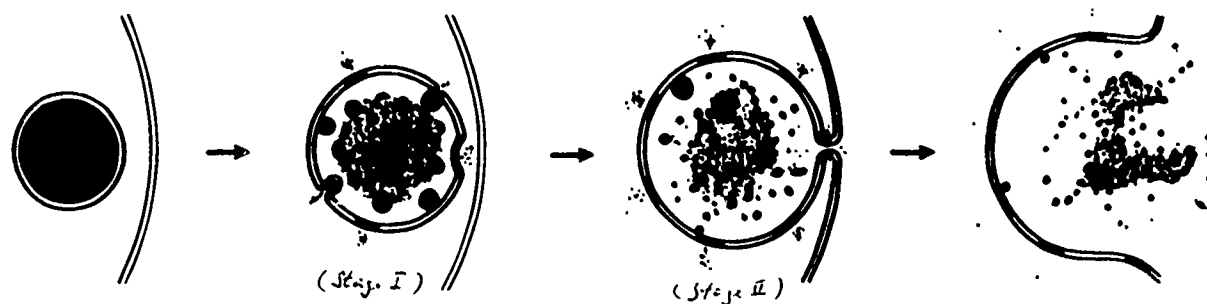
Fig. 7. A two-stage fusion model for exocytosis. The figures from left to right depict the progression of granule exocytosis. Activation of a dense, quiescent granule near the plasma membrane results in an influx of cellular water into the granule. The entry of water causes spontaneous sequestration and coalescence of the matrix-bound phospholipid and other membrane precursors into membrane vesicles (stage I). The influx of water also initiates the granule activation process. Rapid fusion of the newly assembled vesicles (represented by shaded bilayer) into the perigranular membrane results in the enlargement of the perigranular membrane. Since the *de novo* generated vesicles may contain some matrix materials, their fusion with the perigranular membrane can also result in the ejection of granule contents into the cytoplasm. When the expanding perigranular membrane comes into contact with the plasma membrane, their fusion results in pore formation (stage II). Following pore formation, the granule matrix can rapidly unravel and disperse.

membrane-lined common vacuole (Fig. 4), as in compound exocytosis. Fusion of this vacuole with the plasma membrane will result in extrusion of multiple granule matrices. This may be the mechanism by which granules situated deep within the cytoplasm can be exteriorized.

The process of spontaneous membrane assembly postulated here requires no chemical reaction. It is a mere physical phenomenon driven by free energy and entropy which is typical of the interaction between amphipathic molecules and water (Danielli & Davson, 1935; Frank & Evans, 1945; Tanford, 1980). The spontaneity and rapidity of such a process is reflected in the ease with which bilayer membrane can be made *in vitro* (Langmuir & Waugh, 1938; Mueller *et al.*, 1962; Andreoli, 1974). The involvement of an entropy-driven spontaneous process in the mechanism of exocytosis would explain why secretion can occur within seconds of activation (Douglas, 1974; Plattner *et al.*, 1984). The varying sizes and shapes of the new membranes, as seen here for the activated mast cell granules, not only reflect the fluid character of the biological membrane but also the randomness of the spontaneous process.

Conclusion

By invoking the normal physiological cascade involved in the triggering of the anaphylactic reaction, we have observed evidence which strongly suggests the occurrence of a *de novo* membrane assembly process in the mechanism of mast cell granule exocytosis. Mobilization of this process, following antigen challenge of presensitized mast cells, enables tne perigranular membrane of the activated granule to enlarge and fuse with the plasma membrane, forming a pore through which histamine and other mediators of inflammation can be exteriorized. This finding also

explains why activated granules of stimulated mast cells have been reported to undergo 'swelling' (enlargement), and to contain extra membrane in conjunction with histamine release. This observation, together with those reported in mast cells stimulated by a detergent and by compound A23187, supports our hypothesis that a spontaneous process of new membrane assembly occurs in the mechanism of secretory granule exocytosis. Since the site of new membrane assembly is in the secretory granule where preformed membrane precursors are stored (Chock & Schmauder-Chock, 1989), it seems that this process involves a mechanism different from that believed to take place on the smooth endoplasmic reticulum where phospholipid synthesis is coupled to the process of membrane assembly (Wilgram & Kennedy, 1963; Alberts *et al.*, 1983). The underlying mechanism of a granule exocytosis-initiated membrane assembly might involve a combination of spontaneous free energy and entropy changes associated with the mixing of amphipathic molecules with water. The important role that water plays in this membrane assembly process cannot be over-emphasized in view of the fact that most, if not all, biological processes (including enzyme reactions, protein synthesis, nucleic acids synthesis, lipid synthesis, as well as the assembly and disassembly of biologically macromolecules) require the participation of water molecules at some point or other; furthermore, such processes take place in a mostly aqueous cellular medium.

References

ALBERS, R. W., CHOCK, E. S., DONLON, M. A., & CHOCK, S. P. (1985) Localization of calmodulin in the mast cell granules. Fed. Proc. 44, 984 (abstr. 3353).

ALBERTS, B., BRAY, D., LEWIS, J., RAFF, M., ROBERTS, K. & WATSON, J. D. (1983) Molecular biology of the cell. p. 350. New York and London: Garland Publishing Inc.

ANDREOLI, T. E. (1974) Planar lipid bilayer membranes. In Methods in Enzymology (edited by FLEISCHER, S. & PACKER A.) Vol. 32, pp. 513–7. New York: Academic Press.

BLASCHKO, H., FIREMARK, H., SMITH, A. D. & WINKLER, H. (1967) Lipids of the adrenal medulla. Lysolecithin, a characteristic constituent of chromaffin granules. Biochem. J. 104, 545–9.

BLOOM, G. D. & HAEGERMARK, O. (1965) A study on morphological changes and histamine release induced by compound 48/80 in rat peritoneal mast cells. Exptl. Cell Res. 40, 637–54.

BLOOM, G. D. & CHAKRAVARTY, N. (1970) Time course of anaphylactic histamine release and morphological changes in rat peritoneal mast cells. Acta Physiol. Scand. 78, 410–9.

BLOOM, G. D., FREDHOLM, B. & HAEGERMARK, O. (1967) Studies on the time course of histamine release and morphological changes induced by histamine liberators in rat peritoneal mast cells. Acta. Physiol, Scand. 71, 270–82.

CHANDLER, D. E. & HEUSER, J. E. (1980) Arrest of membrane fusion events in mast cells by quick-freezing. J. Cell Biol. 86, 666–74.

CHOCK, E. S., DONLON, M. A., FIORI, C. E. & CATRAVAS, G. N. (1982) Elemental analysis for calcium in rat peritoneal mast cell granules. J. Cell Biol. 95, 409a.

CHOCK, S. P., DONLON, M. A. & CHOCK, E. S. (1984) Localization of calmodulin in the mast cell granules. Fed. Proc. 43, 1934 (abstr. 3026).

CHOCK, S. P. & CHOCK, E. S. (1985) A two-stage fusion model for secretion. Fed. Proc. 44, 1324 (abstr. 5341).

CHOCK, S. P. & SCHMAUDER-CHOCK, E. A. (1985) Evidence of de novo membrane generation in the mechanism of mast cell secretory granule activation. Biochem. Biophys. Res. Commun. 132, 134–9.

CHOCK, S. P. & SCHMAUDER-CHOCK, E. (1987) The mast cell granules: A phospholipid source for prostaglandins synthesis. In Prostaglandins and Lipid Metabolism in Radiation Injury (edited by WALDEN, T. L. & HUGHES H. N.), pp. 127–32. New York: Plenum Press.

CHOCK, S. P. & SCHMAUDER-CHOCK, E. A. (1988) Synthesis of prostaglandins and eicosanoids by the mast cell secretory granule. Biochem. Biophys. Res. Commun. 156, 1308–15.

CHOCK, S. P. & SCHMAUDER-CHOCK, E. A. (1989) Phospholipid storage in the secretory granule of the mast cell. J. Biol. Chem. 264, 2862–8.

CHOCK, S. P. & SCHMAUDER-CHOCK, E. A. (1990) Mini-review. A new model for the mechanism of stimulus-secretion coupling. Biofactors (in press).

CURTIS, S. K., COWDEN, R. R. & NAGEL, J. W. (1979) Ultrastructural and histochemical features of the thymus glands of the adult lungless salamander, Plethodon glutinosus (Caudata: Plethodontidae). J. Morphol. 160, 241–74.

DANIELLI, J. F. & DAVSON, H. (1935) A contribution to the theory of permeability of thin films. J. Cell. Comp. Physiol. 5, 495–508.

DOUGLAS, W. W. (1974) Involvement of calcium in exocytosis and exocytosis-vesiculation sequence. Biochem. Soc. Symp. 39, 1–28.

FONIO, A. (1951) Uber das funktionelle verhalten der isolierten Strukturelements der Thrombocyten, des Hyalomers und des Granulomers. Acta Haemat. 6, 207–12.

FRANK, H.S. & EVANS, M. W. (1945) Free volume and entropy in condensed systems. III. Entropy in binary liquid mixtures; partial molal entropy in dilute solutions; structure and thermodynamics in aqueous electrolytes. J. Chem. Phys. 13, 507–32.

HELLE, K. B. (1973) Biochemical studies of the chromaffin granule. III. Redistribution of lipid phosphate, dopamine-beta-hydroxylase and chromogranin A after freezing and thawing of the isolated granule membranes. Biochim. Biophys. Acta 318, 167–80.

HENDERSON, W. R. & CHI, E. Y. (1985) Ultrastructural characterization and morphometric analysis of human eosinophil degranulation. J. Cell Sci. 73, 33–48.

HUANG, C. (1969) Studies on phosphatidylcholine vesicles. Formation and physical characteristics. Biochemistry 8, 344–52.

HUANG, C. & MASON, J. T. (1978) Geometric packing constraints in egg phosphatidylcholine vesicles. Proc. Natl. Acad. Sci. USA 75, 308–10.

ISHIZAKA, K. (1985) Twenty years with IgE: From the identification of IgE to regulatory factors for the IgE response. J. Immunol. 135(1), i–x.

ISHIZAKA, K., TOMIOKA, H. & ISHIZAKA, T. (1970) Mechanism of passive sensitization. I. Presense of IgE and IgG molecules on human leukocytes. J. Immunol. 105, 1459–67.

ISHIZAKA, T. (1982) Biochemical analysis of triggering signals induced by bridging of IgE receptors. Fed. Proc. 41, 17–21.

ISHIZAKA, T., STERK, A. R., DAERON, M., BECKER, E. L. & ISHIZAKA, K. (1985) Biochemical analysis of desensitization of mouse mast cells. J. Immunol. 135, 492–501.

KAGEY-SOBOTKA, A., MacGLASHEN, D. W. & LICHTENSTEIN, L. M. (1982) Role of receptor aggregation in triggering IgE-mediated reactions. Fed. Proc. 41, 12–7.

KANWAR, U. & KANSAL, M. (1980) Cytochemical studies on the prostate glands of the trematodes, Paramphistomum epiclitum and Paradistomoides orientalis. J. Helminthol. 54, 263–6.

KRUGER, P. G., LAGUNOFF, D. & WAN, H. (1980) Isolation of rat mast cell granules with intact membranes. Exp. Cell. Res. 129, 83–93.

KOWK, R. & EVANS, E. (1981) Thermoelasticity of large lecithin bilayer membrane vesicles. Biophys. J. 35, 637–52.

LAGUNOFF, D. (1973) Membrane fusion during mast cell secretion. J. Cell Biol. 57, 252–9.

LANGMUIR, I. & WAUCH, E. F. (1938) The adsorption of proteins at oil-water interfaces and artificial protein-lipoid membranes. *J. Gen. Physiol.* **21**, 745–55.

LAWSON, D. (1980) Rat peritoneal mast cells: a model system for studying membrane fusion. *Membrane-Membrane Interactions* (edited by GILULA, N. B.), pp. 27–44. New York: Raven Press.

LAWSON, D., RAFF, M. C., GOMPERTS, B., FEWTRELL, C. & GILULA, N. B. (1977) Molecular events during membrane fusion. *J. Cell Biol.* **72**, 242–59.

LICHTENBERG, D., FREIRE, E., SCHMIDT, C. F., BARENHOLZ, Y., FELGNER, P. L. & THOMPSON, T. E. (1981) Effect of surface curvature on stability, thermodynamic behavior, and osmotic activity of dipalmitoylphosphatidylcholine single lamellar vesicles. *Biochemistry* **20**, 3462–67.

MARCUS, A. J., ULMAN, H. L. & SAFIER, L. B. (1969) Lipid composition of subcellular particles of human blood platelets. *J. Lipid Res.* **10**, 108–14.

METCALFE, D. D., KALINER, M., & DONLON, M. A. (1981) The mast cell. *CRC Crit. Rev. Immunol.* **3**, 23–74.

METZGER, H., GOETZE, A., KANELIOPOULOS, J., HOLOWKA, D. & FEWTRELL, C. (1982) Nature of the high-affinity mast cell receptor for IgE. *Fed. Proc.* **41**, 8–11.

MEULLER, P. O., RUDIN, D. O, TI TIEN, H. & WESCOTT, W. C. (1962) Reconstitution of excitable cell membrane structure in vitro. *Circulation* **26**, 1167–70.

MYLROIE, R. & KONIG, H. (1971) Soluble acidic lipoprotein components of adrenomedullary chromaffin granules. Relations to chromagranins. *FEBS Let.* **12**, 121–4.

NAGPAL, N. & KANWAR, U. (1981) The poison gland in the centipede *Otostigmus Ceylonicus*: Morphology and cytochemistry. *Toxicon* **19**, 898–901.

OHKI, S. (1984) Effects of divalent cations, temperature, osmotic pressure gradient, and vesicle curvature on phosphatidylserine vesicle fusion. *J. Membrane Biol.* **77**, 265–75.

PALADE, G. (1975) Intracellular aspects of the process of protein synthesis. *Science* **189**, 347–58.

PLATTNER, H., MATT, H., KERSKEN, H., HAACKE, B. & STURZL, R. (1984) Synchronous exocytosis in *Paramecium* cells. I. A novel approach. *Exp. Cell Res.* **151**, 6–13.

ROHLICH, P., ANDERSON, P. & UVNAS, B. (1971) Electron microscope observations on compound 48/80-induced degranulation in rat mast cells. *J. Cell Biol.* **51**, 465–83.

ROTHMAN, J. E. & LENARD, J. (1977) Membrane asymmetry. *Science* **195**, 743–53.

SCHMAUDER-CHOCK, E. A. & CHOCK, S. P. (1987a) Mechanism of secretory granule exocytosis: Can granule enlargement precede pore formation? *Histochem. J.* **19**, 413–8.

SCHMAUDER-CHOCK, E. A. & CHOCK, S. P. (1987b) New membrane assembly during exocytosis. *Proceedings of the 45th Annual Meeting of the Electron Microscopy Society of America* (edited by BAILEY, G. W.), pp. 782–3. San Francisco: San Francisco Press.

SCHMAUDER-CHOCK, E. A. & CHOCK, S. P. (1989) The localization of cyclo-oxygenase and prostaglandin E_2 in the secretory granule of the mast cell. *J. Histochem. Cytochem.* **37**, 1319–28.

SHEETZ, M. P. & CHAN, S. I. (1972) Effect of sonication on the structure of lecithin bilayers. *Biochemistry* **11**, 4573–81.

SIMSON, J. A. V., HALL, B. J. & SPICER, S. S. (1973) Histochemical evidence for lipoidal material in secretory granules of rat salivary glands. *Histochem. J.* **5**, 239–54.

SMALL, D. M. (1967) Phase equilibria and structure of dry and hydrated egg lecithin. *J. Lipid Res.* **8**, 551–7.

TANFORD, C. (1980) *The hydrophobic effect: Formation of micelles and biological membranes.* 2nd edn. pp. 1–127. New York: John Wiley & Sons, Inc.

UVNAS, B. (1982) Mast Cell Granules. *The Secretory Granules* (edited by POISNER, A. M. & TRIFARO, J. M.), pp. 357–84. Amsterdam: Elsevier Biomedical Press.

WHITE, J. G. & KRIVIT, W. (1966) The ultrastructural localization and release of platelet lipids. *Blood* **27**, 167–86.

WILGRAM, G. F. & KENNEDY, E. P. (1963) Intracellular distribution of some enzymes catalyzing reactions in the biosynthesis of complex lipids. *J. Biol. Chem.* **238**, 2615–9.

YEAGLE, P. L., HUTTON, W. C., MARTIN, R. B., SEARS, B. & HUANG, C. (1976) Transmembrane asymmetry of vesicle lipids. *J. Biol. Chem.* **251**, 2110–12.

Linear Dichroism Characteristics of Ethidium–and Proflavine–Supercoiled DNA Complexes

CHARLES E. SWENBERG,[1] SUSAN E. CARBERRY,[2*] and NICHOLAS E. GEACINTOV[2]

[1]Radiation Biochemistry Department, Armed Forces Radiobiology Research Institute, Bethesda, Maryland 20814, and [2]Chemistry Department and Radiation and Solid State Laboratory, New York University, New York, New York 10003

SYNOPSIS

A flow linear dichroism technique is utilized to study the unwinding of supercoiled DNA induced by the binding of ethidium bromide (EB) and proflavine (PF) at different ratios r (drug added/DNA base). In the case of either EB or PF bound to linear calf thymus DNA, the reduced linear dichroism signals LD/A (LD: linear dichroism; A: absorbance, both measured at the same wavelength), determined at 258, and 520 or 462 nm (corresponding to contributions predominantly from the partially oriented DNA bases, intercalated EB, or PF, respectively) are nearly independent of drug concentration. In the case of supercoiled DNA, the magnitude of LD/A at 258 nm first increases to a maximum value near $r = 0.04$–0.05, and then decreases as r is increased further, mimicking the behavior of the sedimentation coefficients, viscosities, and gel electrophoresis patterns measured by other workers at similar values of r. However, LD/A at 520 nm, which is due to DNA-bound EB molecules, is constant within the range of r values of 0.02–0.06 in which the magnitude of LD/A determined at 258 nm due to the DNA bases exhibits a pronounced maximum. In contrast, in the case of PF, the magnitudes of LD/A determined at 258 or 462 nm are characterized by similar dependencies on r, both exhibiting pronounced maxima at $r = 0.05$; this parallel behavior is expected according to a simple intercalation model in which the DNA bases and drug molecules are stacked on top of one another, and in which both are oriented to similar extents in the flow gradient. The unexpected differences in the dependencies of $(LD/A)_{258}$ and $(LD/A)_{520}$ on r in the case of EB bound to supercoiled DNA, are attributed to differences in the net overall alignment of the EB molecules and DNA bases in the flow gradient. The magnitude of the LD signal at 258 nm reflects the overall degree of orientation of the supercoiled DNA molecules that, in turn, depends on their hydrodynamic shapes and sizes; the LD signals characterizing the bound EB molecules may reflect this orientation also, as well as the partial alignment of individual DNA segments containing bound EB molecules. The differences in the LD characteristics of the bound PF and EB molecules may be due to subtle differences in the mechanisms of binding, perhaps reflecting differences in the torsional dynamics and local rigidities in superhelical DNA [Wu et al. (1988) *Biochemistry* **27**, 8128-8144] induced by these two different intercalating agents.

INTRODUCTION

The existence of circular superhelical DNA in both eukaryotic and prokaryotic cells is well documented,

and its characteristics have been studied extensively.[1-4] Many drug molecules that form intercalation complexes with DNA, of which ethidium bromide (EB) is a classical example, are known to unwind supercoiled DNA.[5-9] Electron micrographs show that supercoiled DNA is characterized by highly twisted, compact structures, while the relaxed DNA forms are characterized by open and more extended structures.[8,10] A number of different methods, based on differences in the hydrodynamic properties

of supercoiled, partially relaxed, and relaxed DNA, have been employed to characterize the degrees of unwinding induced by drug molecules. These methods include gel electrophoresis,[9,11] sedimentation velocity,[5-8] and viscometry.[12,13]

We have recently shown[14] that supercoiled DNA can be oriented in the flow gradient of a Couette cell[15] and that changes in superhelicities induced by polycyclic aromatic drugs or carcinogens can also be monitored by linear dichroism (LD) methods. There are several advantages inherent in the LD technique for studying the unwinding and rewinding of supercoiled DNA induced by exogeneous chemicals: (1) the kinetics of unwinding or rewinding of the DNA molecules on time scales of seconds can be followed[14] by monitoring the LD signal within the DNA absorption band (< 300 nm), and (2) the LD signal can be scanned as a function of wavelength; thus, the orientation of the drug molecules causing the changes in superhelicity can be followed by monitoring the LD signal within the wavelength range of the absorption spectrum of the drug.

In this work, we explore the relationships between the LD signals (and thus the relative orientations) of the supercoiled DNA, and of two typical drug molecules, EB and proflavine (PF) (Figure 1), which cause unwinding of the DNA by an intercalation mechanism. In the case of linear calf thymus DNA, the reduced LD within the absorption bands of the DNA and the drugs is approximately the same and independent of the drug concentration. However, in the case of EB-supercoiled DNA complexes, the LD/A ratios within the DNA and drug absorption bands exhibit different dependences on the drug concentrations; this apparent anomaly, which is not apparent in the case of PF-ϕX 174 complexes, is attributed to differences in the degrees of alignment in the hydrodynamic flow gradient of the supercoiled DNA molecules as a whole, and of individual linear DNA segments containing the bound EB molecules.

MATERIALS AND METHODS

The supercoiled DNA samples (ϕX 174, SV 40, and pBR322) were purchased from Bethesda Research Laboratories (Bethesda, MD); Topoisomerase I was obtained from Applied Genetics (Freeport, NY), while EB and PF were purchased from Sigma Chemical Co. (St. Louis, MO). Calf thymus DNA (Worthington Biochemicals, Freehold, NJ) was prepared and sonicated as previously described;[16] a reduction in the average molecular weight of the DNA molecules by sonication is desirable, since the average chain length of high molecular weight native DNA is reduced in the hydrodynamic flow field in the Couette cell, thus leading to diminishing LD signals as a function of time. The purity of the supercoiled DNA samples was checked by agarose gel electrophoresis. Completely relaxed marker DNA was obtained by incubating the DNA with Topoisomerase I (1 unit/0.5 μg DNA, incubation time 30 m at 37°C). Gel electrophoresis was performed using vertical gel slabs (3 mm thick) of 1% agarose (w/v) in TEA buffer (40 mM Tris base, 5 mM sodium acetate, 1 mM EDTA, pH 8.2, 24°C). The gels were stained with EB, photographed under uv light, and the bands were quantitated by densitometry scanning. All samples contained more than 70% of the supercoiled form I DNA.

The flow LD experiments were performed using a Couette cell consisting of a stationary outer cylinder and a rotating inner cylinder, with the DNA solution placed in the annular gap between the two cylinders. The LD signal is defined as follows:

$$LD = A_{\parallel} - A_{\perp} \qquad (1)$$

In these LD measurements, the propagation direction of a linearly polarized light beam is perpendicular to the axis of rotation and parallel to the flow gradient; the LD signal is equal to the difference in
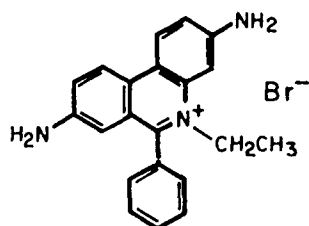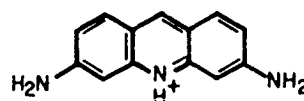
Ethidium Bromide   Proflavine

Figure 1   Structures of EB and PF.

absorbance measured with the polarization vector parallel ($A_{\parallel}$) or perpendicular ($A_{\perp}$) with respect to the direction of flow. The LD signals are a function of (1) the orientations of the transition moments with respect to the flow direction, and can therefore be either positive or negative in sign, (2) the absorption spectra of the oriented species, and (3) the degree of orientation of the macromolecules in the flowing solution. The sign of the LD signal in the absorption region of the DNA (230–300 nm) is negative in sign for both linear[15] and supercoiled[14] DNA.

For the LD experiments, the DNA samples ($7.5 \times 10^{-5}\ M$) were dissolved in 5 mM Tris buffer containing 1 mM EDTA at pH 7.9, 24°C; each LD experiment requires about 1.2 mL of solution containing a minimum of 10 μg of DNA. The details of our LD apparatus are described elsewhere.[16] Here, we briefly describe only the homebuilt Couette cell used in these experiments. The radius of the inner rotating cylinder is $R_i = 1.10$ cm, while that of the outer cylinder is $R_o = 1.15$ cm (annular gap = 0.05 cm). The inner cylinder was filled with fresh doubly distilled water, and rotated at speeds of up to 1300 rpm. The velocity gradient G was calculated from the formula[17]

$$G(\text{s}^{-1}) = \frac{2\pi R V}{(R_o - R_i)} \qquad (2)$$

where R is the mean radius [$R = (R_o + R_i)/2$], and the rotation speed V of the inner cylinder is given in revolutions per second. The velocity gradient in all experiments, unless otherwise noted, was 1840 s^{-1}. These gradients were well below the rates required for shear degradation of linear DNA molecules.[18] Indeed, subjecting the supercoiled DNA (or the sonicated calf thymus DNA) to the hydrodynamic forces in a Couette cell operating at $V = 15$ s^{-1} for at least 30 m did not cause any measurable changes in the LD signals at 258 nm.

Theoretical considerations suggest that the critical velocity gradient G_c, corresponding to the maximum rotation speed at which laminar flow characteristics should still be observed, is equal to[19,20]

$$G_c = \frac{\pi^2}{(0.057)^{1/2}} \times \frac{\rho}{\eta} \times \frac{(R)^{1/2}}{(R_o - R_i)^{5/2}} \qquad (3)$$

where ρ and η are the density and the viscosity of the solution, respectively. For $G > G_c = 800\ \text{s}^{-1}$ (G_c calculated using the dimensions of our Couette cell), Taylor instabilities[19] are expected to set in and the

flow is expected to be nonlaminar. However, the LD signals increase smoothly with increasing G up to G values of at least 3000 s^{-1} (see below), a fact that has been noted previously in the case of linear DNA.[15,21,22] Possible reasons for the apparent absence of nonlaminar flow effects at flow gradients above G_c have been briefly discussed by Lee and Davidson.[17]

In order to follow the changes in conformation of supercoiled DNA as a function of EB (or PF) concentration, small aliquots of concentrated aqueous solutions of the drugs were successfully injected into the DNA solutions, and the LD spectra were scanned after each injection from 240 to 580 nm in the case of EB, or 240 nm to 500 nm in the case of PF. The maximum volume change due to the injection of the concentrated EB solutions was at most 1.5%; these small volume changes were neglected. The monochromator scanning rate was 120 nm/m, and the response time of the signal lock-in amplifier was fixed at 300 ms in order to increase the signal/noise ratio. The concentrations of EB and PF were calculated from the known molar extinction coefficients of both drugs in the absence of DNA (5800 $M^{-1}\ \text{cm}^{-1}$ for EB at 480 nm, and 34,500 $M^{-1}\ \text{cm}^{-1}$ for PF at 445 nm).

RESULTS

Absolute Reduced LD

Typical LD signals of linear and of supercoiled DNA as a function of the velocity gradient are shown in Figure 2. The LD signals are expressed in terms of the output voltage of the lock-in signal amplifier. However, the absolute response of the apparatus was also calibrated utilizing crossed polarizers. The absolute or reduced linear dichroism LD/A, where A is the absorbance of the DNA samples at 258 nm, is about −0.14 in the case of unsonicated calf thymus DNA at $G = 3000\ \text{s}^{-1}$. This value of LD/A is similar to the values given by other workers for native double-stranded DNA.[15,23] The LD signal of the supercoiled DNA is about five times smaller under identical experimental conditions, and thus the characteristic LD/A values are only −0.03 at $G = 3000$ s^{-1}; this is an upper limit for the RF I supercoiled form, since the samples are always contaminated with nicked RF II DNA. The LD signals due to nicked circular DNA[14] or linear DNA are higher than those of supercoiled DNA.

The photosensitization of the DNA-bound drug
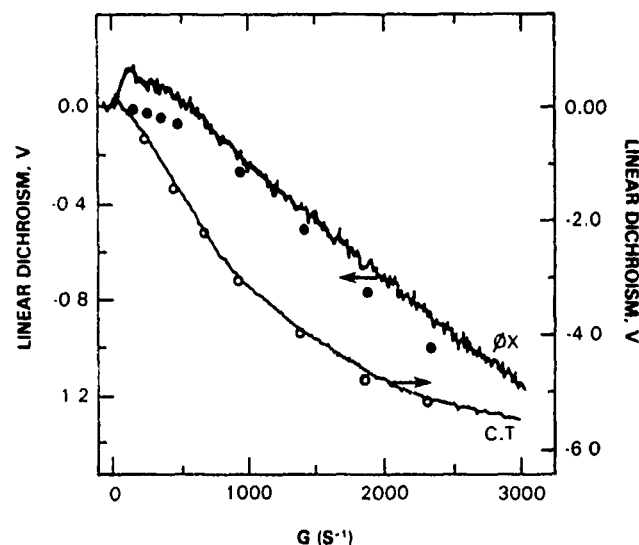
Figure 2 Relative LD signals at 258 nm (arbitrarily expressed in units of volts) of supercoiled (ϕX 174) and calf thymus (C.T.) DNA as a function of the velocity gradient G. Continuous lines: the velocity gradient was increased from zero to the maximum value at a constant rate of 750 s^{-2}; (O) calf thymus DNA, ($\bullet$) supercoiled DNA: the flow gradient was allowed to reach a preselected value and the LD signal was measured 60 s later. DNA concentration: 7.5 × 10^{-5} M.

molecules can, in principle, lead to single-strand breaks resulting in a complete relaxation of the supercoiled DNA. It was therefore verified that there were no measurable changes in the ratio of (supercoiled)/(nicked) DNA molecules during the LD experiments by both gel electrophoresis and the LD technique. Simulating the experimental illumination (and rotation) conditions even at the higher EB concentrations used in these experiments, there were no detectable changes in the ratios of (supercoiled)/(nicked) molecules detectable by the gel electrophoresis assays. As is shown below, the magnitude of the LD signal at 260 nm changes by a factor of greater than three upon complete unwinding of the supercoiled DNA; nevertheless, subjecting the EB-DNA samples to the experimental conditions of the Couette cell (including illumination) at constant EB concentrations did not cause any changes in the magnitude of the LD signals at 260 nm. Therefore, the extent of nicking of supercoiled DNA under our experimental conditions, if any, was negligible.

Dependence of LD on Velocity Gradient G

The LD signals of the DNA at 258 nm in the absence of added drugs were measured in two different ways: (1) the rotation speed was increased at a constant rate, equivalent to a rate of increase in the velocity gradient $G/\Delta t$ = 750 s^{-2}; and (2) the speed of ro-

tation was allowed to reach a steady preselected value, and then the LD signal at 258 nm was measured about 60 s after equilibrium had been reached.

In the case of linear calf thymus DNA, the LD signals were identical when measured by either method (Figure 2). In the case of the supercoiled DNA there is a significant difference between the steady-state and continuous sweep LD values; at low G values (< 500 s^{-1}), the LD signal is positive in sign in the continuous sweep case, and is close to zero in the steady-state case. Above G = 1000 s^{-1} the magnitude of the LD signals is consistently higher in the steady-state case (closed circles) than in the continuous sweep case at all values of G (Figure 2). Independent kinetic measurements show that the response time of the LD signal of supercoiled DNA is about 20–30 s (data not shown). In the case of linear DNA, the response time is less than the time required to change the rotation speed from one fixed value to another (about 5 s). The longer time response of supercoiled DNA suggests that some deformation of the molecule is occurring in the hydrodynamic force field, which leads to a better overall net alignment of the DNA bases with their planes tending to be tilted perpendicular to the flow lines.

At low values of G, the LD of supercoiled DNA is positive in sign, suggesting that at low velocity gradients the DNA bases have a weak net tendency
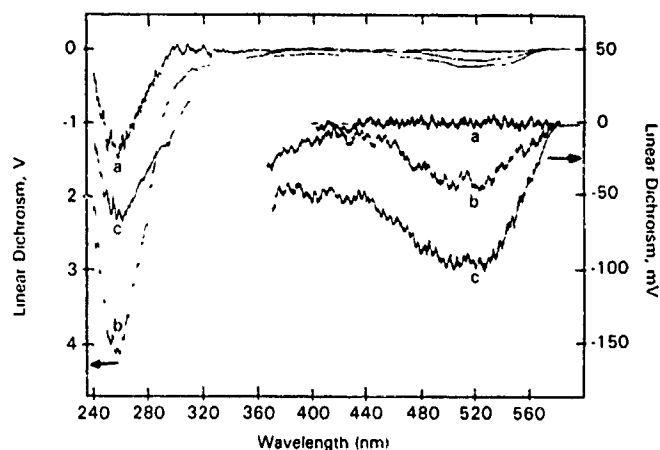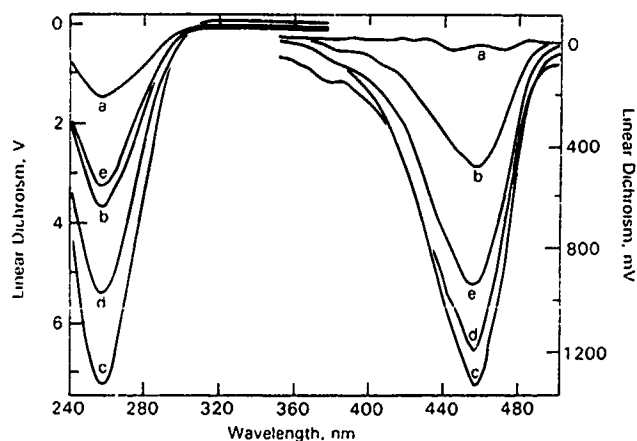
Figure 3 LD spectra of EB-ϕX 174 DNA complexes at three different values of r (moles drug added/mole nucleotide); (a) r = 0.00, (b) r = 0.04, and (c) r = 0.10. DNA concentration: 7.5 × 10^{-5} M. LD scans were performed at a rate of sweep of 120 nm/m at a constant flow gradient (G = 1840 s^{-1}).

of aligning with their planes parallel to the flow lines. A very weak initial positive LD signal at G values below 60 s^{-1} is also observed in the case of linear DNA. Norden and Seth reported that denatured DNA, in contrast to the double-stranded form, is characterized by positive LD spectra;[21] the small positive LD signals at low G values therefore could be due to minor single-stranded regions present in the DNA molecules.

LD Characteristics of EB- and PF–Supercoiled DNA Complexes

Typical LD spectra of ϕX 174 DNA without EB and at two different concentrations of EB (r = 0.04 and

0.10, where r = moles drug molecules added/mole nucleotides) are shown in Figure 3. Within the DNA absorption band (below 300 nm), the LD signal due to ϕX 174 is negative in sign and resembles the absorption spectrum in shape, as in the case of linear DNA.[15,22,23] Above 400 nm, a weak negative LD signal due to EB molecules bound to the DNA is observed. As expected for intercalated drug molecules, the sign of this LD signal is negative.[23-27] Similar LD spectra at different ratios r are shown for PF–ϕX 174 complexes in Figure 4; the negative LD band peaking at 462 nm coincides with the absorption band of PF bound to DNA[24,25] by an intercalation mechanism.[28]

Figure 4 LD spectra of PF-ϕX 174 complexes at different values of r; (a) r = 0.00, (b) r = 0.04, (c) r = 0.05, (d) r = 0.06, and (e) r = 0.10. Other conditions as in caption to Figure 3.

EB-Supercoiled DNA Complexes. The reduced LD signal at 258 nm, which is predominantly due to the net overall orientation of the DNA bases, increases in magnitude by a factor of nearly 4 as r is increased from zero to 0.04 by adding EB to either ϕX 174 DNA or SV40 DNA solutions; however, as r is increased further to a value of 0.10, LD/A diminishes. The LD/A values at 520 nm due to bound EB molecules remain approximately constant in the region of r (0.02–0.06) in which the LD/A ratio at 258 nm exhibits a pronounced minimum (Figure 5A and B). Below r = 0.02, the $(LD/A)_{258}$ ratios are rather uncertain because of the small LD signals and absorbance values.

The unexpected differences in r dependence of the absolute LD in the 258- and 520-nm wavelength regions has also been observed in the case of pBR322 supercoiled DNA (data not shown). The LD signals
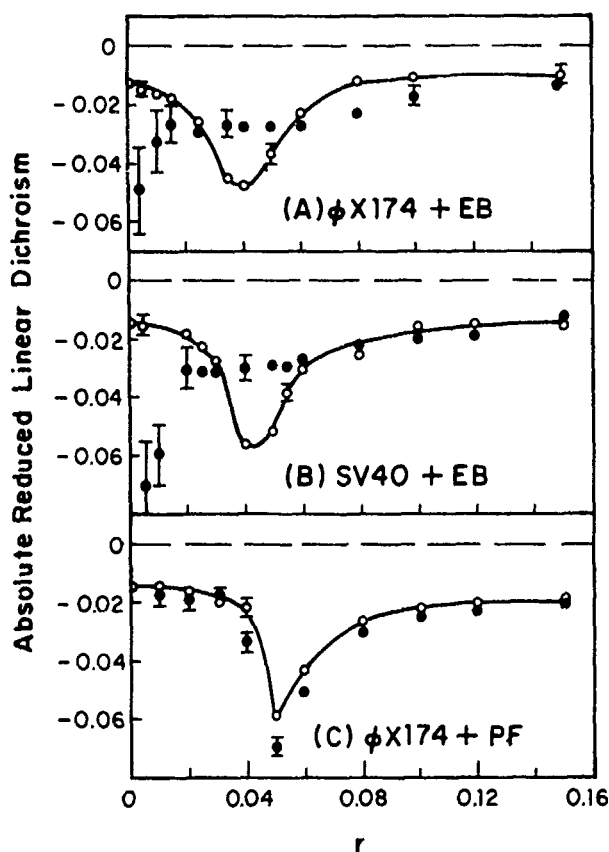
Figure 5 Reduced LD (LD/A, in absolute units) at 258 nm (O, DNA absorption band) and within the bound drug absorption bands (●). (A) EB added to ϕX 174 supercoiled DNA, drug LD/A values determined at 520 nm; (B) EB added to SV40 supercoiled DNA, drug LD/A values determined at 520 nm; (C) PF added to ϕX 174 DNA, drug LD/A values determined at 462 nm. DNA concentration: 7.5 × 10⁻⁵ M. Flow gradient: 1840 s⁻¹.

at r = 0 and r = 0.04–0.05 correspond to supercoiled and completely unwound DNA, respectively (see below); typical ratios of LD signals, LD(r = 0.04–0.05)/LD(r = 0.00), were 3.7, 2.8, and 3.7 for ϕX 174, pBR322, and SV40 DNA, respectively.

PF-ϕX 174 DNA Complexes. The magnitude of the LD signal at 258 nm, for comparable values of r, is significantly larger in the case of PF than in the case of EB; also, the highest magnitude of the LD signal at 462 nm due to intercalated PF (at r = 0.05) is about 4.5 times greater than the analogous EB signal at 520 nm (at r = 0.04). These quantitative differences can be mostly attributed to the larger molar extinction coefficients of PF relative to those of EB. Because the magnitude of the LD signals is proportional to the absorbance of the intercalatively bound drug molecules, the influence of the drugs on the overall LD signals will be greatest at the absorption maxima of the drug molecules. According to measurements in our laboratory (data not shown), PF bound to DNA is characterized by maxima at 256 (molar extinction coefficient ϵ = 29,300 M^{-1} cm^{-1}) and 462 nm (ϵ = 32,700), while the absorption maxima of EB bound to DNA are located at 298 (ϵ = 27,600) and 520 nm (ϵ = 4100); this latter value is in good agreement with the results of Houssier et al.[25] Thus the absorption and LD spectra of intercalated PF molecules nearly coincide below 300 nm with those of the DNA bases, and the overall LD signal near 258 nm is thus greater than in the case of EB–DNA complexes; in the latter case, the absorption maximum of intercalated EB at 296 nm manifests itself as a shoulder in the LD spectra near 300 nm (Figure 3).

The reduced LD values at 258 and 462 nm as a function of r for PF-ϕX 174 DNA complexes are shown in Figure 5C. These two curves resemble one another in shape, both reaching minima at r = 0.05. These results indicate that the PF molecules and DNA bases exhibit similar degrees of orientation in these flow gradient LD experiments, as expected in a simple intercalation model.

LD Characteristics of Drug–Linear DNA Complexes

The reduced LD values of EB– and PF–calf thymus DNA complexes as a function of r within the DNA and drug absorption bands are shown in Figure 6. In contrast to the behavior of supercoiled DNA at similar values of r, the LD/A values at 258 nm and within the absorption bands of the complexed drug molecules are nearly constant as a function of added drug concentration. The slight increase at the higher

r values may reflect the stiffening of the DNA segments due to the intercalative binding of the drug molecules; the reduced LD values at 258 and at 462 nm are nearly identical in the case of PF, as expected for classical intercalation complexes.[2c] The small differences between the $(LD/A)_{258}$ and $(LD/A)_{520}$ values in the case of EB have been reported earlier by others as discussed in the review of Houssier.[26]

The results obtained with the sonicated linear DNA–drug complexes show that the LD signals as a function of r obtained with supercoiled DNA are not due to artifacts of the Couette cell measurements.

DISCUSSION

Correlations Between Magnitude of LD, Sedimentation Coefficients, and Changes in Superhelical Density

The Effects of Drug Concentration. In Waring's paper,[6] the sedimentation coefficients (S_{20}) are plotted as a function of v_c, the ratio of *bound* drug molecules per nucleotide. Our LD results are plotted as a function of r, the concentration of *added* drug molecules per DNA nucleotide. However, we performed equilibrium dialysis measurements at r = 0.05 and found that under our experimental conditions more than 95% of the drug molecules are bound to the DNA (data not shown); this is consistent with previous results of Crawford and Waring[29] in the case of EB, and the known high association constants ($\sim 10^5 M^{-1}$) of EB[25] and PF[30] measured at relatively low ionic strengths, similar to those employed in our experiments. Thus, $r = v_c$ (for r < 0.1); this is confirmed by comparing our values of r corresponding to the minima in the LD/A curves, with the values of v_c corresponding to the minima in the S_{20} coefficients in Waring's experiments.[6] These minima correspond to the "equivalence point," where the sedimentation coefficients are the same at this value of v_c for nicked and for the fully relaxed ϕX 174 DNA forms.[6]
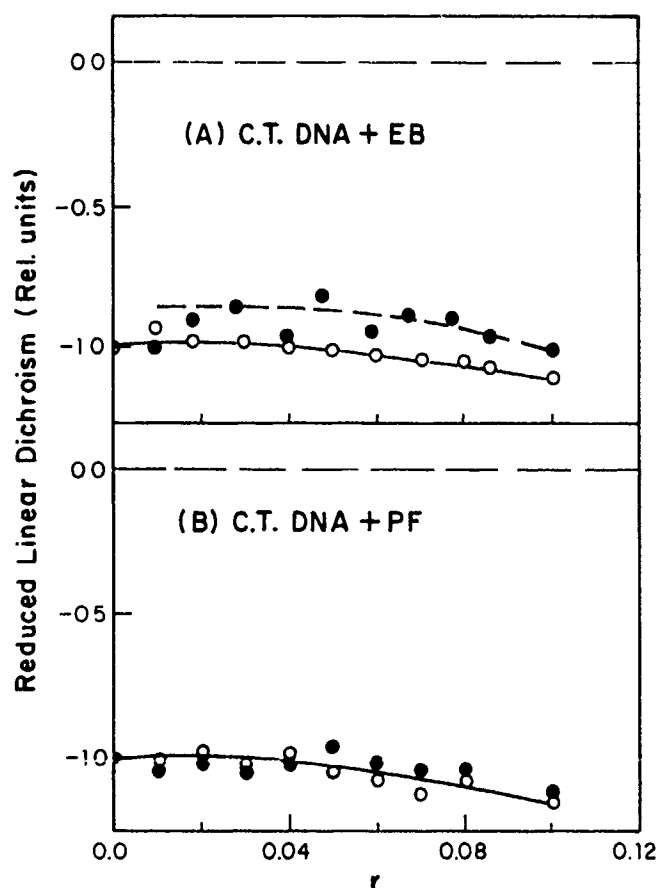
Figure 6 Reduced LD values (in relative units) of EB- and PF-sonicated calf thymus DNA complexes. (A) EB (●, measured at 520 nm), and (B) PF (●, measured at 462 nm); (O) LD/A values determined at 258 nm. DNA concentration: 7.5×10^{-5} M; flow gradient: 1840 s^{-1}.

The Equivalence Point and Unwinding Angles. The equivalence point in our experiments is reached at $r = 0.04 \pm 0.005$ in the case of EB-ϕX 174 DNA complexes (Figure 5A). In Waring's sedimentation experiments, the equivalence point was reached at $\nu_c = 0.04$.[6] In the case of PF and ϕX 174 DNA, our equivalence point occurs at $r = 0.05 \pm 0.005$, whereas in Waring's sedimentation coefficient experiments the equivalence point lies in the range of $\nu_c = 0.045-0.065$, again suggesting that r and ν_c are very close to one another, as indicated also by the experiments of Ramstein et al.[27] for values of $r < 0.1$.

The differences in the ν_c values at the equivalence points have been attributed to differences in the unwinding angles θ per bound drug molecule.[1][6] In the case of EB,[2][7][11] the accepted value for θ is 26°, while for PF[31] $\theta = 17°$. When the superhelix density σ (number of superturns/10 base pairs) is known, the unwinding angle θ can be calculated from ν_c according to the equation[1][2]

$$\theta = (-180\sigma/\nu_c) \quad (4)$$

The superhelix density of ϕX 174 is -0.057[1]; using the values of r deduced from the LD/A minima in Figure 5, θ values of $26 \pm 2°$ and $21 \pm 2°$ are obtained for EB and PF, respectively. The latter value is slightly larger than the one given in the literature.[2]

The results shown in Figure 5A and B, as well as similar results obtained with pBR322 DNA (results not shown), suggest that the LD technique is suitable for following the unwinding of different kinds of supercoiled DNA by EB. In all cases, the same biphasic behavior of the LD signal as a function of r is observed. However, the equivalence point appears at slightly higher values of r in the cases of pBR322 ($r = 0.05$) and SV40 DNA. The superhelical density of the latter is the same as that of ϕX 174[1]; the number of base pairs per ϕX 174,[32][33] pBR322,[34] and SV40[35][36] molecule, is 5386, 4363, and 5243, respectively. From the sequences provided in the cited references, we estimate that the GC content is 46, 54, and 41%, respectively. Therefore, these factors cannot account for the observed differences in the observed r ratios at the equivalence points. Other, more trivial effects such as heterogeneities in superhelical densities,[2] contamination of the samples with nicked and linear forms, can also play a role in determining the apparent values of ν_c.

The Shapes of the Titration Curves. The dependence of the $(LD/A)_{258}$ values of supercoiled ϕX 174 DNA as a function of EB and PF concentrations is remarkably similar to the sedimentation coeffi-

cient curves published earlier by Waring.[6] The increase in the magnitude of the LD signal as r is increased from zero to about 0.04-0.05 is attributed to a drug-induced unwinding of supercoiled DNA, which causes a decrease in the S_{20} coefficient[6] and an increase in the magnitude of the LD signal at 258 nm. Partially or fully unwound forms of ϕX 174 DNA exhibit a greater LD signal due to their larger, more extended hydrodynamic shapes, in contrast to supercoiled DNA, which is characterized by smaller LD values (or higher S_{20} coefficients). At an r value near 0.04, all superturns are removed, giving the DNA molecules an untwisted open circular topology, a state characterized by $\sigma = 0$. In the case of proflavine, this state is reached at a slightly higher value of $r = 0.05$. At still higher r values, left-handed superturns, corresponding to a positive increase in the superhelical density, are introduced as a result of the binding of the drug molecules; this results in a more compact form (lower LD values) and greater S_{20} coefficients.

The LD/A curves are rather symmetrical in the case of EB (Figure 5A and B). In the case of proflavine (Figure 5C), the LD/A signal as a function of r, after passing through the minimum, does not return to its initial value as r is increased further. A similar asymmetry was noted by Waring in his S_{20} vs ν_c curves.[6] The reasons for such asymmetric titration curves have been discussed by Bauer and Vinograd.[1] These reasons include the following: (1) the relative binding affinity of EB (and probably other intercalating drug molecules) depends on the superhelical density, favoring supercoiled forms at $\nu < \nu_c$, and linear DNA forms at $\nu > \nu_c$; (2) the degree of asymmetry depends on the initial values of the superhelical density, and the maximum number of intercalated drug EB molecules that can bind to the DNA at values of $r > 0.1$; it may be difficult to achieve a sufficiently high binding level to rewind the DNA in a positive sense to achieve the same original magnitude of $|\sigma|$.

Tertiary Structure and Contributions of DNA Bases and Drug Molecules to the LD Signals Measured at Different Wavelengths

The characteristics of linear DNA in a hydrodynamic flow gradient have been considered by a number of different authors. Wada[22] and Nordén and Tjerneld[23] approximated the behavior of DNA in terms of the Peterlin-Stuart theory[37] for rigid ellipsoids of revolution; deviations from this theory due to the deformation and extension of the DNA molecules in the hydrodynamic flow field were also

considered by Nordén and Tjerneld.[23] Shimada and Yamakawa[38] derived a theoretical treatment for hydrodynamic orientation of polymers based on the worm-like coil model; Schellman and co-workers used the bead-spring model for descriptions of the polymer chains.[39,40] In both of these models, the flexibility and deformation of DNA molecules in the hydrodynamic flow is taken into account. Overall, the DNA molecules may be viewed as a series of linked, relatively stiff segments that become partially oriented with their axes tending to align themselves parallel to the flow lines, thus accounting for the observed negative LD signals within the DNA absorption band.

Some elements of these models, particularly deformation and partial alignment of DNA segments along the flow lines, may also be applicable to covalently closed circular DNA. However, the closed circular nature of the intertwined DNA strands imposes restrictions on the overall degree of orientation of the individual DNA segments in the hydrodynamic force field.

Superimposed on these effects is the change in the overall hydrodynamic shape and size of the DNA molecules due to the changes in superhelicity induced by the binding of drug molecules. The lower the superhelicity, the greater the apparent hydrodynamic size of the molecules,[1-13] and thus the smaller the overall Brownian rotational motions of the DNA molecules. Therefore, unwinding should be accompanied by a better overall alignment of these molecules along the flow lines in the Couette cell. This effect, independent of any motion of the individual segments, is believed to account for the higher magnitudes of LD signals at the equivalence point relative to the LD signals of the highly compact supercoiled forms. Intuitively, it appears evident that the overall orientations of such segments in the flow field will be lower in the highly twisted supercoiled forms, than in the relaxed or linear DNA forms.

The seemingly anomalous difference in the r dependencies of the $(LD/A)_{258}$ and LD_{520} signals suggests that the unwound DNA segments containing EB molecules may respond differently to the hydrodynamic force field than the closed circular DNA molecule as a whole, or than DNA segments containing few or no EB molecules. At values of r beyond the equivalence point, ethidium molecules are known to bind preferentially to linear rather than to supercoiled DNA[1]; thus the distribution of EB molecules within any single closed circular DNA molecule may be quite heterogeneous, accounting for differences in the response of different regions of the DNA molecules to the hydrodynamic forces tending to align these segments. Any one of these effects, or a combination thereof, could account for the differences in the r dependencies of the LD signals at 258 nm and at 520 nm in the case of the EB-supercoiled DNA complexes.

It is evident that the behavior of the LD signals of the PF molecules as a function of r more closely parallel the LD signal at 258 nm than the analogous EB LD signals; the variations in the LD signals at 258 nm as a function of r are ascribed to the changes in the overall size of the DNA molecules, differences in deformation of the tertiary structure, and the partial alignment of DNA segments along the flow lines. While the exact reasons for these differences in behavior between EB- and PF-supercoiled DNA complexes are not known, these differences may be related to the known differences in the binding geometries of these two drug molecules. As established by other workers,[16,23-27] PF is characterized by an orientation angle $\theta = 90°$ (orientation of in-plane transition moment of the drug molecules with respect to the axis of B-form DNA), as expected for classical intercalation complexes. On the other hand, the transition moments of the EB molecules appear to be tilted with respect to the planes of the DNA bases[25,26,29,41] ($\theta = 60°–75°$), which suggests that the binding geometry may be somewhat different than in the case of PF. Furthermore, different intercalators may affect the local torsional rigidities and dynamics of supercoiled DNA to different extents,[42] which in turn may affect the deformation of the DNA molecules and/or the alignment of individual DNA segments. In addition, there may be differences in the binding affinities of PF and EB to DNA of different superhelical densities.

CONCLUSIONS

The flow LD technique is a suitable hydrodynamic method for rapidly assaying variations in the properties of supercoiled DNA induced by the binding of drug molecules. The conformational properties of the bound drug molecules causing these changes can also be monitored. The 258-nm LD signal reflects the overall shape and hydrodynamic properties of the partially supercoiled DNA molecules, while the 520-nm LD signals due to bound EB molecules may reflect the partial alignment of individual DNA segments containing the bound drug molecules. In contrast, the reduced LD values due to the supercoiled DNA bases at 258 nm and due to complexed PF molecules at 462 nm appear to more closely reflect

analogous degrees of alignment of both moieties in the flow gradients, as expected for a simple inter-calation model of binding.

REFERENCES

1. Bauer, W. & Vinograd, J. (1974) in *Basic Principles in Nucleic Acid Chemistry*, Vol. II, Ts'o, P. O. P., Ed., Academic Press, New York, pp. 265-303.
2. Bauer, W. R. (1978) *Ann. Rev. Biophys. Bioeng.* **7**, 287-313.
3. Scovell, W. M. (1986) *J. Chem. Ed.* **63**, 562-565.
4. Sinden, R. R. (1987) *J. Chem. Ed.* **64**, 294-301.
5. Bauer, W. & Vinograd, J. (1968) *J. Mol. Biol.* **33**, 141-171.
6. Waring, J. (1970) *J. Mol. Biol.* **54**, 247-279.
7. Wang, J. C. (1974) *J. Mol. Biol.* **89**, 783-801.
8. Pulleyblank, D. E. & Morgan, A. R. (1975) *J. Mol. Biol.* **91**, 1-13.
9. Keller, W. (1975) *Proc. Nat. Acad. Sci. USA* **72**, 4876-4880.
10. Liu, L. F. & Wang, J. C. (1975) *Biochim. Biophys. Acta* **395**, 405-412.
11. Espejo, R. T. & Lebowitz, J. (1976) *Anal. Biochem.* **72**, 95-103.
12. Revet, B. M. J., Schmir, M. & Vinograd, J. (1971) *Nature New Biol.* **229**, 10-13.
13. Smit, E. M. & Borst, P. (1971) *FEBS Lett.* **14**, 125-129.
14. Yoshida, H., Swenberg, C. E. & Geacintov, N. E. (1987) *Biochemistry (USA)* **26**, 1351-1358.
15. Wada, A. & Kozawa, S. (1964) *J. Polym. Sci.* **2**, 853-864.
16. Geacintov, N. E., Ibanez, V., Rougee, M. & Bensasson, R. V. (1987) *Biochemistry (USA)* **26**, 3087-3092.
17 Lee, C. S. & Davidson, N. (1968) *Biopolymers* **6**, 531-550.
18. Davison, P. F. (1959) *Proc. Natl. Acad. Sci. USA* **45**, 1560-1568.
19. Taylor, G. I. (1923) *Phil. Trans.* **A223**, 289-343.
20. Jerrard, H. G. (1950) *J. Appl. Phys.* **21**, 1007-1013.
21. Nordén, B. & Seth, S. (1979) *Biopolymers* **18**, 2323-2339.
22. Wada, A. (1964) *Biopolymers* **2**, 361-380.
23. Nordén, B. & Tjerneld, F. (1976) *Biophys. Chem.* **4**, 191-198.
24. Houssier, C. & Kuball, H.-G. (1971) *Biopolymers* **10**, 2421-2433.
25. Houssier, C., Hardy, B. & Fredericq, E. (1974) *Biopolymers* **13**, 1141-1160.
26. Houssier, C. (1981) in *Molecular Electrooptics*, Krause, S., Ed., Plenum, New York, pp. 313-398.
27. Ramstein, J., Houssier, C. & Leng, M. (1973) *Biochim. Biophys. Acta* **335**, 54-68.
28. Neidle, S., Pearl, L. H., Herzyk, P. & Berman, H. M. (1988) *Nucleic Acids Res.* **16**, 8999-9016.
29. Crawford, L. V. & Waring, M. J. (1967) *J. Mol. Biol.* **25**, 23-30.
30. Ellerton, N. F. (1969) *Biopolymers* **8**, 767-786.
31. Waring, M. J. (1981) *Ann. Rev. Biochem.* **50**, 159-192.
32. Sanger, F., Air, G. M., Barrell, B. G., Brown, N. L., Coulson, A. R., Fiddes, J. C., Hutchinson, C. A., III, Slocombe, P. M. & Smith, M. (1977) *Nature* **265**, 687-695.
33. Sanger, F., Coulson, A. R., Friedman, T., Air, G. M., Barrell, B. G., Brown, N. L., Fiddes, J. G., Hutchinson, III, C. A., Slocombe, P. A. & Smith, M. (1978) *J. Mol. Biol.* **125**, 225-246.
34. Maniantis, J., Fritsch, E. F. & Sambrook, J. (1982) in *Molecular Cloning: a Laboratory Manual*, Appendix B, Cold Spring Harbor Laboratory, New York, pp. 479-487.
35. Reddy, V. B., Thimmappaya, B., Dahr, R., Subramanian, K. N., Zain, B. S., Pan, J., Ghosh, P. K., Celma, M. L. & Weissman, S. M. (1978) *Science* **200**, 494-502.
36. Fiers, W., Contreras, R., Haegeman, C., Rogiers, R., van de Voorde, A., Van der Heuverswyn, H., Von Herreweghe, J., Volckaert, G. & Ysebaert, M. (1978) *Nature* **273**, 113-120.
37. Peterlin, A. & Stuart H. A. (1939) *Z. Physik* **112**, 1-19.
38. Shimada, J. & Yamakawa, H. (1976) *Macromolecules* **9**, 583-586.
39. Wilson, R. W. & Schellman, J. A. (1977) *Biopolymers* **16**, 2143-2165.
40. Schellman, J. A. (1980) *Biophys. Chem.* **11**, 321-328.
41. Hogan, M., Dattagupta, N. & Crothers, D. M. (1979) *Biochemistry (USA)* **18**, 280-288.
42. Wu, P., Song, L., Clendenning, J. B., Fujimoto, B. S., Benight, A. S. & Schurr, J. M. (1988) *Biochemistry* **27**, 8128-8144.

Advances in radioprotection through the use of combined agent regimens*

J. F. WEISS†, K. S. KUMAR†, T. L. WALDEN†,
R. NETA‡, M. R. LANDAUER§ and E. P. CLARK†

†Radiation Biochemistry, ‡Experimental Hematology, and §Behavioral
Sciences Departments, Armed Forces Radiobiology Research Institute,
Bethesda, MD 20814-5145, USA

The most effective radioprotective agents exhibit toxicities that can limit their usefulness. It may be possible to use combinations of agents with different radioprotective mechanisms of action at less toxic doses, or to reduce the toxicity of the major protective compound by adding another agent. With regard to the latter possibility, improved radioprotection and reduced lethal toxicity of the phosphorothioate WR-2721 was observed when it was administered in combination with metals (selenium, zinc or copper). The known mechanisms of action of potential radioprotective agents and varying effects of different doses and times of administration in relation to radiation exposure must be considered when using combined-agent regimens. A number of receptor-mediated protectors and other biological compounds, including endotoxin, eicosanoids and cytokines, have at least an additive effect when administered with thiol protectors. Eicosanoids and other bioactive lipids must be administered before radiation exposure, whereas some immunomodulators have activity when administered either before or after radiation exposure. For example, the cytokine interleukin-1 administered simultaneously with WR-2721 before irradiation or after irradiation enhances the radioprotective efficacy of WR-2721. The most effective single agents or combinations of protectors result in a decrement in locomotor activity, an index of behavioral toxicity. Recent evidence indicates that administration of the CNS stimulant caffeine mitigates the behavioral toxicity of an effective radioprotective dose of the phosphorothioate WR-3689 without altering its radioprotective efficacy. These examples indicate that the use of combinations of agents is a promising approach for maximizing radioprotection with minimal adverse effects.

1. Protection by thiols, antioxidants, and immunomodulators

Historically, the development of radioprotective agents has been dominated by the study of sulfhydryl compounds, particularly the aminothiols and the phosphorothioates. Various mechanisms or combinations of mechanisms for radioprotection by thiols have been proposed: at the molecular level, scavenging of reactive oxygen species, hydrogen transfer reactions, mixed disulfide hypothesis, enhancement or protection of repair enzymes, and at the biochemical-physiological level, modification of cellular metabolism, induction of hypothermia, anoxia, mediators and enzymes, and biochemical shock (Foye 1981, Weiss and Kumar 1988). The most effective thiol protectors developed thus far are S-2(? aminopropylamino)ethylphosphorothioic acid (WR-2721) and other

phosphorothioates with slightly differing structures, such as S-2[(3-methylaminopropyl aminolethylphosphorothioic acid (WR-3689) (Davidson *et al.* 1980). A dose reduction factor (DRF) as high as 2·7 against 30-day lethality in mice has been achieved with WR-2721 (Yuhas and Storer 1969), but high levels of protection are accompanied by side-effects that may be unacceptable in many situations.

A number of 'natural antioxidants' with low toxicity, such as glutathione, superoxide dismutase, antioxidant vitamins (vitamins E, A, and C), as well as substances that mimic or induce activity of endogenous antioxidant systems (*e.g.* selenium), have been studied as radioprotectors. Generally, these natural agents provide a low degree of protection compared with phosphorothioates, but they may be of value in certain situations. Although the post-irradiation administration of antioxidants or free radical scavengers would not be expected to have much effect, evidence suggests that this may occur to some extent, and is probably related to modulation of later reactions, *e.g.* interaction of radiation-induced radicals of biomolecules with reactive oxygen species evolved during normal cellular processes (reviewed in Weiss and Kumar 1988). There is some evidence of protection against lethality for mice administered the following antioxidants after irradiation: super-oxide dismutase (Petkau 1987), vitamin A (Seifter *et al.* 1984) and vitamin E (Malick *et al.* 1978). There is evidence, mostly *in vitro*, that thiols administered post-irradiation can enhance DNA repair (Riklis 1983) and reduce mutagenic effects (Grdina *et al.* 1985); however, mercaptopropionylglycine does protect against radiation-induced chromosome aberrations in bone marrow when administered to mice after irradiation (Uma Devi and Thomas 1988).

Although it is unlikely that compounds administered after irradiation will have a greater effect than those administered before irradiation that intercept or immediately repair damage or enhance repair mechanisms, from a practical point of view it is important to develop therapeutic agents, such as immunomodulators or biological response modifiers, that would enhance hematopoietic and immunological responses even when administered during the post-irradiation period.

The first and longest-studied of this class is endotoxin. When studying newer immunomodulators it is useful to recall that although endotoxin is most effective when administered 24 h before irradiation, it provides slight protection when administered shortly before or even after radiation exposure (Ainsworth 1988). An effective category of radioprotectors of the immunomodulator class is polysaccharides. The extensive studies of Patchen (reviewed in Patchen *et al.* 1988) indicate that glucan (β-1,3 polyglucose) acts as a biological response modifier when it protects against radiation exposure, e.g. when particulate glucan is given 24 h before irradiation. However, the work of Maisin *et al.* (1986) indicates that glucan and related polysaccharides may also act as free radical scavengers, because high levels of protection can be obtained by some polysaccharides when they are given shortly before irradiation (similar to aminothiols). Our studies (Weiss and Kumar 1988), using synthetic radioprotector/immunomodulators other than glucan, such as diethyldithiocarbamate (DDC) and levamisole, suggest that many immuno-modulators can modulate oxidative processes and some exhibit both pro-oxidant and antioxidant properties. These anomalies point out that it is sometimes difficult to classify radioprotective agents into rigid categories. Also different mechanisms may predominate, depending on dose and time of delivery. Differences in cell biochemistry among organs or between normal and tumor tissue can result in

differential effects, including protection in one tissue and radiosensitization or toxicity in another. DDC is an example of a thiol protector with different effects (Kumar *et al.* 1986). These factors must ultimately be taken into consideration when choosing protectors of differing mechanisms for use in combinations.

2. Receptor-mediated radioprotection

Identification of specific receptors for many radioprotectors presents a great advantage as it allows a better understanding of the mechanisms of action of radioprotective agents at the cellular level. This diverse 'class' of radioprotective agents, having known receptors, has many subclasses and would include the bioactive lipids, naturally occurring peptides, and some synthetic compounds. Bioactive lipids that are radioprotective include metabolites of arachidonic acid, such as prostacyclin (PGI_2) and leukotriene C_4 (LTC_4); synthetic analogs of prostaglandins, such as 16,16 dimethyl prostaglandin E_2 ($diPGE_2$); and other phospholipid moieties (platelet activating factor (PAF)). The radioprotective activity of endotoxin, a lipopolysaccharide, is probably related to its lipid component (reviewed by Ainsworth 1988). The extracellular and intracellular activities thought to be involved in receptor-mediated protection are shown in figure 1.

Of the compounds acting through receptor mediation, the most active appear to be $diPGE_2$ (Hanson and Ainsworth 1985, Walden *et al.* 1987), LTC_4 (Walden *et al.* 1988), PGI_2 (Hanson 1987b), and PAF (Hughes *et al.* 1989). $DiPGE_2$ and LTC_4 effectively protect hematopoietic stem cells and intestinal crypt cells and enhance survival of irradiated mice (Hanson and Ainsworth 1985, Hanson 1987a, Walden *et al.* 1987, 1988). Of the many arachidonic acid metabolites tested, PGI_2 (Hanson 1987b) and the prostaglandin analogue misoprostol (Hanson *et al.* 1988) also provide a high degree of intestinal protection. All of these compounds are only effective when given before irradiation.

The studies of Walden and co-workers show that the maximum protection attainable by treatment with bioactive lipids (30-day survival of irradiated mice) is in the range of protection afforded by the phosphorothioates. However, when a comparison is made based on administration of equitoxic doses ($1/4$ LD_{10}), they are not as effective: WR-2721 or $WR-3689 > diPGE_2 > LTC_4 = PAF$. The major problems with $diPGE_2$ are extensive diarrhea and behavioral toxicity at radioprotective doses. The eicosanoids mediate many important physiological and pathological reactions, ranging from vasoregulation to inflammation, thus complicating the elucidation of the mechanisms responsible for their radioprotective properties. In addition, the eicosanoids also function as mediators of radiation injury (inhibitors of prostaglandin synthesis, such as indomethacin, can be radioprotective). Protection may involve events at the cell membrane level and induction of cell hypoxia, as well as profound physiological effects (Walden 1987).

Many biological response modifiers, such as endotoxin and glucan, induce the peptide cytokines interleukin-1 (IL-1) and tumor necrosis factor (TNF), and some of the properties of endotoxin may be due to prostaglandin and leukotriene induction as well. A common feature of synthetic immunomodulators that are protective is their ability to induce cytokines, such as colony-stimulating factors (CSF) and interleukins (Chirigos and Patchen 1988). Although the radioprotective effects of a variety of biological response modifiers may be due to enhancement of hematopoietic recovery, or other effects on a variety of immune cells, this may come about by the release of cytokines, which in turn induce the release of many
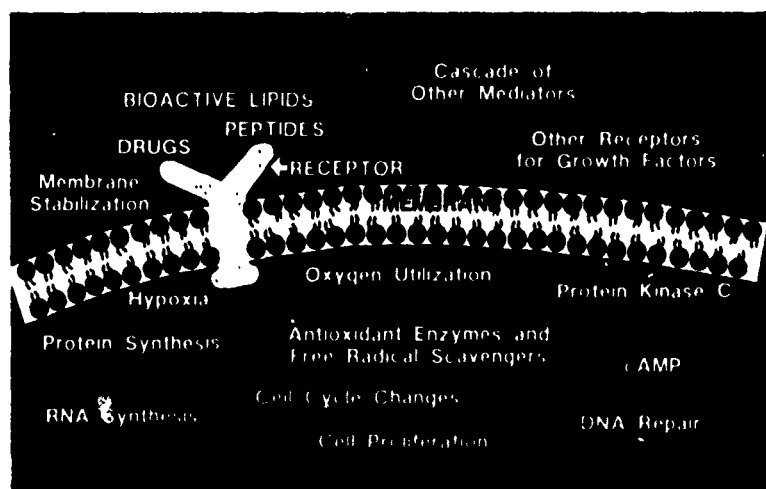
J. F. Weiss et al.

Figure 1. Cellular activities related to receptor-mediated radioprotection.

mediators, such as the products of arachidonic acid metabolism, and pathways that can be considered inflammatory (Neta 1988). Identification of IL-1 and TNF as protective and therapeutic agents against radiation (Neta 1988, Neta *et al.* 1988) presents direct evidence that inflammatory pathways participate in prevention of radiation damage and in repair, because these two cytokines are key inflammatory mediators, produced endogenously in response to multiple exogenous insults (infections, trauma and other physical stresses).

IL-1 provides varying degrees of protection, depending on the time of administration in relation to radiation exposure, probably involving a variety of mechanisms (Neta *et al.* 1988, 1989). These may include induction of hematopoietic growth factors (G-CSF, GM-CSF, IL-3 and IL-6) and induction of scavenging acute-phase proteins and superoxide dismutase, and probably other mechanisms not yet recognized (Durum *et al.* 1989). The protective effects of single doses of IL-1, whether administered before or after irradiation, contrast with G-CSF, which is effective in improving survival of mice and neutrophil recovery only when it is administered after irradiation in multiple doses (Laver *et al.* 1990). Most studies of biological response modifiers and cytokines indicate a limit of protection of 1·3 DRF.

Other peptide hormones, such as luteinizing hormone-releasing hormone (LHRH), may also protect through receptor mediation. Pre-treatment of rats with analogs of LHRH produces specific protection from radiation-induced injury to the testes (Schally *et al.* 1987). This may have important clinical applications. Methyl-xanthines, isoproterenol and norepinephrine act through receptors to increase cellular cyclic AMP levels, which might contribute to protective activity.

3. The problem of toxicity and combinations of radioprotective agents

A major question in chemical radioprotection remains: can protective mechanisms be separated from mechanisms of toxicity? As Maisin and Bacq (1975) have emphasized, the goal of non-toxic radioprotection appears difficult to attain because radioprotection and toxicity seem to be intimately linked in all organisms, particularly in mammals. The problem of toxicity of single protectors and combinations

is more acute when the intended use is at radiation accident sites or in space, where performance is an important factor. Behavioral and other toxicities are less problematic in clinical applications, where side-effects can be controlled. Clinical studies with WR-2721 have shown that it produces a variety of side-effects, including nausea, vomiting and hypotension (Blumberg *et al.* 1982). Animal studies indicate that WR-2721 also produces a decrement in performance (Bogo *et al.* 1985, Landauer *et al.* 1987). The use of WR-2721 as an adjunct to radiotherapy and chemotherapy should prove beneficial (Glover *et al.* 1988), especially if side-effects could be minimized. Similarly, because of exploitable differences in eicosanoid metabolism between normal and tumor tissue, the use of these bioactive lipids as protectors (or inhibition of their synthesis) in cancer treatment may some day be a reality (Walden 1987, Hanson *et al.* 1988). Protective cytokines, such as IL-1 and G-CSF, may also have considerable side-effects, but they are in clinical use.

Performance decrement must be evaluated when developing radioprotectors for uses where behavioral toxicity would be an unacceptable side-effect. In a series of studies, Landauer and co-workers demonstrated that the most effective protectors have the greatest behavioral side-effects, as measured by alterations in locomotor activity (Landauer *et al.* 1989b). In general, biological compounds produce decrements at least as large as chemical radioprotectors. Studies demonstrate that when radioprotective efficacy is compared on the basis of doses with equal behavioral toxicity, WR-2721 and WR-3689 (which have undesirable behavioral effects) are still superior to other radioprotectors tested.

There is now considerable evidence suggesting that the use of combinations of agents is a valid concept (Maisin *et al.* 1968, Patchen *et al.* 1989, Sztanyik and Santha 1976, Uma Devi and Thomas 1988, Weiss *et al.* 1987). A review of data on combined radioprotection indicates that the maximum achievable DRF, using combinations of protectors, will be approximately 3. However, it is extremely unlikely that this will prove practical because of concomitant toxicity. A more reasonable approach is to use combinations providing a lower DRF but acceptable toxicity. In addition, DRFs obtained with combined lower doses of protectors can be further extended by bone marrow transplants and other supportive care administered after irradiation. When the intended use of a combination of protectors is as an adjunct to radiotherapy, appropriate preclinical testing must be done to determine how the combination alters tumor protection versus normal tissue protection.

Throughout the remainder of this paper we discuss protection aginst γ- or X-irradiation by combinations of agents, illustrated also by previously unpublished data. In all radioprotection studies reported in the tables, CD2F1 male mice were irradiated bilaterally with cobalt-60 at 1 Gy/min. The $LD_{50/30}$ for saline-treated mice was 8·0–8·5 Gy. Other experimental details are given in Weiss *et al.* (1987) and Landauer *et al.* (1987).

4. Combinations of metals and phosphorothioates

Treatment of mice with salts of various metals (copper, zinc or selenium) provided a small radioprotective effect. Therefore, it was of interest to determine whether combinations of metals and thiol compounds would be beneficial. We first concentrated on selenium (Se) because of its known inter-relationship with endogenous antioxidant defense systems, such as vitamin E and glutathione peroxidase (Jacobs *et al.* 1983). The effect of Se, as sodium selenite, on the acute toxicity and

radioprotective effect of WR-2721, was studied in male CD2F1 mice (Weiss *et al.*
1987). Injection of 1·6 mg/kg Se 24 h before WR-2721 (800–1200 mg/kg, i.p.)
decreased the lethal toxicity of WR-2721 significantly. Se injection alone
(1·6 mg/kg) 24 h before cobalt-60 irradiation increased survival (DRF = 1·1). An
enhancement of the protective effect of WR-2721 also occurred when Se was
injected 24 h before WR-2721 (200–600 mg/kg, i.p., 0·5 h before irradiation). For
example, after exposure to 22 Gy (1 Gy/min), 30-day survival was 100 per cent
when mice were treated with both Se and 600 mg/kg WR-2721, and 13 per cent
when they were treated with WR-2721 alone. The DRFs for 30-day survival after
400 mg/kg WR-2721 were 2·6 with Se and 2·2 without Se pre-treatment.

Pre-administration of zinc aspartate 2 min before cysteamine or 2-β-
aminoethylisothiouronium-Br-HBr (AET) increased the radioprotective effect of
the thiols (Floersheim and Floersheim 1986). Brown *et al.* (1988) demonstrated that
zinc chloride administration 5 min before WR-2721, resulted in an increase in both
the hematopoietic and gastrointestinal DRFs.

In subsequent studies we compared the effects of Se, zinc (Zn) as zinc chloride
and copper (Cu) as copper sulfate. We used lower doses than those used previously
in combination with thiols, and WR-2721 was also administered at a relatively low
dose. Mice were either pre-treated with the metals, or the metals were administered
simultaneously with WR-2721. Table 1 compares the effects of the metals on the
lethal toxicity of WR-2721 (1000 mg/kg). Cu pre-administration (3 h or 24 h)
resulted in an increase in survivors, but simultaneous administration with
WR-2721 was not effective. Zn was effective when it was given 3 h before
WR-2721. Although this study was done with a small number of animals, the
results suggest that Se was more effective than the other metals when it was given
simultaneously with WR-2721.

Table 2 shows that pre-treatment with each of the three metals at −3 h enhances
radioprotection by WR-2721 (200 mg) at 14 Gy exposure when all treatments were
i.p. However, when WR-2721 was administered orally and the metals i.p., Se was
not effective, whereas Cu and Zn had a small effect. Table 3 shows the comparative
radioprotective effects of solutions of metals and WR-2721 combined. In this
situation, Se was the most effective, in a similar way to its effect on the lethal
toxicity of WR-2721 (Table 1).

Table 1. Effect of metals (0·8 mg/kg, i.p.) on lethal toxicity of WR-2721 (1000 mg/kg, i.p.,
CD2F1 male mice).

Treatment	30-day survivors
WR-2721	1/30
Cu at −3 h	9/10
Cu at −24 h	7/10
WR-2721 and Cu simultaneously	1/10
Zn at −3 h	8/10
Zn at −24 h	0/10
WR-2721 and Zn simultaneously	1/10
Se at −3 h	4/10
Se at −24 h	3/10
WR-2721 and Se simultaneously	3/10

Table 2. Effect of pre-treatment with metals (0·8 mg/kg, i.p., −3 h) on radioprotection by WR-2721 in CD2F1 male mice.

	Treatment	30-day survivors
WR-2721 (700 mg/kg, p.o.), 1 h before irradiation (14 Gy cobalt-60)	WR-2721	7/48 (15%)
	+Cu	11/32 (34%)
	+Zn	18/32 (56%)
	+Se	3/32 (9%)
WR-2721 (200 mg/kg, i.p.), 30 min before irradiation (14 Gy cobalt-60)	WR-2721	15/40 (38%)
	+Cu	34/40 (85%)
	+Zn	27/40 (68%)
	+Se	34/40 (85%)

The results of metal effects on toxicity and radioprotection by WR-2721 suggest different mechanisms for the potentiation by metals of thiol radioprotection. Floersheim and Floersheim (1986) suggested that Zn stabilizes thiol protectors, but there is little experimental evidence for this mechanism. Inhibition of alkaline phosphatase by metals would alter the kinetics of conversion of WR-2721 to its active free thiol WR-1065. This might occur with higher concentrations of Zn (Brown *et al.* 1988) or Se (Weiss *et al.* 1987). The improvement in radioprotective effect of WR-2721 by Se and/or suppression of toxic metabolites formed during metabolism of WR-2721 may be due to induction of glutathione peroxidase activity by Se administration (Kumar *et al.* 1988). It is possible that other endogenous protective organometallic compounds are formed when the metals are injected, or the metals are forming new compounds by reacting with WR-1065. This appears to be most likely in the case of Se (Kumar and Weiss 1989).

Because oxygen plays an important role in the modulation of radiation sensitivity, modulation by metals of oxygen uptake by WR-1065 was investigated using an *in vitro* model system (Kumar and Weiss 1989). The highest rate of oxygen consumption by WR-1065 occurred in the presence of Cu, followed by Se, and Zn had very little effect. Purdie *et al.* (1983) suggested that WR-1065 is oxidized to the disulfide, and the consequent anoxia may contribute to protection by the drug. Our studies indicate that formation of the disulfide of WR-1065 is accelerated in the presence of increased levels of Cu. Earlier *in vivo* work by Yuhas *et al.* (1973)

Table 3. Radioprotection in CD2F1 male mice by combined treatment with WR-2721 and metals. Solutions of WR-2721 (200 mg/kg) and metals (0·8 mg/kg) administered i.p. simultaneously 30 min before irradiation.

Treatment	30-day survivors	
	14 Gy	15 Gy
WR-2721	8/16 (50%)	1/16 (6%)
WR-2721 and Cu	11/16 (69%)	9/16 (56%)
WR-2721 and Zn	13/16 (81%)	5/16 (31%)
WR-2721 and Se	16/16 (100%)	13/16 (81%)

showed that the protective effect of WR-2721 was probably influenced by oxygen tension. Denekamp *et al.* (1982) reported that an optimum level of oxygen is needed for maximum protection with WR-2721, and protection is lower below and above that level of oxygen. It is difficult to correlate our *in vitro* results with the observed radioprotective effects in mice of the metal and WR-2721 combinations, but the studies established that metal ions are important factors in the interaction between sulfhydryl compounds and oxygen with respect to radioprotection.

An important adjunct to studies on radioprotection by combinations of agents are determinations of behavioral toxicity of single agents compared with combinations of agents. Automated quantitation of spontaneous locomotor activity has been found to be a sensitive measurement of the behavioral toxicity of radioprotectors (Landauer *et al.* 1987). Table 4 summarizes the effects of combinations of metals and WR-2721 on mouse locomotor activity. Mice ($n = 11$/group) were tested during the nocturnal phase of their light/dark cycle. All treatments resulted in locomotor decrements. Administration of metals alone resulted in an earlier onset of locomotor decrement than the WR-2721 treatment, but it took longer to recover from the decrement produced by WR-2721. When WR-2721 was administered with the metals, the Cu combination resulted in the most severe locomotor decrement, due mainly to the longer recovery time. The Zn and WR-2721 mixture appears to be the least toxic because WR-2721 alone produced a greater performance decrement than the combination. Information on the behavioral toxicity, lethal toxicity and radioprotective effects of combinations can be useful for comparative assessments of combined radioprotective regimens.

5. Combinations of receptor-mediated and other biological compounds with phosphorothioates

The first indication that biological response modifiers or immunomodulators might be effective in combination with thiols resulted from studies of endotoxin and AET. Administration of endotoxin at 24 h and AET 15 min before radiation exposure of mice resulted in greater than additive protection (Ainsworth *et al.* 1970). Unpublished work by Walden, using detoxified endotoxin (monophosphoryl lipid A) injected at −24 h, produced an additive effect with WR-2721 administered at −30 min.

The combined use of WR-2721 and diPGE$_2$ has been investigated (Hanson 1987a, Steel *et al.* 1988, Landauer *et al.* 1989b). The studies have shown a favorable protective response with γ-irradiation. When WR-2721 was administered 15 min before irradiation with 0·4 mg/kg diPGE$_2$ given 5 min before irradiation, 30-day survival increased as compared with that of WR-2721 alone. In this case, protection by the combined agents was slightly less than additive. The DRF for WR-2721 (200 mg/kg) was 1·9; for diPGE$_2$, 1·45; and for the combination, 2·15. A protective response that was greater than additive was obtained for survival at 6 days when diPGE$_2$ was administered 1 h before irradiation and before WR-2721 (Hanson 1987a). Greater protection of murine intestinal crypt cells was observed after the combined treatment, but protection by high doses of WR-2721 (approximately 300–400 mg/kg) could not be improved by the addition of diPGE$_2$. The greater protection produced by using the combination of agents in this study could have resulted from the order of administration, which produced different physiological responses, or from modified catabolism of the radioprotectors. Misoprostol, a synthetic analog of prostaglandin E$_1$, was effective in protecting intestinal clono-

Table 4. Behavioral toxicity (locomotor decrement) in CD2F1 male mice treated i.p. simultaneously with metals (0·8 mg/kg) and WR-2721 (200 mg/kg).

Treatment	Onset of locomotor decrement (min)	Maximum locomotor decrement		Time to recover from decrement (h)
		(min)	percentage	
WR-2721	25	25	70	4·0
Se	15	15	70	0·8
WR-2721 and Se	10	20	95	4·5
Cu	10	10	66	0·6
WR-2721 and Cu	10	30	80	7·0
Zn	10	10	35	0·3
WR-2721 and Zn	20	30	70	3·5

genic cells when combined with WR-2721 (Hanson *et al.* 1988). The combination of misoprostol (25 μg/mouse) followed by a high dose of WR-2721 (10 mg/mouse) extended the longevity of mice irradiated with 20 Gy and 23·5 Gy.

When WR-2721 followed by diPGE$_2$ was administered before fission neutron irradiation, there was no improvement in the survival of mice compared with those given WR-2721 alone (Steel *et al.* 1988). Behavioral toxicity studies conducted on mice receiving the combination of WR-2721 and diPGE$_2$ demonstrated a greater behavioral decrement measured by locomotor activity than those produced by either agent alone (Landauer *et al.* 1989b).

Although Maisin *et al.* (1986) failed to find improved radioprotection with polysaccharides and AET, Patchen *et al.* (1990) reported enhanced protection by WR-2721 in combination with glucan. The protective effect (DRF 1·2) of particulate glucan administered at −20 h was additive with the protective effect of WR-2721 (200 mg/kg, −30 min). Furthermore, an even greater protection was obtained when Se was also given at −20 h. Treatment with each of the three agents, which act by different mechanisms, resulted in an increase in hematopoietic stem cells (endogenous spleen colony-forming unit assay). Treatment with the combination of the three agents was most effective in this regard, as well as in accelerating bone marrow and splenic granulocyte–macrophage colony-forming cell regeneration (Patchen *et al.* 1990). A greater than additive effect was obtained when WR-2721 was given before irradiation and soluble glucan (Glucan-F) was administered after irradiation (Patchen *et al.* 1989). This study established a potential role for the post-irradiation use of immunomodulators in combination with traditional thiol radioprotectors. Such combinations appear to depend on the sequential thiol-mediated cell protection and immunomodulator-mediated hematopoietic stimulation.

We demonstrated that IL-1 was effective in improving the survival of irradiated CD2F1 mice when it was administered at times ranging from 20 h before to 2 h after radiation exposure. When administered after irradiation in combination with WR-2721 (200 mg/kg, −30 min), IL-1 enhanced survival at radiation doses (15–16 Gy) causing hematopoietic and gastrointestinal injury (Neta *et al.* 1989). Table 5 shows the effect of simultaneous administration of IL-1 (human recombinant interleukin-1α, Hoffmann-LaRoche) and WR-2721 at 30 min before irradiation. IL-1 alone has no protective effect at the high radiation doses tested. Greater than additive

Table 5. Radioprotective effects of combinations of WR-2721 and IL-1 in CD2F1 male
mice. Simultaneous i.p. administration 30 min before irradiation.

Treatment	30-day survivors	
	14 Gy	15 Gy
WR-2721 (200 mg/kg)	14/32 (44%)	0/24 (0%)
+IL-1 (4 μg/kg)	23/24 (96%)	6/16 (38%)
+IL-1 (400 μg/kg)	16/16 (100%)	13/16 (81%)
	18 Gy	20 Gy
WR-2721 (400 mg/kg)	14/32 (44%)	1/32 (3%)
+IL-1 (4 μg/kg)	30/32 (94%)	15/32 (47%)
+IL-1 (400 μg/kg)	25/32 (78%)	6/32 (19%)

protection was obtained with combinations of IL-1 and 200 mg/kg WR-2721 (1/4
the LD_{10} dose) or 400 mg/kg WR-2721. The higher dose of IL-1 (400 mg/kg) did
not provide much benefit over the lower dose (4 μg/kg). WR-2721 may be
protecting hematopoietic stem cells, which in turn may be amplified because of
IL-1 administration. Whether similar explanations can be used to account for im-
proved protection with WR-2721 and IL-1 in the gastrointestinal dose range is
being investigated. Although the biochemical mechanisms of protection by IL-1
are unclear, it is known that IL-1 treatment of mice induces ceruloplasmin and
metallothionein (reviewed by Neta 1988), both of which have antioxidant and
possible radioprotective effects. The induction of superoxide dismutase by IL-1
also was observed recently *in vitro* (Masuda *et al.* 1988). Vaishnav *et al.* (1989)
showed that IL-1 can induce manganese–superoxide dismutase *in vivo*, but only at
6 h after administration with the higher dose (400 μg/kg). Therefore, superoxide
dismutase may contribute to the radioprotective effect of IL-1, but may not be the
only radioprotective mediator.

It would be useful to combine more than one cytokine with a phosphorothioate,
because additive protection has been observed with combinations of cytokines or
biological response modifiers: IL-1 and TNF (Neta *et al.* 1988), IL-1 and G-CSF
(Laver *et al.* 1990) and glucan and BM41.332 (Patchen *et al.* 1988). Presently, the
only recommended biological factors for the treatment of radiation injuries in
humans are recombinant G-CSF and GM-CSF (Browne *et al.* 1990) because more
clinical data are available for these agents. Because WR-2721 is also in clinical use,
animal studies on combinations of pre-irradiation administration of phosphoro-
thioates combined with post-irradiation administration of G-CSF or GM-CSF
show promise for early acceptance for human use (Patchen and MacVittie,
unpublished work). The further addition of post-irradiation bone marrow trans-
plants has been shown previously to be of value with a number of protectors, for
example, in combination with IL-1 (Oppenheim *et al.* 1989).

6. Combinations of caffeine and phosphorothioates

Research on chemical radioprotectors needs to be expanded to include studies
on drugs that will prevent radiation-induced behavioral disruption and per-

Table 6. Effect of caffeine on radioprotection by WR-3689 in CD2F1 male mice. Simultaneous oral administration 1 h before irradiation.

Treatment	30-day survivors		
	10 Gy	11 Gy	12 Gy
WR-3689 (400 mg/kg) +caffeine (40 mg/kg)	12/32 (38%) 14/32 (44%)	— —	— —
WR-3689 ( ) mg/kg) +caffeine (4 ng/kg)		4/8 (50%) 10/16 (63%)	2/8 (25%) 4/16 (25%)

formance decrement, as well as studies on agents that will modify the behavioral toxicity of radioprotectors (Bogo 1988). Landauer *et al.* (1989a) recently determined that the CNS stimulant caffeine can mitigate the locomotor decrement produced by WR-3689. These data and results on radioprotection by combinations of caffeine and WR-3689 will be published in detail elsewhere. The timing of caffeine administration in relation to administration of the phosphorothioate appears to be important in mitigating the behavioral effect, but not the radioprotective efficacy, of WR-3689. Caffeine administration does not have an adverse effect on the radioprotective efficacy of WR-3689 when the drugs are administered by various routes. Table 6 shows the survival of irradiated mice (10–12 Gy) after simultaneous oral administration of WR-3689 and caffeine 1 h before irradiation. No significant difference in survival was observed. Although caffeine is generally considered to be a sensitizer, results on radiosensitization effects are, in general, obtained from *in vitro* cell irradiation studies. There is evidence that, in mice, caffeine provides some protection of jejunal crypt cells, as do other inhibitors of cyclic AMP phosphodiesterase (Lehnert 1979). The results on combinations of caffeine and WR-3689 provide encouragement that the toxicities of major radioprotective compounds can be ameliorated.

Acknowledgements

References

AINSWORTH, E. J., 1988, From endotoxins to newer immunomodulators: Survival-promoting effects of microbial polysaccharide complexes in irradiated animals. *Pharmacology and Therapeutics*, **39**, 223–241.

AINSWORTH, E. J., LARSEN, R. M., MITCHELL, F. A., and TAYLOR, J. F., 1970, Survival-promoting effects of endotoxin in mice, dogs, and sheep. *Radiation Protection and Sensitization, Proceedings of the Second International Symposium on Radiosensitizing and Radio-Protective Dugs*, edited by H. L. Moroson and M. Quintiliani (Taylor & Francis, London), pp. 381–388.

BLUMBERG, A. L., NELSON, D. F., GRAMKOWSKI, M., GLOVER, D., GLICK, J. H., YUHAS, J. M., and KLIGERMAN, M. M., 1982, Clinical trials of WR-2721 with radiation therapy. *International Journal of Radiation Oncology, Biology, Physics*, **8**, 561–563.

BOGO, V., 1988, Behavioral radioprotection. *Pharmacology and Therapeutics*, **39**, 73–78.

BOGO, V., JACOBS, A. J., and WEISS, J. F., 1985, Behavioral toxicity and efficacy of WR-2721 as a radioprotectant. *Radiation Research*, **104**, 182–190.

BROWN, D. Q., GRAHAM, W. J., MACKENZIE, L. J., PITTOCK, J. W., and SHAW, L. M., 1988, Can WR-2721 be improved upon? *Pharmacology and Therapeutics*, **39**, 157–168.

BROWNE, D., WEISS, J. F., MACVITTIE, T. J., and PILLAI, M. V. (eds), 1990, *Treatment of Radiation Injuries* (Plenum, New York) (In press).

CHIRIGOS, M. A., and PATCHEN, M. L., 1988, Survey of newer biological response modifiers for possible use in radioprotection. *Pharmacology and Therapeutics*, **39**, 243–246.

DAVIDSON, D. E., GRENAN, M. M., and SWEENEY, T. R., 1980, Biological characteristics of some improved radioprotectors. *Radiation Sensitizers, Their Use in the Clinical Management of Cancer*, edited by L. W. Brady (Masson, New York), pp. 309–320.

DENEKAMP, J., MICHAEL, B. D., ROJAS, A., and STEWART, F. A., 1982, Radioprotection of mouse skin by WR-2721: the critical influence of oxygen tension. *International Journal of Radiation Oncology, Biology, Physics*, **8**, 531–534.

DURUM, S., OPPENHEIM, J. J., and NETA, R., 1989, Immunophysiological role of inter-leukin-1. *Immunophysiology: Role of Cells and Cytokines in Immunity and Inflammation*, edited by J. J. Oppenheim and E. Shevach (Oxford University Press, Oxford), pp. 210–225.

FLOERSHEIM, G. L., and FLOERSHEIM, P., 1986, Protection against ionizing radiation and synergism with thiols by zinc aspartate. *British Journal of Radiology*, **59**, 597–602.

FOYE, W. O., 1981, Radioprotective drugs. *Burger's Medicinal Chemistry*, edited by M. E. Wolff (Wiley, New York), pp. 11–45.

GLOVER, D., FOX, K. R., WEILER, C., KLIGERMAN, M. M., TURRISI, A., and GLICK, J. H., 1988, Clinical trials of WR-2721 prior to alkylating agent chemotherapy and radiotherapy. *Pharmacology and Therapeutics*, **39**, 3–7.

GRDINA, D. J., NAGY, B., HILL, C. K., WELLS, R. L., and PERAINO, C., 1985, The radioprotector WR-1065 reduces radiation-induced mutations at the hypoxanthine-guanine phosphoribosyl transferase locus in V79 cells. *Carcinogenesis*, **6**, 929–931.

HANSON, W. R., 1987a, Radioprotection of murine intestine by WR-2721, 16,16-dimethyl prostaglandin E_2 and the combination of both agents. *Radiation Research*, **111**, 361–373.

HANSON, W. R., 1987b, Radiation protection by exogenous arachidonic acid and several metabolites. *Prostaglandin and Lipid Metabolism in Radiation Injury*, edited by T. L. Walden and H. N. Hughes (Plenum, New York), pp. 233–243.

HANSON, W. R., and AINSWORTH, E. J., 1985, 16,16-Dimethyl prostaglandin E2 induces radioprotection in murine intestinal and hematopoietic stem cells. *Radiation Research*, **100**, 290–297.

HANSON, W. R., HOUSEMAN, K. A., and COLLINS, P. W., 1988, Radiation protection *in vivo* by prostaglandins and related compounds of the arachidonic acid cascade. *Pharmacology and Therapeutics*, **39**, 347–356.

HUGHES, H. N., WALDEN, T. L., and STEEL, L. K., 1989, Radioprotective efficacy of platelet activating factor in mice. *Abstracts of Papers for the 37th Annual Meeting of the Radiation Research Society, Seattle, WA*, p. 186.

JACOBS, A. J., RANKIN, W. A., SRINIVASAN, V., and WEISS, J. F., 1983, Effects of vitamin E and selenium on glutathione peroxidase activity and survival of irradiated mice. *Proceedings of the 7th International Congress of Radiation Research*, edited by J. J. Broerse, G. W. Barendsen, H. B. Kal, and A. J. van der Kogel (Martinus Nijhoff, Amsterdam), D5–15.

KUMAR, K. S., and WEISS, J. F., 1989, Effect of metals on oxygen consumption by radioprotective thiols *in vitro*. *Frontiers of Radiation Biology, Proceedings of the 21st Annual Meeting of the European Society for Radiation Biology*, edited by E. Riklis (VCH, Weinheim/Deerfield Beach, FL, and Balaban, Rehovot/Philadelphia) (In press).

KUMAR, K. S., SANCHO, A. M., and WEISS, J. F., 1986, A novel interaction of diethyl-dithiocarbamate with the glutathione/glutathione peroxidase system. *International Journal of Radiation Oncology, Biology, Physics*, **12**, 1463–1467.

KUMAR, K. S., VAISHNAV, Y. N., and WEISS, J. F., 1988, Radioprotection by antioxidant enzymes and enzyme mimetics. *Pharmacology and Therapeutics*, **39**, 301–309.

LANDAUER, M. R., DAVIS, H. D., DOMINITZ, J. A., and WEISS, J. F., 1987, Dose and time relationships of the radioprotector WR-2721 on locomotor activity in mice. *Pharmacology, Biochemistry and Behavior*, **27**, 573–576.

LANDAUER, M. R., DAVIS, H. D., KUMAR, K. S., and WEISS, J. F., 1989a, Caffeine mitigates the behavioral toxicity of the radioprotector WR-3689. *Abstracts of Papers for the 22nd Annual Meeting of the European Society for Radiation Biology, Brussels*, p. 146.

LANDAUER, M. R., WALDEN, T. L., and DAVIS, H. D., 1989b, Behavioral effects of radioprotective agents in mice: combination of WR-2721 and 16, 16 dimethyl prostaglandin E_2. *Frontiers of Radiation Biology, Proceedings of the 21st Annual Meeting of the European Society for Radiation Biology*, edited by E. Riklis (VCH, Weinheim/Deerfield Beach, FL and Balaban, Rehovot/Philadelphia) (In press).

LAVER, J., GILLIO, A., ABBOUD, M., GASPARETTO, C., WARREN, D., O'REILLY, R. J., and MOORE, M. A. S., 1990, Myeloprotective effects of interleukin-1 following exposure to chemoradiotherapy. *Treatment of Radiation Injuries*, edited by D. Browne, J. F. Weiss, T. J. MacVittie, and M. V. Pillai (Plenum, New York) (In press).

LEHNERT, S., 1979, Radioprotection of mouse intestine by inhibitors of cyclic AMP phosphodiesterase. *International Journal of Radiation Oncology, Biology, Physics*, **5**, 825–833.

MAISIN, J. R., and BACQ, Z. M., 1975, Toxicity, *International Encyclopedia of Pharmacology and Therapeutics: Sulfur-Containing Radioprotective Agents*, edited by Z. M. Bacq (Pergamon, New York), pp. 15–39.

MAISIN, J. R., KONDI-TAMBA, A., and MATTELIN, G., 1986, Polysaccharides induce radioprotection of murine hemopoetic stem cells and increase the LD 50/30 days. *Radiation Research*, **105**, 276–281.

MAISIN, J. R., MATTELIN, G., FRIDMAN-MANDUZIO, A., and VAN DER PARREN, J., 1968, Reduction of short- and long-term radiation lethality by mixtures of chemical protectors. *Radiation Research*, **35**, 26–44.

MALICK, M. A., ROY, R. M., and STERNBERG, J., 1978, Effect of vitamin E on post-irradiation death in mice. *Experientia*, **34**, 1216–1217.

MASUDA, A., LONGO, D. L., KOBAYASHI, Y., APPELLA, E., OPPENHEIM, J. J., and MATSU-SHIMA, K., 1988, Induction of mitochondrial manganese superoxide dismutase by interleukin-1. *FASEB Journal*, **2**, 3087–3091.

NETA, R., 1988, Role of cytokines in radioprotection. *Pharmacology and Therapeutics*, **39**, 261–266.

NETA, R., KUMAR, K. S., and WEISS, J. F., 1989, Enhancement of survival of irradiated mice by treatment with interleukin-1 (IL-1) alone and in combination with WR-2721. *Abstracts of the 37th Annual Meeting of the Radiation Research Society, Seattle, WA*, p. 185.

NETA, R., OPPENHEIM, J. J., and DOUCHES, S. D., 1988, Interdependence of the radioprotective effects of human recombinant interleukin 1α, tumor necrosis factor α, granulocyte colony-stimulating factor, and murine recombinant granulocyte-macrophage colony-stimulating factor. *Journal of Immunology*, **140**, 108–111.

OPPENHEIM, J. J., NETA, R., TIBERGHIEN, P., GRESS, R., KENNY, J., and LONGO, D., 1989, Interleukin 1 enhances survival of lethally irradiated mice treated with allogeneic bone marrow cells. *Blood*, **74**, 2257–2263.

PATCHEN, M. L., D'ALESANDRO, M. M., CHIRIGOS, M. A., and WEISS, J. F., 1988, Radioprotection by biological response modifiers alone and in combination with WR-2721. *Pharmacology and Therapeutics*, **39**, 247–254.

722

PATCHEN, M. L., MACVITTIE, T. J., and JACKSON, W. E., 1989, Postirradiation glucan administration enhances the radioprotective effects of WR-2721. *Radiation Research,* **117,** 59-69.

PATCHEN, M. L., MACVITTIE, T. J., and WEISS, J. F., 1990, Combined modality radioprotection: The use of glucan and selenium with WR-2721. *International Journal of Radiation Oncology, Biology, Physics* (In press).

PETKAU, A., 1987, Role of superoxide dismutase in modification of radiation injury. *British Journal of Cancer,* **55** (Suppl. VIII), 87-95.

PURDIE, J. W., INHABER, E. R., SCHNEIDER, H., and LABELLE, J. L., 1983, Interaction of cultured mammalian cells with WR-2721 and its thiol WR-1065: implications for mechanisms of radioprotection. *International Journal of Radiation Biology,* **43,** 517-527.

RIKLIS, E., 1983, DNA repair as a probe of radiosensitivity and radioprotection. *Radioprotectors and Anticarcinogens,* edited by O. F. Nygaard and M. G. Simic (Academic Press, New York), pp. 363-380.

SCHALLY, A. V., PAZ-BOUZA, J. I., SCHLOSSER, J. V., KARASHIMA, T., DEBELJUK, L., GANDLE, B., and SAMPSON, M., 1987, Protective effects of analogs of luteinizing hormone-releasing hormone against X-radiation-induced damage in rats. *Proceedings of the National Academy of Sciences, USA,* **84,** 851-857.

SEIFTER, E., RETTURA, G., PADAWER, J., STRATFORD, F., WEINZWEIG, J., DEMETRIOUS, A. A., and LEVENSON, S. M., 1984, Morbidity and mortality reduction by supplemental vitamin A or β-carotene in CBA mice given total body radiation. *Journal of the National Cancer Institute,* **73,** 1167-1177.

SINGH, A., and SINGH, H., 1982, Time-scale and nature of radiation-biological damage: approaches to radiation protection and postirradiation therapy. *Progress in Biophysics and Molecular Biology,* **39,** 69-106.

STEEL, L. K., WALDEN, T. L., HUGHES, H. N., and JACKSON, W. E., 1988, Protection of mice against mixed fission neutron-γ (n:γ = 1:1) irradiation by WR-2721, 16,16-dimethyl PGE$_2$, and the combination of both agents. *Radiation Research,* **115,** 605-608.

SZTANYIK, L. B., and SANTHA, A., 1976, Synergistic effect of radioprotective substances having different mechanisms of action. *Modification of Radiosensitivity of Biological Systems* (International Atomic Energy Agency, Vienna), pp. 47-59.

UMA DEVI, P., and THOMAS, B., 1988, Bone marrow cell protection and modification of drug toxicity by combination of protectors. *Pharmacology and Therapeutics,* **39,** 213-214.

VAISHNAV, Y. N., KUMAR, K. S., WEISS, J. F., and NETA, R., 1989, Induction of superoxide dismutase: A mechanism for radioprotection by interleukin-1 (IL-1)? *Abstracts of Papers for the 37th Annual Meeting of the Radiation Research Society, Seattle, WA,* p. 185.

WALDEN, T. L., 1987, A paradoxical role for eicosanoids: Radioprotectants and radiosensitizers. *Prostaglandin and Lipid Metabolism in Radiation Injury,* edited by T. L. Walden and H. N. Hughes (Plenum, New York), pp. 263-271.

WALDEN, T. L., PATCHEN, M. L., and MACVITTIE, T. J., 1988, Leukotriene-induced radioprotection of hematopoietic stem cells in mice. *Radiation Research,* **113,** 338-395.

WALDEN, T. L., PATCHEN, M., and SNYDER, S. L., 1987, 16,16-Dimethyl prostaglandin E$_2$ increases survival in mice following irradiation. *Radiation Research,* **109,** 440-448.

WEISS, J. F., and KUMAR, K. S., 1988, Antioxidant mechanisms in radiation injury and radioprotection. *Cellular Antioxidant Defense Mechanisms,* Vol. II, edited by C. K. Chow (CRC Press, Orlando), pp. 163-189.

WEISS, J. F., HOOVER, R. L., and KUMAR, K. S., 1987, Selenium pretreatment enhances the radioprotective effect and reduces the lethal toxicity of WR-2721. *Free Radical Research Communications,* **3,** 33-38.

YUHAS, J. M., PROCTOR, J. O., and SMITH, L. M., 1973, Some pharmacologic effects of WR-2721: Their role in toxicity and radioprotection. *Radiation Research,* **54,** 222-233.

YUHAS, J. M., and STORER, J. B., 1969, Chemoprotection against three modes of radiation death in the mouse. *International Journal of Radiation Biology,* **15,** 233-237.